Report No. CG-D-43-82

(10)

AD A130609

LORAN-C SIGNAL STABILITY STUDY :

ST. MARYS RIVER

DECEMBER 1982

FINAL REPORT

Prepared by

U.S. DEPARTMENT OF TRANSPORTATION
United States Coast Guard
Office of Research and Development
Washington, D.C. 20590

NOTICE

This document is disseminated under the sponsorship of the Department of Transportation in the interest of information exchange. The United States Government assumes no liability for its contents or use thereof.

The contents of this report do not necessarily reflect the official view or policy of the Coast Guard; and they do not constitute a standard, specification, or regulation.

This report, or portions thereof may not be used for advertising or sales promotion purposes. Citation of trade names and manufacturers does not constitute endorsement or approval of such products.

Technical Report Documentation Page

1. Report No.	2. Government Accession No.	3. Recipient's Catalog No.
CG-D-43-82	AD-A130609	

4. Title and Subtitle	5. Report Date
LORAN-C SIGNAL STABILITY STUDY: ST. MARYS RIVER	December 1982
	6. Performing Organization Code: G-DST-1
7. Author(s): R. J. WENZEL, D. C. SLAGLE	8. Performing Organization Report No.: CG-D-43-82
9. Performing Organization Name and Address: Department of Transportation, U.S. Coast Guard, Office of Research and Development, Washington, DC 20593	10. Work Unit No. (TRAIS): 2110
	11. Contract or Grant No.
12. Sponsoring Agency Name and Address: Department of Transportation, U.S. Coast Guard, Office of Research and Development, Washington, DC 20593	13. Type of Report and Period Covered: FINAL REPORT, May 1980 to May 1982
	14. Sponsoring Agency Code: G-DST-1

15. Supplementary Notes

16. Abstract

The Coast Guard operated an experimental "Loran-C mini-chain" in the St. Marys River, Michigan from the beginning of 1976 to the end of 1980. The impetus for the experiment was a Congressionally directed Winter Navigation Program on the Great Lakes and the St. Lawrence Seaway. Certain key stretches of these waterways, such as the St. Marys River, have particularly stringent navigation requirements. The mini-chain experiment was an investigation to see if Loran-C could satisfy those requirements. At the same time, the Coast Guard had a mandate to investigate the suitability of Loran-C for use in restricted waterways (harbor and harbor entrance (HHE) areas) throughout the United States. The St. Marys River became a test bed for the entire HHE Loran-C R&D program. Once the Great Lakes Loran-C chain became operational, the mini-chain was no longer required in the St. Marys River.

At the conclusion of the mini-chain experiment, the Coast Guard had the opportunity to explore the final untested concept of the HHE program: the so-called Supplemental LOP. This report documents the results of these tests and shows a Supplemental LOP is a viable concept but not necessary in the St. Marys River. With the existing chain being controlled from a site in the St. Marys River, 25 meter, 99.9% probability performance is possible. The report shows how this appears to be the "best achievable" Loran-C performance due to a problem known as phase modulation. It suggests that ongoing experiments outside the St. Marys River concentrate on determining if the effects of this problem can be reduced.

17. Key Words	18. Distribution Statement
Loran-C, Differential Loran-C, Supplemental LOP, Harbor Monitor, Harbor-Harbor Entrance, Error Ellipse Temporal Variations, Double Range Difference, Phase Modulation	Document is available to the U.S. Public through the National Technical Information Service, Springfield, Va 22161

19. Security Classif. (of this report)	20. Security Classif. (of this page)	21. No. of Pages	22. Price
Unclassified	Unclassified		

Form DOT F 1700.7 (8-72) Reproduction of completed page authorized

METRIC CONVERSION FACTORS

Approximate Conversions to Metric Measures

Symbol	When You Know	Multiply by	To Find	Symbol
	LENGTH			
in	inches	*2.5	centimeters	cm
ft	feet	30	centimeters	cm
yd	yards	0.9	meters	m
mi	miles	1.6	kilometers	km
	AREA			
in^2	square inches	6.5	square centimeters	cm^2
ft^2	square feet	0.09	square meters	m^2
yd^2	square yards	0.8	square meters	m^2
mi^2	square miles	2.6	square kilometers	km^2
	acres	0.4	hectares	ha
	MASS (weight)			
oz	ounces	28	grams	g
lb	pounds	0.45	kilograms	kg
	short tons (2000 lb)	0.9	tonnes	t
	VOLUME			
tsp	teaspoons	5	milliliters	ml
Tbsp	tablespoons	15	milliliters	ml
fl oz	fluid ounces	30	milliliters	ml
c	cups	0.24	liters	l
pt	pints	0.47	liters	l
qt	quarts	0.95	liters	l
gal	gallons	3.8	liters	l
ft^3	cubic feet	0.03	cubic meters	m^3
yd^3	cubic yards	0.76	cubic meters	m^3
	TEMPERATURE (exact)			
°F	Fahrenheit temperature	5/9 (after subtracting 32)	Celsius temperature	°C

*1 in = 2.54 (exactly). For other exact conversions and more detailed tables, see NBS Misc. Publ. 286, Units of Weights and Measures, Price $2.25, SD Catalog No. C13.10:286.

Approximate Conversions from Metric Measures

Symbol	When You Know	Multiply by	To Find	Symbol
	LENGTH			
mm	millimeters	0.04	inches	in
cm	centimeters	0.4	inches	in
m	meters	3.3	feet	ft
m	meters	1.1	yards	yd
km	kilometers	0.6	miles	mi
	AREA			
cm^2	square centimeters	0.16	square inches	in^2
m^2	square meters	1.2	square yards	yd^2
km^2	square kilometers	0.4	square miles	mi^2
ha	hectares (10,000 m^2)	2.5	acres	
	MASS (weight)			
g	grams	0.035	ounces	oz
kg	kilograms	2.2	pounds	lb
t	tonnes (1000 kg)	1.1	short tons	
	VOLUME			
ml	milliliters	0.03	fluid ounces	fl oz
l	liters	2.1	pints	pt
l	liters	1.06	quarts	qt
l	liters	0.26	gallons	gal
m^3	cubic meters	35	cubic feet	ft^3
m^3	cubic meters	1.3	cubic yards	yd^3
	TEMPERATURE (exact)			
°C	Celsius temperature	9/5 (then add 32)	Fahrenheit temperature	°F

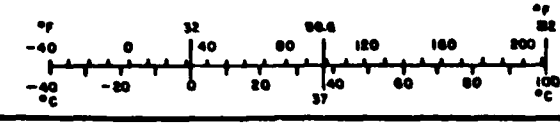

TABLE OF CONTENTS

TABLE OF CONTENTS (CONTINUED)

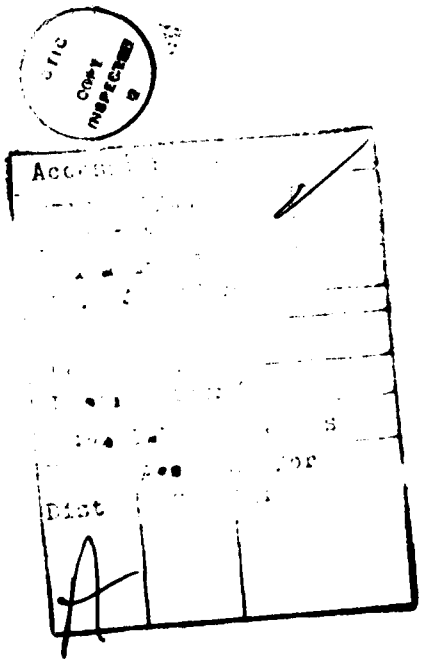

LIST OF ILLUSTRATIONS

LIST OF ILLUSTRATIONS (CONTINUED)

LIST OF ILLUSTRATIONS (CONTINUED)

LIST OF ILLUSTRATIONS (CONTINUED)

LIST OF TABLES

1. INTRODUCTION

1.1 Coastal Confluence Zone and Harbor/Harbor Entrance Loran-C

In 1974, after several years of deliberation, the U.S. Department of Transportation (DOT) announced that Loran-C was to be the federally sponsored radionavigation system for U.S. Coastal Confluence Zone (CCZ) and Harbor/Harbor Entrance (HHE) applications. This required an expansion of the existing Loran-C system which had been developed over a 15 year period for the U.S. Department of Defense.

One of the first orders of business after the decision was made involved the design of the expanded system. Logically, one would argue that the goal of the design process would be to insure the requirements are met. Interestingly, the requirements were not completely known and therein lies a long tale. Although an in-depth discussion of the matter is not warranted here, an overview of how and why the implementation decision could be made without knowing the exact requirements should be presented. This provides important background for understanding the implications of the results of this report.

As stated in reference 1, the applicable planning document at the time of the "CCZ/HHE implementation" decision, "The coastal confluence includes those waters contiguous to major land masses or island groups where ships tend to converge toward harbors and where significant traffic exists in patterns essentially parallel to the coastlines." Much is said as a lead-in to the statement of system accuracy requirements in the CCZ, but we can summarize by noting that since the CCZ does not involve "truly restricted" waterways, the requirements can be stated in universal terms. Reference 1 defines the CCZ system requirement as that which "would be satisfied with a radio-navigation system having the capability of fixing position to a repeatable accuracy of 1/4 NM, to 50 NM off the coast with reduced accuracies available at greater distances."

It was known in 1974 that a Loran-C system could be implemented to satisfy this requirement. It was also known, however, that several other systems could also meet the requirement. Indeed, the U.S. government was operating several such systems at the time. These systems had evolved over the years, in most cases, as a result of Department of Defense requirements of the time. This proliferation of government operated systems, with what reference 1 called a resulting "dissipation of funds," was one of the first problems encountered by the new Department when DOT was created in 1967. Resolution of the "dissipation" problem, for the CCZ arena, was accomplished by the 1974 announcement.

The HHE area was defined by reference 1 to include "those waters inside the mouths of bays and rivers along which terminal facilities are located." The requirements were addressed along the following lines:

> Quantitative statements of the needs for radionavigation services in this environment can only be made in general terms and must reflect the uniqueness of the environment

in each area. The question of coverage; i.e., whether the technique will be provided at all, is an administrative question, dependent for decision upon the degree of benefit accruable in any particular locality, versus the cost of acquiring it.

As can be seen, no universal statement, as was possible for the CCZ application, is possible for the HHE system. To complete the description of events leading up to the implementation decision, it should be noted that by the early 1970's there was also a proliferation of proposed systems which, on paper anyway, were being offered as solutions to the "HHE problem," whatever that might prove to be. Again on paper, however, it was possible to show that a Loran-C system could be designed to be similarly effective. This versatile characteristic of the Loran-C system, of course, was the key to its selection. It could meet the identifiable CCZ requirement and thus provide the tool for halting the "dissipation of funds" in that arena. At the same time it could be made available for HHE applications until such time as it could be established that an alternative system could satisfy a need with the required "degree of benefit" where Loran-C could not.

This background discussion explains how the "HHE Loran-C" decision could be announced without a definitive statement of the requirements. To see how the implementation could proceed, we must introduce some general navigation system design considerations.

1.2 Loran-C System Implementation

All navigation systems are based on the measurement of some physical quantity (e.g., differences in the times of arrival of electronic signal for loran). The measurements can only be made to a certain finite accuracy resulting in measurement errors which, ultimately, result in uncertainty in the derived positions. For most systems (certainly loran), the expected accuracy of the measurement varies from point to point throughout the navigation system service area. Also for most systems (again, certainly for loran), the effects of the geometry which transform the measurement error to position error vary throughout the service area.

The combination of these two considerations leads to the fact (often overlooked in planning documents) that the accuracy provided by an existing or proposed Loran-C system will vary significantly throughout the service area. Thus, if the U.S. Loran-C system were designed so that (95%) position errors were not to exceed 1/4 NM anywhere in the desired coverage area, it follows directly that considerably better accuracies can be expected in many areas. (20-meter/95% accuracies are currently observed in many areas.)

Ideally, the system design would attempt to insure that those "by-product" high accuracy regions were located exactly where the high payoff HHE applications were located. This ideal could not be achieved for several reasons. First, of course, HHE accuracy requirements were not known. Even if one were to attempt an educated guess, however, it would soon become apparent that the number of stations required to satisfy "potential needs" in <u>all</u> HHE areas greatly exceeds that required for the simple CCZ implementation. Lacking a quantifiable statement of the "degree

of benefit accruable" necessary to answer the "administrative question," such guesses could not be transformed into budgetary action.

This uncertainty, however, is a double-edged sword. On one side, the benefits to justify a more extensive network could not be quantified. On the other side there was the risk that a "bare-bones CCZ system" implementation would require prohibitively expensive upgrades if future events showed extensive HHE applications were warranted. Under such conditions, other systems which could not be competitive to a properly designed HHE Loran-C network might prove competitive with a "twice designed" Loran-C system. It must be recalled that, as the clock ticked and these risks were being considered, the economies to be accrued by stopping the "dissipation of funds" by multiple CCZ systems were being postponed.

The versatility of the Loran-C system was again brought to bear in solving this apparent dilemma - through the concept of so-called "chain enhancement techniques." The techniques consisted of:

- Differential Loran-C
- Supplemental LOP(s)
- Mini-Chain(s)

With the availability of these techniques, the CCZ implementation could proceed and the HHE question could be resolved along the following lines:

- HHE requirements, whatever they may prove to be, will be satisfied in most areas by the system designed to satisfy the CCZ requirements. This is a consequence of either the fact that requirements in a particular area are mild or that the "by-product" areas featuring truly precise service can be strategically located.

- In most of the areas in which CCZ Loran-C may not provide adequate "HHE-level" service, the problem will be due to signal instabilities rather than the effects of adverse geometry. In these areas, Differential Loran-C can provide the required stability. In concept, Differential Loran-C is implemented by the installation of a local monitor, or a small network of local monitors, along with a radio communications link to the users in the HHE area of concern. Periodic corrections can be broadcast to the user and, when applied to the user's measurements, reduce the instabilities to an acceptable level.

- In the areas in which the problems are due to poor geometry rather than signal instabilities, Differential Loran-C is not the answer. In these cases, conditions can be improved by the addition of a single station to an exiting Loran-C chain. Ideally, this so-called Supplemental LOP will improve the geometry to the desired extent.

- Because the Loran-C signals are transmitted in groups of pulses that are repeated every "group repetition interval," there is a limit to the number of stations that can be assigned to a chain - pulse groups from different stations must not overlap in time. Thus, the Supplemental LOP technique can only be used for a small number of HHE areas. Another alternative, when existing geometry must be improved, is the installation of

an entire chain of low-powered stations. With this so-called "Mini-Chain" approach, geometry can be optimized for the area of concern and the resulting system proves less costly than the CCZ system which features high powered transmissions.

- The final approach is the use of some combination of any of the above techniques.

With this implementation strategy, Congress approved funding and the U.S. Coast Guard was directed to begin the CCZ implementation and start an R&D program to investigate HHE implementation techniques.

1.3 The U.S. Coast Guard HHE Loran-C R&D Program

With allowances for the normal budgetary cycle, the U.S. Coast Guard HHE Loran-C R&D program began in the late 1970's. The program began by considering many program elements but evolved to concentrate on the four areas described in reference 2. The four areas are:

- HHE Guidance Equipment. Assuming an area features adequate Loran-C geometry and signal stability, and, assuming the Loran-C coordinates of critical portions of an HHE area are known, the question centers on determining the best method to present position information to the navigator. "Old time" loran receivers, which provided only time difference numbers, proved entirely adequate in applications wherein there was plenty of time to manually plot the loran number on charts or adequate room to "follow an LOP." They are still adequate in many areas - but not in restricted waterways. The ways to use "computer navigators" and electronic graphical devices to present loran-derived information had to be explored.

- HHE Trackline Surveying. This element examined one of the three assumptions stated above: how to determine the Loran-C coordinates of critical portions of an HHE area. Once earlier studies established there was no viable means of predicting Loran-C coordinates to an accuracy approaching expected requirements, it had to be determined if an economically feasible method to measure the coordinates could be developed.

- Augmentation Techniques. This element was established to explore the feasibility of the techniques: Differential Loran-C, Supplemental LOP, Mini-Chain. Questions such as "how does one design a Differential Loran-C network? What is the residual variation, i.e., that which defines the best achievable stability? Do short baseline warrant any special design consideration?" had to be answered.

- Stability Studies. This element is designed to determine how stable the CCZ system signals are in areas of potential HHE application. Where the need seems indicated, it should consider the stability which could be achieved by the application of any of the augmentation techniques.

Notice that the program does not attempt to determine the benefits of possible HHE implementations. Rather, it seeks to provide "Loran-C peculiar" knowledge to support implementation decisions which, again, are

"administrative questions." We should emphasize there are at least two other "missing links" in the whole implementation question. Neither are "Loran-C per se" issues and are not specifically examined under the heading "Loran-C R&D." They do apply to the "HHE question," however and should be mentioned. Loran-C R&D studies have made major contributions to current understanding of these "other" issues.

The first "missing link" is what we will call "guidance error." This is analogous to what would be called "flight technical error" in an aviation application: the inability of the mariner to perfectly follow the guidance equipment indicators. By examining channel characteristics, determing expected Loran-C instabilities, and accounting for vessel width, we can be fairly explicit in specifying how much room is "left over" for guidance error. Obviously, if the remainder is a negative number, all would agree this is unsatisfactory. If the remainder is 50 meters or more, all would probably agree this is satisfactory. Until we know what to say about 5, 10, 20, 30 meters, however, we cannot say the final word. This missing link will be addressed in several subsequent sections of this report.

The other missing link is vital in determining the "degree of benefit accruable" which reference 1 indicates is necessary for an implementation decision. It relates to the fact that knowledge of one's position is not the total answer in guiding large vessels through restricted waterways. Information pertaining to other traffic and channel conditions, e.g., ice, current, etc, is equally important. The implication is that no positioning system, e.g., Loran-C, NAVSTAR-GPS, etc, no matter how accurate, can be the total solution. This concept is reflected in the conclusions we have drawn in past Loran-C studies and will present in this and future reports.

1.4 The St. Marys River Loran-C Mini-Chain Experiment

As discussed in reference 3, an experiment was being conducted in the early 1970's to extend the navigation system in the Great Lakes and St. Lawrence Seaway. Of considerable concern was the ability of large vessels to transit several key restricted waterways under all conditions of channel ice and restricted visibility. In 1972 the Maritime Administration (MARAD) began experimentation with an electronic navigation system which used pulsed laser and radar techniques. This was one of the "proliferating solutions looking for a problem" of the time. The St. Marys River in Michigan's Upper Peninsula, the narrow passage connecting Lake Superior with Lake Huron, was selected as the test area. The design goal for the system was 10 feet. Since the minimum channel width is 300 feet and the largest vessels are 105 feet in beam, this design goal leaves almost 90 feet, on either side, for guidance error.

Reference 3 indicates the system being examined by MARAD, called "precise radionavigation system" (PRANS), "showed promise." This is a general characteristic of all of the precision systems that were proliferating at the time. It is interesting to note that the same PRANS system has been examined several times since in other areas and, in general, "shown promise." With the 1974 Loran-C decision, further exploration of PRANS - in the St. Marys River - was halted, and Loran-C came under consideration.

It was known from the start that Loran-C could not be made much better than about a "100 foot system." Discussion with local mariners were held and the indication was that a reliable 100 foot system would be enough. Herein was one of the first important contributions Loran-C made to the "requirements issue" which the previous section identified as the first "missing link." If Loran-C could allow 100 foot errors - on either side of the channel, that leaves only 100 feet in the narrowest channels - obviously not enough for vessels which can be as wide as 105 feet! As reference 3 explains, however, "a system was not really needed in several of the river's narrow sections, such as the West Neebish Island 'rock cut,' where the sides of the channel could literally be seen."

The first expansion under the CCZ implementation was not scheduled for completion until 1977 and coverage in the Great Lakes was not expected until 1980. Combined with the fact that the navigation season extension experiment was ongoing, this made it possible to justify the installation of an experimental "mini-chain," the equipment for which was available "off-the-shelf." With a considerable amount of inter-agency and inter-government cooperation, a Loran-C mini-chain was designed, installed and brought on-air in January 1976. The exclusive nature of the chain, the "tight" requirements of the St. Marys River, and the early availability made it ideally suited as the HHE Loran-C R&D test bed. The chain was operated until the end of 1980 and led to the development of Loran-C grid prediction methods, practical guidance equipment and trackline survey techniques, and a Loran-C stability study methodology. The St. Marys River region and the stations of the mini-chain are shown in figure 1-1.

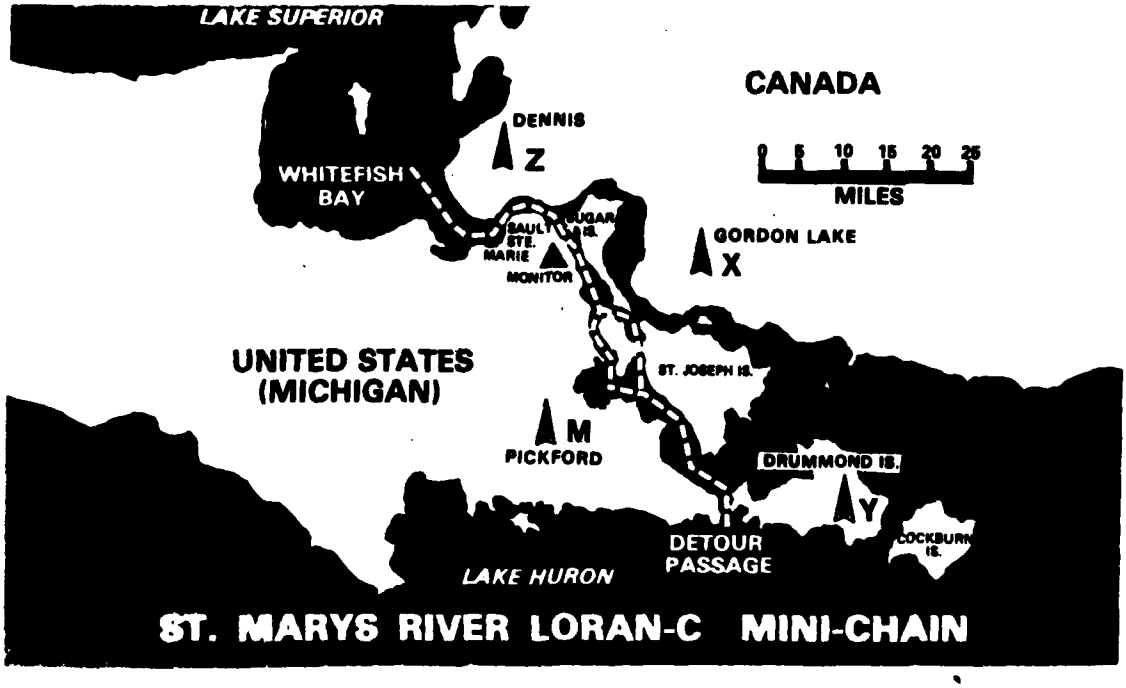

Figure 1-1 St. Marys River Loran-C Mini-Chain

1.5 Mini-Chain Experiment Results

The key findings of the Mini-Chain experiment, as documented in reference 3, are as follows:

- Grid Prediction Methods can be developed to yield practical results for CCZ applications if they include adequate Loran-C data samples. When applied to restricted waterways however, data taking requirements are excessive. (See references 4 and 5).

- Practical techniques can be developed to measure the Loran-C coordinates of critical portions of tracklines the vessels must follow through the restricted waterways. These techniques are preferable to grid prediction techniques and, in practice, have proven less time consuming. (See references 6 and 7).

- Practical guidance equipment can be developed for use in a restricted waterway. Assuming adequate signal stability, the only additional requirement for the successful implementation of such equipment is the waypoint data available from a properly conducted trackline survey. (See reference 8).

- There is no difference between the fundamental limitations of a mini-chain and a "normal-sized" chain.

- The temporal variations noted in the St. Marys River Loran-C readings (see references 9 and 10) exceeded initial expectations. Considerable account, however, must be taken of the severe conditions in the St. Marys River region (reference 3). With expected weather variations, however, the Loran-C readings should be expected to vary significantly - even for a mini-chain (see references 11 and 12).

- Knowledge of "own ship's position" is not the total answer - even in a carefully controlled channel with one-way traffic. In poor visibility with "icy river" conditions, knowledge of ice conditions at an upcoming turn (thus, how a vessel with considerable inertia must be prepared to enter the turn) is every bit as important as Loran-C derived information of vessel location.

- Mariners who used the Loran-C guidance equipment for 2 years found it entirely adequate, when used in conjunction with the ship's radar, for knowing where they were. They indicated, however, that loran/radar information, i.e., knowledge of where they and other vessels were, was not the total answer.

- The final conclusion was that the mini-chain yielded errors less than 29 meters at the 99 percentile in the narrow reaches. With the application of daily corrections, this error could be reduced to 20 meters. With real-time differential corrections, this could be reduced to 16 meters in the narrow reaches. Although this is sufficient for most channels, it must be concluded Loran-C cannot be used as a stand-alone system for "blind" transit of every channel in the St. Marys River.

1.6 The Great Lakes Chain Experiment

In 1979, the U.S. Coast Guard sought funding to make the Mini-Chain permanently operational. This would have entailed the approval of initial funds to upgrade the chain reliability and the approval of recurring operational funds. Initially, about forty percent of the upgrade funds were approved. This was enough to begin the procurement of much of the equipment required for the upgrade. In early 1980, however, the request for follow-on funds was disapproved. Thus, the "administrative question" was not answered in favor of the mini-chain.

In March 1980, the Great Lakes Loran-C chain was declared operational. Faced with the prospect of having to close down the mini-chain at the end of 1980, the Coast Guard sought and received approval to keep one station of the chain operating for a short test period. With this Supplemental LOP, the final "chain enhancement" technique could be studied. As a prelude to the experiment, and as the first stage of the CCZ system stability studies - the final Loran-C R&D effort - data from the available Great Lakes chain signals were collected throughout the second half of 1980. When the mini-chain was secured at the end of the 1980 shipping season, the Gordon Lake, Ontario mini-station was added to the Great Lakes chain for a 6 month experimental period. After the Supplemental LOP was secured in July 1981, data collection in the St. Marys River continued for a year. Guidance equipment demonstrations, using the Great Lakes chain signals, continued throughout the 1981 and 1982 shipping seasons.

The results of the Great Lakes chain Supplemental LOP experiment and the continuing Great Lakes chain stability study in the St. Marys River region are presented in this report.

2. Great Lakes Chain Experiment Overview

2.1 Preliminary Great Lakes Chain Stability Study Equipment.

Applicable elements of the Great Lakes Loran-C Chain, identified as group repetition rate 8970, are shown in figure 2-1. The chain master station is at Dana, Indiana and the X and Y secondary stations are at Seneca, New York and Baudette, Minnesota, respectively. Both the 8970-X and 8970-Y baselines were originally controlled by use of observations made at the so-called A-1 monitor site at Muskegon, Michigan. In case of failures at the A-1 site, control is based on observations made at the A-2 site which, for those two baselines, was located at Plumbrook, Ohio. During the Supplemental LOP experiment, the station at Gordon Lake, Ontario transmitted signals as the 8970-Z baseline. A-1 and A-2 control for this new baseline was based on observations made at Riverside, Michigan - the same site that was used as the prime chain monitor for the mini-chain experiment. The 8970 chain has a fourth secondary station, located at Malone, Florida which, since the signals cannot be reliably tracked in the St. Marys River region, was not considered in this experiment.

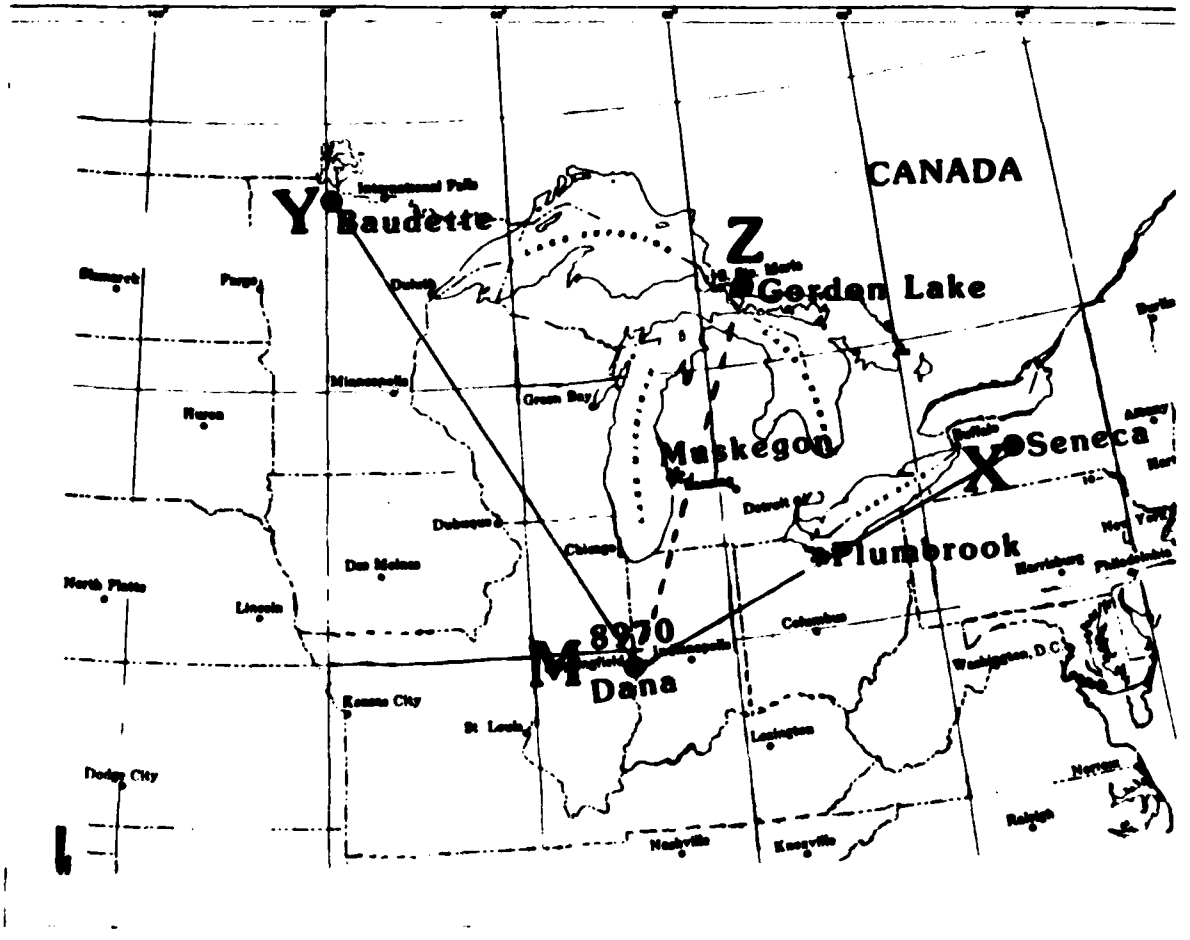

Figure 2-1 Great Lakes Loran-C Chain Northern Stations

Figure 2-2 shows the St. Marys River region in greater detail and indicates the data collection sites which were used for this study. The sites at Pt. Iroquois, Dunbar Forest and Detour Village are at the same locations as the data collection sites used for the mini-chain stability studies. The new site at Rocky Point was installed, as will be discussed, so that the narrow portions of the river can be examined in greater detail than was possible in the mini-chain study.

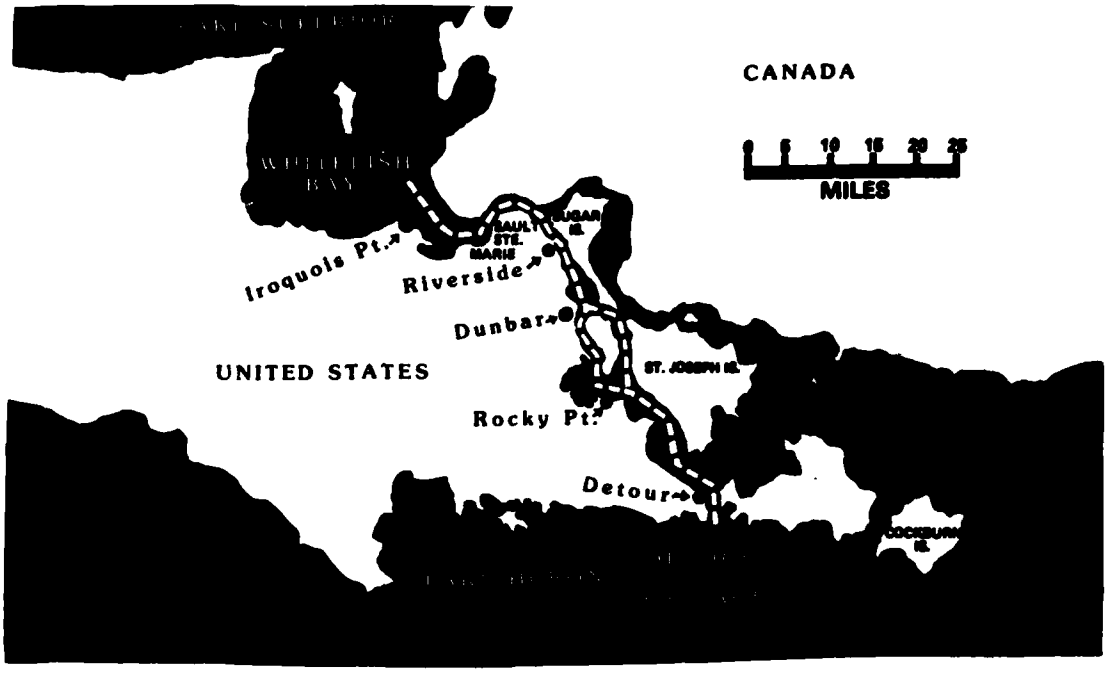

Figure 2-2 St. Marys River Stability Study Monitor Sites

As indicated at the end of Section 1, the stability study reported herein was the first step in the larger continental U.S.-wide stability study which was to be the first element of the HHE R&D effort to extend outside the St. Marys River area. As originally planned, these efforts were to feature upgraded data collection sets rather than the aging, hard to maintain sets used for the studies of reference 3. Because of the need to wrap up the mini-chain studies, however, this development became a lesser priority and the new sets were not ready when the Great Lakes chain became operational.

Although the mini-chain stability study ran through late May 1980, concurrent Great Lakes chain data was taken from mid-December 1979 through mid-April 1980. The data was presented in reference 3 which cautioned that the Great Lakes chain was not declared operational until March 1980. With the mini-chain stability study concluded, the Great Lakes chain study formally began on 20 May 1980.

Figure 2-3 shows the original data collection set, featuring the Internav 204 receiver, in block diagram form. Figure 2-4 shows the actual equipment as installed at the Dunbar Forest site. (An AN/BRN-5 receiver and peripherals are also shown. As discussed in Section 2.3, this equipment was not used for the Great Lakes chain study).

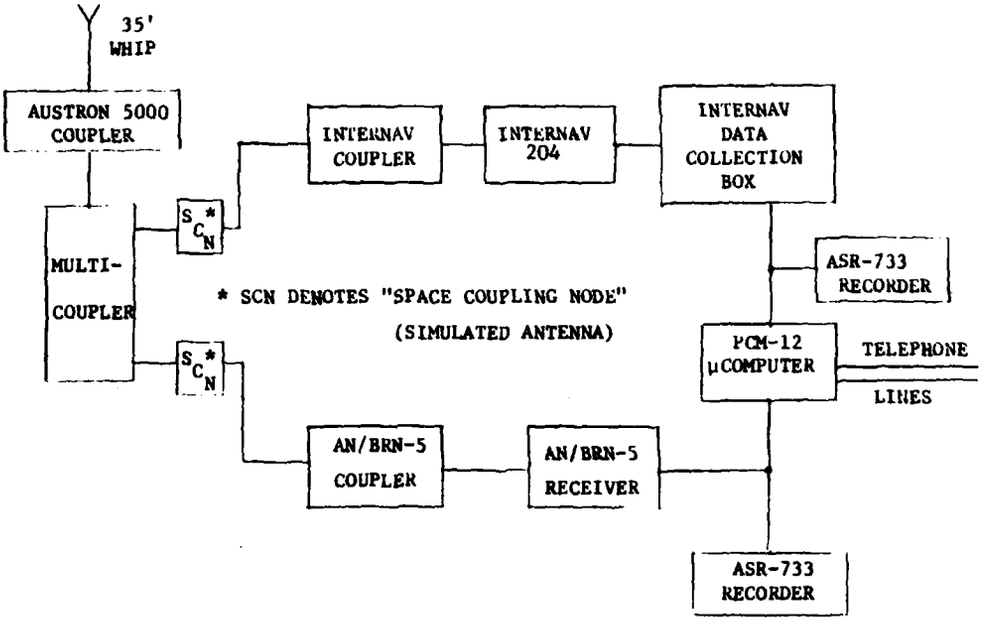

Figure 2-3 Original Data Collection Set Block Diagram

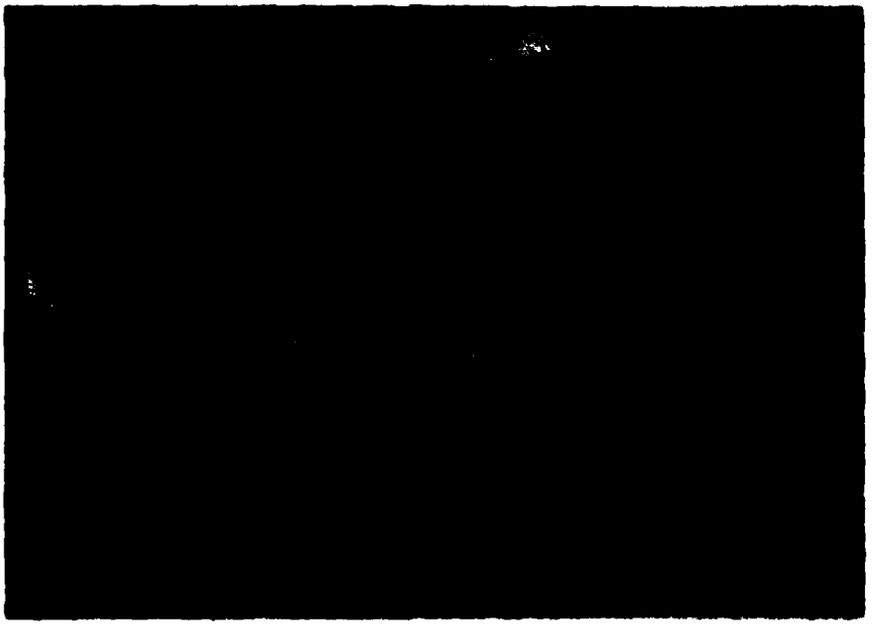

Figure 2-4 Original Data Collection Set at Dunbar Forest Site

The Internav 204 receiver tracks the signals and provides the time difference readings to the Internav data collection set. The data collection set has an internal clock which can be used to determine how often the set collects data from the receiver. For this experiment, as in the mini-chain experiment, data collection was initiated every 10 minutes. When data collection began, the set obtained data from the receiver and averaged the reading over a 90 second period. The resulting average, for all stations being tracked, was sent to the PCM-12 micro-computer for storage. Computer storage was adequate to hold readings for about 2 days. The computer was interfaced to a phone line so that readings could be retrieved by personnel stationed at Riverside without having to visit the site.

At Riverside, mini-chain personnel would call each data site at least once a day and obtain a printout on a local teleprinter of each 10 minute sample. Mini-chain personnel would scrutinize the data for signs of equipment problems and, if none were found, average six successive readings during a certain hour of the day to obtain a "system sample" hourly average. The system sample readings would be transmitted via teletype message to the U.S. Coast Guard R&D Center at Groton, Ct. where the data would be stored for analysis. (The adequacy of this "once per day" sampling for characterizing the system stability is discussed in references 1 and 10.) This procedure continued from May 1980 through July 1981 when the Internav 204-based data collection sets were removed and retired from service.

2.2 USCG Harbor Monitor Sets.

The HHE Loran-C Stability Studies are being conducted with the use of data sets which are presently located throughout the coastal areas of the continental U.S. Operational data sites as of the end of calendar year 1982 are at locations indicated in figure 2-5. As noted earlier, the stability studies comprise the final element of the HHE Loran-C R&D program to get started. Development of the equipment, the so-called Harbor Monitor Sets, was initiated in late 1979 and prototype units were not available until after the St. Marys River Great Lakes chain stability studies began.

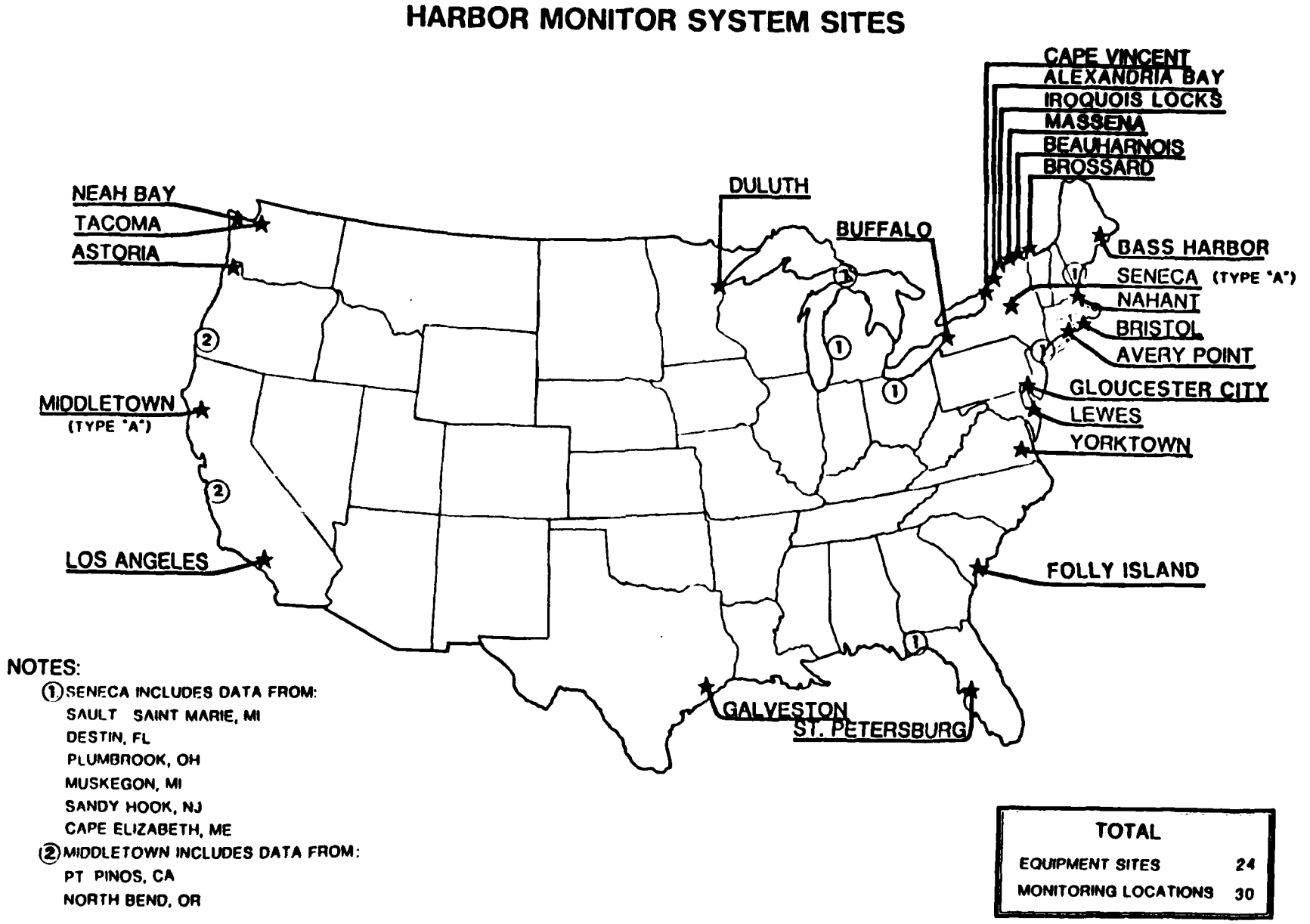

Figure 2-5 Location of Harbor Monitor Sites

The equipment set was developed by the Coast Guard Research and Development Center in Groton, Ct. A prototype installation was accomplished at Pt. Allerton, Massachusetts, convenient to the R&D Center, in September 1980. In February 1981, after several months of field tests/refinements, harbor monitor sets were installed at the same St. Marys River data collection sites that were being used for on-going studies. An additional harbor monitor set was installed at Rocky Point. The sets remained installed until the end of May 1982 when the Great Lakes chain experiment in the St. Marys River was concluded.

The harbor monitor set consists of a survey grade Loran-C receiver, the Internav 404, a small micro-computer, and miscellaneous support equipment allowing battery back-up power and remote (via telephone) access to the collected data. Like the equipment set described in paragraph 2.1 above, the harbor monitor set is used to collect data suitable for a "low density data analysis." A difference is that hourly samples are automatically processed by the equipment and samples are taken twice a day - at noon and midnight. A block diagram of the harbor monitor set is provided in figure 2-6.

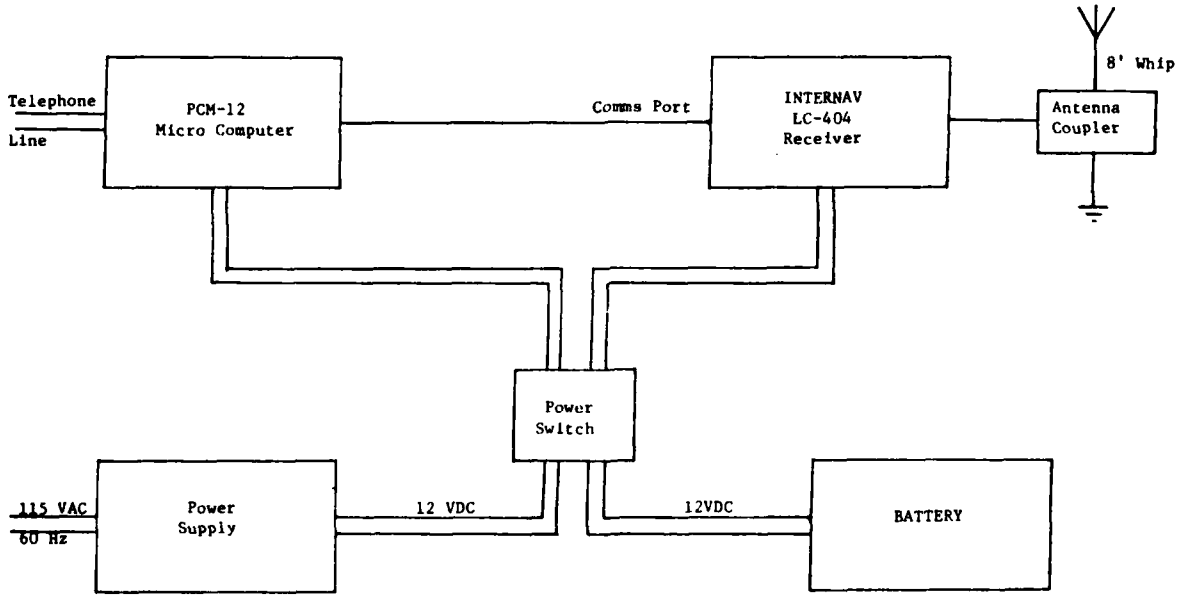

Figure 2-6 Harbor Monitor Set Block Diagram

Simulator tests have shown the Loran-C receiver has a "servo loop time constant" of about 6-8 seconds under conditions typically encountered at harbor monitor sites. Thus the computer obtains a sample of the receiver output every 40 seconds so that the samples can be treated as statistically independent. The micro-computer uses a real-time clock to begin the

sampling period at the prescribed time. At the end of the sampling period, the mean, standard deviation, and minimum and maximum values of each time difference are recorded. Depending upon the number of signals being observed, available memory will hold from 10 to 20 days of data. Phone line access to the micro-computer allows retrieval of the stored data. It also allows a remotely located operator to prompt the computer to exercise any receiver command which a local operator could enter via the front panel controls. Finally, the entire micro-computer program can be changed via the phone line. The data collected with the harbor monitor sets comprise the bulk of the data leading to the conclusions of this report.

The harbor monitor set at Dunbar is shown in figure 2-7.

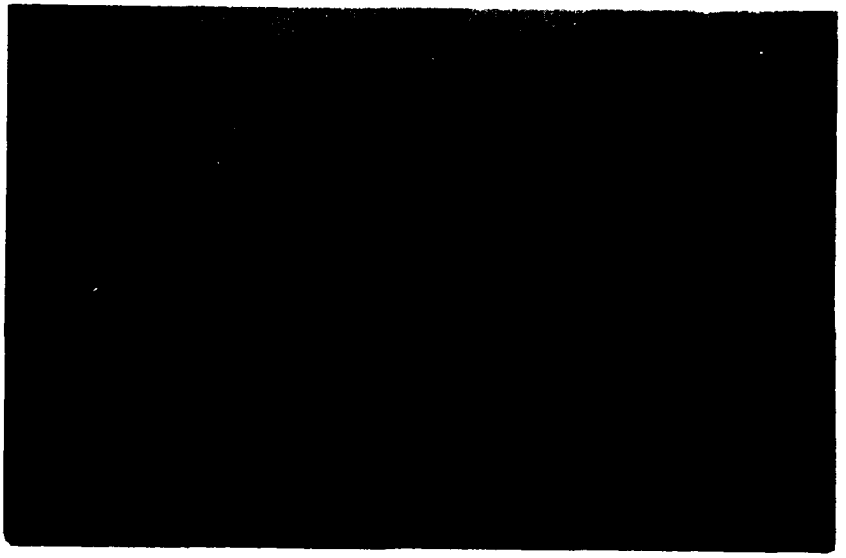

Figure 2-7 Harbor Monitor Set at Dunbar Forest

2.3 Early Problems in Experiment Execution

A number of problems were encountered in data collection in the first year of the experiment. We could ignore most of these problems if the report were to concentrate only on the results of the second year efforts. Since the Supplemental LOP experiment was conducted in the first year, however, a general description of the problems should be presented. It will help explain, for example, why subsequent analyses are direct in some cases but very involved in others.

The first source of problems was the necessity to operate with limited personnel resources. From the end of May 1980 to the end of 1980, the mini-chain was still being operated in support of on-going guidance equipment demonstrations. This was the first priority. The same personnel were tasked with support of the collection of Great Lakes chain data. Early deployment of the harbor monitor sets would have helped in this regard but, as indicated earlier, development was not completed until mid-February 1981.

The Loran-C receivers (Internav 204 and AN/BRN-5) and the data collection sets that were used throughout the mini-chain stability study required considerable maintenance and were on their last legs. Given a choice as to what area to emphasize with available support resources, the Internav 204 receiver was chosen. This is a general purpose, moderately priced receiver whereas the AN/BRN-5 is a DOD "super-receiver." Importantly, with a narrow band "RF front end," the Internav 204 is representative of typical receivers available to the public. The AN/BRN-5 features a front end which is as wide as any ever built for Loran-C and, as mentioned in reference 3, can "see things typical receivers do not see" and "not see things typical receivers will see." Thus, the AN/BRN-5's were not used to track Great Lakes chain signals. This greatly reduced support requirements.

The Internav 204 receiver, however, can only track two secondary stations. Until the Gordon Lake station was added to the Great Lakes chain, this posed no problems. There was a short period of time, however, before the harbor monitor sets (which can track four secondaries) were installed, in which signals from all three secondary stations of interest were on air. Thus, although all stations were tracked at one site or another during this period, data for all signals for all sites was not obtained.

Another problem was brought about by the Great Lakes chain signal variations in the St. Marys River area in the late Fall/early Winter months. These variations were much larger than typically encountered in the mini-chain signals. In the mini-chain experiment, for example, a sudden (from one day to the next) time difference variation of several hundred nanoseconds was a sure sign of equipment problems. For the Great Lakes chain signals, because of the remoteness of the St. Marys River to the chain monitor/control station (Muskegon), such variations were considered typical. Although this is at times true, equipment problems cannot be ruled out and separating the effects of propagation path changes from equipment problems becomes tricky. An illustration of this problem can be seen by examining the data from Riverside and Pt Iroquois presented in figure 2-8.

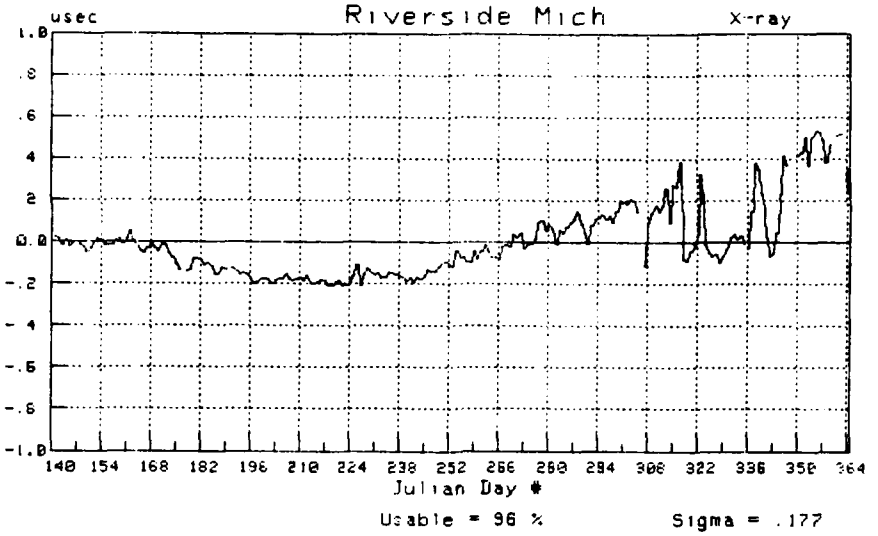

a.

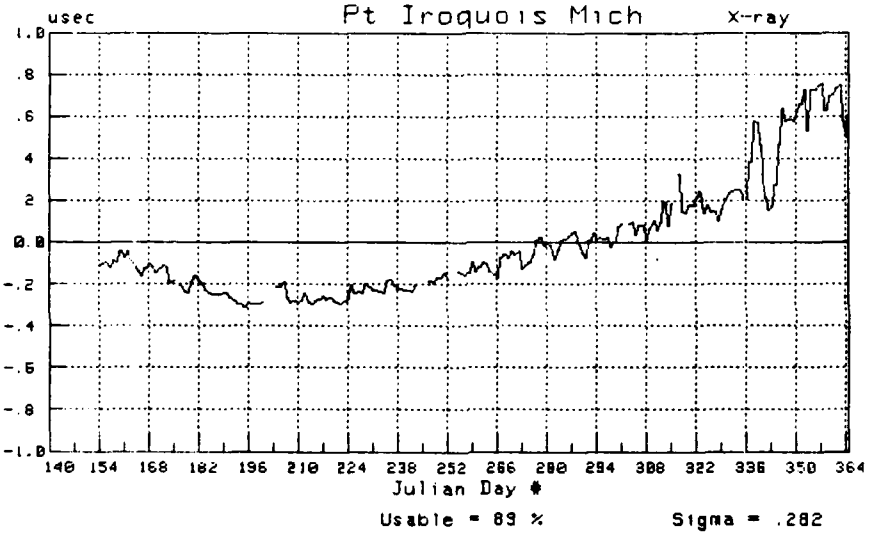

b.

Figure 2-8 Great Lakes Chain Xray TD Observations

The plots indicate that variations are mild in the summer but can become severe as winter sets in. This is entirely in line with what studies such as references 11 and 12 or any number of earlier, related reports say we should expect. If we subtract the data record of figure 2-8.a from that of figure 2-8.b, however, we obtain the data record shown in figure 2-9. Ideally, this should give us an indication of what type of variations can be expected at Pt. Iroquois if Great Lakes chain control were moved to Riverside or if Differential Loran-C corrections could be relayed from Riverside to Pt. Iroquois In figure 2-10 we accomplish the same "Differential Loran-C simulation" for the 8970-Y baseline.

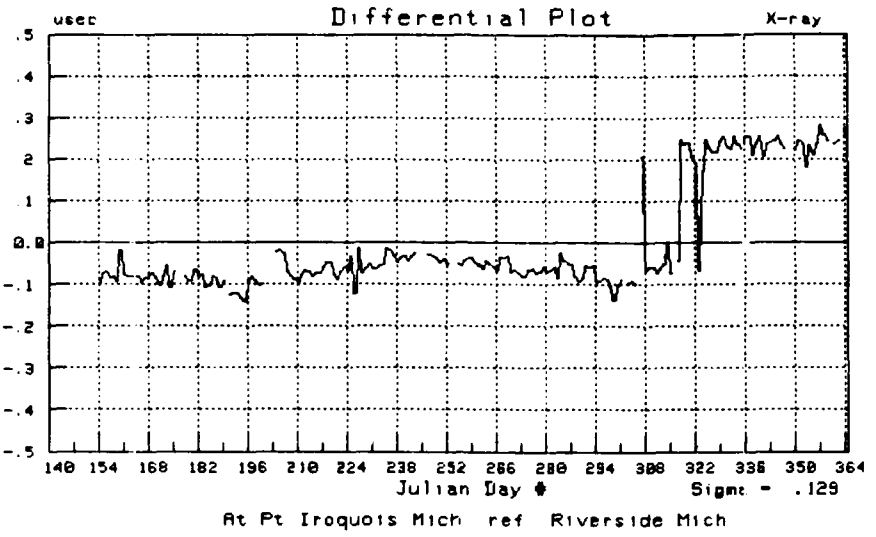

Figure 2-9 Simulated Differential Loran-C Performance at Pt. Iroquois 8970-X Baseline

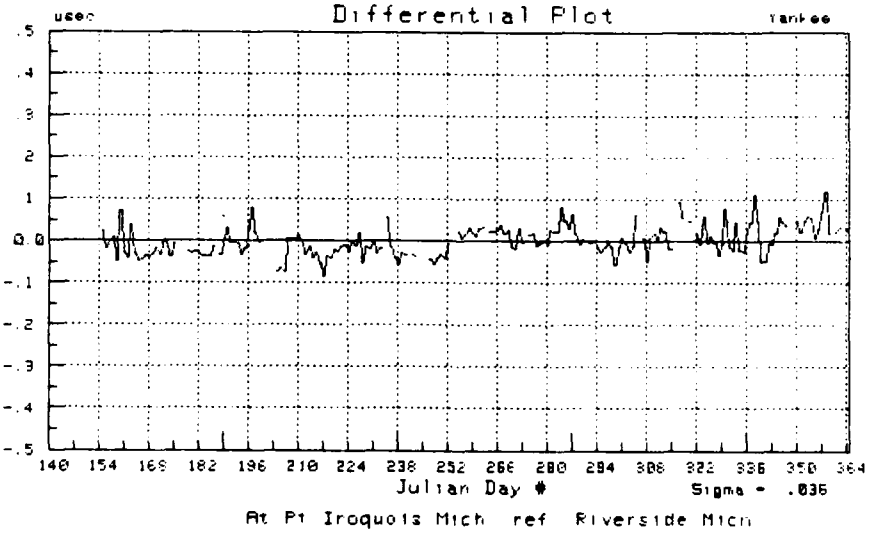

Figure 2-10 Simulated Differential Loran-C Performance at Pt. Iroquois 8970-Y Baseline

The plots of figure 2-8 represent the data that was reported to the R&D Center and forwarded to Coast Guard Headquarters in January 1981. Upon receipt of the data, the authors called mini-chain personnel to challenge the validity of the reported data. It was then discovered that data was being reported, at times, from different receivers at Riverside (without any annotations). There were three receivers in use at Riverside: an Austron 5000 which was used to control the mini-chain, an Internav 303 used as a backup to the Austron 5000 and another Internav 303 being used to record Great Lakes chain data. There were also two different receiving antennas. The block diagram of figure 2-11 illustrates the situation.

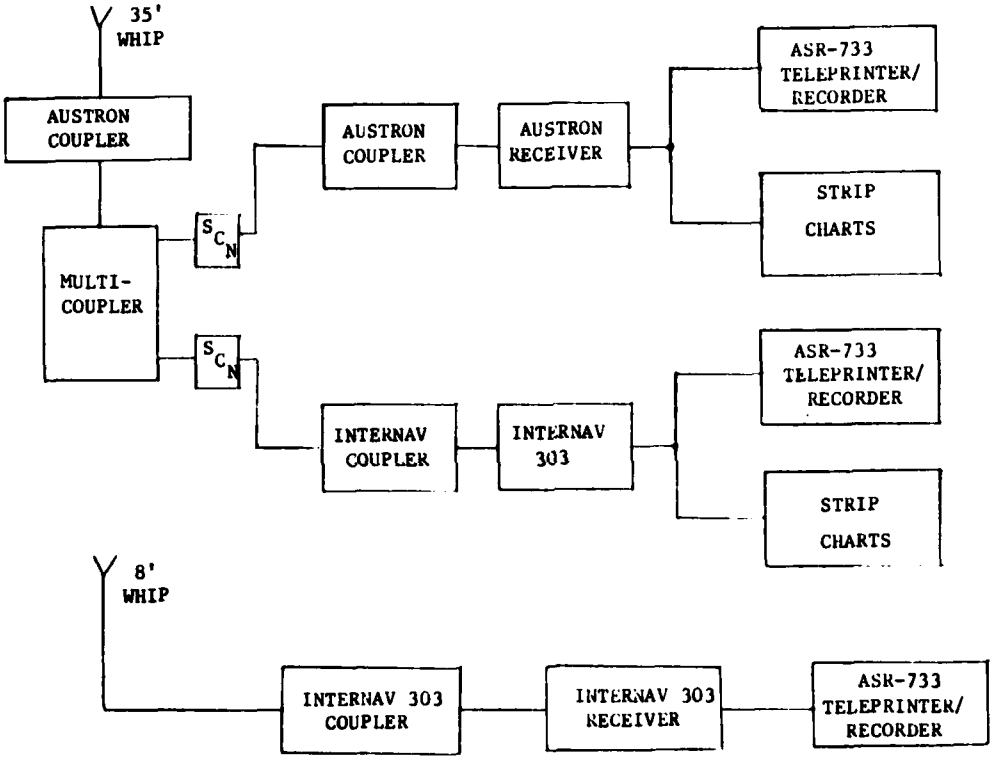

Figure 2-11 Riverside Receiving System Block Diagram

The Internav receiver which was using the same antenna as the Austron 5000 was normally locked to the mini-chain signals (as a backup chain control receiver in case of Austron 5000 failure). As it turns out, the Austron 5000 did not fail but the Internav 303 tracking the Great Lakes chain did. At the times of such failures the Internav 303 which used the Austron 5000 antenna was locked to the Great Lakes chain - without changing antennas - until repairs could be made. The "track record" of the "Great Lakes chain antenna" Internav 303 was subsequently shown to be as follows:

Up to 1 Nov.	- in operation
1-3 Nov.	- in maintenance
4-12 Nov.	- in operation
13-18 Nov.	- in maintenance
19 Nov.	- in operation
20 Nov. - 31 Dec.	- failed

To complete the story, we should examine figure 2-12 which shows the antenna plot plan at Riverside and the Great Lakes chain LOPs at Riverside.

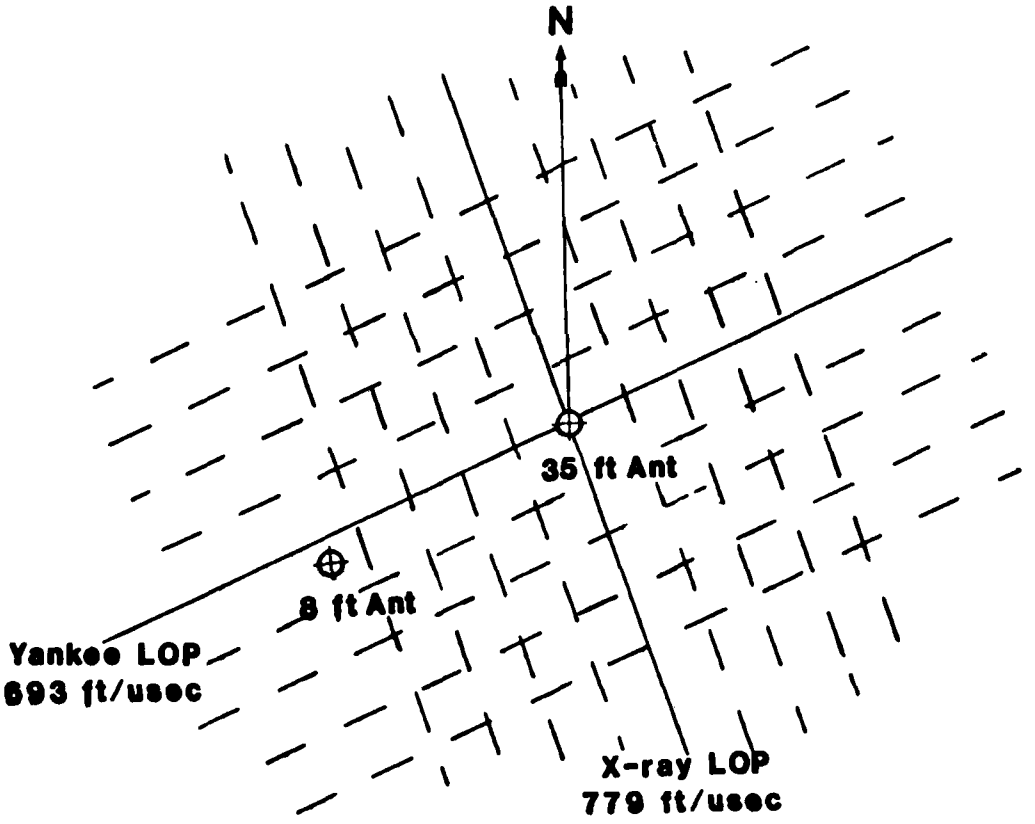

Figure 2-12 Riverside Antenna Plot Plan and LOPs

From the plot plan we can see why the antenna switch causes a greater shift on the Xray LOP than on the Yankee LOP. Calculations show the offsets, ideally, would be 256 nsec for X and 30 nsec for Y. The calculations, however, do not account for equipment differences in the total

receiver path. Fortunately, side-by-side data comparisons could be made from records obtained shortly after the "8' whip antenna Internav 303" was repaired. A correlation showed the actual offsets were 295 nsec for X and 65 nsec for Y. With these corrections applied to the Riverside data, the simulated Differential Loran-C performance at Pt. Iroquois appears as shown in figure 2-13.

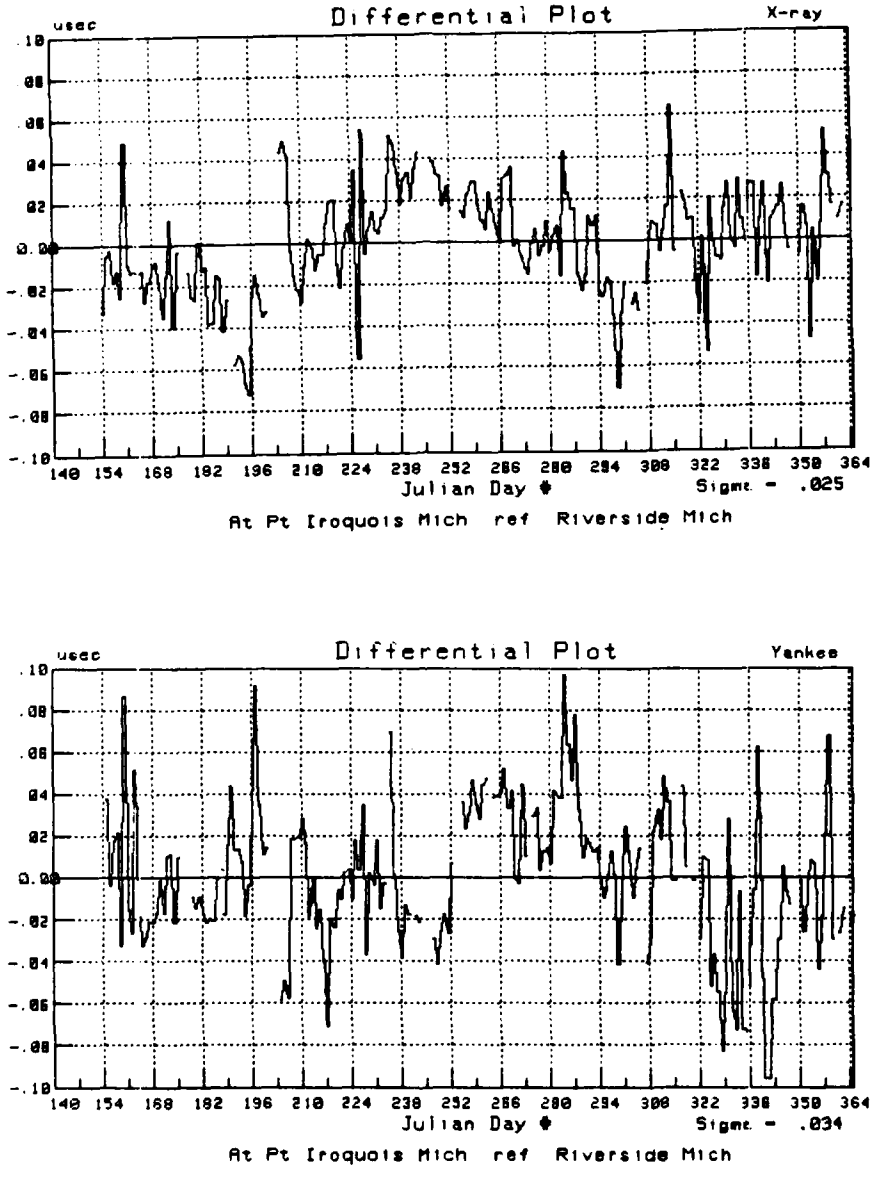

Figure 2-13 Corrected Differential Loran-C Plots for Pt. Iroquois

Among other things, the above discussion illustrates the difficulties associated with data collection/analysis in places where the TD variations are large. We should note that this is generally only a problem where "post mission analysis" to simulate Differential Loran-C (or hypothesize a propagation model as in reference 3 or similar reports) is to be attempted. Specifically, if 500-1000 nsec variations occur "naturally," and the goal of the study is to simply see how good/bad things are, the periodic appearance and disappearance of 200 nsec equipment related offsets will make little difference in the overall conclusion of the study. If, however, the goal of the study is to hypothesize explanations for, or corrections to the data, considerably more care must be taken. We note finally, that a similar correction should be made to the plot of figure 6-15 in reference 3 which, uncorrected, is reproduced as figure 2-14.

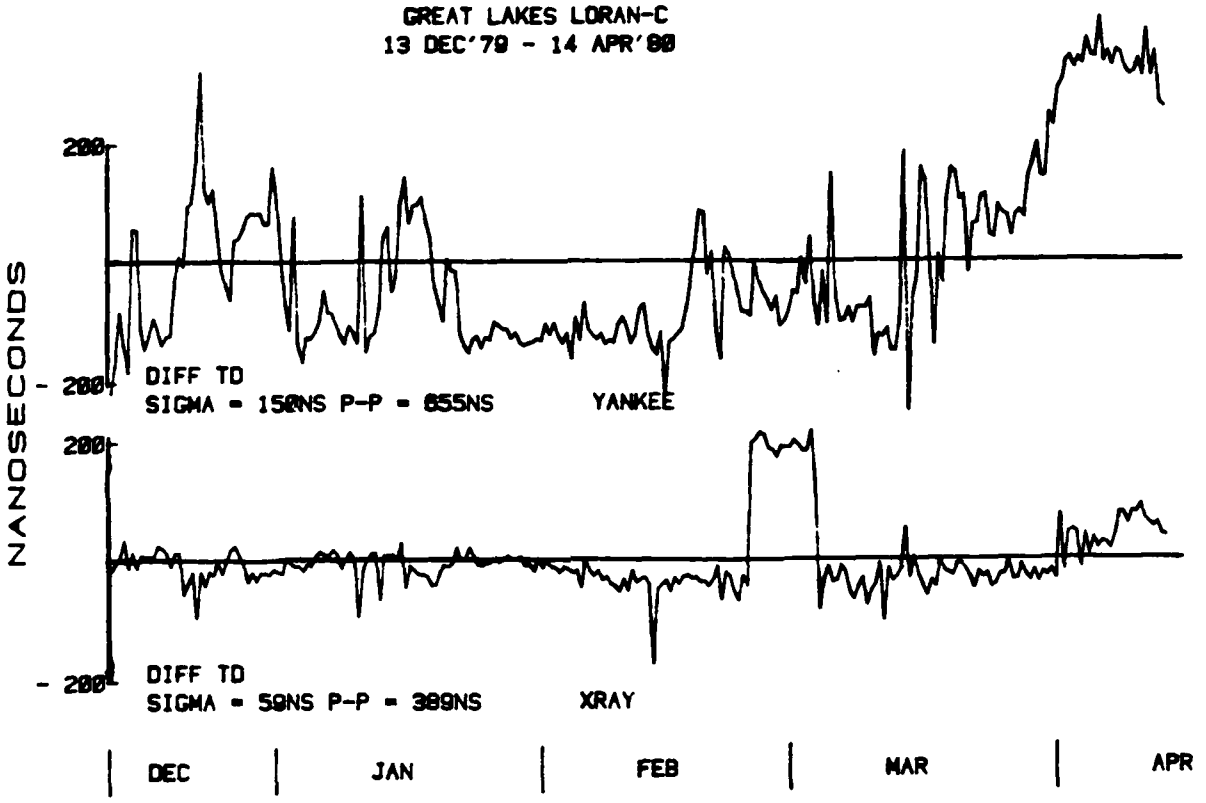

Figure 2-14 Reproduction of Figure 6-15 from Mini-Chain Final Report

In the "case of the moving antenna," we were fortunate in having teleprinter records which indicated which antenna was being used. In other cases we were not so lucky. The first one we should mention involved what mini-chain personnel called "receiver set-up." This apparently was a standard procedure developed during the mini-chain experiment and had become institutionalized by the time of the authors' first visit to the St. Marys River in January 1981. In examining local teleprinter records during that visit, the authors noted that the Internav 204 receiver at Dunbar was routinely "slipping on and off" the correct cycle. The Detour receiver was

operating steady - on the incorrect cycle. When this was pointed out to mini-chain personnel, they indicated a "set-up" was required and dispatched a junior technician to accomplish the task.

The "set-up" procedure proved to be a receiver "deriver" adjustment - the critical adjustment which allows the receiver to determine which cycle to lock on to. Typically, this is a "factory adjustment" which must be accomplished with extreme care. With the Internav 204, and access to a "cycle number" available in the teleprinter message, it is possible to properly make the adjustment in the field - again, if extreme care is taken. It is also possible, however, to make an error which will change the receiver track point and compromise the experiment.

To properly make the adjustment one must first recognize that the cycle numbers will, by nature, be very "noisy" - they reflect signal envelope slope measurements and their noisiness is a reflection of "signal-slope-to noise ratio" (much lower than standard SNR for Loran-C). The person making (or checking) the adjustment must also have a full understanding of the Loran-C parameter known as ECD (envelope-to-cycle-difference as defined in reference 13). Beyond the simplistic definition of reference 13, the person making (or checking) the adjustment must have a full understanding of how ECD is measured by the receiver being adjusted.

Finally, the person making the adjustment should have a full understanding of phase modulation/skywave interference - the reasons there is such a thing as the "desired cycle to track." (Phase modulation is defined in reference 13. The implications regarding cycle selection are treated in reference 14.) If one does not have the required understanding, one can incorrectly assume that if the receiver indicates readings which are approximately correct (say, within one to two hundred nanoseconds) after the adjustment, the adjustment has neccesarily been properly made.

Before proceeding with the discussion which seems to be leading towards doom, we should emphasize that Loran-C can be made to work. Factory adjustments of the deriver are not difficult to get right. Even field adjustments are not difficult - if the technician understands what is happening. Even uninitiated technicians have a high probability of success. A final complicating factor, however, is the peculiar receiving system arrangement used at the mini-chain stability study sites. The arrangement, previously shown as part of figure 2-3, is shown in figure 2-15 along with the "as designed" configuration.

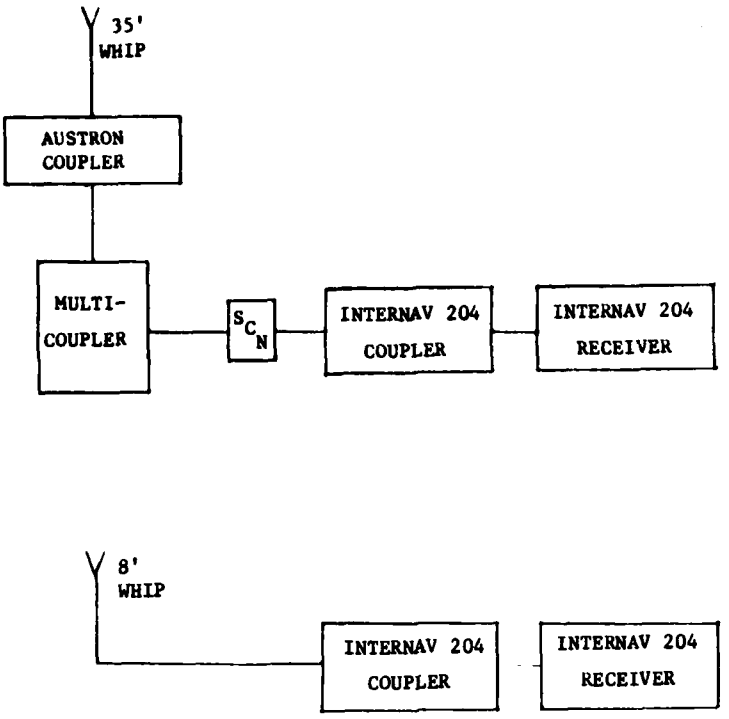

Figure 2-15 "As Designed" vs Installed Internav 204 Receiving System

As discussed earlier, the multicoupler was used since the Internav 204 could not track three secondary stations. As a general comment we can say that the additional band-limiting caused by the additional coupler simply makes it more difficult to distinguish between successive cycles of the received signals.

With all of these factors it is not surprising to find that "cycle slips" occured. The effects can be seen in the plots of figures 2-16 and 2-17 wherein we simulate Differential Loran-C at Dunbar and Detour (corrections obtained at Riverside).

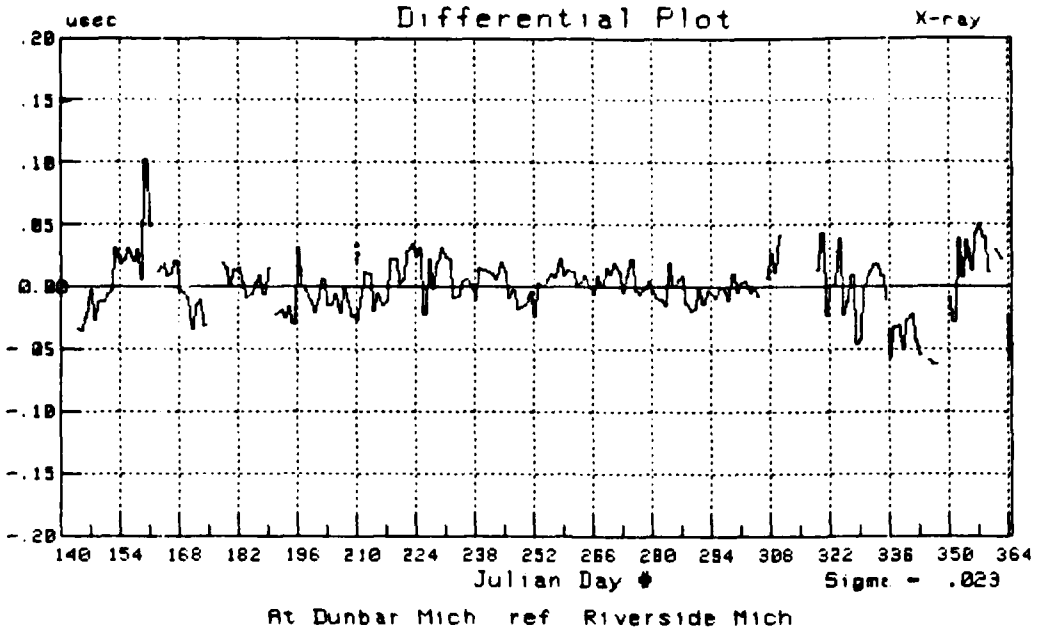

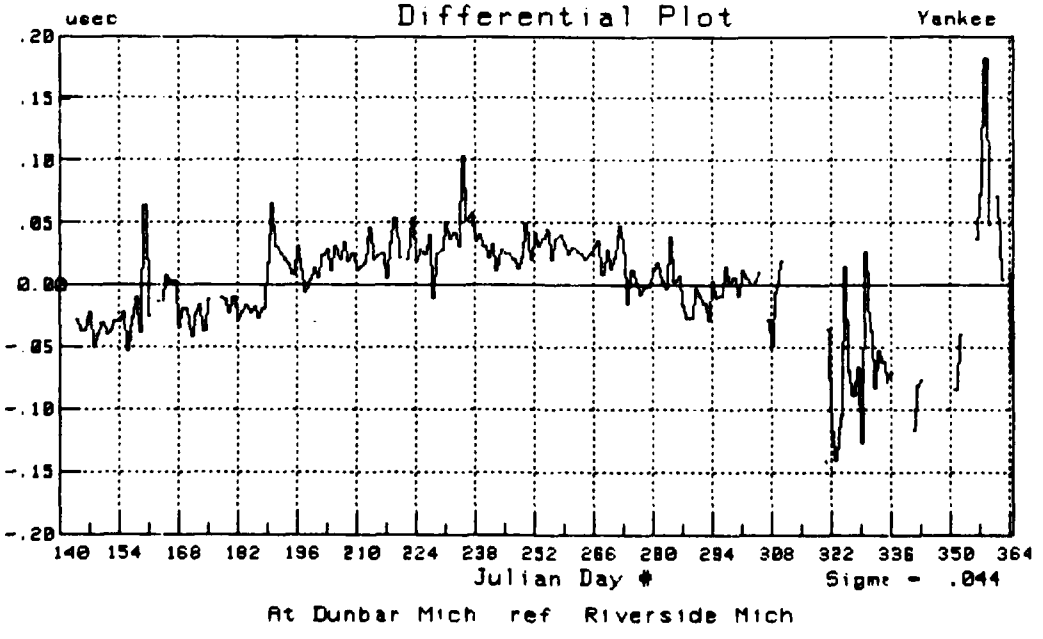

Figure 2-16 Simulated Differential Loran-C at Dunbar

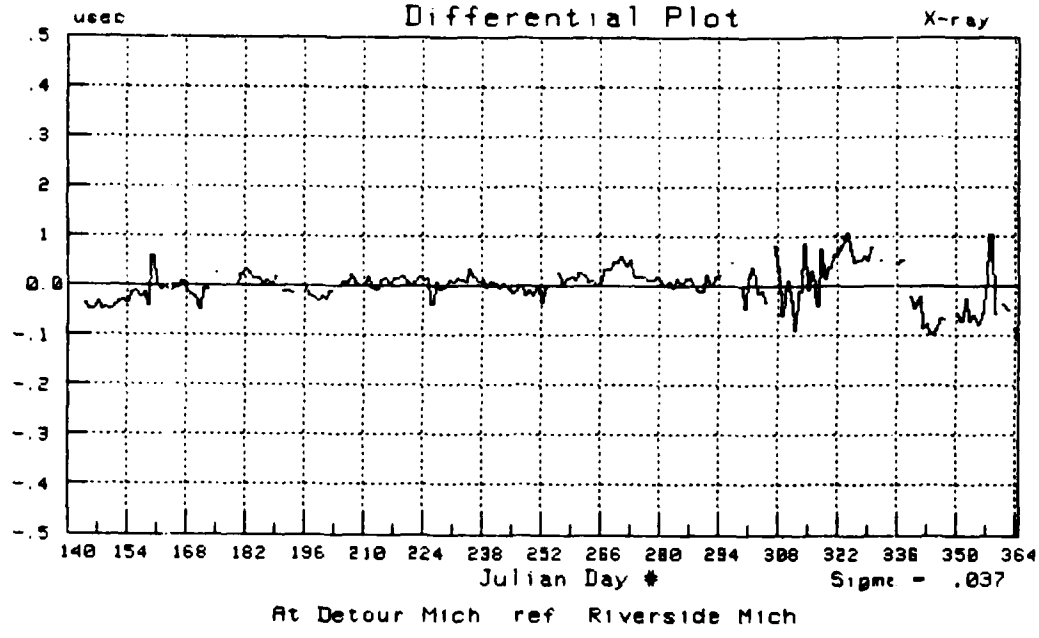

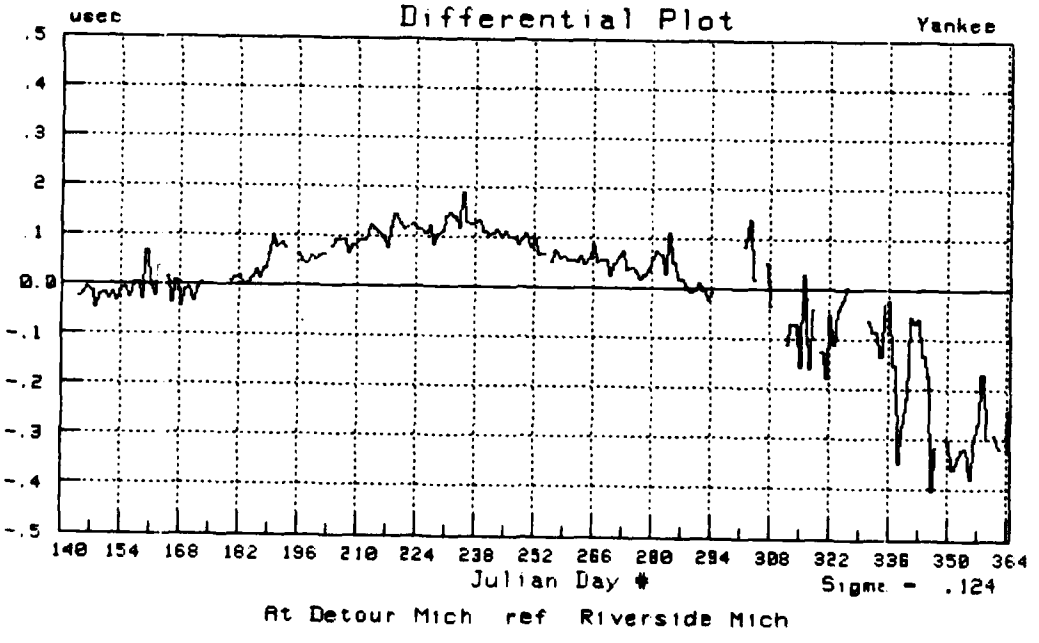

Figure 2-17 Simulated Differential Loran-C at Detour

Again, the data contained in the plots was first reported to Coast Guard Headquarters in January 1981. As in the "case of the moving antenna," explanations were discovered by scrutinizing teleprinter records. In this case however, it was not possible to correct the data. One can observe a "general offset," remove it, and observe that the resulting data is generally "noisier" than at times of proper receiver operation. One can thus imagine that things would be better had the cycle slips not occured. One cannot, however, say how much better and must simply call the experiment "compromised."

2.4 Subsequent Problems in Experiment Execution

Harbor Monitor Sets were deployed in the St. Marys River region in early February 1981 while the Internav 204 receiver problems described above were being examined. When initial Harbor Monitor Set data was reviewed in March, it was noted that the receiver at Dunbar Forest was locked to the wrong cycle. This was a considerable source of concern since it had just been established that the strategy of the Harbor Monitor project would feature no field adjustments of the "deriver" circuitry. Since the deployed Internav 404 sets had just been received "from the factory," the concern was acute.

Investigation revealed, however, that the 404's had been installed without their own antenna. The "35-foot-whip-coupler-multi-coupler-space coupling node-coupler" arrangement was being used. The fact that problems were only encountered with one TD - in spite of "our best efforts" - speaks well for Loran-C. In early April 1981 R&D Center personnel visited the sites and installed the receivers "as designed" - i.e., with their own antennas/couplers and the receivers selected the correct cycle throughout the remaining 14 months of the experiment.

As will be discussed in Section 3, the original plan was for the Supplemental LOP experiment to run through mid-1981 at which time an implementation decision would be made. The plan did not contend, however, with the fact that mini-chain personnel resources would be dwindling by early 1981. Thus it was necessary to decide whether to obtain and attempt to train new personnel for the last few months of the experiment. This led to the preliminary analysis discussed in Section 3 which concluded this would not be necessary (also, most probably, not possible). Although it would soon no longer be possible to operate the supplemental station 24 hours a day, it was recognized this was not necessary. Beginning in April, the 8970-Z station was only operated for about 4 hours a day - coming on-air about 1 hour prior to each data collection period of the day.

This mode of operation caused an unexpected problem at just about the time the previously mentioned problems had been solved. When the 8970-Z station went off-air, the receiver tracking circuitry would begin to "wander." Thus, the signal had to be re-acquired just before the sampling period. This was not an unexpected requirement - the Harbor Monitor Sets were supposed to "wake up" about 30 minutes before sampling time to make sure all was fine - with plenty of time to take corrective action if things were not. This design feature, unfortunately, proved to be improperly implemented.

The situation was complicated by the fact that there was a schedule coordination problem at first. It was not until this was resolved that the design flaw was uncovered. Immediately after the design flaw was corrected, the mini-chain personnel observed daylight savings time without thinking to inform R&D Center personnel. Having had inadequate time to gain confidence in the design "fix," R&D Center personnel implemented several "fixes to the fix" before uncovering the "secret of the changing time zones." Having violated the maxim "if it's not broken don't fix it," several more days were required to determine which of the redundant fixes was causing the current loss of data.

During the entire episode, unfortunately, X and Y data was generally being lost as well as Z data. In many cases, Internav 204 data was available, through a correlation, to fill in data gaps. Nevertheless, considerable data was lost.

Shortly after the 8970-Z station was secured on 1 July 1981, considerable confidence in the Harbor Monitor Sets had been gained. As the final assignment for the mini-chain personnel, therefore, the Internav 204 sets were removed from the data collection sites. This caused the final problem that should be mentioned.

When the old sets were removed, considerable effects were noticed in the Harbor Monitor Set data records. Investigation revealed there was an indirect tie-in between the two antenna systems which was finally broken with the removal of the old equipment. Mini-chain personnel were directed to return to each site (Riverside and Rocky Point were not affected) to reconstruct the tie-in. Working in conjunction with R&D Center personnel, they performed experiments for which extensive sets of data were taken: with the tie-in, without, with, etc. Subsequent analysis indicated it is possible to precisely account for the offsets (95% confidence bounds less than 5 nanoseconds) so that the results of 2 months of data collection efforts would not be lost. (The remainder of the experiment was conducted with the tie-in eliminated).

2.5 Problem Resolution and Summary

Shortly after the Great Lakes chain became operational, chain operators began to observe what they felt were indications of problems at the Muskegon chain control site. Specifically, on one day in March 1980, local phase adjustments (LPAs) totalling 400 nsec were inserted in the 8970-Y baseline in the evening and removed the next morning. Experienced with operations in "milder" chains, the operators assumed this indicated a control site problem. Full scale investigation of the problem did not start until late 1980 and, pending resolution of the problem, chain operators suggested use of the Riverside site for chain control.

For reasons discussed in Section 3, this was an attractive answer to the question of how to conduct Great Lakes chain guidance equipment tests in the St. Marys River after the mini-chain was secured. It also provided a convenient means of detecting equipment problems in a timely fashion - with local control of the entire chain, 200 nsec TD jumps would be readily

discernible. By the Spring of 1981, chain operators were convinced there were really no problems at Muskegon but the original suggestion had brought to mind sufficient other advantages to support a move of the prime monitor to Riverside. The shift of control was accomplished in late May 1981.

This was the big step in resolving the problem of the detection of equipment related offsets. Another big step, of course, was the installation of the receivers in the manner intended by the manufacturer (i.e., without the intervening multicoupler, etc). Another key step was the institution of a program at R&D Center to scrutinize the data on a day-to-day basis for signs of equipment problems. This led to the rapid detection of the offsets induced by the removal of the Internav 204 sets. A final step worth mentioning is that with the installation of the Harbor Monitor sets, one less group of people (mini-chain personnel) was involved in the experiment.

The problems caused when the 8970-Z station was being operated intermittently resulted in an unfortunate loss of data but, as mentioned, Internav 204 data was generally available to fill in the gaps and the problems were resolved before the Supplemental experiment was completed. Table 2-1 summarizes the key features of the 2 year experiment.

20 May - 31 December 1980	- Mini-Chain in operation - Old data collection sets used for Great Lakes chain data collection - "Moving Antenna" Problems - Cycle Slip Problems
1-18 January 1981	- Mini-Chain Secured - Old data collection sets still in use. Cycle Slip Problems persist
19 January - 31 March 1981	- Gordon Lake on-air full time - Old data collection sets used to collect <u>some</u> of the 3-secondary data
12 February - 2 April 1981	- Harbor Monitor Sets installed incorrectly. Some data usable
1 April - 1 July 1981	- Gordon Lake on-air periodically - Harbor Monitor Sets have periodic problems
27 May 1981 - 27 May 1982	- Gordon Lake secured - 8970-X and -Y controlled at Riverside. - Only data problems occurred when old data collection sets removed

Table 2-1 Summary of St. Marys River Great Lakes Chain Stability Study

2.6 Comments on Stability Studies

As explained at the beginning of Section 2.3, the preceeding presentation of experiment problems will assist in subsequent discussions of the data. It will not, for example, be necessary to interrupt the discussions of Sections 3 and 4 to explain why data is missing from late 1980 or early 1981. We could, however, have accomplished the purpose without risk of appearing so verbose or painfully detailed.

Cognizant of the risk, however, the authors concluded that a presentation of such details has an important place in Loran-C literature. The literature is replete with theories about the nature of Loran-C variations. It is similarly replete with reports on data collection efforts. Like reference 3, there is generally incomplete agreement between the theories and the data. In reference 3, for example, a propagation model which is nearly identical to the one to be used in this study was found to explain only a small portion of the variations observed in the data. Again, similar examples can be found in other studies.

In general, such reports point to unexplained equipment problems, unaccountable receiver problems, etc. If some studies seem to have encountered fewer problems than that of reference 3, it should be cautioned that the St. Marys River region, indeed, the entire Great Lakes region, presents a particularly harsh environment for year-round experiments of this nature.

It is the opinion of the authors that, in spite of the problems listed in the preceeding sections, there will be be considerably fewer "unexplained problems" in this report than is generally the case. Indeed, if we examine the data of past studies, we find numerous problems that are overlooked and suspect that if even the problems which were not overlooked were listed, the list would be considerably longer than that presented herein. We feel we have made considerable progress in the execution of Loran-C stability studies and, rather than glossing over the problems which were encountered and solved, we wish to present our methods. Our hope is that if it appears we have been somewhat more successful than our predecessors, future experimentors will not erroneously conclude it is because technology has progressed to the point at which problems "fix themselves" and undertakings such as this have now become trivial.

If one carefully examines the methods used in stability studies, one generally finds that there are at least two entities involved: those that conduct the experiment and those who analyze the results and prepare the test report. With few exceptions, this has been the general method for Loran-C stability studies conducted over the years. In some cases, Coast Guard chain operators collect the data and a contractor performs the analysis. In other cases, special teams (e.g., mini-chain personnel) are tasked with collecting the data whereas contractors, or R&D Center personnel or USCG Headquarters personnel try to make some sense out of it all. A recent study reported in reference 15 (actually, the first report under the Harbor Monitor program) Canadian Coast Guard, St. Lawrence Seaway Development Corporation, St. Lawrence Seaway Authority and R&D Center personnel participated in data collection while the analysis was conducted

at USCG Headquarters. Recent FAA studies have featured similar approaches. We have concluded that these approaches are extremely susceptible to failure.

A problem is that even if somebody associated with the experiment truly understands the subtleties of the Loran-C system, that person tends to be an analyst situated very late in the review cycle. It is not uncommon for such a person to first see the data months after the measurements are made. Examples of the preceeding sections show such a method of operation generally uncovers problems too late - inadvertent actions of those who operate and maintain the instrumentation could have compromised the data. Even if those associated with day-to-day operations are fully knowledgeable, they typically do not have the tools (e.g., those which allow for massive data base manipulation) necessary to detect subtle equipment problems.

Once the Harbor Monitor program got into full swing, R&D Center, properly equipped for data scrutiny, became solely responsible for equipment maintenance/operation and data collection/review. It now seems inconceivable to the authors to attempt any other approach.

This is not to imply all problems with the USCG Harbor Monitor program have been solved. R&D Center, for example, is still not performing all of the data review - a considerable learning process is involved. Enough progress has been made, however, for us to assert that the only fully successful approach is to have one knowledgeable, properly equipped entity responsible for the entire effort and fulfilling all aspects of that responsibility on a day-to-day basis.

3. PRELIMINARY PERFORMANCE ANALYSIS

3.1 Need for a Preliminary Analysis

The fate of the mini-chain was described briefly in Section 1.6. Before the end of the Mini-Chain experiment, the Coast Guard sought funding to make the chain operational. This involved several years of acquisition, constuction and installation funds followed by continuing funds for recurring operational costs. The first year funds were approved but no further approval was obtained. A detailed description of how something like this is possible would involve an explanation of the federal budgetary process and extend far beyond the scope of this report. We note, however, that the funds were adequate to make one of the stations operational so the question of whether or not to proceed with such action led to the exploration of the Supplemental LOP - the one chain augmentation technique that had not been explored.

A very quick analysis showed that of the mini-chain stations, the Gordon Lake site was best situated to provide good geometry: the resulting LOP would be predominently oriented along-track in the narrow reaches of the river. With this baseline controlled at a site of our choice, this could allow a stable cross-track indication - assumed to be the prime requirement in the river. Since the other stations of the Great Lakes chain would be controlled (i.e., TD's held steady) at distant Muskegon, it was recognized that some form of chain augmentation would be required in the St. Marys River - perhaps even Differential Loran-C. The hope was that the Supplemental LOP would improve matters to the extent that a "mild" form of corrections, e.g., daily, would provide adequate performance.

The R&D effort began under these circumstances. By early 1981, however, enough had been seen to suggest that even twice daily corrections would still leave substantial variations in the 8970-X and -Y signals. This led to a tentative conclusion that if the Great Lakes chain were to be used in the St. Marys River, either a move of the Muskegon monitor site or the implementation of real-time Differential Loran-C would be required. With this fact tentatively established, the marginal utility of the Supplemental LOP was reduced. Combined with the rapidly approaching date at which a decision regarding the replacement of chain operators had to be made, this forced the preliminary analysis described in the rest of this section.

3.2 Requirements Statement

As mentioned in Section 1, there are some unanswered questions regarding how good the Loran-C (or any navigation) system must be to satisfy precision navigation requirements in restricted waterways. Indeed, the more fundamental question regarding how much of the total problem of negotiating restricted passages is a navigation problem is not yet answered. These questions still exist now, will likely remain for many years, and certainly could not be answered in early 1981. In trying to determine whether or not

Loran-C should be improved in a given area, however, some performance metric had to be used. Drawing upon common sense, and aided by informal results from guidance equipment demonstrations, we formulated an assumed set of requirements. In somewhat cruder form, these were used in the Supplemental LOP decision. After refinement, they were used and documented in the St. Lawrence Seaway work of reference 15, were mentioned earlier in this report (Section 1.3), and will be used for the remainder of this report.

In developing the requirement, we first assume that cross-track error is the key parameter. Along-track error is of concern at the time of a turn. Assuming, as is the case, the turns are "mild" (i.e., no 90° turns), and assuming along-track errors are not significantly worse than cross-track errors (also, generally the case), we need only concentrate on cross-track error.

This means we must abandon such "standard" navigation system performance metric as CEP or drms - i.e., one-dimensional quantities. It also means we must be concerned about channel course. Thus, we must examine all reaches of the river.

We also must recognize that we cannot state accuracies at 50% or even 95% probability levels. We choose instead, the 99.9% probability level recognizing that this is not much different, for example, than the 99.99% level but does not (as a 99.99% probability figure does) exceed the availability of the basic system.

Thus we start, as in reference 3 and 15, by listing the half-channel width for each reach of the river. From this we subtract the "half-vessel width" for the largest vessels expected - 105 feet. What remains is how far the centerline of the vessel can stray from the center of the channel without part of the vessel extending outside the channel. This defines the total allowable error. (Having part of the vessel extend outside the channel does not, of course, guarantee the bottom will be scraped. We arbitrarily assume however, this situation is to be avoided.)

Next, we compute the 99.9% probability cross-track error of the Loran-C and subtract this value from the total allowable error figure. The result indicates how far the edge of a vessel, following the loran indications with no "guidance error," will come to the edge of the channel.

At this point, the discussion becomes "fuzzy" in some cases. For this reason we present the results in tabular form - listing the "room for guidance error" as the final column. If the entry is a negative number the conclusion is not fuzzy - this implies part of the vessel is outside the channel. Such situations will be annotated with three asterisks. If the entry is a positive number, but less than 5 meters, we show two asterisks, tacitly assuming this is inadequate. This is probably not so fuzzy an assumption. If the result is a number between 5 and 10 meters we have enterred the fuzzy region but still assume this is inadequate. One asterisk is assigned to such reaches. If we have more than 10 meters left for guidance error, we are still in the fuzzy area but, for current decision making purposes, assume we have adequate room. (One can expand upon the concept by simply adding an asterisk wherever at least one appears and to all reaches featuring results in the 10 to 15 meter range).

With this assumed performance requirement we can present the basis for the preliminary analysis and decision.

3.3 Analysis Results, Raw Loran-C, No Supplemental LOP

Figure 3-1 shows the half channel widths in the St. Marys River. In subsequent discussions we will have to give a more detailed description of the channel (e.g., courses, etc). Such detail is illustrated in Table 3-1.

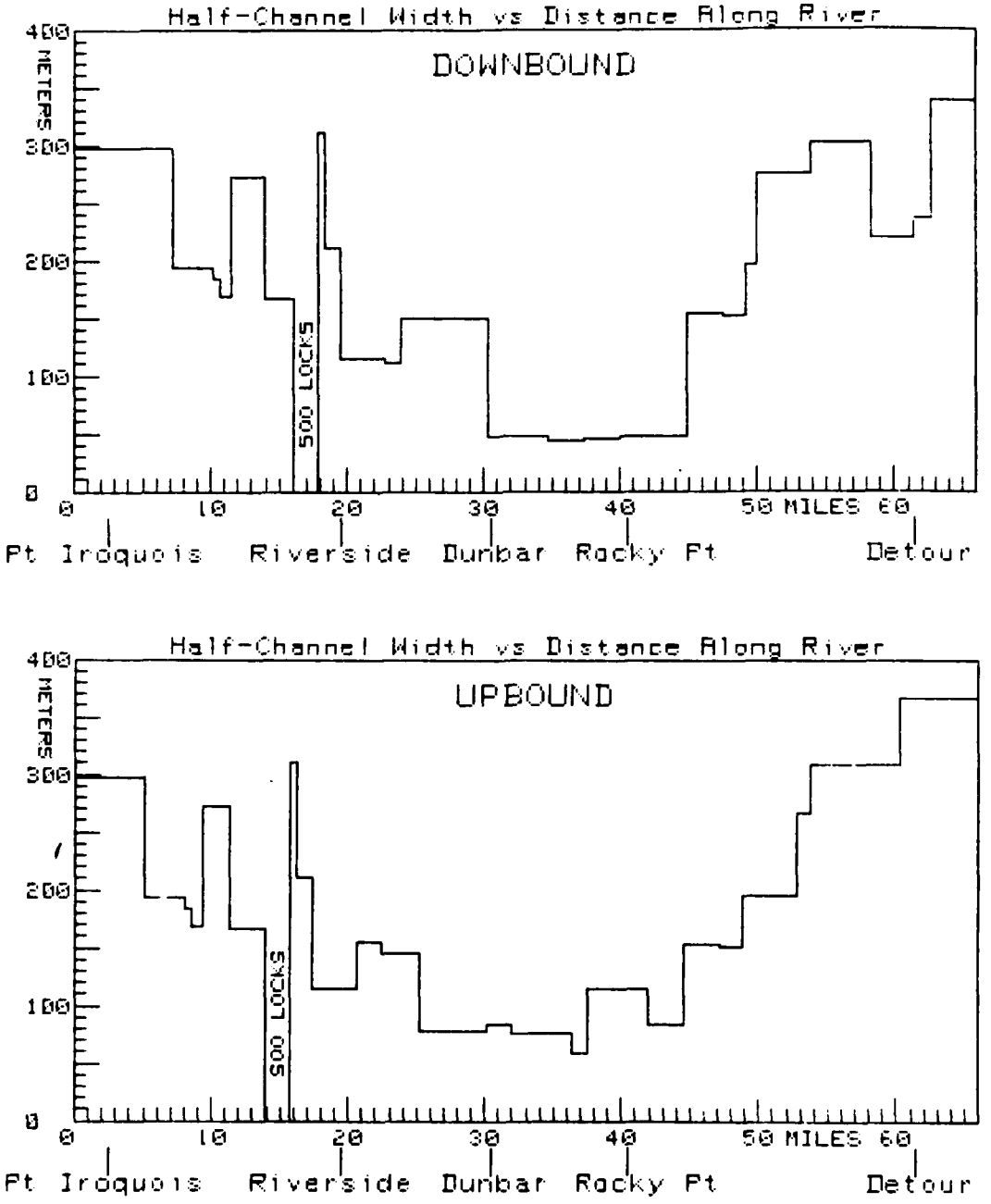

Figure 3-1 St. Marys River Half-Channel Widths

Reach Fm W.P.	Reach To W.P.	Reach Center	Course	Half-Width
1	2	45-59.0 N 83-52.9 W	002.6°T	367 m
2	8	46-02.9 N 83-56.5 W	295.5	309
8	10	46-04.5 N 84-00.6 W	330.5	266
10	11	46-06.2 N 84-00.8 N	006.6	195
11	12	46-07.9 N 84-00.7 W	337.2	195
12	13	46-08.7 N 84-01.8 W	308.1	151
13	14	46-09.9 N 84-03.9 W	308.8	154
14	16	46-11.4 N 84-06.2 W	322.2	83
16	18	46-13.9 N 84-06.6 W	016.8	115
18	20	46-15.8 N 84-06.4 W	314.9	59
20	22	46-17.5 N 84-07.1 W	356.5	77
22	24	46-19.4 N 84-09.1 W	291.2	77
24	26	46-19.9 N 84-11.0 W	292	83
26	28	46-21.7 N 84-12.5 W	330.3	79
28	30	46-24.7 N 84-14.6 W	339.6	145
30	32	46-26.4 N 84-15.9 W	323.7	155
32	33	46-28.3 N 84-17.5 W	332.9	115
33	34	46-29.8 N 84-19.1 W	289.2	211
34	35	46-30.1 N 84-20.1 W	297.3	310
35	36	46-30.1 N 84-21.6 W	267.2	LOCKS
36	37	46-29.9 N 84-24.0 W	256.1	167
37	38	46-28.1 N 84-28.0 W	232.1	272
38	39	46-28.1 N 84-28.0 W	209.9	169
39	40	46-27.7 N 84-28.5 W	237.1	183
40	41	46-27.2 N 84-30.7 W	253.1	194
41	42	46-28.3 N 84-34.5 W	318.6	297

UPBOUND

Reach Fm W.P.	Reach To W.P.	Reach Center	Course	Half-Width
1	3	45-57.9 N 83-53.1 W	180.3°T	338 m
3	5	45-59.8 N 83-53.3 W	169.7	236
5	7	46-01.4 N 83-54.7 W	140.9	219
7	9	46-03.4 N 83-58.5 N	115.3	301
9	11	46-05.9 N 84-00.8 W	186.5	275
11	12	46-08.7 N 84-01.8 W	157.2	195
12	13	46-09.9 N 84-03.9 W	128.1	151
13	14	46-11.4 N 84-06.2 W	128.8	154
14	15	46-11.9 N 84-07.7 W	128.5	48
15	17	46-14.4 N 84-10.3 W	168.5	46
17	19	46-16.4 N 84-11.9 W	143.1	43
19	21	46-19.2 N 84-12.9 W	181.7	48
21	31	46-23.6 N 84-14.1 W	159.2	150
31	32	46-26.5 N 84-16.0 W	143.6	110
32	33	46-28.3 N 84-17.5 W	152.9	115
33	34	46-29.8 N 84-19.1 W	109.2	211
34	35	46-30.1 N 84-20.1 W	117.3	310
35	36	46-30.1 N 84-21.6 W	087.2	LOCKS
36	37	46-29.9 N 84-24.0 W	076.1	167
37	38	46-28.1 N 84-28.0 W	052.1	272
38	39	46-28.1 N 84-28.0 W	029.9	169
39	40	46-27.7 N 84-28.5 W	057.1	183
40	41	46-27.2 N 84-30.7 W	073.1	194
41	42	46-28.3 N 84-34.5 W	138.6	297

DOWNBOUND

Table 3-1 Description of St. Marys River Reaches

At this point we should introduce a refinement which affects the requirements statement of the previous section and the reach description. Most of the "wide" channels of the St. Marys River feature 2-way traffic. Thus our requirement "formula," which features consideration of only one vessel, and a "goal" of holding to the channel centerline cannot be directly applied. The 2-way traffic channels are from waypoints 11 to 14 and 32 to 42.

One approach to the refinement is to simply "cut these channels in half." Thus, for example, the reach from waypoint 34 to waypoint 35 could be considered as illustrated in figure 3-2. The channel is 620 meters wide.

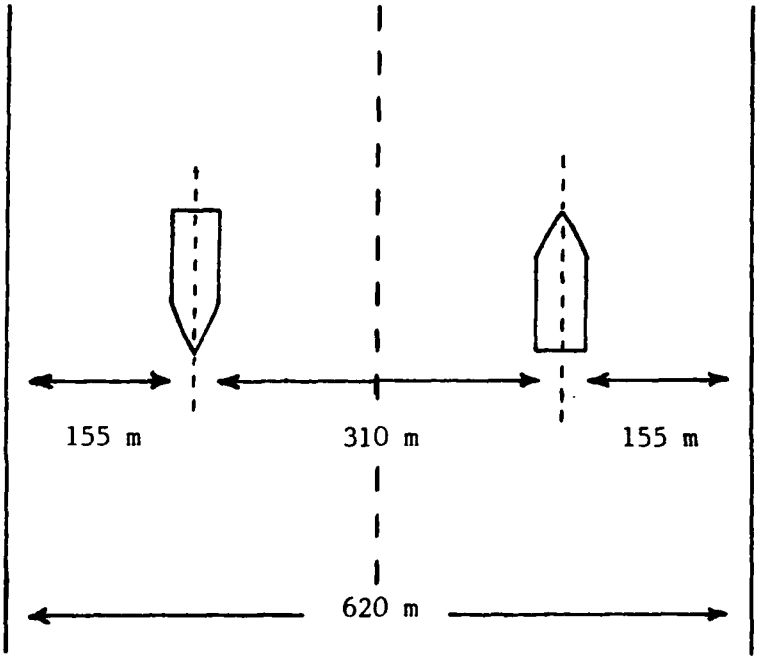

Figure 3-2 Channel From Waypoint 34 to Waypoint 35

The illustration suggests the cross-track error margin (for loran and guidance error) should be 155 meters minus 1/2 the vessel beam. As a practical matter, this is not representative of what takes place and will yield pessimistic results. Under "visual conditions," the vessels follow the same, "true" channel centerline. This "single centerline" is similarly featured in PILOT. When a vessel does encounter another vessel coming the other way, it will move right as indicated. It will not, however, move a distance approaching 155 meters as suggested.

The actual procedure used to move off the centerline - and back - is difficult to describe but easy for a seasoned mariner to accomplish. To summarize the result, we can simply assume that each vessel moves about

30-50 meters to the right. Thus, there is a separation of about 30-50 meters for the largest vessels. The distinction between 30 and 50 meters will not prove critical in our further discussions of the St. Marys River. Thus, we will use the smaller figure and subtract it from the "Half-channel width" column entry of table 3-1 - for the 2-way traffic channels - in constructing further tables and plots.

To reconstruct the early 1981 decision process, we should examine the data available at the time - the data which extended from 20 May to 31 December 1980. For the first part of the discussion we need only consider the Riverside data. The TD data is shown in figure 3-3. In figure 3-4 we transform this data to a scatter plot of fixes. In assigning the reference point for the plot, we choose the average of all of the data. This tends to put the data in the best possible light.

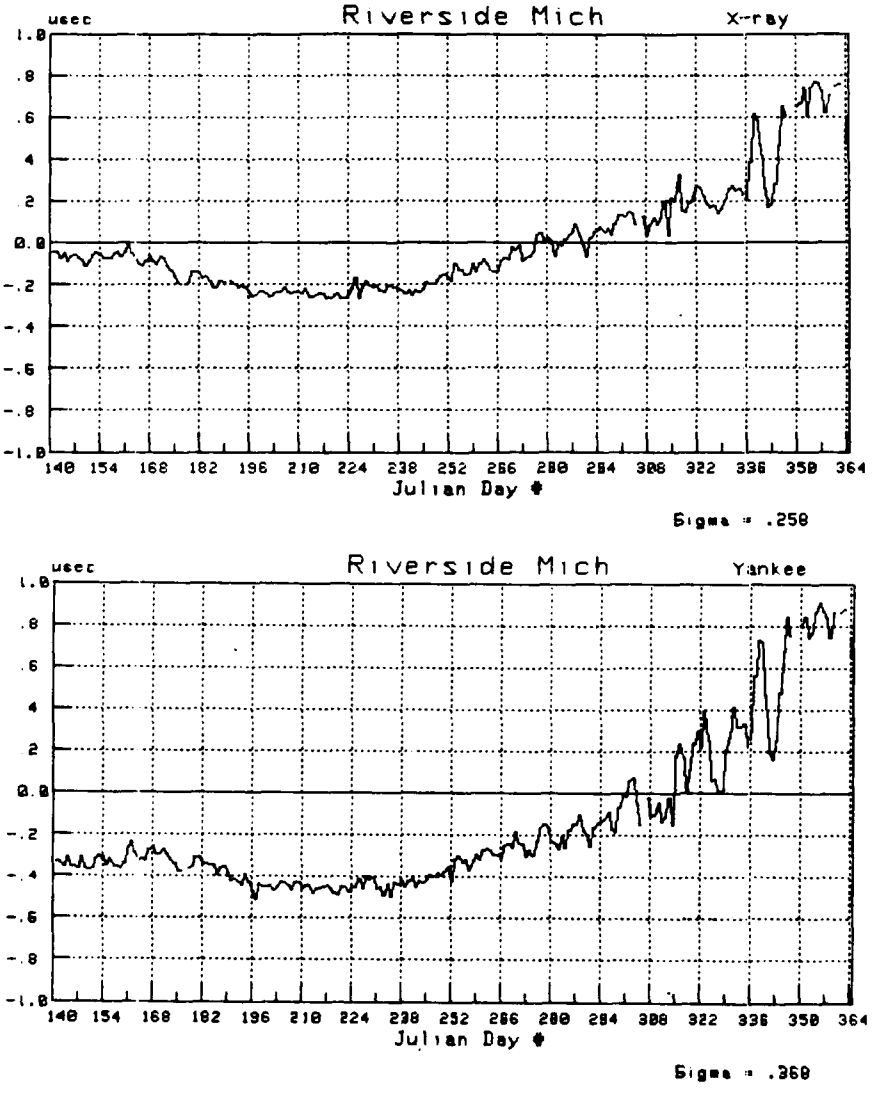

Figure 3-3 8970-X and -Y Time Difference Readings at Riverside - 1980

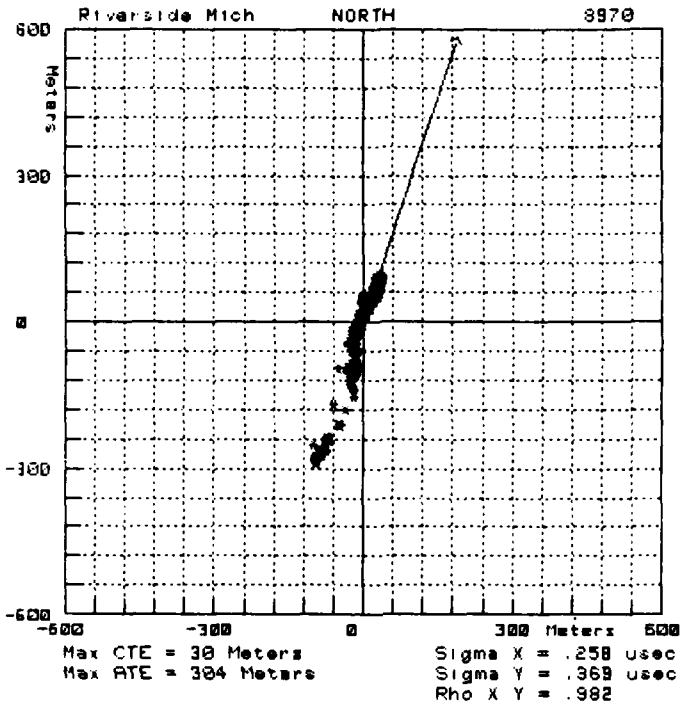

Figure 3-4 Scatter Plot of 8970-X and -Y Derived Fixes at Riverside

We can speed the analysis by scrutinizing the plot of figure 3-4 to determine what course provides the smallest cross-track error. We find this "best possible" course is 018°T (or 198° T). Figure 3-5 shows the data of figure 3-4 converted to cross-track error using this course for the computation. We see the error never gets larger than 30 meters - for this "best possible" course. Glancing through Table 3-1, however, we see there are only a few reaches which feature courses close to this. More generally, the courses are nearly perpendicular to this optimal course so that the value indicated for "ATE" in figure 3-4 (i.e., 304 meters) is more representative of what we can expect. Detailed analysis shows that, assuming the Riverside data can be considered typical - as the data from other sites shown in Section 2 indicates, the cross-track error will exceed the channel boundaries in 87% of the reaches.

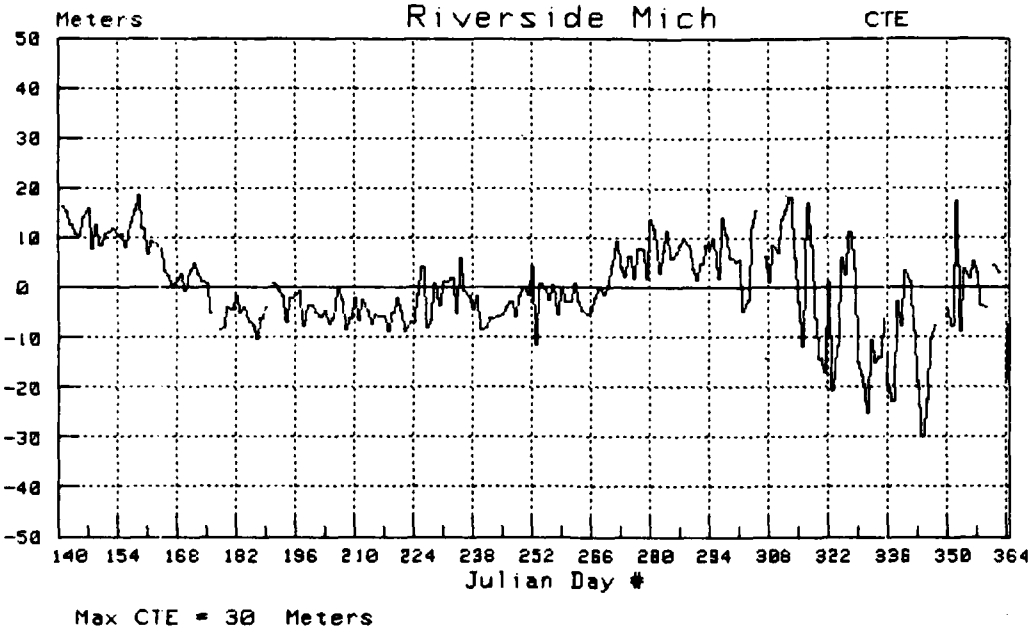

Figure 3-5 Riverside TD Data Converted to Cross-Track Error

There is one refinement we can make to have the "raw Loran-C" situation look as good as possible. If we examine the scatter plot of figure 3-4 we see that the data is not symmetrical about the arbitrarily chosen reference point. If we adjust the reference point so that the "max left" and "max right" cross-track errors are balanced, we obtain some improvement. In this case, the number of reaches with inadequate Loran-C performance is reduced to 68% of the total. In figure 3-6 we reproduce a slightly modified version of the channel description of figure 3-1. First, we decrease the half-channel width by 30 meters in those reaches featuring 2-way traffic. Next, we decrease all half-channel widths by 16 meters - the half-width of the largest vessels. What remains is the total error budget to be shared by the loran and guidance error terms. On this plot, we superimpose a plot of the maximum loran cross-track error for each reach. Again, the points being plotted are computed by applying the Riverside data to the geometry and course of each reach.

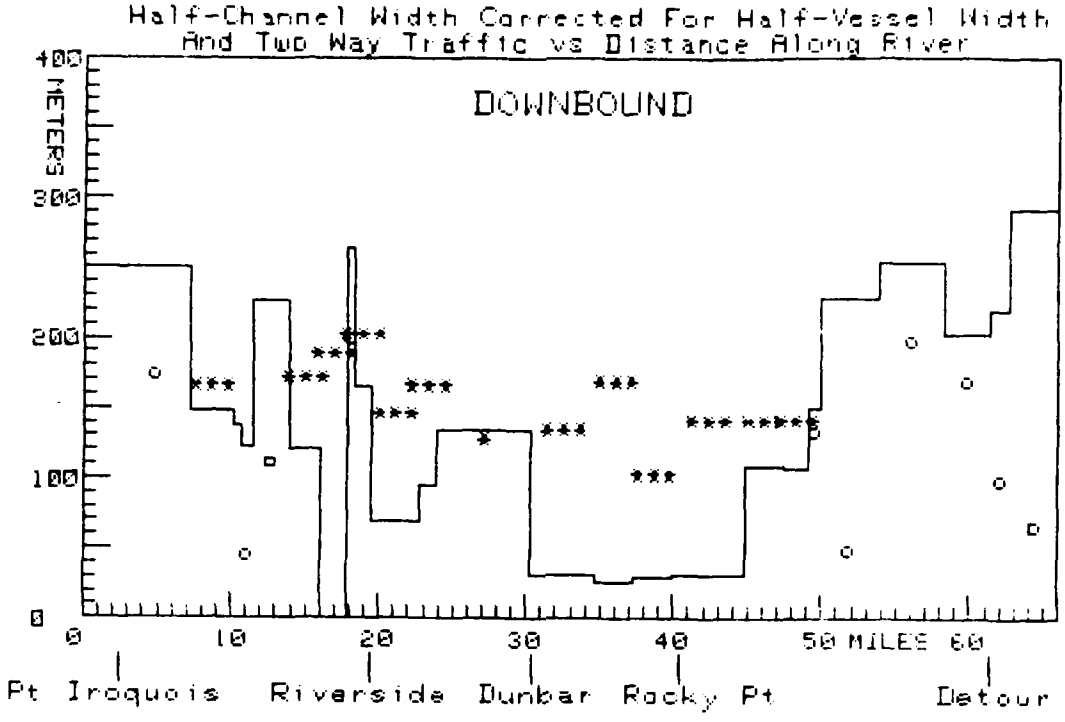

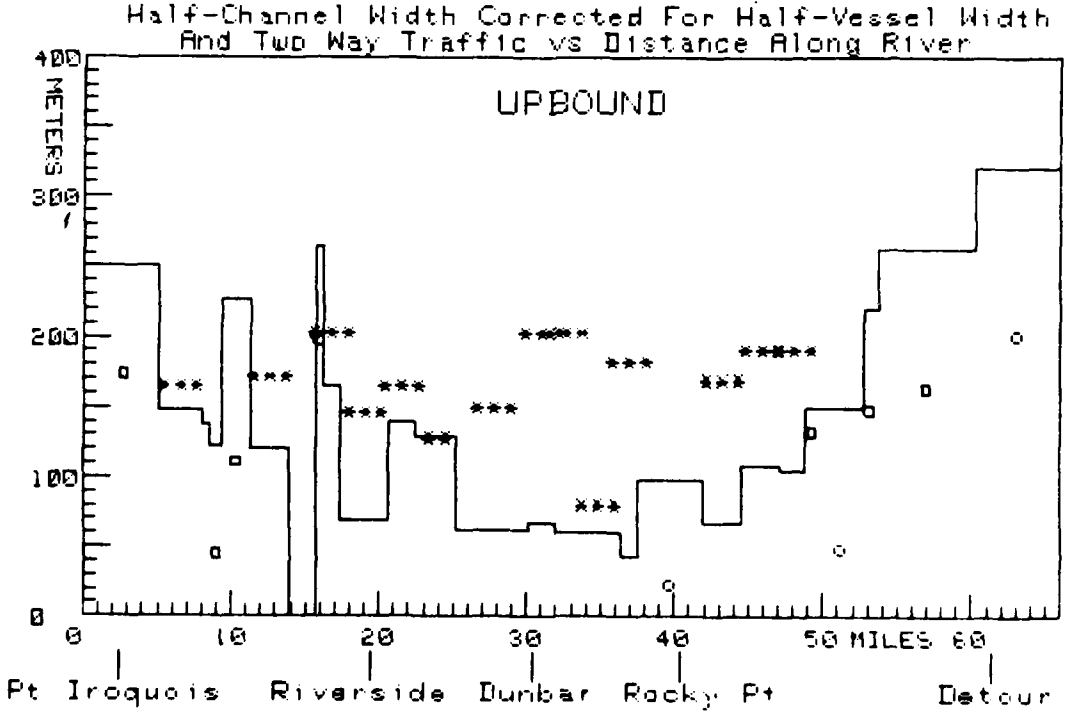

Figure 3-6 "Raw" 8970-X and -Y Loran-C Performance vs Total Error Margin

We have plotted the maximum Loran-C cross-track errors with circles if the Loran-C satisfies our assumed requirements in the particular reach. The errors are marked with the appropriate number of asterisks (as previously discussed) if they fail to satisfy the assumed requirements in the reach. From this we can conclude that the "raw Loran-C" performance of the Great Lakes chain, as originally configured, is not acceptable for precision use in the St. Marys River.

3.4 Analysis Results, No Supplemental LOP, Daily Corrections

One of the simplest ways to enhance Loran-C performance is to apply periodic (e.g., daily) corrections to the waypoint data used by the guidance equipment. In the St. Marys River, an in-place voice communications network makes this possible. The method is practical if a single correction, derived from observations made at a single shore station can suffice. We can obtain a crude simulation of the expected performance of such an arrangement by manipulation of the data presented in figure 3-3. Specifically, we can subtract each data point from the next day's reading to arrive at a measure of how large an error we can expect just before the time of the next correction. Such a simulation does not account for any spatially related component of the time difference variations. Thus, it is valid only in the immediate vicinity of Riverside. If we apply the results to other reaches of the river we will obtain very optimistic results. Nevertheless, the excercise is instructional and should be carried out. The resulting time differences are shown in figure 3-7 and a scatter plot of the position fixes is shown in figure 3-8.

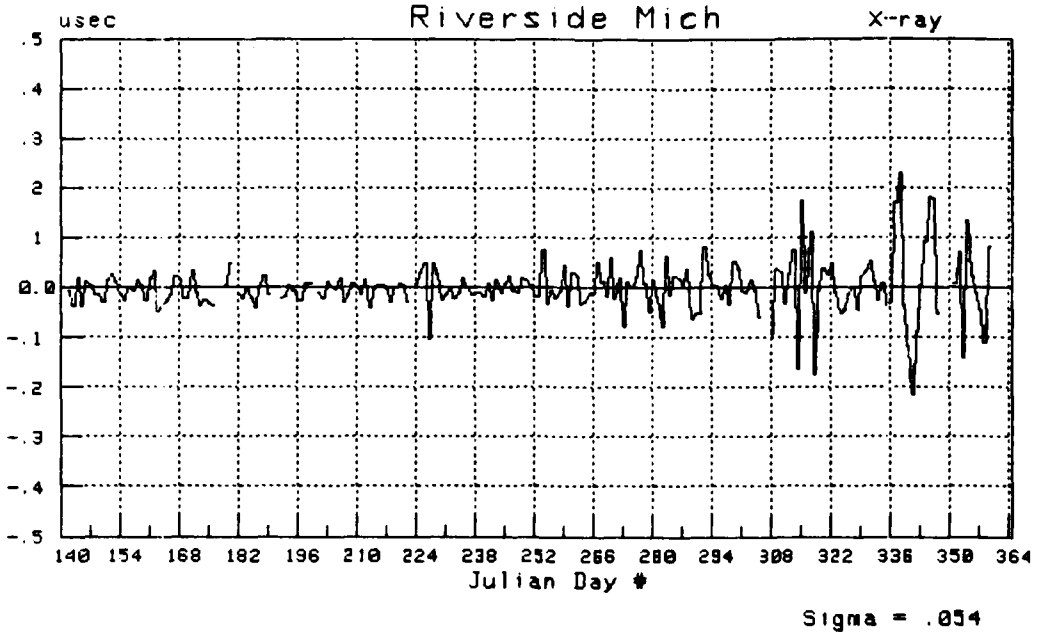

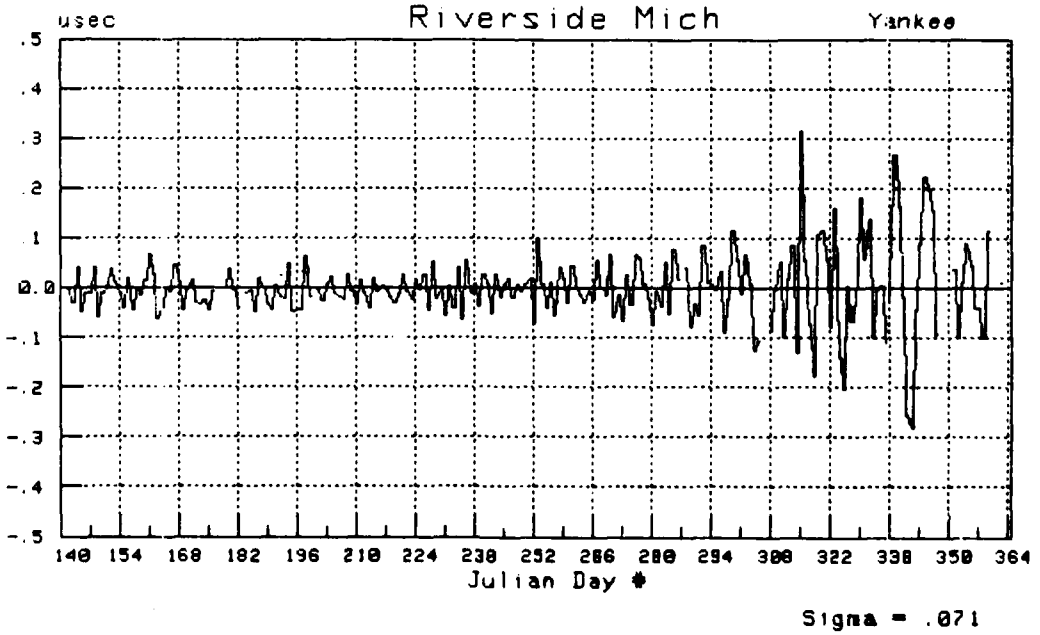

Figure 3-7 Riverside TD's with 24-hour Old Corrections Applied

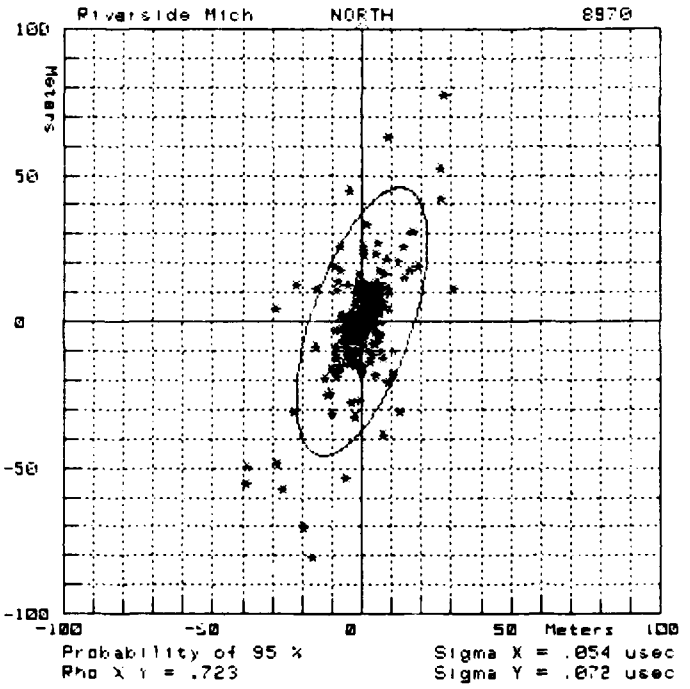

Figure 3-8 Scatter Plot for Data of Figure 3-7

Comparing figure 3-8 to figure 3-4, we see a substantial reduction in the error. We can also note that, by effectively removing the "seasonal" component of the variation, we have effectively eliminated the symmetry problem. If we argue that this same reduction in time difference variation will apply throughout the river, we can apply the data of figure 3-8 to each reach and, given the appropriate course, compute the maximum cross-track error. The results, for each reach, are superimposed on the plot of the (modified) half-channel width plot in figure 3-9.

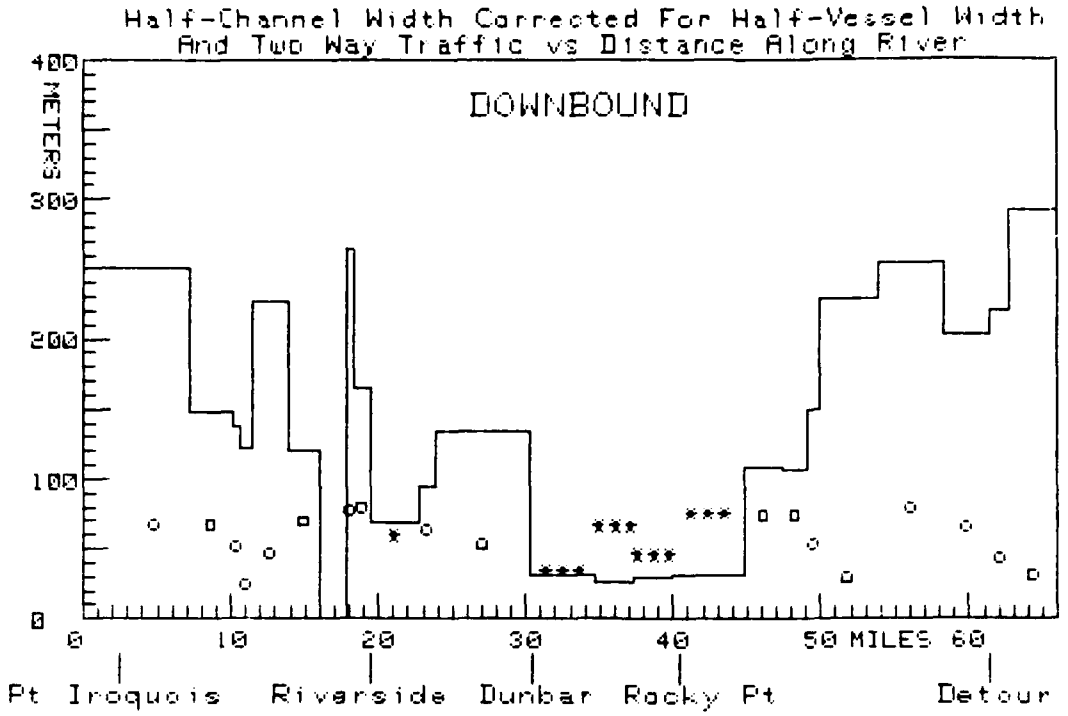

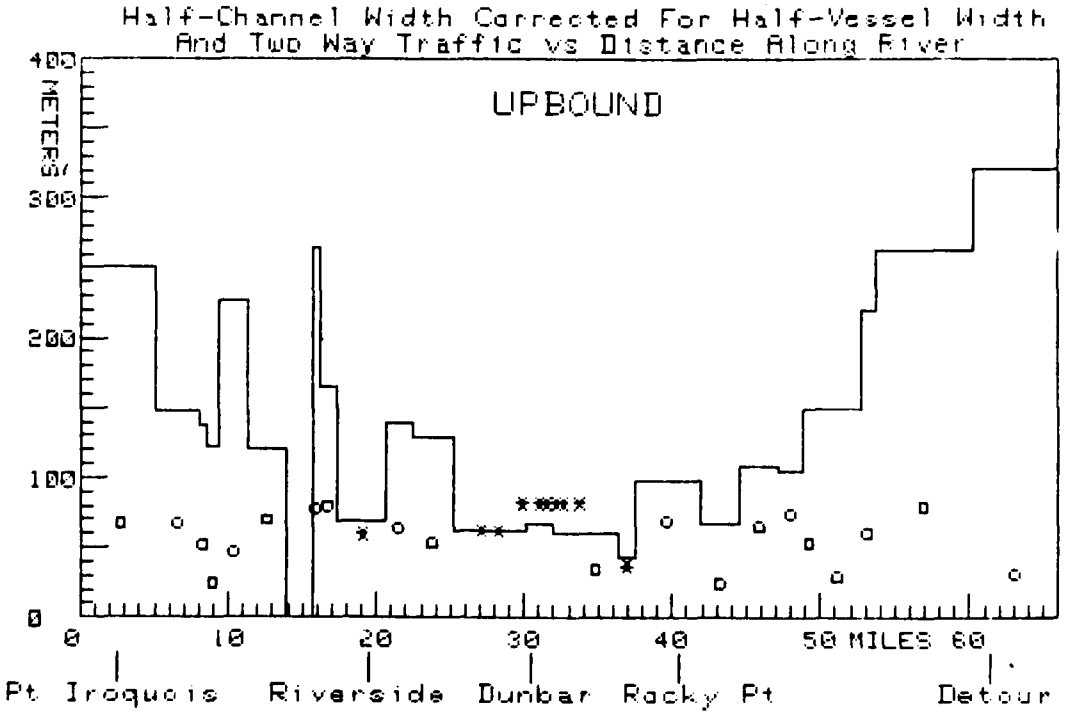

Figure 3-9 Application of Riverside Data (Daily Corrections) to Each Reach of the St. Marys River

Again, we indicate the maximum Loran-C cross-track error with a circle if the assumed requirements are satified in a reach. Asterisks indicate the errors for reaches in which the assumed requirements are not met. Clearly, this simple enhancement technique does not yield adequate performance (note, we expect spatially related variations to increase the errors even above those indicated). If precision Loran-C navigation is to be provided in the St. Marys River, a more elaborate enhancement technique must be sought.

To be a little more specific, we can note that there are really two classifications we can assign to the reaches of the St. Marys River: wide and narrow. The narrow reaches extend from waypoint 14 to waypoint 32 (about mile 20 to mile 45). From figure 3-9 we can see that an argument can be made that the requirements are satisfied in the wide reaches by the application of 24-hour corrections. Even a concern that we are ignoring the spatially correlated component can be argued away since the only reach which is "borderline" (from waypoint 32 to waypoint 33 - at about mile 20 downbound) is close to Riverside.

Interestingly, we would be satisfying these requirements with what could be called a "60-80 meter system." At this point, we may be able to temporarily simplify the difficult question "what is the goal of Loran-C in the St. Marys River?" If the goal is to simply provide adequate positioning information in the wide reaches, leaving the narrow reaches for "some other system," we have found a way to do it. Thus, unless we can argue that a supplemental LOP makes for an easier, less expensive implementation, the only way to support an argument in favor of the supplemental LOP approach is to show it satifies requirements in the narrow reaches as well as the wide reaches.

Turning to implementation considerations, the cost to the government is certainly minimized by the "daily correction" method - assuming it is up to the user to obtain the daily correction (somehow). Alternatively, since it can probably be considered impractical to expect a user to obtain the correction unassisted, we should consider what the government can provide. As a lead-in to the next sections, we will simply assume the cost of a supplemental LOP is not much more than that of operating shore based monitors and broadcasting corrections. This is not as wild an assumption as it might seem: the Coast Guard is well-practiced at transmitting Loran-C signals whereas implementation of even a "mild differential Loran-C" network would be a new start. This approximate relative cost should be recalled as we proceed with the examination of alternate enhancement techniques.

3.5 Supplemental LOP Performance Prediction Techniques

As previously indicated, it was originally assumed (and probably remains true) that the preferable approach to improving performance is the addition of another LOP. If the resulting performance is adequate, this provides a "stand-alone-loran" solution to the problem (i.e., no auxiliary communication network required). By January 1981, the results outlined in the previous sections were known and the viability of the Supplemental LOP as a single solution to the problem came under serious question. Since data

from the new LOP was not yet available, but, as previously indicated, action was required, it was necessary to employ a prediction method to hypothesize expected performance. As a result of the mini-chain experiment, there was a considerable data base and a promising model available for these predictions. These were used for the analysis.

Before proceeding with a discussion of the analysis, we should outline the features of the model. It is the so-called double-range-difference (DRD) model, the classical approach to explaining/predicting seasonal Loran-C variations. It is discussed in many references and used in reference 3. Reference 15 devotes an Appendix to it and uses it throughout the main body of the report. The following is a short refresher.

In figure 3-10 we show the hyperbolic lines of a hypothetical Loran-C baseline. Note that the lines are labelled in kilometers - properly indicating a constant difference in the distances from two fixed transmitter locations. These distances do not normally change over reasonable periods of time.

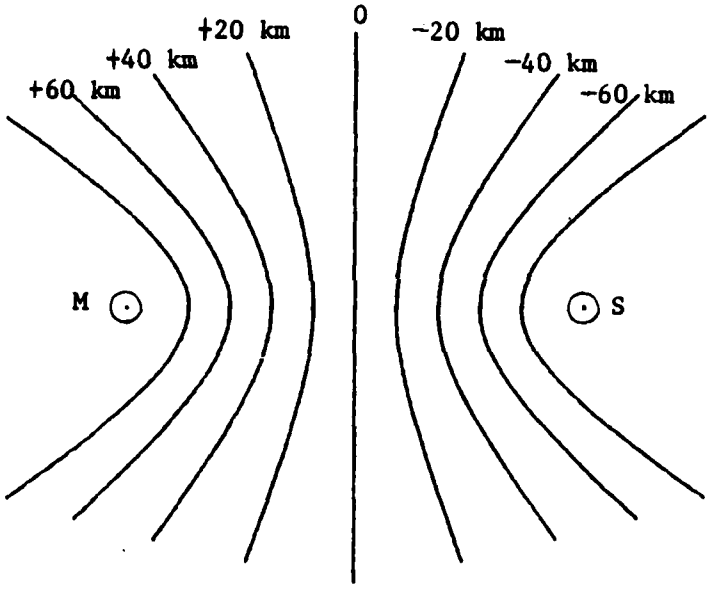

Figure 3-10 LOP's of a Hypothetical Loran-C Baseline

The underlying principle in loran is that there is some uniform speed, v_1, at which the signals travel. We choose a hypothetical value of 2×10^8 m/sec (or 0.2 km/usec) in re-labelling the LOP's at the bottom of figure 3-11.a. Although this value is very low, it is of the correct order of magnitude and, being a nice round number, makes the discussion easy to follow. We say this is the speed of the signals at time t_1 and that it is valid over the entire service area. In figure 3-11.a., again for simplicity, we assume that the emission delay is held constant at zero, i.e., the two stations transmit simultaneously.

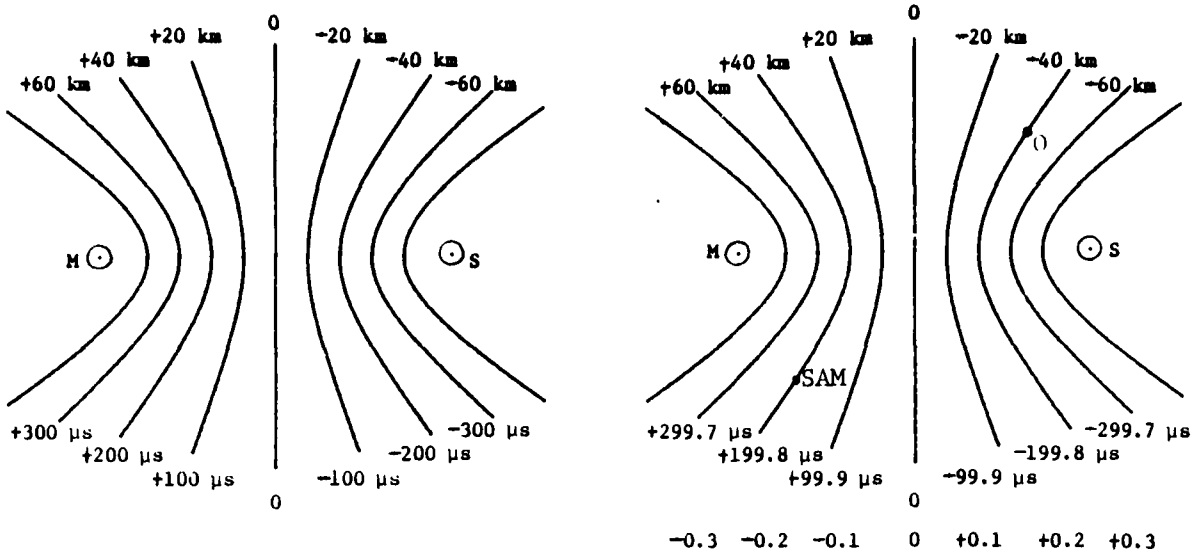

TD's at Time t_1 With Propagation Speed v_1

(a)

TD's at Time t_2 With Propagation Speed v_2

Numbers in bottom Row Indicate TD Change From t_1 to t_2

(b)

Figure 3-11 LOP's for a Hypothetical Loran-C Baseline - Re-Labelled for Various Propagation Speeds

Next, we suppose that at time t_2, the speed has changed by one part in a thousand, i.e., to $v_2 = 1.001\ v_1 = 2.002 \times 10^8$ m/sec. Again, we say that this speed holds true over the entire service area. Under these circumstances, the time differences all change by about one part in a thousand and the LOP's at time t_2 should be labelled as shown in figure 3-11.b. Note that the distances have not changed - just the time differences. In the bottom row of numbers in figure 3-11.b. we have indicated the TD change from time t_1 to time t_2.

What we have presented thus far is, of course, a simplification that indicates changes in TD's are determined by the LOP of the observer. To more accurately reflect what happens, we indicate a system area monitor (SAM) and an observer on two of the hyperbolas of figure 3-11. Notice that the formulation thus far indicates the TD's at the SAM change from time to time. Again, figure 3-11 represents uniform velocity changes and a constant emission delay.

Actual chain control practices do not allow the situation of figure 3-11 to occur: corrections are made to keep the time difference at SAM constant

throughout the year. It would be wonderful if the corrections could be made to the speed of propagation - this would keep the time differences constant everywhere. This, of course, is not possible, so corrections are made to the emission delay. Thus, if we assume the time difference observed at the SAM at time t_1 is the "assigned number," the time differences actually observed at time t_2 will be as shown in figure 3-12. As indicated by the reading on the perpendicular bisector of the baseline, the emission delay has been adjusted to exactly cancel the propagation speed change related variation at the SAM.

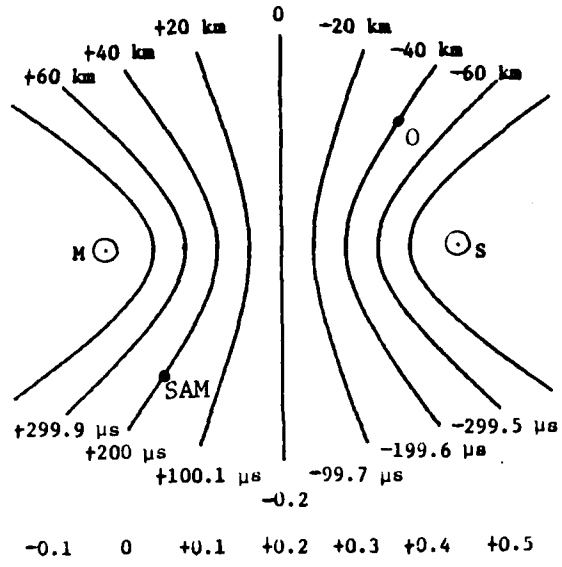

Figure 3-12 LOP's of Hypothetical Baseline Adjusted to Reflect Actual Chain Control Procedures

Now it can be seen that the TD change at the location of the observer is not fully determined by the hyperbola of the observer. Instead, it is determined by consideration of two hyperbolas. Specifically, it is determined by the difference between the hyperbola of the observer and the hyperbola of the SAM. Since each hyperbola represents a range difference, the relationship between the two hyperbolas comprises a double range difference - leading to the term employed to describe the model.

To relate all of this to what actually takes place, we note first that the emission delay is not actually close to zero: it varies about some large number chosen to ensure signals from each station of the chain do not overlap in reception time. This has no impact on the results of the previous discussion. We also note that propagation speeds are not, in general, uniform throughout the coverage area. Thus, lines of equal time difference are not perfect hyperbolas. This also, however, does not adversely impact upon the discussion since we are concerned more about

changes in speeds than actual speeds. Finally, we note that changes in the speed of propagation are generally not uniform over a large area. This is discussed in considerable detail in reference 15. Over a small area such as the St. Marys River, however, we might expect this is not a problem.

If the model is approximately a true description of the mechanism involved with seasonal variations in time differences, the next question to ask is what effect does this have over the course of a year. The Appendices of reference 15 give a simplified answer to this question with some simple plots which represent greatly smoothed time difference records at either end of a hypothetical Loran-C baseline. The plots are reproduced below.

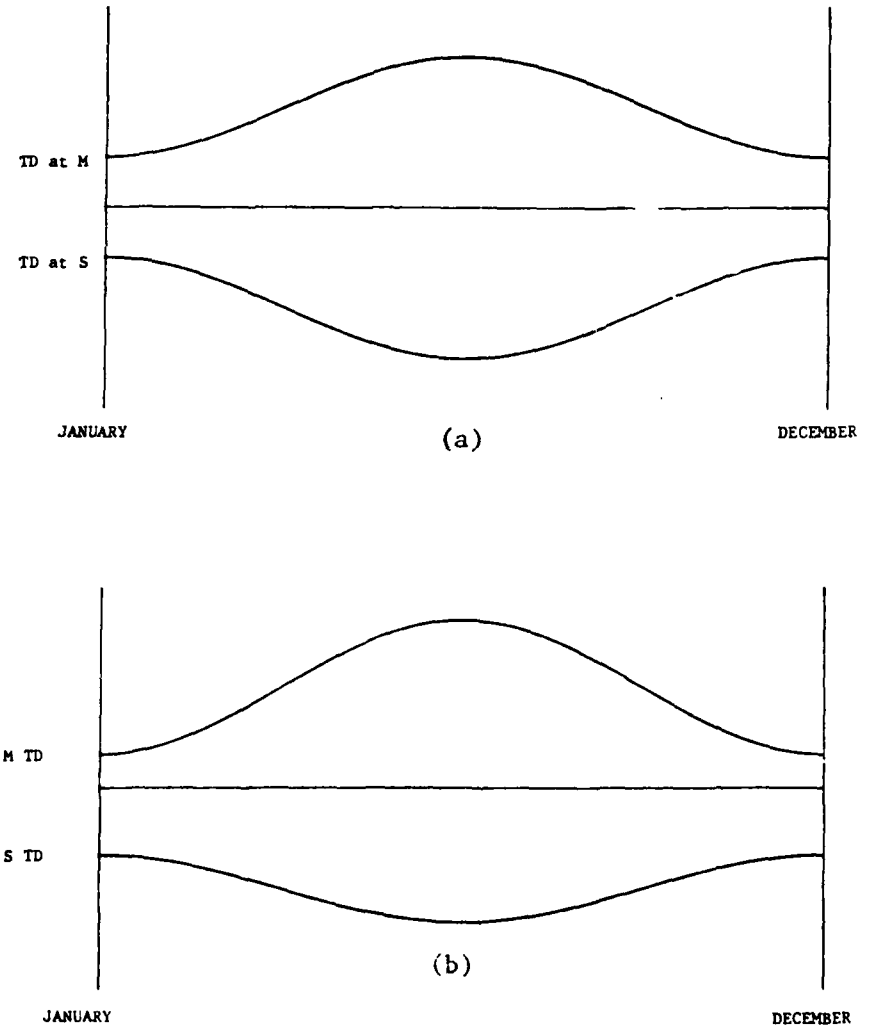

Figure 3-13 Smoothed Plots of Year-Round TD Records at Each End of Hypothetical Loran-C Baselines

The curve at the top of each figure represents the TD as observed at the master station. The plots at the bottom represent the TD as observed at the secondary station. In figure 3-13.a., we indicate what we expect to occur when the SAM is, in a DRD-sense, about halfway between the master and the secondary. The plot of figure 3-13.b. suggests the SAM is closer, in a DRD-sense to the secondary. Reference 15 shows these plots along with some representative plots of actual data. Since section 4 of this report will contain numerous data plots which confirm the concept, we will skip a presentation of data at this point. We should note however, that the general trend is as follows: when it gets cold, the signals travel faster (see reference 11).

If we consider this fact, along with the concepts of figures 3-11 and 3-12, we can confirm the plots of figure 3-13 are as expected. First, notice that the TD at the master station is larger in the summer than it is in the winter. Let's assume that the summer value is the reference. With an observer at the master station, the time of transit of the signal from the master station to the observer is independent of the speed. The signal from the secondary station, however, has a long way to go. Since it travels faster in the winter, we expect it to get to the observer at the master station sooner in the winter than in the summer. This decreases the time difference so that, as indicated, we see a smaller TD in the winter than we do in the summer. From reciprocal arguments, we expect the TD observed at the secondary station to be larger in the winter than in the summer - again, as indicated in the plots.

To take the argument a little bit further, suppose the propagation changes are uniform and that the SAM is located on the perpendicular bisector of the baseline. In this case, the distance from the SAM to the two stations being the same, the TD at the SAM stays constant no matter how the speed changes (so long as changes are uniform over the service area) and no emission delay adjustments are necessary. Thus, we expect the variations observed at either end of the baseline to be equal and opposite.

Alternatively, suppose the SAM is located "hyperbolically" closer to the secondary that it is to the master, with uniform propagation speed changes. In this case, we would expect the SAM (if not allowed to order emission delay adjustments) to see the TD's <u>increase</u> in the winter - as they do at the secondary station - but not to as great an extent as at the secondary station. Since the SAM <u>is</u> allowed to make corrections, however, the emission delay is forced <u>negative</u> in the winter. This is the general trend that an observer at the secondary station would like to see - although not quite enough to keep the TD's constant year-round - and the <u>opposite</u> of what an observer at the master station would like to see. Thus, the variations are reduced at the secondary and worsened at the master site - just as indicated in figure 3-13.b.

To complete this preliminary discussion of the model we can note that Muskegon, the SAM for the 8970 - X and -Y baselines, is closer to the master station than the observer in the St. Marys River is for both baselines. Thus, applying the concepts of the above discussion, we expect the TD's observed in the St. Marys River to be more positive in the winter than they are in the summer. This is exactly the trend we see indicated by the plots of figure 3-3.

The simplest way to apply this model to year-round performance predictions is discussed in detail in reference 15. First we note that the loran fixes obtained over the course of a year will form an elliptical pattern. Given certain arguments about the nature of the variations, we can draw the pattern, the so-called error ellipse, for any desired probability, if we know the joint second order statistics of the time differences. For 2-TD fixes this means we must know the standard deviations of each TD and the correlation coefficient between the two TD's.

To obtain estimates of these statistics, we recognize first that we have two predominant components - one that is spatially correlated (i.e., correlated from site-to-site) and one that is spatially independent (i.e., independent from site-to-site). A more elaborate breakdown of the components of the Loran-C variations is possible but this simple classification is generally found to be sufficient.

Next, we argue that the spatially correlated component is the seasonal component which is sinusoidal in nature and, generally, weather driven. Thus, it is very nearly perfectly correlated (correlation coefficient of +1 or -1 - depending on the sign of the DRD) from site-to-site and from baseline to baseline. The spatially independent components, as the name implies, are independent from site-to-site but, assuming the signals are reasonably strong - as they are in most HHE applications - have a correlation coefficient of +0.5 at any given site. This argument follows from the fact that the measurement of the master signal time-of-arrival is common to both TD measurements at a given site and that "transmitted noise," i.e., variations inherent in the system, dominate atmospheric noise effects.

Reference 15 used an elaborate analysis procedure to show that a representative figure to use for the standard deviation of the spatially independent component variation is 11 nsec. Thus, to complete our statistical description we need only to find a way of determining the standard deviation of the spatially correlated component. We will have to explore this in section 3.8. At this point, however, we should simply imagine what will happen if the 8970-Z baseline contains no spatially correlated component. Although this will lead to considerably optimistic results, we should first examine the performance implications if this ideal were somehow achieved. Realizing the implications of the concepts discussed in this section, we will appreciate the need for further examination if the results appear promising.

3.6 Analysis Results, "Raw 8970-X and -Y TD's," Ideal 8970-Z Performance

Suppose we operate the 8970-Z station at Gordon Lake, Ontario, and control the time difference for this baseline with a SAM located at Riverside, Michigan. If we leave the control of the 8970-X and -Y baselines at Muskegon, we will have, in the vicinity of Riverside, two signals with variations as indicated in figure 3-3 and one very stable signal. As indicated in the previous section, our studies to date indicate the best stability we ever expect, over the course of a year, corresponds to a time difference standard deviation of 11 nanoseconds. To simulate what could

occur if we were somehow able to achieve this ideal, we can generate a sequence of values representing samples of a stationary, white, Gaussian random process, with a zero mean and a standard deviation of 11 nanoseconds. We will use this sequence to simulate 8970-Z TD readings so that the readings expected (ideally) in the vicinity of Riverside are as shown in figure 3-14.

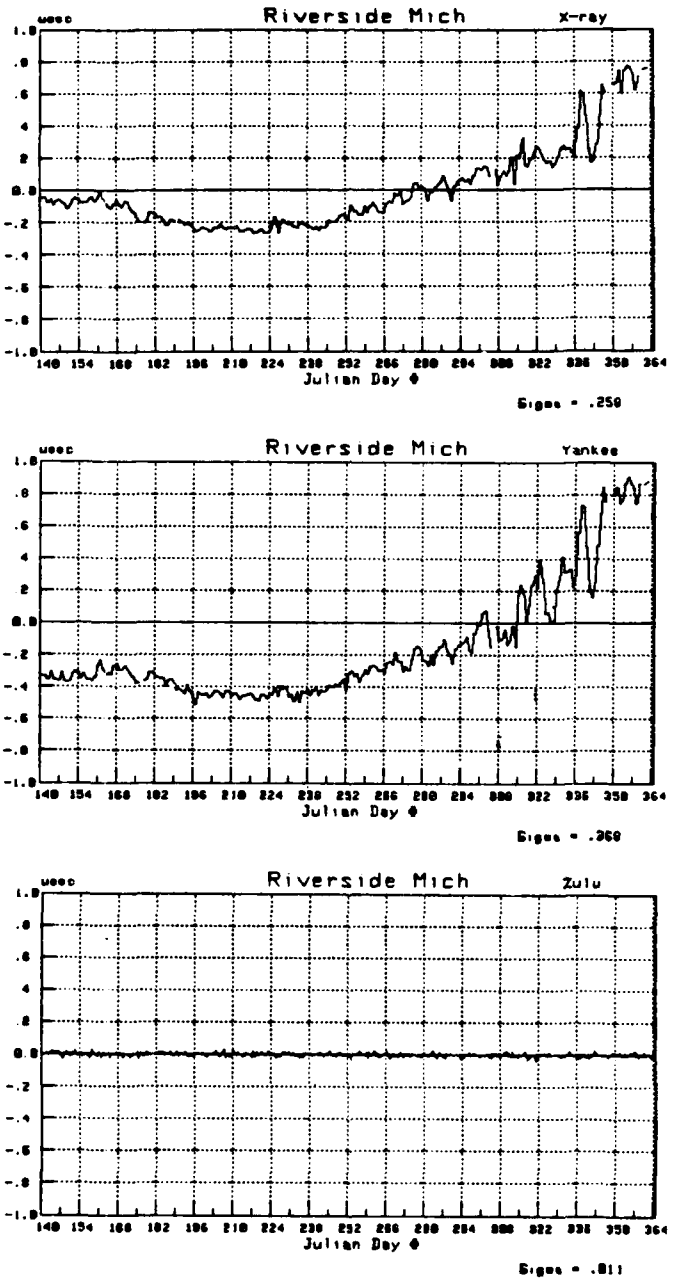

Figure 3-14 Expected TD Variations at Riverside With Ideal 8970-Z Performance

Using the so-called G-Matrix, described in Appendix A and used in PILOT, we combine these three sequences of readings to obtain a sequence of position fixes. In scatter plot form, the results are as indicated in figure 3-15.

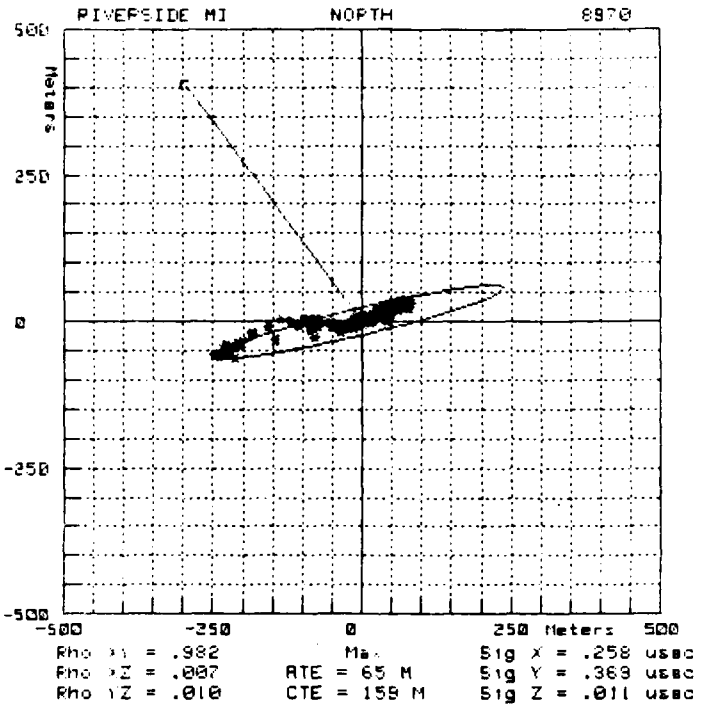

Figure 3-15 Scatter Plot of Expected 3-TD Fixes at Riverside (Ideal 8970-Z Performance)

Proceeding as before, and drawing upon knowledge of observations made at Pt. Iroquois, let us assume that the Riverside readings for 8970-X and -Y are representative of what is to be expected throughout the St. Marys River. To be consistent, let us assume the "11 nsec standard deviation" assumption for 8970-Z also holds true throughout the region. We have no basis for supporting this latter assumption. Indeed, with the concepts described in the previous section, we know this will not be true: 8970-Z variations will increase as we move away from Riverside. Nevertheless, we will use this assumption as the basis for our first look at the 3-TD situation and simply recall the results will be optimistic. We hypothesize the performance for all reaches as indicated in the plot of figure 3-16. The significance of the circles and asterisks is as before.

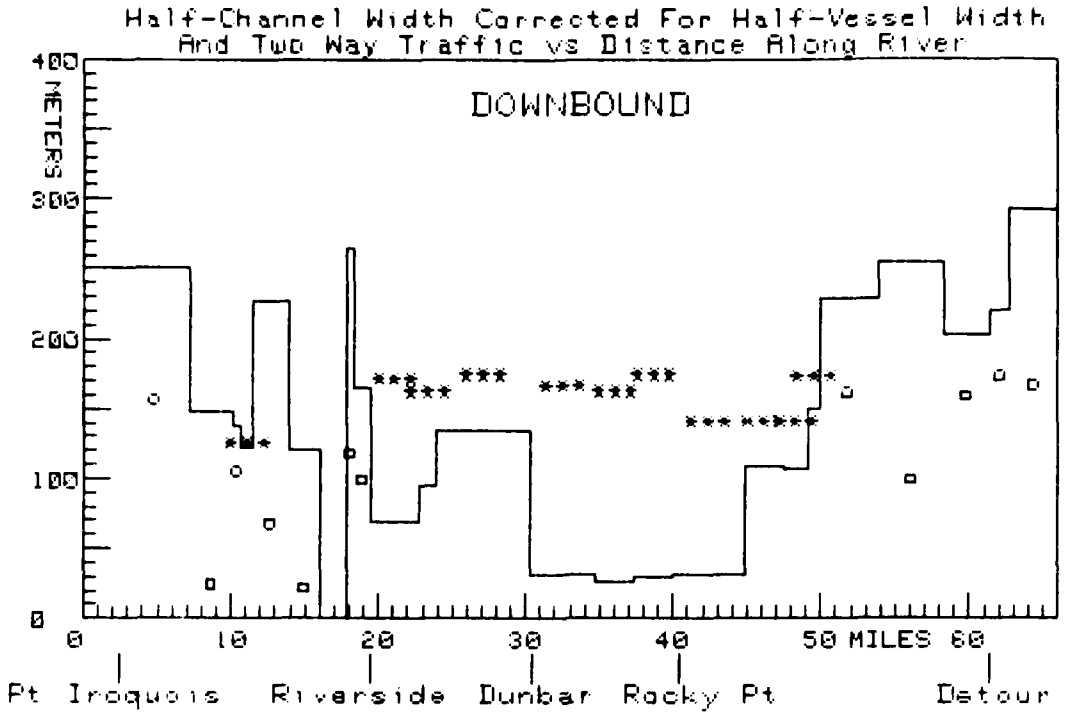

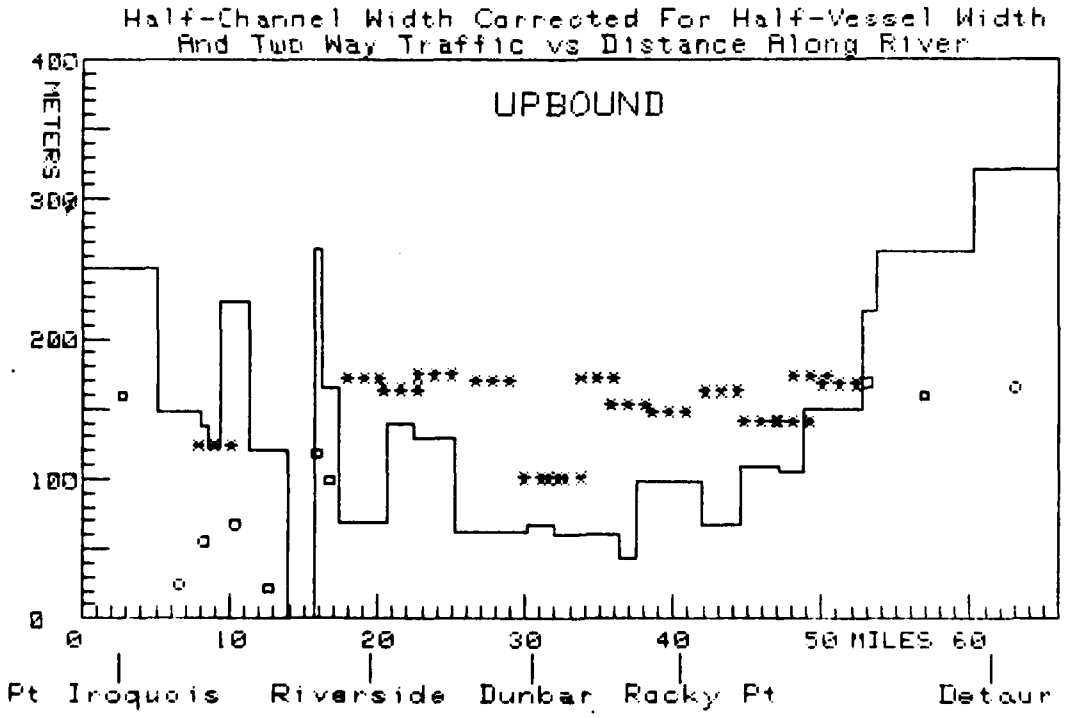

Figure 3-16 3-TD Fix Performance - Raw 8970-X and -Y Data, Ideal 8970-Z Performance

The results show the performance is clearly unacceptable. Indeed, the performance is worse than we would obtain by the "daily correction" approach: here we have problems in the wide reaches as well as in the narrow reaches.

It is interesting to note that the results are barely better than in the 2-TD "raw data" case (actually worse in some reaches). Depending upon one's facility with matrix manipulation, an intuitive explanation for this is possible. Very simply, however, we can simply imagine that the two unstable TD's are "out-voting" the third, stable TD. This suggests we might try to match the 8970-Z station with only one of the existing TD's, particularly if we recall the 8970-Z TD generally provides an LOP which is oriented along-track. Figure 3-17 shows the LOP's at Riverside and suggests that the "YZ" TD combination might give better results.

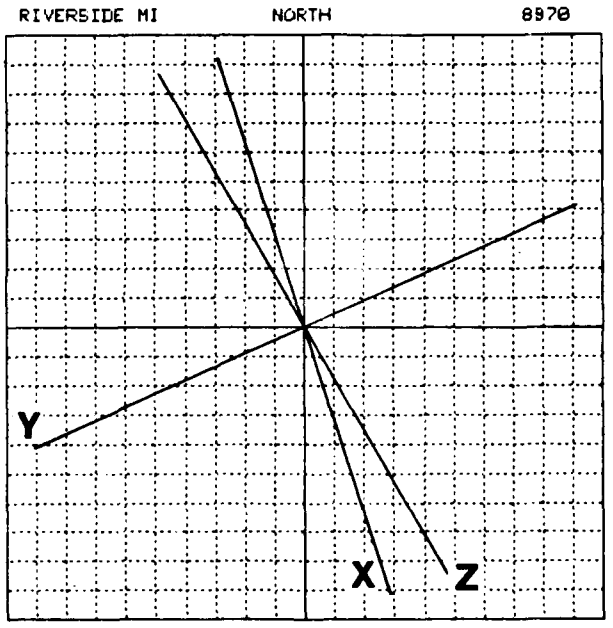

Figure 3-17 8970-X, -Y and -Z LOP's at Riverside

We will again simulate the expected performance by applying the 8970-Y Riverside data to the geometry and course of each reach, along with a simulated "11 nsec standard deviation" 8970-Z data record. We should recall that, because our assumptions about the 8970-Z variations ignore any spatially related variations, our results will again be very optimistic. The performance is as indicated in figure 3-18.

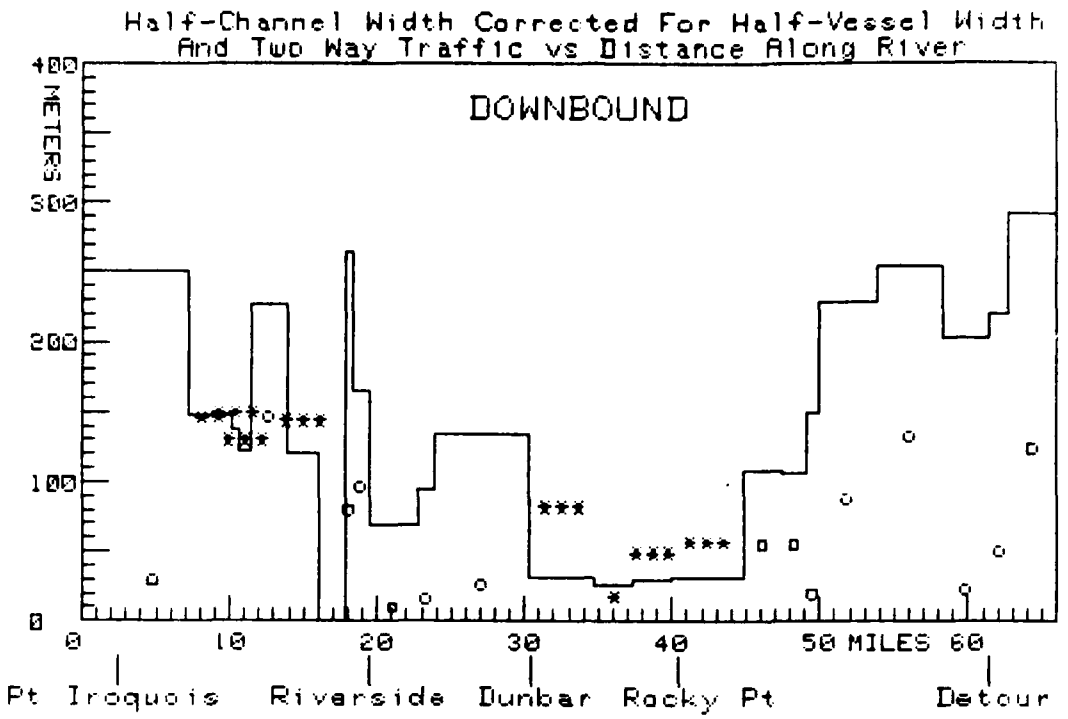

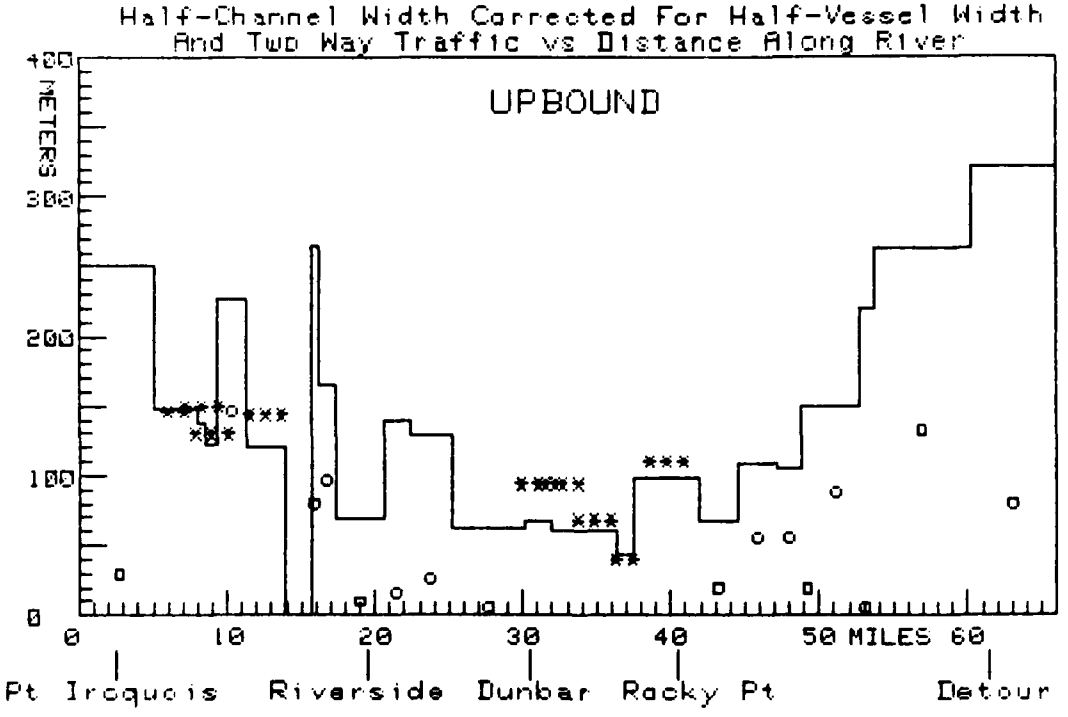

Figure 3-18 8970-Y (Raw) and 8970-Z (Ideal) 2-TD Fix Performance

We see that the results are much better than in the 3-TD fix case so that the supplemental LOP "comes close" to providing an alternative method of yielding adequate cross-track performance in the wide reaches. At this point we can make some very important statements about the utility of the supplemental LOP approach in the St. Marys River. First, however, we should examine the "XZ" 2-TD fix performance (8970-X -"raw," 8970-Z - ideal) which is as indicated in figure 3-19.

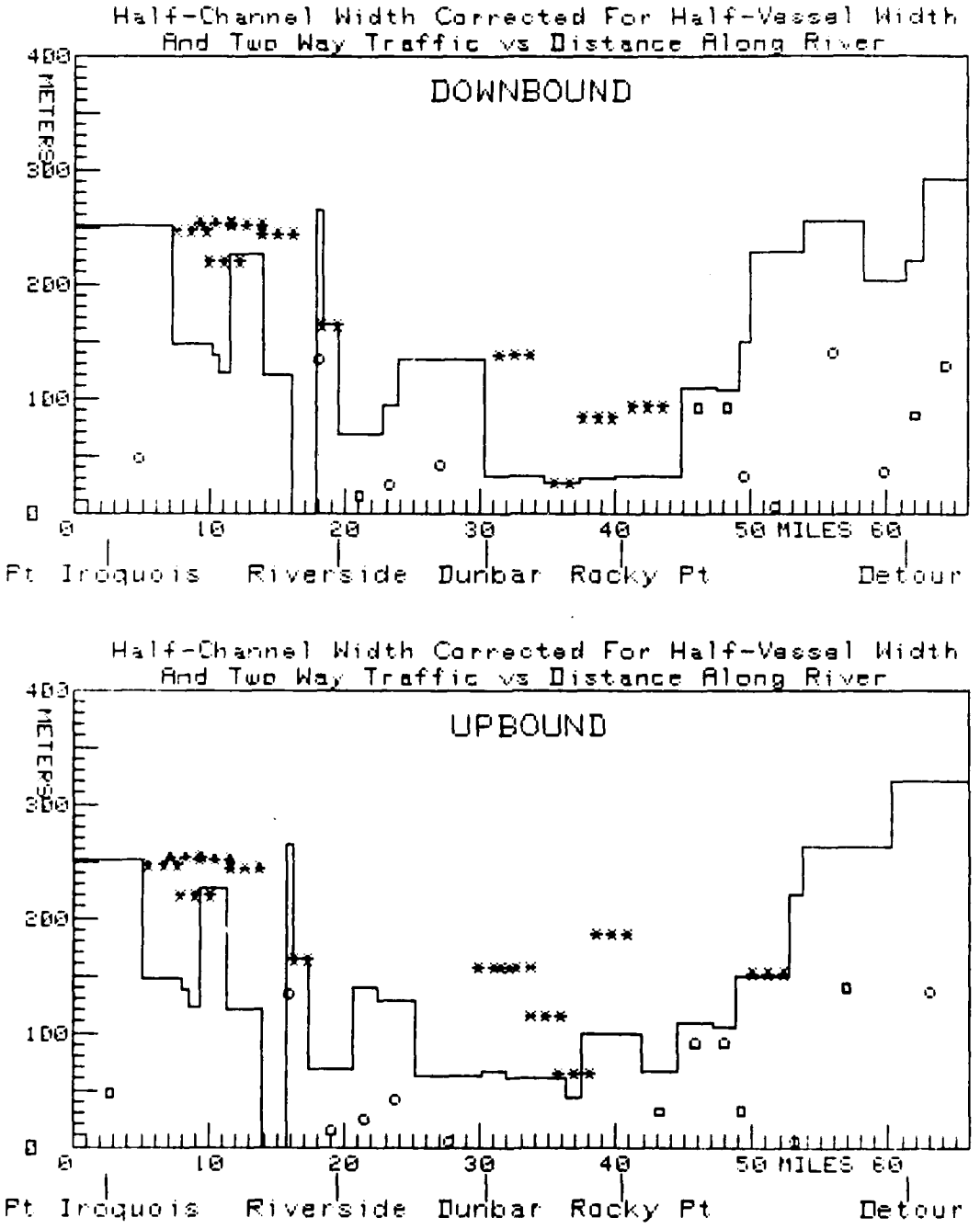

Figure 3-19 8970-X (Raw) and 8970-Z (Ideal) 2-TD Fix Performance

Clearly, the results for this combination are unacceptable. Thus, we have examined four situations featuring the use of "raw" data from one of the two existing baselines: MXY, MXZ, MYZ, and MXYZ fixes. There is actually another combination which can be used for navigation - XYZ - since the PILOT receiver is "master independent." We will explore this in later sections. For now we should simply note that only one of the possible combinations shows any promise of yielding adequate performance (i.e., the MYZ combination). This is an important concept to emphasize because one of the claimed advantages of the supplemental LOP approach is redundancy/reliability. The argument begins with the fact that single station availability is on the order or 99.9+%. If signals from three stations are required, and only three stations exist, the "fix availability" is about 99.7+%. Whereas this may seem like a high percentage to some, others argue that 99.7% excludes about 26-1/2 hours per year. If four stations provide signals and if the goal is simply to obtain a fix (of any quality), one can generally expect to be satisfied 99.9994+% of the time (i.e., being frustrated less than 3 minutes per year).

This certainly seems like a worthwhile goal but, generally, assumes that "fix quality" is not important. In the St. Marys River, however, we simply cannot support this argument and since only one combination seems to show promise (recall, we have assumed "ideal" 8970-Z performance), the reliability argument evaporates. Indeed, it can be argued that the mere existence of poor combinations of TD's is a serious argument against the supplemental LOP (he who suggests you avoid this problem by simply "passing the word" to use only MYZ is dangerously naive about the success with which Loran-C system information is promulgated).

To summarize, we can say that lacking some additional enhancement technique (e.g., daily corrections), the 8970-Z signal has possible utility only as a "replacement LOP," not a supplemental LOP. Even this is subject to further review if we consider spatial variations, and is true only for the wide reaches. All of this having been said, we must emphasize this does not rule out the supplemental LOP as a viable technique for other HHE areas. Examination of figure 3-17 gives an indication of why improvement is difficult in the St. Marys River: 8970-X and -Y geometry is not a problem. Indeed, it is hard to improve upon the existing geometry. The problem is that the existing LOP's are not stable. Thus, while we appear headed towards ruling out the supplemental LOP as a "stand-alone" solution in the St. Marys River, we can identify it as a viable approach to the Loran-C problem in the Houston/Galveston area where, although the TD's are reasonably stable, the geometry is horrible.

To complete the discussion of this section, we should recall that when we discussed the use of cross-track error as the prime metric for judging whether or not performance is adequate, we argued that as long as the along-track error was of approximately the same size, we did not have to consider this performance measure. This simplifies the discussion since there is no simple way to tabulate the across-track requirements. We should note, however, that with the "MYZ" combination, we will encounter substantial along-track errors - as figure 3-20 suggests.

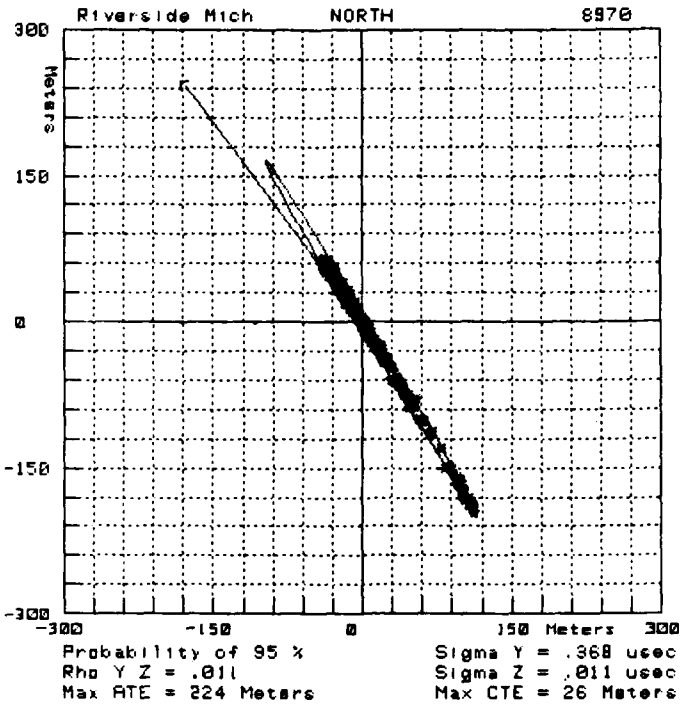

Figure 3-20 Scatter Plot for 2-TD 8970-Y (Raw) and 8970-Z (Ideal) Fixes at Riverside

Additionally, we note there are some problems in the wide reaches of the river - even for the "best case" MYZ combination - even ignoring spatial variations. To examine what could happen, we can hypothesize a sinusoidal variation - of the type indicated in figure 3-13 - in the 8970-Z record over the period of a year. Results of the Mini-Chain experiment suggest the sinusoid can be expected to have a peak-to-peak swing of about 6 nanoseconds per kilometer. To simulate the expected variation at a particular site, we compute the double range difference (DRD) in kilometers and multiply this by the sinusoid. When we accomplish this for the reach between waypoints 12 and 13, for example, we obtain the more realistic prediction of 8970-Z variations shown in figure 3-21.

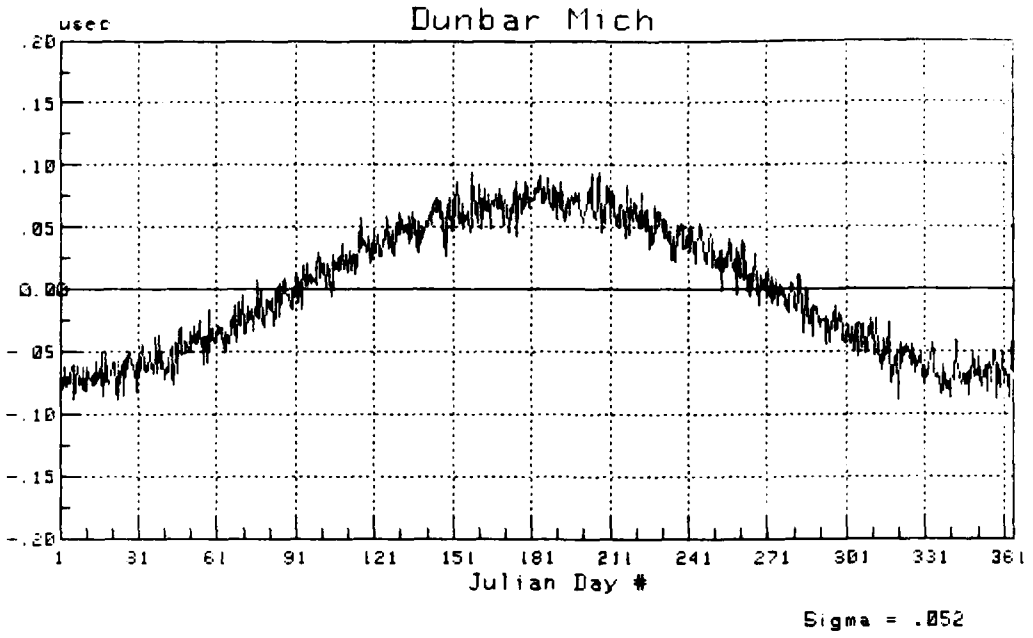

Figure 3-21 Modified Prediction of 8970-Z Variations, Waypoints 12 - 13

When we combine this with the 8970-Y (raw) variations, we compute a maximum cross-track error of 200 meters - a substantial increase over the "ideal" performance prediction of 26 meters. From all of this we can see that the supplemental LOP is an inadequate "stand-alone" solution to the St. Marys River requirements. Thus, if the new LOP is to be of any benefit, it will have to be used in addition to another enhancement technique such as the use of daily corrections. We explore this next.

3.7 Analysis Results, Daily Corrections to 8970-X and -Y, With Supplemental LOP

Following the standard approach, we use 8970-X and -Y data obtained at Riverside and apply 24-hour old corrections. We argue this is representative of what to expect throughout the region - realizing we are either ignoring spatial variations, or requiring there to be several monitors (thus making the implementation become more complex). We assume ideal 8970-Z performance is available throughout the region - again cautioning this will lead to optimistic results. Under these assumptions, the performance will be as indicated in figure 3-22.

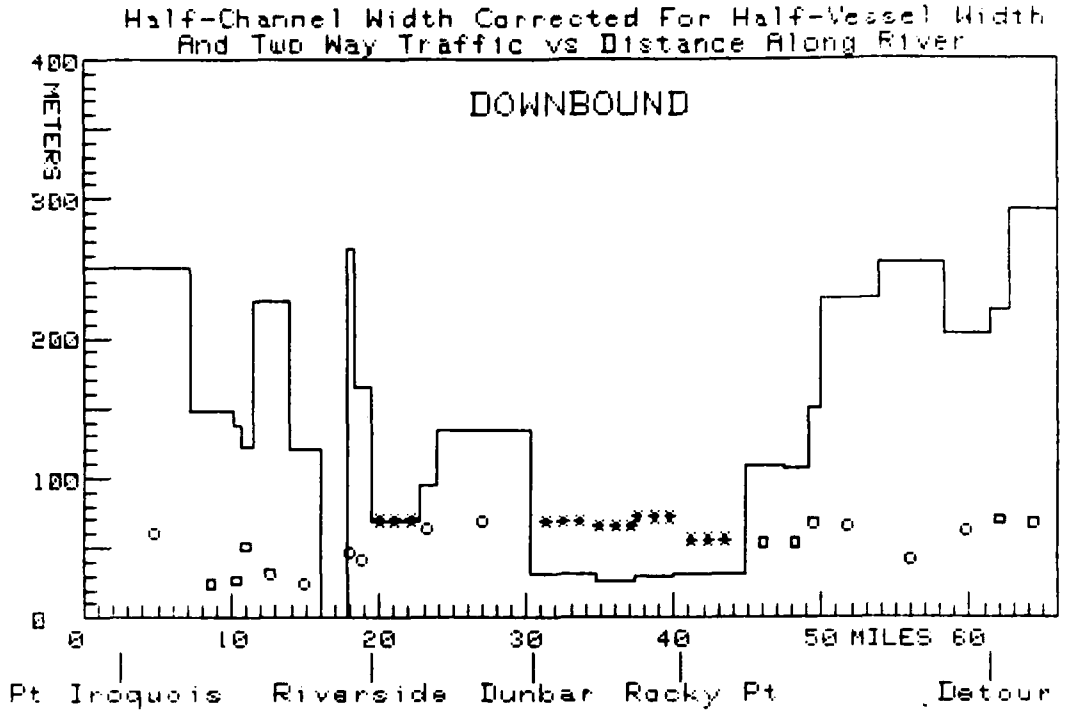

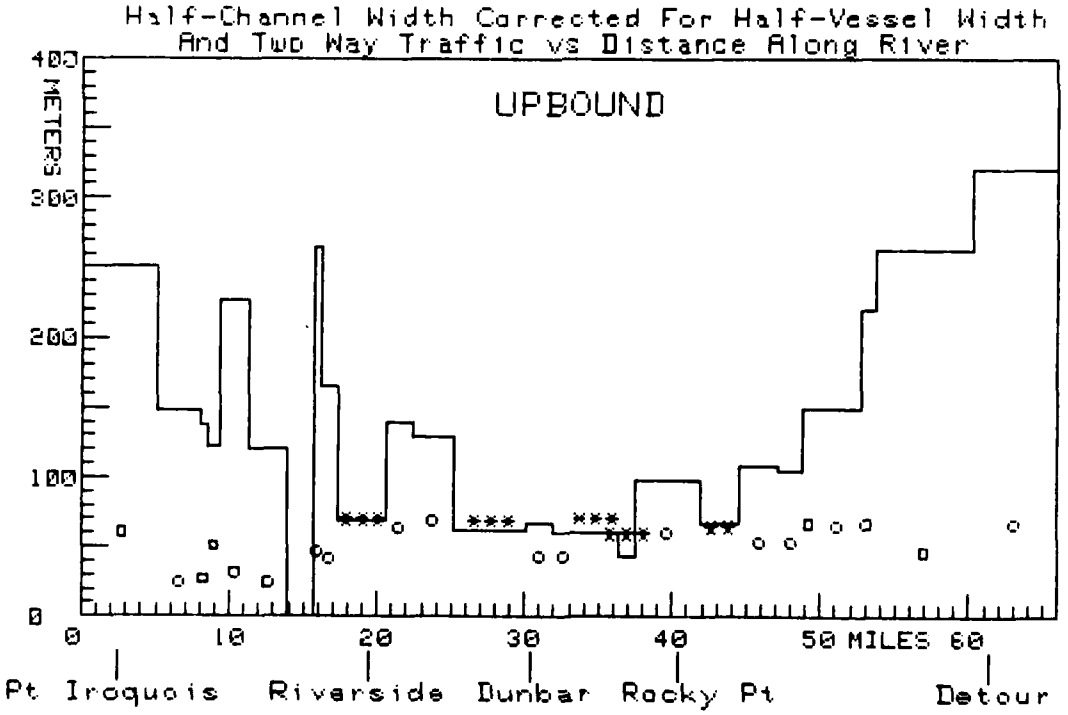

Figure 3-22 3-TD Fix Performance - 8970-X and -Y (Daily Corrections) 8970-Z (Ideal)

We see this combination satisfies the requirements in the wide reaches but not in the narrow reaches. Recalling the discussion of Section 3.4, and the performance as indicated in figure 3-9, however, we see this is no substantive change from what was obtained by simply applying 24-hour corrections. Thus, we arrived at consideration of this "joint enhancement technique" having concluded daily corrections had to be applied. We have now seen, there is no firm basis for the argument that the supplemental LOP must be provided in addition to the daily corrections. At this point in the January 1981 decision process, enough was seen to determine that operational implementation of the supplemental LOP could not be justified. Thus, the decision was made to cancel implementation plans.

There are other reasons for continuing examination of the concept, however, and since this was an R&D project, the supplemental LOP was operated for 6 months - through mid-1981. Additionally, there was a desire at the time to do something to provide high performance Loran-C in the St. Marys River. Finally, as previously mentioned, problems with Muskegon were suspected so that use of Riverside to control 8970-X, -Y, and -Z, at least on a temporary basis, was suggested. This allowed a very close approximation to differential Loran-C, with a relatively simple implementation. Thus, in May 1981, while the supplemental LOP experiment was being conducted, control of 8970-X and -Y was moved to Riverside.

As expected, performance was improved throughout the St. Marys River. Additionally, as noted in Section 2, it became much easier to conduct stability studies since, with mild TD variations, equipment problems could be more easily discerned. Data was collected at sites along the river for a full year and comprises the most intense data collection effort we will conduct during the stability studies. The results of this effort will be presented in Section 4.

Before considering those results, however, we should consider the final set of predictions made in support of the decision to shut down the Gordon Lake station. We felt it worthwhile to see if, given control of 8970-X and -Y from somewhere in the St. Marys River, there would be some over-riding reason to continue with the Gordon Lake station. The results of this analysis are presented in the next section.

3.8 Analysis Results, Control of the 8970-X and -Y Baselines from the St. Marys River Region

Year-round data to support this analysis was, of course, not available in early 1981. Thus, full use was made of the DRD model. Since Section 4 will contain a fully empirical analysis of the issues, this presentation serves the purpose of comparing the two approaches.

At this point, we return to the discussion of Section 3.5 wherein we stated that we needed to obtain joint second order statistics of the expected time difference variations. Once we have these, we can generate error ellipses - the expected pattern of the fixes obtained over a year. We argue that it is adequate to consider the TD variations as being comprised

of a seasonal and a short-term component (a more detailed discussion is provided in reference 15). We have further argued that the short-term standard deviation should be 11 nsec and the short term correlation coefficient between any two baselines should be +0.5. We have established that the seasonal variations follow the sinusoidal pattern as in figure 3-13 and that they are, essentially, perfectly correlated (correlation coefficient of +1 or -1) from one baseline to another. To use this fact, we need to obtain a way of properly describing the seasonal component with a standard deviation figure.

As reference 15 suggests, we can accomplish this if we know the peak-to-peak value of the expected smoothed TD swing. Since we expect this component to be sinusoidal, we divide the peak-to-peak swing in half and multiply by 0.707 to obtain an rms value which we will use for our estimate of the standard deviation of this component. Appendix C of reference 15 outlines the method of combining the short-term and seasonal statistics to obtain the desired "total" statistics - a total standard deviation for each baseline and a total correlation coefficient.

By examining the Mini-Chain data plots of reference 3, we find we can expect a sinusoidal component with a peak-to-peak swing of about 6 nsec/km as noted in the previous section. Thus, we expect the standard deviation of the seasonal component, at any point, to be:

$$2 \text{ nsec/km} \times \text{DRD (in km)}$$

Using this basis, we compute the expected statistics that are indicated in Table 3-2.

It is interesting to examine the table to see how our model suggests the standard deviation of the 8970-Z signal varies throughout the river. The so-called "vicinity of Riverside" appears to extend from about reach 20 to about reach 36 (except for the Yankee signal). There is one addition we should make to this table. As suggested in the previous section, we do not need to be "master-dependent." Specifically, if the Dana signal is off-air, we can use the Seneca (normal Xray) signal as the master and, along with the Yankee and Zulu signals, obtain a 2-TD fix. Using the same approach as used for Table 3-2, we compue the DRD's for this configuration and generate the predicted statistics shown in Table 3-3.

Reach Fm W.P.	To W.P.	σ_x (nsec)	σ_y (nsec)	σ_z (nsec)	ρ_{xy}	ρ_{xz}	ρ_{yz}
1	2	35.7	169.2	103.6	-0.94	-0.93	0.99
2	8	30.1	145.4	80.8	-0.91	-0.90	0.99
8	10	20.4	132.3	76.0	-0.82	-0.80	0.99
10	11	22.0	123.9	64.9	-0.84	-0.81	0.99
11	12	24.6	115.7	53.2	-0.87	-0.83	0.98
12	13	22.5	110.3	49.8	-0.84	-0.80	0.98
13	14	18.3	101.8	46.3	-0.76	-0.70	0.98
14	16	14.5	91.5	42.3	-0.60	-0.53	0.97
16	18	16.3	78.8	28.4	-0.68	-0.55	0.97
18	20	18.9	70.1	18.1	-0.76	-0.47	0.94
20	22	19.3	61.0	14.1	-0.75	-0.29	0.83
22	24	16.4	49.2	11.5	-0.65	0.11	0.68
24	26	13.1	44.2	13.1	-0.43	0.05	0.38
26	28	12.2	33.8	11.8	-0.26	0.27	0.64
28	30	11.4	18.3	11.0	0.08	0.22	0.32
30	32	11.1	11.9	11.0	0.41	0.50	0.43
32	33	11.0	13.0	11.0	0.39	0.50	0.46
33	34	11.5	19.9	11.0	0.03	0.50	0.22
34	35	12.5	22.3	11.6	-0.20	0.57	-0.04
35	36	15.1	24.4	13.8	-0.45	0.71	-0.36
36	37	21.1	26.8	20.2	-0.67	0.86	-0.65
37	38	29.0	26.8	29.7	-0.76	0.93	-0.77
38	39	34.8	24.4	37.3	-0.78	0.95	-0.79
39	40	36.7	23.4	39.9	-0.77	0.96	-0.78
40	41	43.8	24.2	48.7	-0.81	0.97	-0.82
41	42	53.3	34.6	58.1	-0.90	0.98	-0.90

Reach Fm W.P.	To W.P.	σ_x (nsec)	σ_y (nsec)	σ_z (nsec)	ρ_{xy}	ρ_{xz}	ρ_{yz}
1	3	33.5	174.3	111.7	-0.93	-0.92	0.997
3	5	35.5	164.8	98.6	-0.94	-0.93	0.995
5	7	33.6	155.2	88.9	-0.93	-0.92	0.994
7	9	22.5	143.2	82.9	-0.85	-0.83	0.994
9	11	21.4	125.5	66.9	-0.83	-0.81	0.98
11	12	25.5	115.7	53.2	-0.87	-0.83	0.98
12	13	23.4	110.3	49.8	-0.84	-0.80	0.98
13	14	19.1	101.8	42.3	-0.76	-0.70	0.98
14	15	12.3	86.9	43.0	-0.38	-0.31	0.98
15	17	11.0	71.5	35.7	-0.01	0.07	0.96
17	19	11.0	59.6	29.9	0.18	0.27	0.95
19	21	11.0	44.8	20.1	0.11	0.26	0.88
21	31	11.4	23.4	11.3	0	0.41	0.42
31	32	11.1	11.7	11.0	0.43	0.49	0.49
32	33	11.0	13.0	11.0	0.39	0.50	0.46
33	34	11.2	19.9	11.0	0.03	0.50	0.22
34	35	12.1	22.3	11.6	-0.20	0.57	-0.04
35	36	14.5	24.4	13.8	-0.45	0.71	-0.36
36	37	20.2	26.8	20.2	-0.67	0.86	-0.65
37	38	28.0	26.8	29.7	-0.76	0.93	-0.71
38	39	33.8	24.4	37.3	-0.78	0.95	-0.79
39	40	35.7	23.4	39.9	-0.77	0.96	-0.78
40	41	42.8	24.2	48.7	-0.81	0.97	-0.82
41	42	52.4	36.9	53.1	-0.90	0.98	-0.90

Table 3-2 Loran-C Chain 8970-X, -Y, and -Z Predicted TD Statistics in St. Marys River Reaches With Riverside as SAM

Reach				
Fm W.P.	To W.P.	σ_y (nsec)	σ_z (nsec)	ρ_{yz}
1	2	203.3	137.4	0.9998
2	8	173.5	108.6	0.9960
8	10	149.6	93.1	0.9942
10	11	143.0	83.7	0.9939
11	12	137.8	74.8	0.9923
12	13	130.1	69.1	0.99
13	14	116.5	67.5	0.98
14	16	101.0	51.4	0.98
16	18	90.9	39.8	0.97
18	20	85.5	31.8	0.95
20	22	76.8	26.9	0.93
22	24	61.4	18.9	0.85
24	26	51.4	18.1	0.84
26	28	39.0	14.5	0.73
28	30	20.9	11.5	0.49
30	32	12.6	11.0	0.46
32	33	13.3	11.1	0.48
33	34	22.5	11.3	0.42
34	35	27.5	11.3	0.39
35	36	33.8	11.2	0.33
36	37	43.6	11.0	0.21
37	38	52.2	11.0	0.03
38	39	55.7	11.3	-0.13
39	40	56.5	11.5	-0.20
40	41	64.7	12.1	-0.33
41	42	85.5	12.0	-0.34

Reach				
Fm W.P.	To W.P.	σ_y (nsec)	σ_z (nsec)	ρ_{yz}
1	3	205.8	143.2	0.9978
3	5	198.4	132.3	0.9970
5	7	186.8	120.5	0.9969
7	9	162.6	102.4	0.9953
9	11	143.6	85.1	0.9940
11	12	137.8	74.8	0.9923
12	13	130.1	69.1	0.99
13	14	116.5	67.5	0.98
14	15	92.5	48.3	0.98
15	17	72.6	36.7	0.97
17	19	58.8	29.0	0.94
19	21	45.2	20.2	0.88
21	31	26.2	12.3	0.59
31	32	12.3	11.0	0.47
32	33	13.3	11.1	0.48
33	34	22.5	11.3	0.42
34	35	27.5	11.3	0.39
35	36	33.8	11.2	0.33
36	37	43.6	11.0	0.21
37	38	52.2	11.0	0.03
38	39	55.7	11.3	-0.13
39	40	56.5	11.5	-0.20
40	41	64.7	12.1	-0.33
41	42	85.5	12.0	-0.34

Table 3-3 Loran-C Chain 8970 Predicted TD Statistics in St. Marys River Reaches With Riverside as SAM, Without Dana (Normal Master) Signal, Using Seneca as Master

Following the procedure outlined in Appendix A, we can use the statistics to generate error ellipses for any of the 2-TD fix combinations or the 3-TD fix combination. The ellipses will represent the 99.9% probability contour. By projecting the ellipse onto a rotated coordinate system determined by the channel course, we obtain the expected (99.9% probability) cross-track error for each reach. These values are listed in Tables 3-4 and 3-5 which also indicate the channel characteristics.

Reach Fm W.P.	Reach To W.P.	Corrected Half-Width Minus 16 m	MXY CTE	MXY Error Margin	MXZ CTE	MXZ Error Margin	MYZ CTE	MYZ Error Margin	XYZ CTE	XYZ Error Margin	MXYZ CTE	MXYZ Error Margin
1	2	351 m	73 m	278 m	56 m	294 m	141 m	210 m	108 m	243 m	130 m	221 m
2	8	293	68	225	35	188	24	269	12	271	19	274
8	10	220	12	208	9	211	41	179	44	176	55	165
10	11	149	55	94	41	108	94	54	74	75	89	60
11	12	149	15	134	17	132	53	96	53	96	49	80
12	13	105	36	69	15	90	8	97	18	87	10	93
13	14	108	35	73	17	91	9	99	14	94	13	95
14	16	67	20	47	11	56	11	53	18	49	29	38
16	18	99	44	55	32	67	58	41	49	50	60	39
18	20	43	17	26	8	35	5	38	15	28	10	33
20	22	61	26	35	24	37	33	28	35	26	37	24
22	24	61	24	37	15	46	20	41	17	44	14	47
24	26	66	24	42	37	29	18	48	18	48	10	56
26	28	63	11	52	8	55	6	57	14	49	17	46
28	30	129	11	118	9	120	8	121	15	114	13	116
30	32	139	11	128	9	130	8	131	23	116	12	127
32	33	69	11	58	8	61	8	61	26	43	13	56
33	34	165	15	150	46	119	14	151	43	122	10	155
34	35	264	[illegible]	250	40	224	12	252	43	221	12	252
35	36	LOCKS	17	--	58	--	17	--	44	--	17	--
36	37	121	18	103	56	65	18	103	35	86	26	95
37	38	226	24	202	49	177	24	202	29	197	30	196
38	39	123	30	93	49	74	30	93	30	93	23	100
39	40	137	21	118	46	91	21	116	27	110	33	104
40	41	148	15	133	41	107	15	133	24	124	42	106
41	42	251	36	215	38	213	36	215	44	207	35	216

Table 3-4 Loran-C Chain 8970-X, -Y, and -Z Predicted Performance in St. Marys River Reaches (Upbound Channel) With Riverside as SAM

Reach From W.P.	Reach To W.P.	Corrected Half-Width Minus 16 m	MXY CTE	MXY Error Margin	MXZ CTE	MXZ Error Margin	MYZ CTE	MYZ Error Margin	XYZ CTE	XYZ Error Margin	MXYZ CTE	MXYZ Error Margin
1	3	292 m	67 m	225 m	53 m	239 m	137 m	155 m	105 m	187 m	125 m	167 m
3	5	220	46	174	40	180	116	104	94	126	101	119
5	7	203	23	180	9	194	46	157	52	151	40	173
7	9	255	71	184	40	215	30	225	11	244	13	242
9	11	229	55	174	40	189	94	135	74	155	91	138
11	12	149	15	134	17	132	33	116	53	96	49	80
12	13	108	36	69	15	90	7	101	18	87	10	93
13	14	108	35	73	17	91	99	100	14	94	13	95
14	15	32	35	-3***	20	12	17	15	11	21	17	15
15	17	30	12	18	12	18	23	7*	23	7*	48	-18***
17	19	27	18	9*	12	15	9	18	11	16	27	0**
19	21	32	14	18	17	15	18	14	18	14	35	-3*
21	31	134	11	123	9	125	8	126	20	114	16	118
31	32	94	11	83	9	85	8	86	33	61	12	82
32	33	69	11	58	8	61	15	54	26	43	13	56
33	34	165	15	150	46	119	42	123	43	122	10	155
34	35	264	14	250	40	224	37	227	43	221	12	252
35	36	LOCKS	17	—	58	--	49	—	44	—	17	--
36	37	121	18	103	56	65	51	70	35	86	26	95
37	38	226	24	202	49	177	54	172	29	197	30	196
38	39	123	30	93	49	74	52	93	30	93	23	100
39	40	137	21	118	46	91	52	85	27	110	33	104
40	41	148	15	133	41	107	46	102	24	124	42	106
41	42	251	36	215	38	213	20	231	44	207	35	216

Table 3-5 Loran-C Chain 8970-X, -Y, and -Z Predicted Performance in St. Marys River Reaches (Downbound Channel) With Riverside as SAM

The channel widths have been adjusted to account for 2-way traffic, as previously discussed, and for vessel "half-widths" of 16 meters. Subtracting the 99.9% Loran-C cross-track error from this channel characteristic results in the entry in the column marked "error margin." Recall this is the value which gives an indication of what is left over for "guidance error." As before, we mark any reaches which do not satisfy our assumed criteria with an appropriate number of asterisks. In constructing Tables 3-4 and 3-5, we use the notation "XYZ" to indicate the situation wherein Seneca is serving as the "master" station.

In examining Table 3-4, we find first that our assumed requirements are satisfied (if we can believe the predictions) in all reaches of the upbound channel. Table 3-5 indicates the requirements in the downbound channel are almost satisfied but there are a few problem reaches. In view of the conclusion of the preceeding section (i.e., that we do not need the 8970-Z station), we should begin further exploration of the problem by examining the MXY combination.

Using the "MXY" combination, the reach from waypoint 17 to 19 is "borderline" - a 9 meter error margin is available for guidance error at the 99.9% probability level. The real problem is in the reach from waypoint 14 to 15. The actual error ellipse for this reach is as shown in figure 3-23.

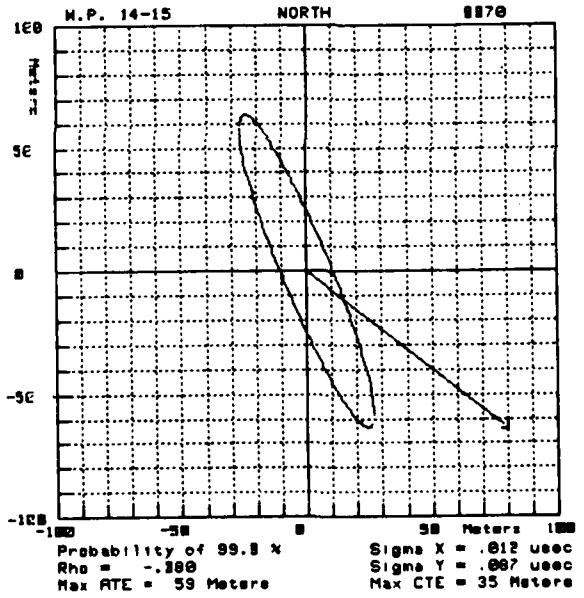

Figure 3-23 8970 MXY Predicted 99.9% Probability Error Ellipse Between Waypoints 14 and 15 Using Riverside as SAM

In figure 3-24 we show the 8970-X and -Y LOP's at the reach of interest. We note that for these baselines, the geometry changes very slowly over the river so that these LOP's are representative of what to expect in most reaches of interest.

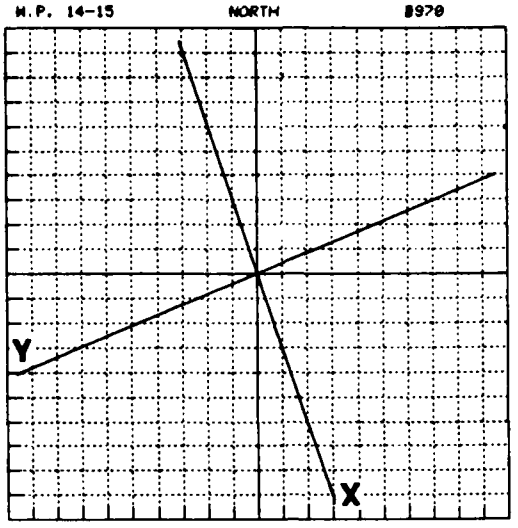

Figure 3-24 8970-X and -Y LOP's Between W.P. 14 and W.P. 15

Combining the information contained in Tables 3-1 and 3-3, we see that between waypoints 14 and 15, the problem arises from the combination of the "tightness" of the reach, the suboptimal course, and the large variation we expect in the 8970-Y signal. We cannot do anything about the first two factors but have some ways to reduce the variation. The simplest approach is to recall that we are hypothesizing a move of the monitor station and, thus far, have found we can make a substantial improvement in performance. To proceed therefore, we should simply realize that although Riverside is a convenient location, we have not yet established it is near optimal. Indeed, from figure 3-1 we see that Riverside is at the northern extreme of the series of narrow reaches - actually, about at waypoint 33. A better location would be more towards the center of the narrow reaches.

Returning to examination of the downbound channel section of Table 3-5, we see that as we move south of the problem reach (from waypoint 14 to waypoint 15), the 8970-Y variation is reduced fairly quickly. Thus, the location of the monitor in the vicinity of Dunbar Forest would seem a better choice. Before exploring this option, we should complete the examination of the effect of the supplemental LOP. As before, we find there are no problems along the upbound channel. The downbound channel is "borderline" for the "MYZ" and "XYZ" combinations but has significant problems for the MXYZ combination. Curiously, the MXZ combination, which gave results identified as "clearly unacceptable" in Section 3.6, now gives the best results. This indicates the far-reaching affects a monitor station move can have.

To summarize what this indicates, we again must conclude that if we prefer any alternative to the MXY combination, it is a situation wherein 8970-Z is being viewed as a "replacement LOP" rather than a supplemental LOP. There is marginal improvement to be gained by use of the Gordon Lake

station but, before overturning the decision mentioned in the previous section (not that anything seen thus far could truly justify such action), we should examine the performance expected if we choose Dunbar Forest as the monitor station.

To do this, we must recompute all of the DRD's and, hence the predicted statistics. The results of this re-computation are presented in Tables 3-6 and 3-7. These statistics are converted to 99.9% probability cross-track errors to obtain the performance results indicated in Tables 3-8 and 3-9.

Reach				
Fm W.P.	To W.P.	σ_y (nsec)	σ_z (nsec)	ρ_{yz}
1	2	162.2	121.1	0.9965
2	8	132.5	92.3	0.9936
8	10	108.6	76.8	0.9914
10	11	102.0	67.5	0.99
11	12	96.8	58.6	0.99
12	13	89.1	53.0	0.98
13	14	71.6	51.4	0.98
14	16	60.2	35.5	0.97
16	18	50.2	24.4	0.92
18	20	45.0	17.3	0.83
20	22	36.5	13.7	0.69
22	24	22.1	11.0	0.17
24	26	14.2	11.2	0.27
26	28	11.6	13.0	0.58
28	30	25.9	17.2	0.83
30	32	36.7	19.3	0.87
32	33	49.8	20.9	0.89
33	34	61.8	21.8	0.89
34	35	67.3	21.8	0.89
35	36	74.0	21.4	0.89
36	37	84.1	20.6	0.87
37	38	92.6	19.1	0.84
38	39	96.4	17.6	0.81
39	40	97.2	17.0	0.80
40	41	105.6	15.8	0.75
41	42	126.5	16.0	0.75

Reach				
Fm W.P.	To W.P.	σ_y (nsec)	σ_z (nsec)	ρ_{yz}
1	3	165.0	126.9	0.9965
3	5	157.6	115.9	0.9965
5	7	146.0	104.2	0.9955
7	9	121.9	86.1	0.9936
9	11	103.0	68.9	0.99
11	12	96.8	58.6	0.99
12	13	89.1	53.0	0.98
13	14	71.6	51.4	0.98
14	15	51.8	32.5	0.96
15	17	32.5	21.6	0.90
17	19	19.9	15.1	0.78
19	21	11.3	11.0	0.50
21	31	20.6	15.6	0.78
31	32	37.5	19.3	0.87
32	33	49.8	20.9	0.89
33	34	61.8	21.8	0.89
34	35	67.3	21.8	0.89
35	36	74.0	21.4	0.89
36	37	84.1	20.6	0.87
37	38	92.6	19.1	0.84
38	39	96.4	17.6	0.81
39	40	97.2	17.0	0.80
40	41	105.6	15.8	0.75
41	42	126.5	16.0	0.75

Table 3-6 Loran-C Chain 8970 Predicted TD Statistics in St. Marys River Reaches With Dunbar as SAM, Without Dana (Normal Master) Signal, Using Seneca as Master

Reach Fm W.P.	To W.P.	σ_x (nsec)	σ_y (nsec)	σ_z (nsec)	ρ_{xy}	ρ_{xz}	ρ_{yz}
1	2	36.7	127.3	86.5	-0.94	-0.93	0.9935
2	8	31.0	103.6	63.8	-0.91	-0.89	0.99
8	10	21.3	90.5	59.0	-0.82	-0.79	0.99
10	11	22.8	82.1	48.1	-0.84	-0.80	0.98
11	12	25.5	74.0	36.5	-0.86	-0.80	0.97
12	13	23.4	68.7	33.3	-0.83	-0.75	0.96
13	14	19.1	60.2	29.9	-0.75	-0.65	0.95
14	16	15.1	50.0	26.0	-0.59	-0.47	0.93
16	18	17.0	37.6	27.5	-0.64	-0.57	0.94
18	20	19.8	29.3	17.3	-0.66	-0.46	0.84
20	22	20.1	21.1	13.5	-0.57	-0.26	0.71
22	24	17.2	12.5	11.2	-0.09	0.16	0.53
24	26	13.7	11.0	12.6	0.36	0.06	0.47
26	28	12.6	14.9	14.5	0.65	-0.11	0.13
28	30	11.7	29.5	20.2	0.49	0.54	0.88
30	32	11.3	39.0	21.1	0.34	0.43	0.89
32	33	11.0	50.2	21.1	0.15	0.29	0.89
33	34	11.2	59.6	19.7	-0.11	0.11	0.87
34	35	12.1	62.4	16.9	-0.33	-0.02	0.80
35	66	14.5	64.7	14.1	-0.57	-0.11	0.68
36	37	20.2	67.3	11.0	-0.79	0.26	0.10
37	38	28.0	67.3	15.1	-0.88	0.78	-0.62
38	39	33.8	64.7	21.4	-0.91	0.90	-0.80
39	40	35.7	63.6	23.9	-0.91	0.92	-0.83
40	41	42.8	64.5	32.1	-0.93	0.95	-0.90
41	42	52.4	75.6	41.3	-0.95	0.97	-0.93

Reach Fm W.P.	To W.P.	σ_x (nsec)	σ_y (nsec)	σ_z (nsec)	ρ_{xy}	ρ_{xz}	ρ_{yz}
1	3	34.4	132.5	94.6	-0.93	-0.92	0.9947
3	5	36.5	122.9	81.5	-0.94	-0.92	0.9934
5	7	34.6	113.3	71.8	-0.93	-0.91	0.9919
7	9	23.4	101.4	65.9	-0.85	-0.83	0.99
9	11	22.3	83.7	50.0	-0.86	-0.79	0.98
11	12	25.5	74.0	36.5	-0.86	-0.80	0.97
12	13	23.4	68.7	33.3	-0.83	-0.75	0.96
13	14	19.1	60.2	29.9	-0.75	-0.65	0.95
14	15	12.7	45.5	26.8	-0.38	-0.28	0.93
15	17	11.2	30.6	20.1	0.01	0.12	0.88
17	19	11.0	19.9	15.3	0.28	0.36	0.78
19	21	11.1	11.1	11.0	0.48	0.50	0.49
21	31	11.7	24.1	18.4	0.52	0.56	0.85
31	32	11.2	39.6	19.9	0.32	0.44	0.88
32	33	11.0	50.2	21.1	0.15	0.29	0.89
33	34	11.2	59.6	19.7	-0.11	0.11	0.87
34	35	12.1	62.4	16.9	-0.33	-0.02	0.80
35	36	14.5	64.7	14.1	-0.57	-0.11	0.68
36	37	20.2	67.3	11.0	-0.79	0.26	0.10
37	38	28.0	67.3	15.1	-0.88	0.78	-0.62
38	39	33.8	64.7	21.4	-0.91	0.90	-0.80
39	40	35.7	63.6	23.9	-0.91	0.92	-0.83
40	41	42.8	64.5	32.1	-0.93	0.95	-0.90
41	42	52.4	75.6	41.3	-0.95	0.97	-0.93

Table 3-7 Loran-C Chain 8970-X, -Y, and -Z Predicted TD Statistics in St. Marys River Reaches With Dunbar as SAM

Reach Fm W.P.	Reach To W.P.	Corrected Half-Width Minus 16 m	MXY CTE	MXY Error Margin	MXZ CTE	MXZ Error Margin	MYZ CTE	MYZ Error Margin	XYZ CTE	XYZ Error Margin	MXYZ CTE	MXYZ Error Margin
1	2	321 m	62 m	259 m	53 m	268 m	98 m	223 m	81 m	240 m	91 m	230 m
2	8	263	44	219	27	236	21	242	14	249	20	243
8	10	220	11	209	9	211	22	198	24	196	36	184
10	11	149	43	106	36	113	59	90	50	99	60	89
11	12	149	18	131	18	131	33	116	33	116	29	120
12	13	105	18	87	9	96	7	98	12	193	10	95
13	14	108	18	90	11	97	8	100	20	88	9	99
14	16	67	12	55	8	59	7	60	9	58	16	51
16	18	99	26	63	32	67	21	78	27	72	33	66
18	20	43	12	31	8	35	7	36	12	31	9	34
20	22	61	20	41	24	37	10	51	18	43	16	45
22	24	61	12	49	18	43	8	53	14	47	12	49
24	26	67	12	55	18	49	8	59	15	52	9	58
26	28	63	12	51	8	55	10	53	15	48	12	51
28	30	129	11	118	11	118	9	120	18	111	24	105
30	32	139	15	124	18	121	17	122	33	106	24	115
32	33	69	12	57	14	55	15	54	38	31	33	36
33	34	165	36	129	88	77	42	123	84	81	10	155
34	35	264	32	232	76	188	37	227	82	182	12	252
35	36	LOCKS	47	--	108	--	49	--	85	--	29	--
36	37	121	50	71	105	16	51	70	79	42	43	78
37	38	226	55	171	87	139	54	172	64	162	59	167
38	39	123	55	68	81	42	52	71	56	67	56	67
39	40	137	53	84	82	55	52	85	62	75	59	78
40	41	148	46	102	73	75	46	102	59	89	62	86
41	42	251	46	205	18	233	20	231	26	225	19	232

Table 3-8 Loran-C Chain 8970-X, -Y, and -Z Predicted Performance in the St. Marys River Reaches (Upbound Channel) With Dunbar as SAM

Reach Fm W.P.	Reach To W.P.	Corrected Half-Width Minus 16 m	MXY CTE	MXY Error Margin	MXZ CTE	MXZ Error Margin	MYZ CTE	MYZ Error Margin	XYZ CTE	XYZ Error Margin	MXYZ CTE	MXYZ Error Margin
1	3	292 m	58 m	234 m	50 m	242 m	95 m	197 m	78 m	214 m	94 m	198 m
3	5	220	41	179	40	180	79	141	68	152	72	148
5	7	203	12	191	9	194	27	176	32	171	24	179
7	9	255	47	208	30	225	26	229	15	240	14	241
9	11	229	43	186	36	193	60	169	50	179	62	167
11	12	149	18	131	18	131	33	116	33	116	29	120
12	13	108	18	90	9	99	7	101	12	96	10	95
13	14	108	18	90	11	97	8	100	20	88	9	99
14	15	32	18	14	12	20	12	20	11	21	10	22
15	17	30	11	19	11	19	9	21	9	21	22	8*
17	19	27	12	15	8	19	7	20	11	18	13	14
19	21	32	8	24	14	18	7	25	6	26	10	22
21	31	134	11	123	11	123	9	125	15	119	20	114
31	32	94	15	79	18	74	16	78	33	61	24	70
32	33	69	12	87	14	55	15	54	26	43	33	36
33	34	165	36	129	88	77	42	123	84	81	10	155
34	35	264	32	232	76	188	37	227	82	182	12	252
35	36	LOCKS	47	—	108	—	49	—	85	—	29	—
36	37	121	50	71	105	16	51	70	79	42	43	78
37	38	226	55	171	87	139	54	172	64	162	59	167
38	39	123	55	68	81	42	52	71	56	67	56	67
39	40	137	53	84	82	55	52	85	62	75	59	78
40	41	148	46	102	73	75	46	102	59	89	62	86
41	42	251	46	205	18	233	20	231	26	225	19	232

Table 3-9 Loran-C Chain 8970-X, -Y, and -Z Predicted Performance in St. Marys River Reaches (Downbound Channel) With Dunbar as SAM

From Table 3-8 we see that, again, the upbound channel is not a problem. More importantly, Table 3-9 shows that the downbound channel is not a problem (except for one "borderline" reach in the 3-TD case).

At this point we should inject a comment regarding the 3-TD fix performance which, perhaps contrary to intuition, is proving less adequate than certain 2-TD combinations. There is no theoretical reason why the 3-TD performance could not be made better than any 2-TD case. The required implementation is non-trivial and is not presently available. When we speak of implementation, of course, we are talking about PILOT and the problem is the way that PILOT "weights" the 3 TD's in the position solution. As mentioned in Appendix A, the PILOT approach attempts to optimize "tracker jitter" performance. Thus, it most heavily counts the strongest signal received rather than the signal which is hyperbolically closest to the monitor (i.e., rather than DRD considerations). The calculations of the weighting function could be changed. (Actually, at least for the St. Marys River area - as Section 4 will show - it is just as easy to compute a DRD-based weighting function as it is to compute the present one.) When this is accomplished, however, one has done the wrong thing if the "TD-offset" feature of PILOT is used to correct for seasonal variations. Of course, one could make PILOT flexible enough to use either approach but we expect it would prove necessary to take a combined approach. Recognizing that all of this is in itself "more R&D work," we avoid the issue by simply examining what presently exists. Since the 3-TD performance is approximately the same as the best 2-TD performance in all cases, we claim the conclusions of the report will be the same no matter what is done with PILOT. It is important, however, to provide an explanation for the seeming anomaly and not pass up an opportunity as the Loran-C R&D program enters its final phase to note: there's more to Loran-C than meets the eye.

Regarding the "MXY" combination, Table 3-7 shows how the previous problem which we had with the monitor at Riverside has been solved: in the reach from waypoint 14 to 15, the 8970-Y standard deviation has been reduced from about 87 nsec to about 46 nsec.

3.9 Summary of Preliminary Performance Analysis

We are now ready to complete the discussion of our predictions and should note that we have not uncovered a situation wherein, for the St. Marys River and the existing 8970 chain, there is a noticable performance advantage to be gained by the additional secondary station. To summarize the findings described in this section, and to reinforce the conclusions, we present Table 3-10.

Technique Considered	Section Discussed	Conclusion Wide Reaches	Conclusion Narrow Reaches
"Raw" MXY	3.3	UNSAT	UNSAT
MXY With Daily Corrections	3.4	SAT	UNSAT
"Raw" MXY Riverside SAM	3.8	SAT	UNSAT (but close)
"Raw" MXY Dunbar SAM	3.8	SAT	SAT
"Raw" MXY Plus Ideal Z	3.6	UNSAT	UNSAT
MXY With Daily Corrections Plus Ideal Z	3.7	SAT	UNSAT
"Raw" MXY Riverside SAM Plus Z	3.8	SAT	UNSAT (but close)
"Raw" MXY Dunbar SAM Plus Z	3.8	SAT	SAT

Table 3-10 Summary of Examined Techniques and Performance Conclusions

The table illustrates how the "With" and "Without" situations are identical - performance-wise. Under these circumstances, the only possible argument for the Supplemental LOP is the "redundancy/reliability" argument.

The issue of redundancy/reliability, as previously noted however, has problems. For all cases we have examined, whereas performance can improve at times, it can also degrade at times (depending upon the combination being employed). A remaining argument in favor of the extra station is what can be called "confirmation," i.e., the concept that using three LOP's is better than using two.

This "confirmation" argument has merit but before we put too much emphasis on it, we should take a broader look at the system. We must recognize that we are stretching Loran-C to its limits (actually, beyond) in considering it as a "stand-alone" solution in the narrow reaches. At these limits, equipment (e.g., receiver) charactertics are more likely causes of problems than the propagation/weather effects that are so predominant under "normal" circumstances. The point is that with one receiver, one antenna, one coupler, etc., you still have a single system and the "redundancy" argument is not truly supportable.

This is not a new concept. Even for the Mini-Chain, it was concluded that Loran-C could not be considered a stand-alone system for "blind" transit of the narrow reaches of the river. Given radar, however, a truly redundant system is available. Local mariners indicate that radar return is entirely adequate in the narrow reaches. This reenforces the statement made in reference 3, and repeated in Section 1.4, that "a system was not really needed in several of the river's narrow sections, such as the West Neebish Island 'rock cut'." As the final point to present in the discussion of predicted performance, we must mention that these "narrow sections" are the "tight" reaches of the downbound channel that we have been discussing in the last few sections. We should begin the empirical analysis of Section 4 recalling this fact and that, whereas we accomplish "an HHE Loran-C R&D" purpose by seeing what, if anything, can be done to optimize Loran-C performance in these reaches, negotiation of those reaches is more properly described as a "radar problem."

4. Analysis of Data

4.1 Harbor Monitor Set Data With Riverside as SAM

The Harbor Monitor sets were installed in the St. Marys River in mid-February 1981 and removed in late May 1982. Riverside became the SAM for the 8970-X and -Y baselines in late May 1981. Since we want to concentrate on what happens with a local control site, we will examine the data obtained from May 1981 to May 1982. Figure 4-1 shows the 8970-X data at the five data collection sites and figure 4-2 shows the 8970-Y data.

We have arranged the data "modulo 1 calendar year" to be consistent with the sinewave concept illustrated in figure 3-13. Thus, the first 140 days plotted represent 1982 data whereas the remaining data was obtained in 1981. Additionally, we have arranged the plots, from top to bottom, in order of increasing double range difference. Thus, for example, Pt. Iroquois, hyperbolically closer to the Xray secondary station (at Seneca, N.Y.) than SAM is, appears at the top of figure 4-1. Detour, hyperbolically closer to the master station (at Dana, In.) than the SAM is, appears at the bottom.

We can recall from figure 3-17 that the 8970-Y LOP's run approximately across track in the St. Marys River region. Thus, as we proceed from one end of the river to the other, we expect a fairly large accumulation in the 8970-Y DRD and thus a fairly large change in the seasonal component of the variation. The 8970-X LOP's, conversely, run approximately along track so there should be a smaller DRD change along the river and, therefore, a smaller change in the seasonal component of the variations. Again, to properly illustrate the concept, we have used the same vertical axis scale with all the plots.

In examining the plots, we see right away that the general pattern is as expected. The records certainly do not look like the pure sinewaves of figure 3-13, but the sinusoidal component, which becomes more predominant as the distance from the SAM increases, is discernible. In figure 4-3 and 4-4, we show heavily filtered versions of the same data records which make the pattern a bit more noticable.

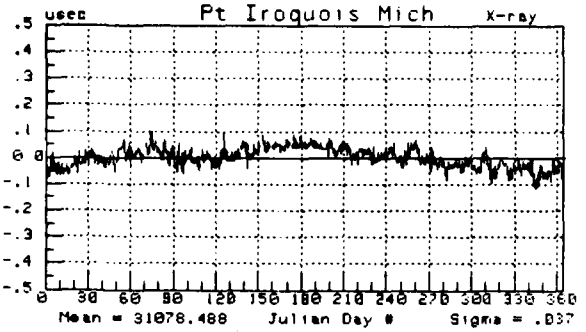

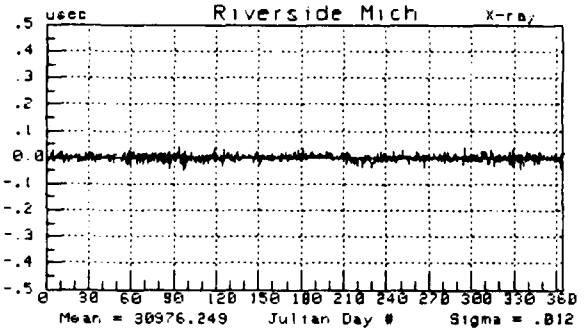

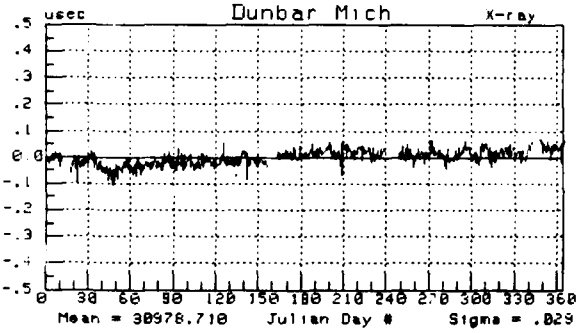

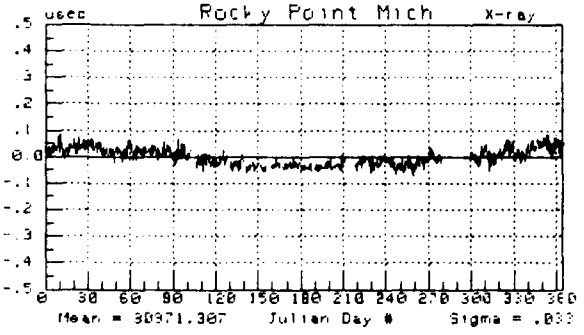

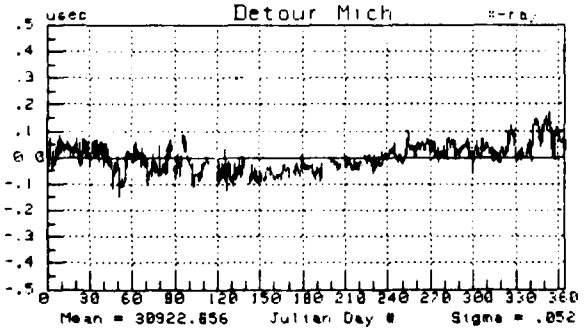

Figure 4-1 Harbor Monitor Site Data for 8970-X Baseline

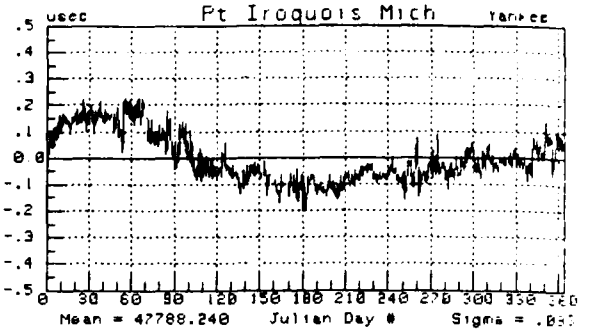

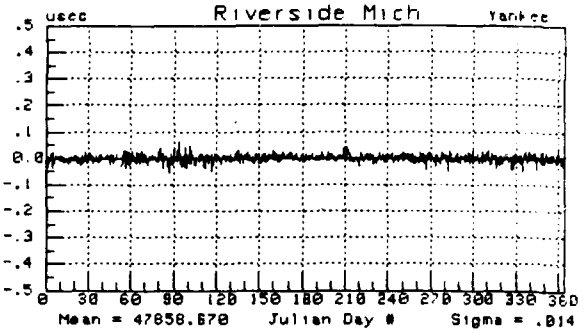

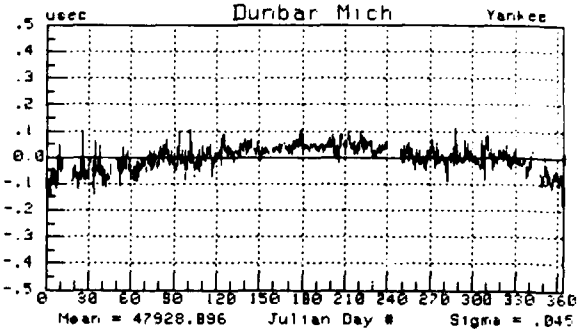

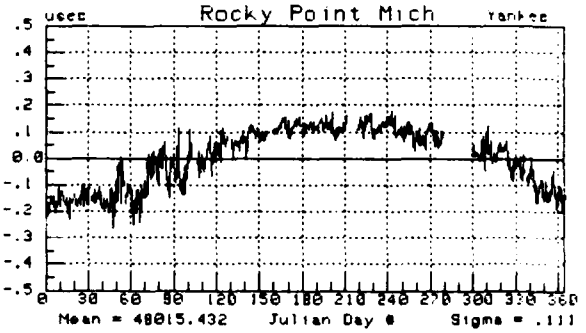

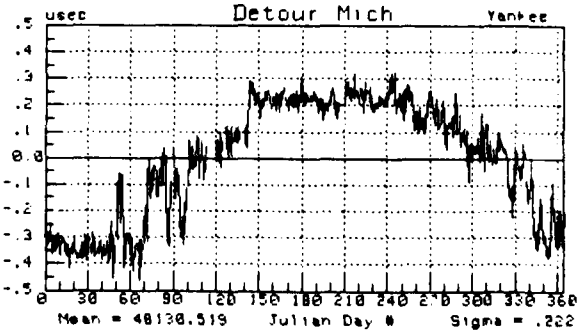

Figure 4-2 Harbor Monitor Site Data for 8970-Y Baseline

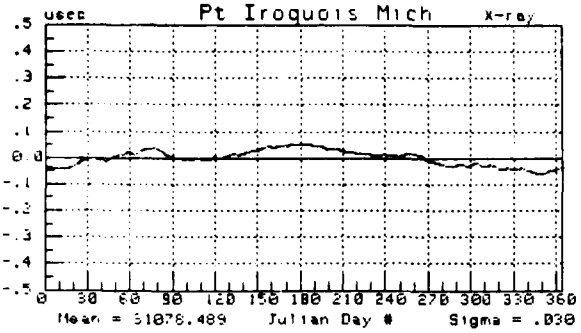

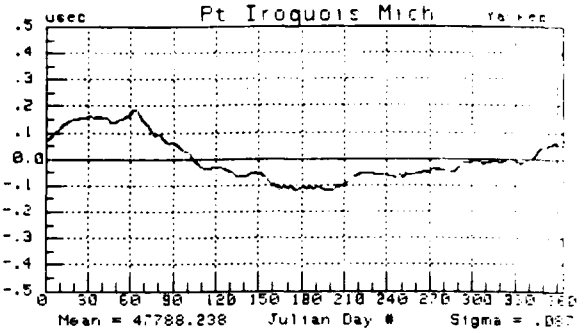

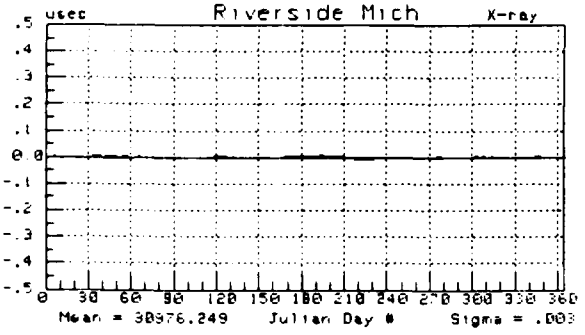

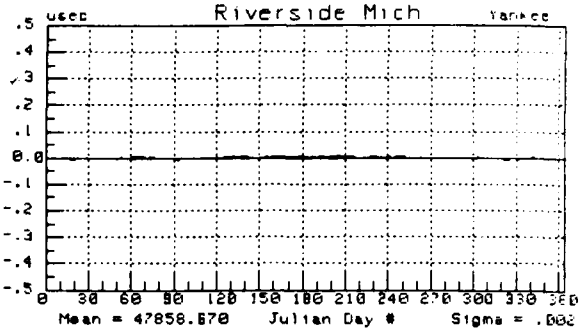

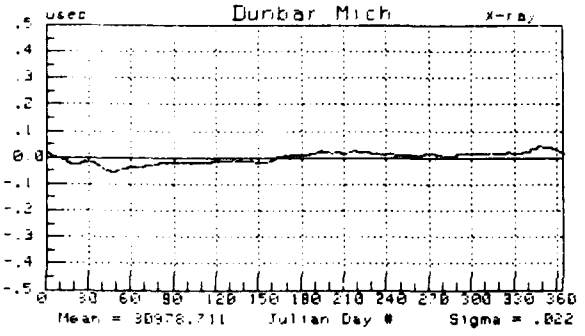

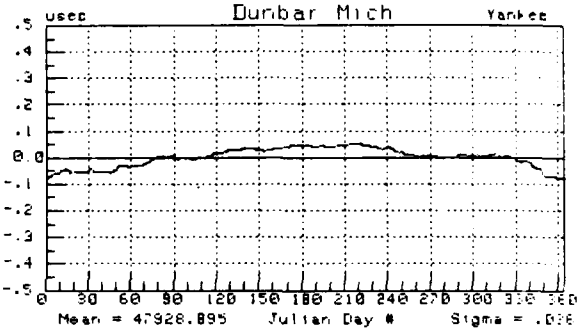

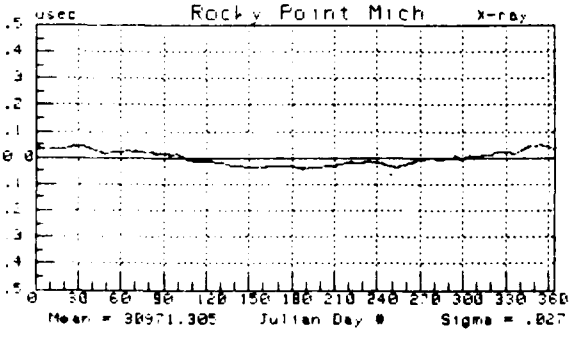

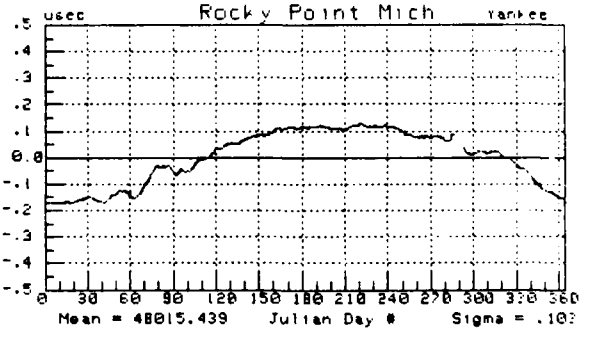

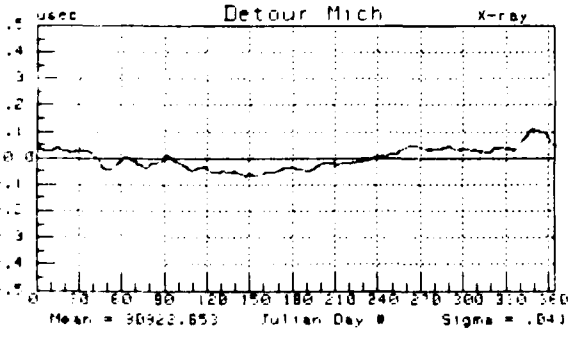

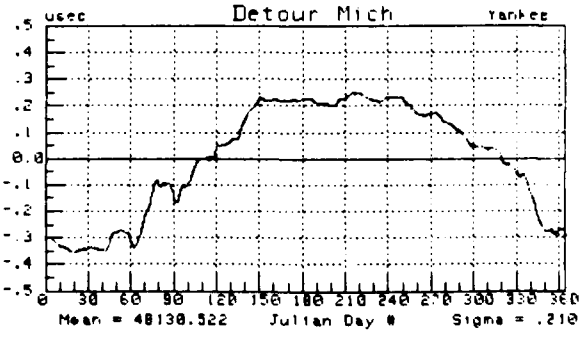

Figure 4-3 Filtered Version of 8970-X Data

Figure 4-4 Filtered Version of 8970-Y Data

Closer examination will show some problems with the data records. These problems will be the subject of considerable discussions in later sections. For now we should point out there will be two goals of the analyses to follow. First, of course, we want to compare empirical results to the "Gordon Lake utility" predictions of the previous section. More importantly, however, since this is the first in-depth examination of multiple harbor monitor site data under the ongoing stability studies, we want to check for more far-reaching implications. Specifically, recall that in Section 3 we implied there is a "floor" to the expected Loran-C performance - determined, so we suggested, by how the local geometry transforms 11 nsec standard deviations to fix error. This "floor" represents the performance one can expect when operating in the immediate vicinity of the SAM or, alternatively, is within a factor of $\sqrt{2}$ of what can be expected when operating in the immediate vicinity of a single differential monitor station. (The monitor station broadcasts some amount of noise as well as structured information). The most important question we can answer involves the suitability of the 11 nsec figure.

We do not wish to downplay the importance of the "Gordon Lake utility" question. As should be clear from Section 3, however, it will be an easy matter to confirm the soundness of the "terminate" decision. We want to take greater pains with the data, however, and must emphasize that the motivation comes from considerations outside the St. Marys River area. Hopefully, these greater pains will shed some light on the "floor" question and provide some insight for further experimentation under the Harbor Monitor program. Thus, in the next few sections, we will comment on St. Marys River performance so that, those matters being put to rest, we can examine the larger questions.

We begin the analysis of the data by recognizing the critical "position parameter" used in Section 3 was cross-track error. Thus, for each data collection site, we convert the TD data of figures 4-1 and 4-2 to the cross-track error plots shown in figure 4-5. The courses used in the computations come from those reaches closest to the data collection sites: from W.P. 41 to 42 (Pt. Iroquois), from W.P. 30 to 32 (Riverside), from W.P. 26 to 28 (Dunbar), from W.P. 13 to 14 (Rocky Point), and from W.P. 1 to 2 (Detour).

The first use we want to make of the results indicated in figures 4-1, 4-2 and 4-5 is to compare them to the predictions of Section 3. We can compare the statistics of figures 4-1 and 4-2 to the predictions directly. For comparing the cross-track readings to the predictions, we argue that although the fixes have not resulted in perfectly symmetrical "left and right of course" error records, they almost have. Thus, we will use the average of the two extreme readings for the comparison. Since we have about 700 data points for each site, we argue it is reasonably appropriate to compare these extremes to the 99.9% probability predictions of the previous section. Thus, we obtain the "predicted vs observed" comparisons shown in table 4-1. The predicted values come directly from appropriate entries in tables 3-2, 3-3, and 3-4 except in the case of Riverside where we know the expected "sigmas" are 11 nsec and the expected "rho" is 0.5. This corresponds to an expected cross-track error (99.9% probability level) of 12 meters.

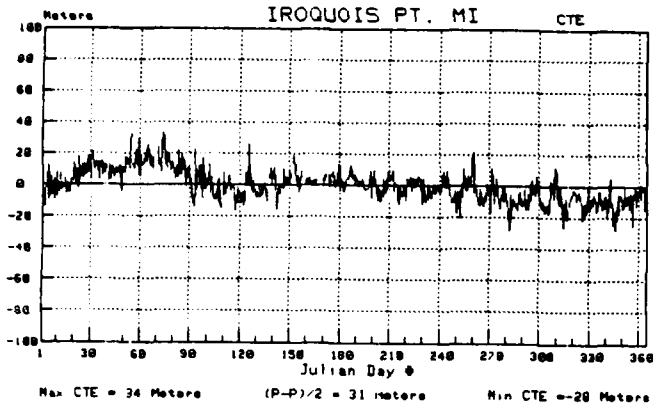

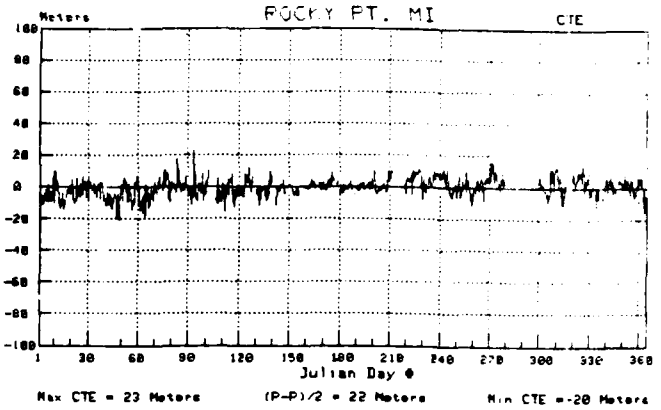

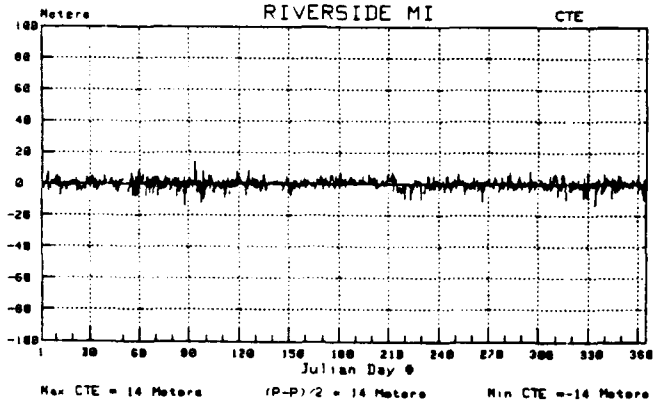

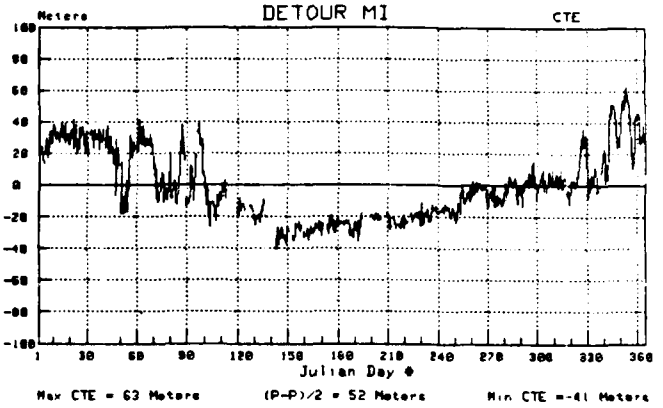

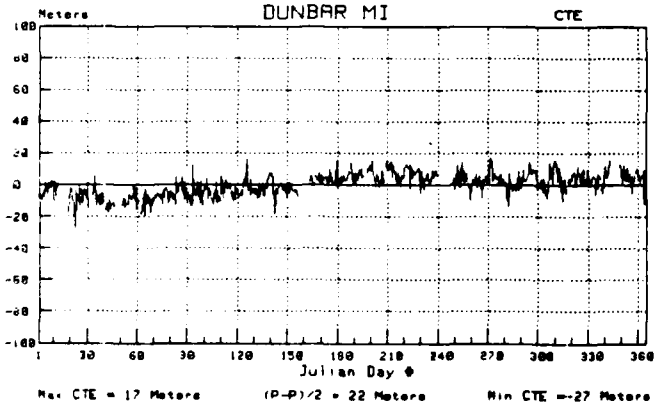

Figure 4-5 Data of Figures 4-1 and 4-2 Converted to Cross-Track Error

Site	Parameter	Predicted	Observed
Pt. Iroquois	σ_x	53 nsec	37 nsec
(W.P. 41-42)	σ_y	35 nsec	93 nsec
	ρ_{xy}	-0.90	-0.18
	CTE	36 m	31 m
Riverside	σ_x	11 nsec	12 nsec
(W.P. 30-32)	σ_y	11 nsec	14 nsec
	ρ_{xy}	0.50	0.48
	CTE	11 m	14 m
Dunbar	σ_x	12 nsec	29 nsec
(W.P. 26-28)	σ_y	34 nsec	45 nsec
	ρ_{xy}	-0.26	0.52
	CTE	11 m	22 m
Rocky Point	σ_x	18 nsec	28 nsec
(W.P. 13-14)	σ_y	102 nsec	111 nsec
	ρ_{xy}	-0.76	-0.334
	CTE	35 m	22 m
Detour	σ_x	36 nsec	55 nsec
(W.P. 1-2)	σ_y	169 nsec	222 nsec
	ρ_{xy}	-0.94	0.105
	CTE	73 m	56 m

Table 4-1 Comparison of Critical Parameters: Predicted vs Measured

At first glance, the comparison of Table 4-1 seems to be sending us conflicting signals: the comparison is very close in some cases but way off in others and no particular pattern emerges. To look for some meaning, let

us return to our model and what it says should determine the statistics of the TD's. Recall we expect the total standard deviation to come from the combination of two independent components. Because of the independence, we expect the total standard deviation to be the root-sum-square of the standard deviation for each component. We expected a standard deviation of 11 nsec for the spatially independent component and expected the standard deviation of the seasonal component to be directly proportional to the DRD.

Suppose we were wrong about the 11 nsec figure. Let's consider the Dunbar results and see if we can obtain a better estimate. In the interest of brevity, we did not list all of the computations leading to the standard deviation predictions. In the case of Dunbar, we expected a standard deviation of the X seasonal component of 5.2 nsec (notice we give the value to the nearest 100 picoseconds - that's what the calculator said!). The standard deviation of the Y seasonal component was expected to be 32 nsec. Root-sum-squared with 11 nsec, these lead to the 12 nsec and 34 nsec figures of table 3-2 and 4-1. Suppose, however, we should have used an estimate of 28.5 nsec for the standard deviation of the spatially independent component. This would combine, root-sum-squared, with the 5.2 and 32 nsec figures to yield "total sigmas" of 29 and 43 nsec, comparing very nicely with the observed values of 29 and 45 nsec, respectively.

Making the numbers come out nice, as above, is easy for one site (two equations, one unknown makes it easy but not guaranteed). What about another site? For Rocky Point, the X seasonal component standard deviation was estimated to be 14.6 nsec and the Y seasonal component standard deviation was estimated to be 101.2 nsec. If we root-sum-square these with the "new estimate" of the spatially independent component standard deviation, i.e., the 28.5 nsec figure, we obtain "total sigma" estimates of 32 and 105 nsec. Again we have nice agreement with the observations of 28 nsec and 111 nsec. The agreement is so nice that it's worth a table or two.

		Old Estimate of Spatially Independent Component			Enlightened Estimate of Spatially Independent Component		
Site	Parameter	Predict	Observe	% Error	Predict	Observe	% Error
Dunbar	σ_x	12	29	142%	29	29	0%
	σ_y	34	45	32%	43	45	5%
Rocky Point	σ_x	18	28	56%	32	28	12%
	σ_y	102	111	8%	105	111	6%

Table 4-2 Comparison of Old and New Estimate of Spatially Independent Component

From table 4-2 we see that the old estimate gave us "embarrassing" agreement between predicted and observed results whereas the enlightened estimates are uniformly respectable. Much more important, however, there is a pattern to the table. The first indication of the pattern is that there is not much improvement between the old and enlightened estimate in the "Rocky Point - Y" case - the case wherein we expected the largest "total sigma." Indeed, we see that with the old estimate, there is a uniformly observed pattern to the estimate error: the larger the expected standard deviation, the smaller the % error. This is consistent with what we would expect with an incorrect estimate of the spatially independent component which is a strong contributor to the "total sigma" for small DRD's but approaches an insignificant level for the larger DRD's.

At this point we must contain our enthusiasm and recognize we are considering only 2 of 5 sites. We note, however, that we have considered 2 of 3 sites which, in general, feature small DRD's. For Detour and Pt. Iroquois, i.e., the sites with the larger DRD's, we have another degree of freedom at our disposal in that we can revise our estimate of the DRD effect. Since the DRD effect is not a larger contributor to the results at Dunbar and Rocky Point (in general), we may be able to accomplish this without significantly compromising the "nice" results of the "enlightened" section of table 4-2. This refinement, which we will save for later sections, however, should not be accomplished before we attend to the matter of Riverside.

Regarding Riverside, notice how table 4-1 indicates we have, essentially, perfect agreement with the predictions of Section 3 - for "rho" as well as the sigmas (and, of course for CTE which is directly determined by the other three). Thus, we sacrifice this outstanding agreement if we employ our "enlightened" estimate. All of this suggests there is, at least, one more degree of freedom to the problem and, indeed, the model we will employ in Section 4.3 features such a term. Specifically, since Riverside data was obtained with the "wideband" Austron 5000 receiver, whereas the data at the other sites was obtained with the "narrowband" Internav 404 receivers, we can expect that there are variations seen by one receiver type that are not seen by the other. Thus, there is a chance we may be able to explain all of this yet. What has to happen, however, is that the high "spatially independent" components have to prove strongly correlated from one Internav 404 site to the other. As mentioned, we will explore this beginning with Section 4.3. For now, however, we should complete the examination of "what is" in the St. Marys River. In other words, although we may find an "Austron 5000 vs Internav 404 related" explanation for the larger-than-expected variations, that does not change the fate of a PILOT (uses an Internav 404) equipped mariner in an Austron 5000 controlled chain.

To examine the performance implications of the data, we should turn to consideration of the scatter plots. These are shown in figure 4-6 along with corresponding predicted error ellipses. The predictions are made using the statistics generated as in Section 3. The statistics indicated on the plots will be slightly different than those shown in Table 4-1 since we will now make predictions about what we expect for each site, vice the midpoint of the nearest reach.

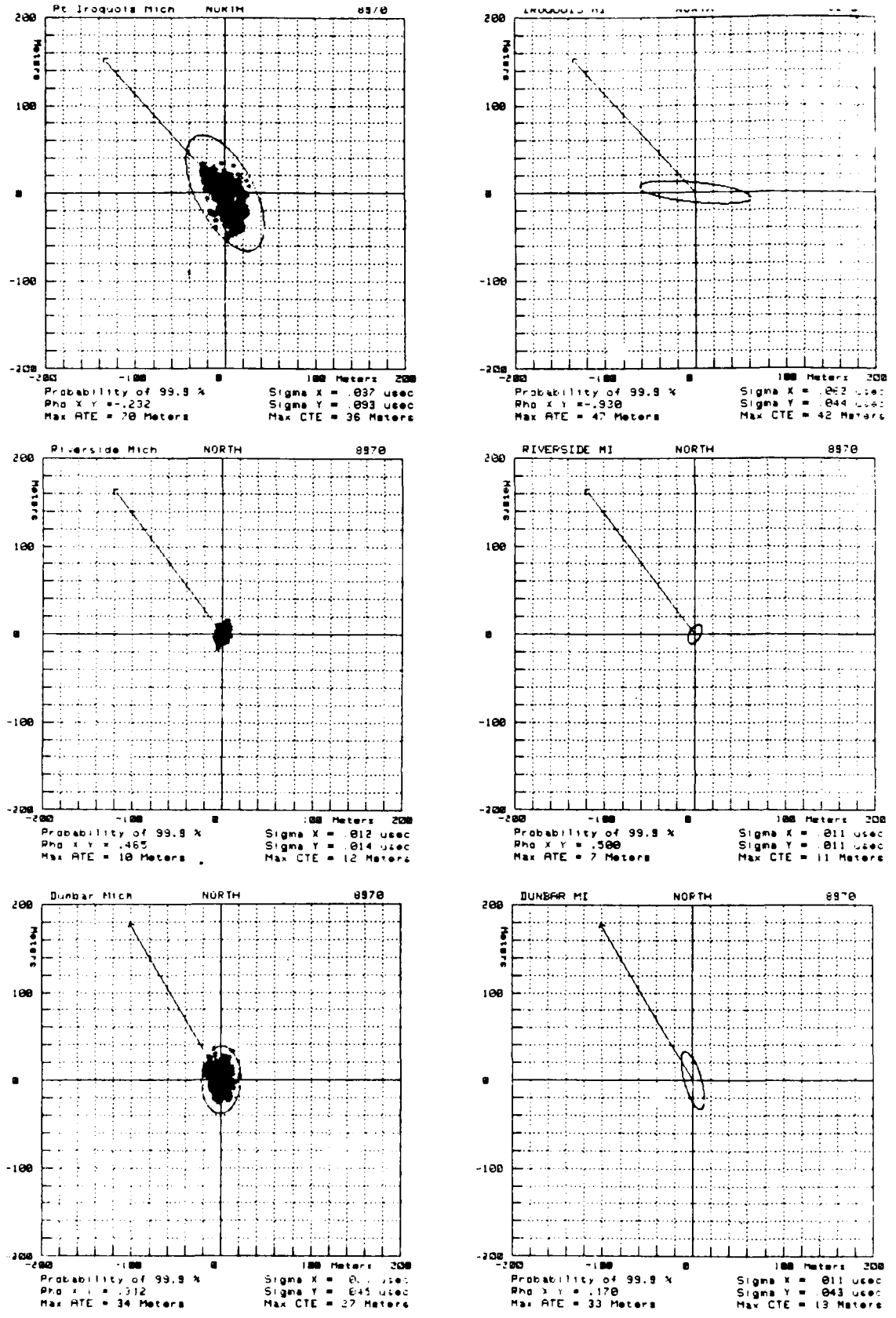

Figure 4-6 Comparison of Scatter Plots of Harbor Monitor Site Data With Predicted Error Ellipses

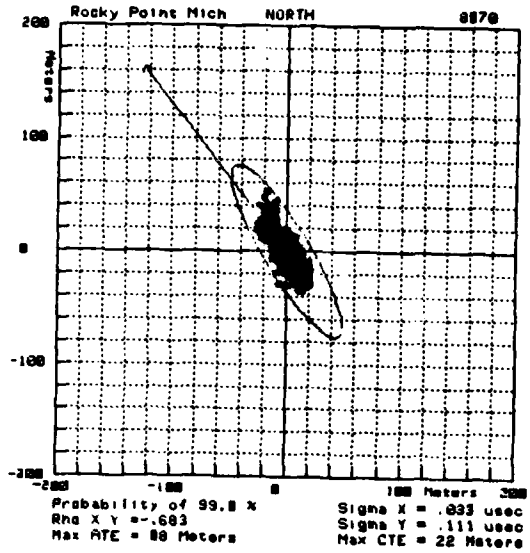

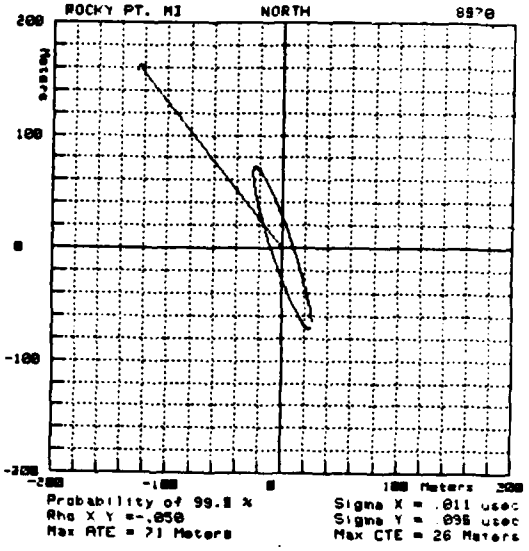

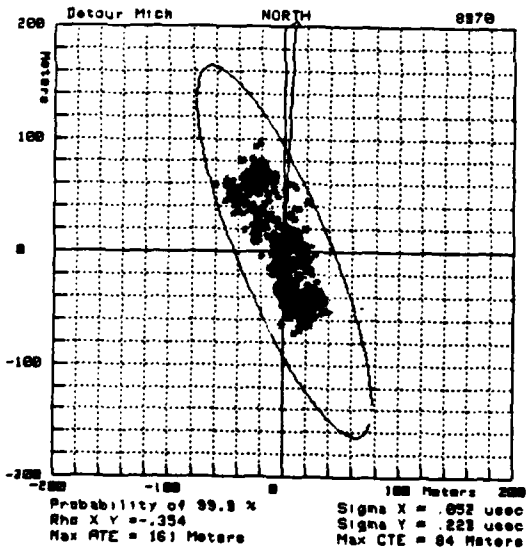

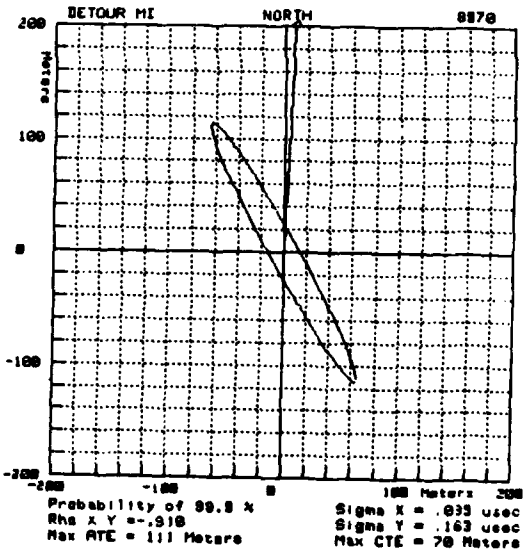

Figure 4-6 (Con't) Comparison of Scatter Plots of Harbor Monitor Site Data With Predicted Error Ellipses

Examining the plots of figure 4-6 provides some insight that we could not get by considering either the raw data or the raw statistics alone. Specifically, when we want to comment on navigation performance, we need to consider cross-track error and, since the courses change from site to site in figure 4-5, there is no simple way to "interpolate" bewteen the reaches considered. The reason we have to interpolate can be seen in table 4-3 which combines the channel characteristics from table 3-4 with the measured performance of table 4-1.

Reach	Half-Width Minus 16 m	Maximum Measured CTE	Measured Error Margin
1-2	351 m	56 m	295 m
13-14	108	22	86
26-28	63	22	41
30-32	139	14	125
41-42	251	31	220

Table 4-3 Measured Performance for Reaches Near Harbor Monitor Sites

It would be great if we could say that since table 4-3 shows there is plenty of room left for guidance error, we can infer that such will be the case in all reaches. We must note, however that, although table 4-3 does not show it, one reach (after we account for half the vessel width) has only 27 meters "left over" and since measured errors in the general vicinity of that reach are as large as 22 meters, we can expect some problems. Moreover, we cannot tell from table 4-3 whether or not there is some reach between Rocky Point and Dunbar which, because of an adverse course, has a cross-track error significantly larger than 22 meters. Figure 4-6 helps us see what is happening better.

From figure 4-6, we see there is substantial disagreement between the observations and our predictions at Pt. Iroquois: the error pattern is larger than the predicted ellipse and has a significantly different orientation than expected. We note, however, the channel requirements are very mild between Pt. Iroquois and Riverside so that the observations do not suggest there will be any problems in that part of the river. Indeed, once we get to Riverside, the only problem related to the ellipse orientation is exhibited in the Dunbar observations. Regarding the size of the error patterns, as compared to the predicted error ellipses, we can say that the general problem is that XRAY, the LOP which determines most of the along-track error, has variations which are bigger than expected. Thus, the ellipses appear "fatter" than anticipated, though of about the expected "length."

From table 3-5 (page 3-36), we note that the only reaches the data suggests we should be concerned about are those tight downbound reaches from waypoint 14 to waypoint 21. These are between Dunbar and Rocky Point. Notice that our predictions show that in going from Riverside to Rocky Point, the error ellipse "rotates" from a major axis alignment approximately northeast to a major axis alignment approximately northwest. The data shows this actually happens. Notice also, however, that we expect the rotation to be essentially complete by the time we have proceeded south along the river to Dunbar. The data indicates this has not happened. From table 3-1, we see that the courses in the tight reaches are, in general, approximately northwest in orientation. Thus, the anamolous behavior in the Dunbar data suggests we would be in trouble in these reaches (ignoring for the moment that we have established that negotiation of the reaches is, if anything, a radar problem).

The above arguments(that's all they are) were offered to explain why we see no reason to try to use the data to interpolate between harbor monitor sites in the tight reaches. It is very clear that performance far exceeds all requirements in the wide reaches, and even in the narrow reaches of the upbound channel. We have also seen enough to suggest that there will be (as expected) problems in the narrow reaches of the downbound channel. This having been established, we can conclude our examination of measured performance with Riverside as SAM and move to a consideration of what might happen with Dunbar as SAM.

4.2 Harbor Monitor Set Data With Dunbar as SAM

Following the approach of Section 4.1, we want to begin with a presentation of what the data suggests would have occurred with Dunbar as SAM. In order to accomplish this simulation, we must compute the data sequence "Dunbar minus Riverside" for each baseline. If we subtract this sequence from the data records for each of the five sites, we simulate our best estimate of what would have occurred had there been an Austron 5000 in control of the chain at Dunbar, and a harbor monitor set at Riverside from May 1981 to May 1982. Appropriately altered TD records are shown in figures 4-7 and 4-8. This data is converted to cross-track error plots in figure 4-9 and table 4-4 presents a comparison of predictions vs measurements for the critical parameters.

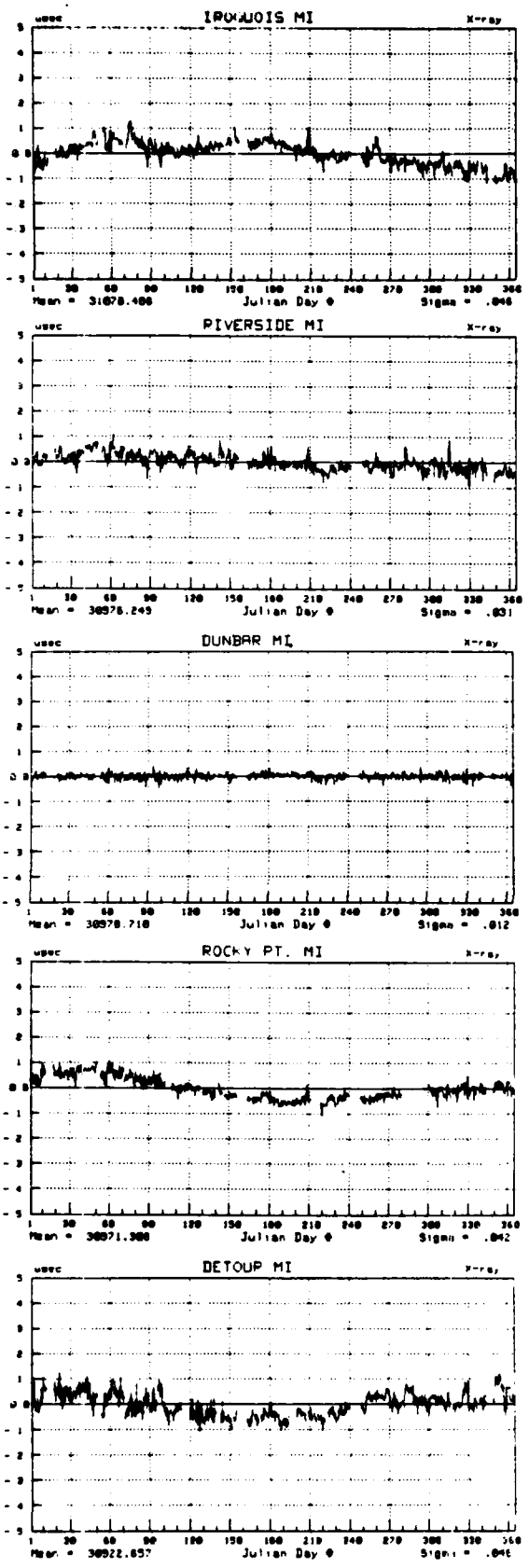

Figure 4-7 Adjusted (For Dunbar as SAM) Harbor Monitor Data for 8970-X Baseline

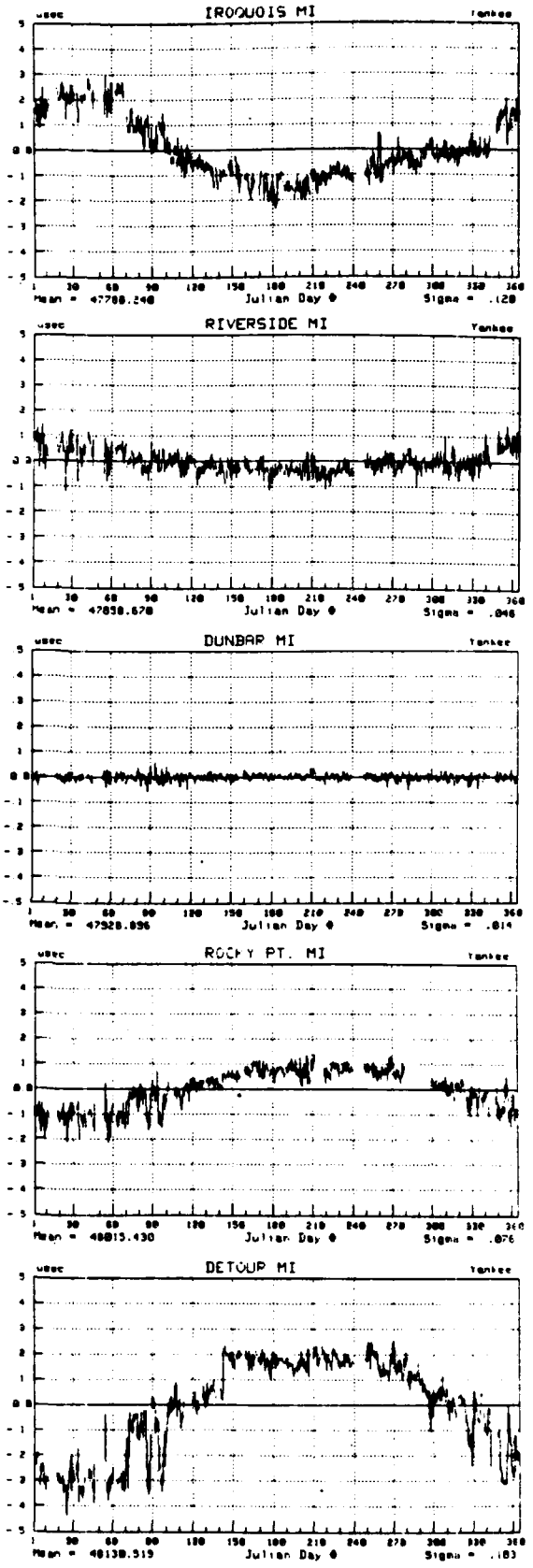

Figure 4-8 Adjusted (For Dunbar as SAM) Harbor Monitor Data for 8970-Y Baseline

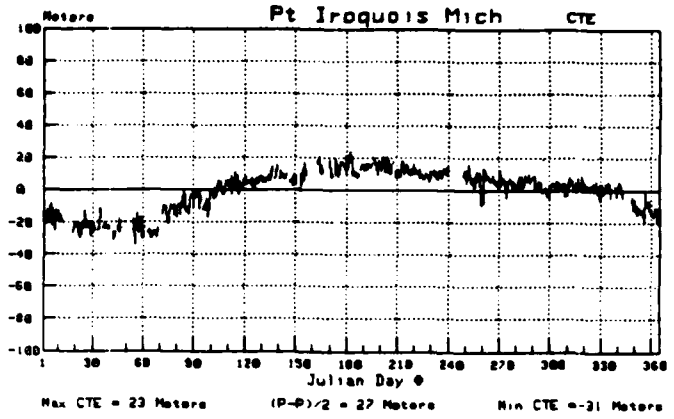

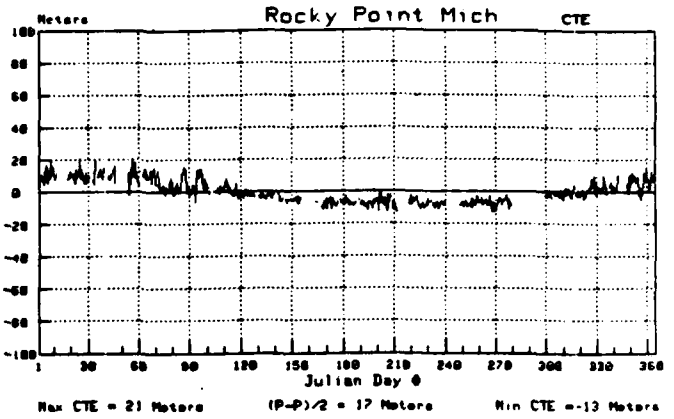

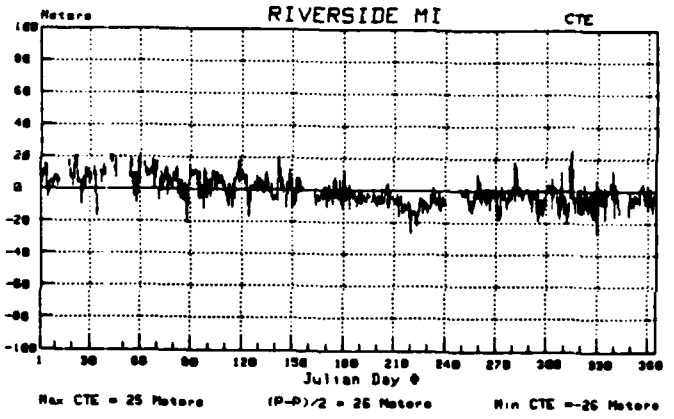

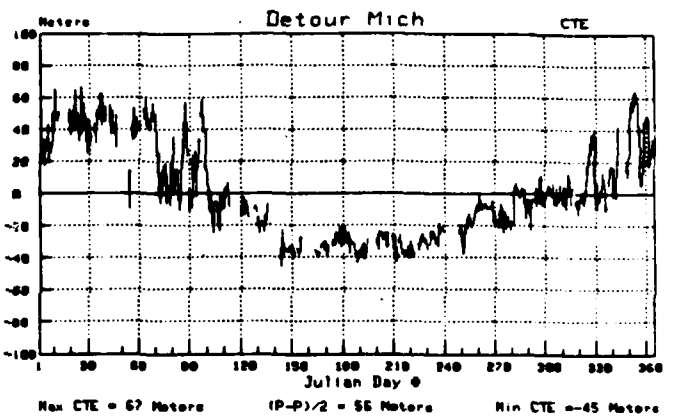

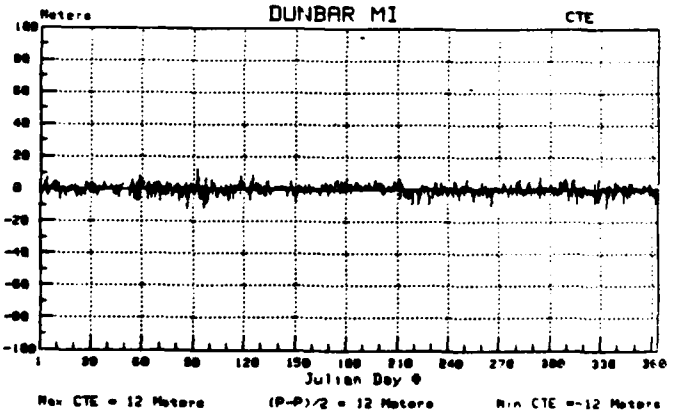

Figure 4-9 Data of Figures 4-7 and 4-8 Converted to Cross-Track Error

Site	Parameter	Predicted	Observed
Pt. Iroquois	σ_x	53 nsec	46 nsec
(W.P. 41-42)	σ_y	76 nsec	120 nsec
	ρ_{xy}	-0.95	0.14
	CTE	46 m	27 m
Riverside	σ_x	11 nsec	31 nsec
(W.P. 30-32)	σ_y	39 nsec	46 nsec
	ρ_{xy}	0.34	0.40
	CTE	15 m	26 m
Dunbar	σ_x	11 nsec	12 nsec
(W.P. 26-28)	σ_y	11 nsec	14 nsec
	ρ_{xy}	0.50	0.48
	CTE	11 m	12 m
Rocky Point	σ_x	19 nsec	42 nsec
(W.P. 13-14)	σ_y	60 nsec	76 nsec
	ρ_{xy}	-0.75	-0.64
	CTE	18 m	17 m
Detour	σ_x	37 nsec	46 nsec
(W.P. 1-2)	σ_y	127 nsec	183 nsec
	ρ_{xy}	-0.94	-0.13
	CTE	62 m	55 m

Table 4-4 Comparison of Critical Parameters: Predicted vs Measured

Again, we see the agreement between the predicted and measured parameters is not as good as we would like. We have already established, however, some of the reasons why. The results look good enough for us to conclude, as before, that we do not have problem in the wide reaches or in the upbound narrow reaches. The downbound narrow reaches are still a concern. To examine these, we again turn to a side-by-side comparison of the predicted error ellipses and the "measured" data scatter plots. These are presented in figure 4-10.

Recall we are interested in the four reaches from waypoint 14 to waypoint 21. These are located between Dunbar and Rocky Point. If we can expect any form of structured behavior in the spatial variations, we expect the results in these reaches, which are closer to the SAM, will be somewhat better than the results indicated at Rocky Point. We should emphasize that the results will only be slightly better - i.e., nowhere near as good as indicated at Dunbar. This is because we are simulating the Dunbar performance with the Austron 5000 data and, as previously indicated, do not expect a user (equipped with an Internav 404) to be able to duplicate this performance.

We notice from the Rocky Point data that the maximum cross-track error is 17 meters. Since the narrowest reach features a "total error margin" of 27 meters, we see we have "borderline" performance. We should note that the course in the narrowest reach (from waypoint 17 to waypoint 19) is essentially the same as that used to process the Rocky Point data (i.e., the course of the reach from waypoint 13 to 14). Thus, we expect no help from a "benign" course change. Thus, we need to obtain a method of interpolating between sites to say the final word about performance in the downbound channel narrow reaches.

We have, of course, already argued that negotiating those reaches is not a loran problem - no matter what the performance. Nevertheless, attempting to extend the results is a useful exercise for R&D purposes. It may also shed some light on the seemingly high "spatially independent" component variations we are seeing in the data. Finally, it may give us a method of stating the expected performance change with the use of the Gordon Lake signal. Since we do not have a full year of data for 8970-Z, we will have to come up with an alternate method of including Gordon Lake in the "empirical predictions." If we can do this, we can say the "final word" about the supplemental LOP experiment in the St. Marys River. These are the reasons which motivate the following section.

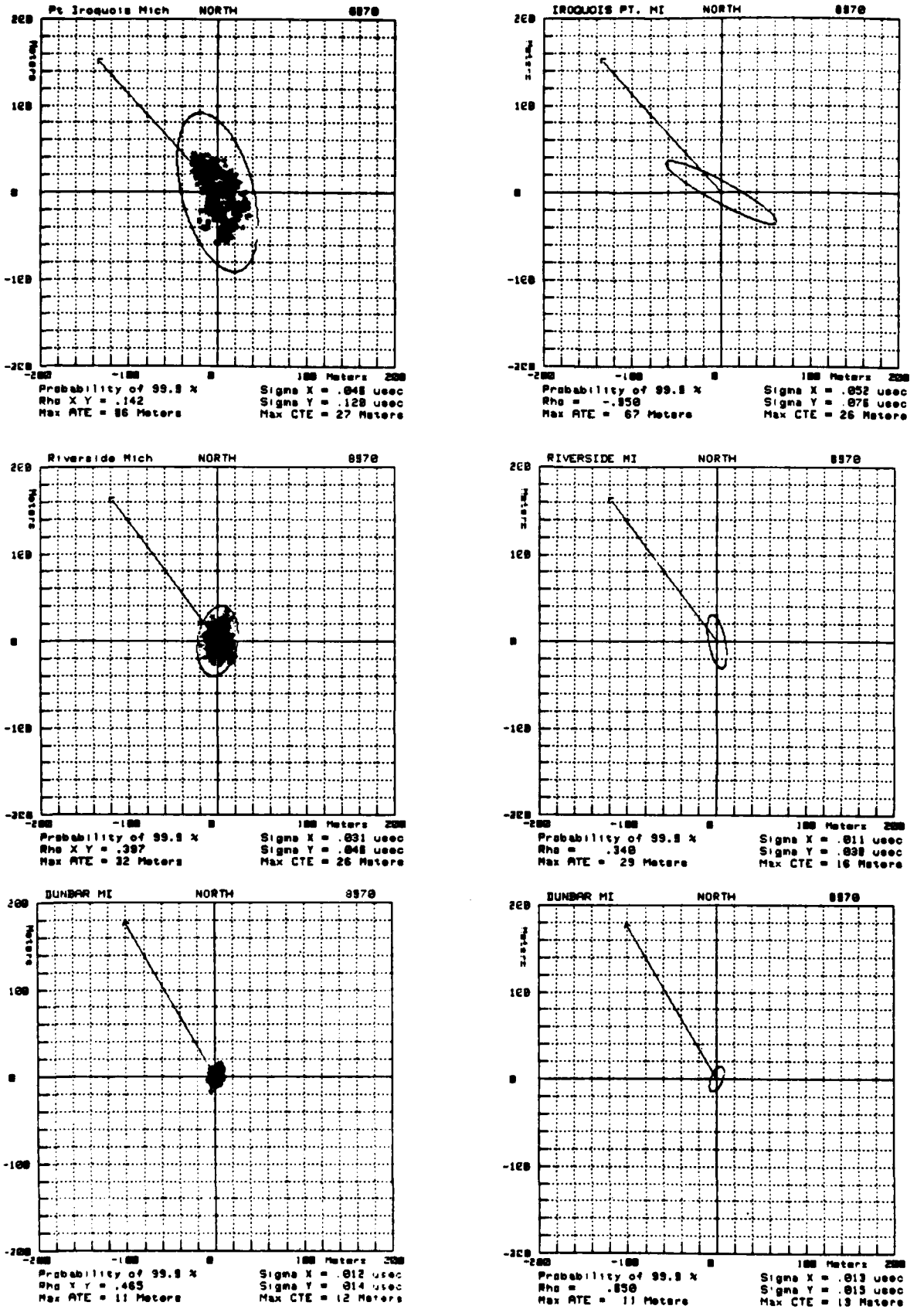

Figure 4-10 Comparison of Scatter Plots of "Dunbar-SAM Modified" Harbor Monitor Data With Predicted Error Ellipses

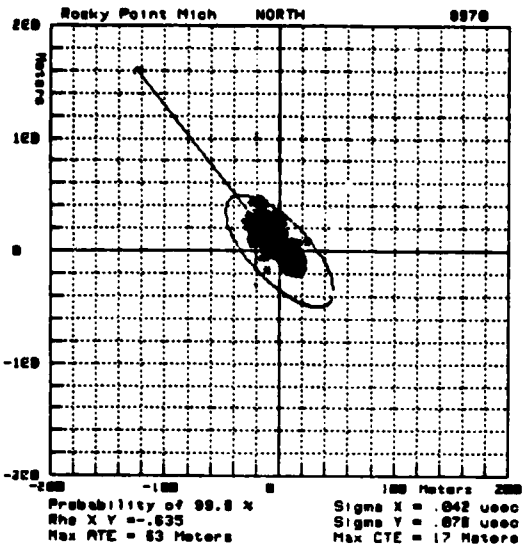

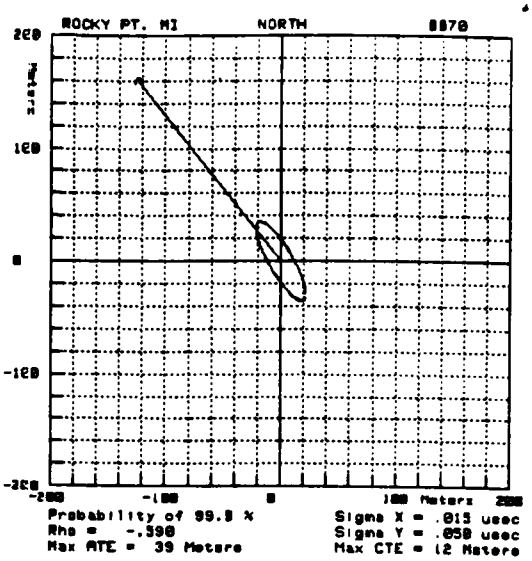

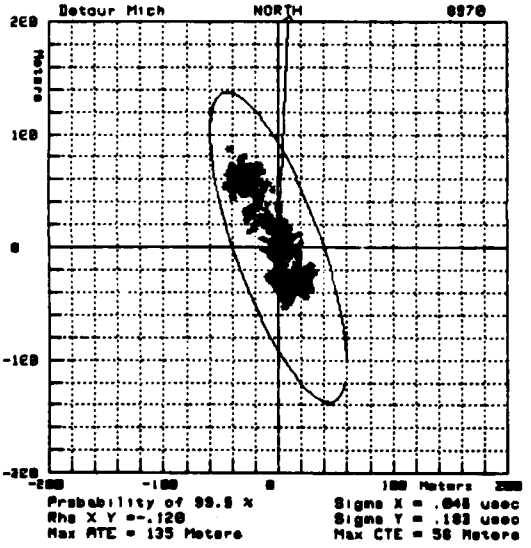

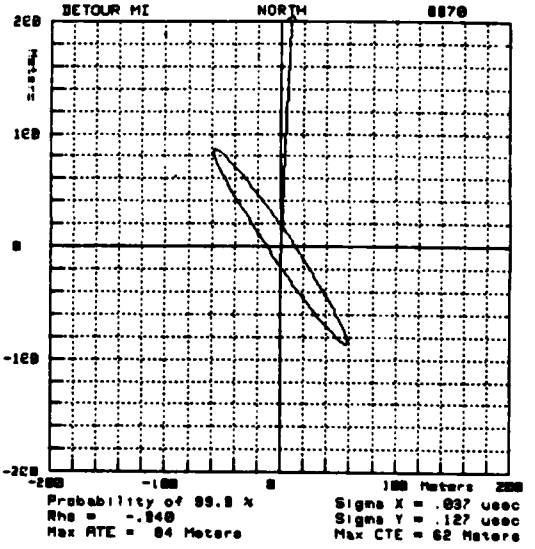

Figure 4-10 (Con't) Comparison of Scatter Plots of "Dunbar-SAM Modified" Harbor Monitor Data With Predicted Error Ellipses

4.3 Empirical Use of the Double Range Difference Model

The basic technique being applied here was employed in the mini-chain stability study as documented in reference 3. We arrange the measured data in a form which implies the observations are samples of a vector random process. Thus, we represent the observations with the notation, $\underline{z}(n)$, where

$$\underline{z}(n) = (z_1(n)\ z_2(n)\ z_3(n)\ \ldots\ )^T$$

We wish to model the observations as follows:

$$\underline{z}(n) = \underline{A} \begin{bmatrix} dTD(n) \\ \underline{C}(n) \end{bmatrix} + \underline{e}(n)$$

The elements of the $\underline{A}$-matrix which operate upon the dTD(n) term will represent the appropriate double range difference. The dTD(n) term indicates propagation speed changes (actually, the inverse of the speed change) and will have units of usec/km. The $\underline{C}(n)$-vector sequence represents "common error" terms - reflecting our suspicion that the harbor monitor sites see the world differently than the Austron 5000 does. The $\underline{e}(n)$-vector sequence represents the error in the model.

The model can be applied in several forms. One simple way is to apply it to a single baseline. In this case, the $\underline{C}(n)$-vector sequence becomes a scalar sequence and the model is written:

$$\underline{z}(n) = \underline{A} \begin{bmatrix} dTD(n) \\ C(n) \end{bmatrix} + \underline{e}(n)$$

In this single baseline case, $z_1(n)$ is the data record from site 1, $z_2(n)$ is the data record from site 2, etc. C(n) represents the common error sequence for the baseline. $e_1(n)$ is the error in the model fit to the data of site 1, e_2 for site 2, etc, and,

$$\underline{A} = \begin{bmatrix} a_1 & 1 \\ \cdot & \cdot \\ \cdot & \cdot \\ \cdot & \\ a_N & \end{bmatrix}$$

a_i is the double double range difference for site i.

If we wish to apply the model to several TD's simultanteously (e.g., TD_X, TD_Y, and TD_Z), we let $z_1(n)$ be the TD_X data record for site 1, $z_2(n)$ be the TD_Y data record for site 1, $z_3(n)$ be the TD_Z data record for site 1, $z_4(n)$ be the TD_X data record for site 2, etc. In this case the $\underline{C}$-vector sequence is:

$$\underline{C}(n) = (C_X \; C_Y \; C_Z)^T$$

and

$$\underline{A} = \begin{bmatrix} a_{x1} & 1 & 0 & 0 \\ a_{y1} & 0 & 1 & 0 \\ a_{z1} & 0 & 0 & 1 \\ a_{x2} & 1 & 0 & 0 \\ . & . & . & . \\ . & . & . & . \\ a_{zN} & 0 & 0 & 1 \end{bmatrix}$$

Notice that we imply there is a different common error term for each of the baseline signals. This is a defendable model of what takes place as discussed in the next section. Notice also that if we use the single baseline model and apply it to several baselines separately, we will obtain different results than those obtained with the combined-TD model. Specifically, in the first case we obtain a different dTD(n) sequence each time we run the model whereas in the latter case we say there is only one dTD. This second case is what we are forced to use if we claim changes in propagation speeds are uniform. In general applications under the harbor monitor program, with widely spaced monitors, we can expect to encounter difficulty with the uniform approach. Thus, we acknowledge that both approaches exist and simply note that once the model is applied, the "trick" is to generate some clever argument to interpret the results.

With the tightly spaced monitors in the St. Marys River (tightly spaced with respect to the signal sources), we would like to see the uniform propagation model yield good results. This is particularly important since we have an incomplete 8970-Z data base. If the model works well when applied to the combined 8970-X and -Y data, it is reasonable to argue the results <u>should</u> be applicable to the 8970-Z data. If the model results do <u>not</u> agree with the limited 8970-Z data, we have reason to suspect there is something special about a short baseline chain. Conversely, if we cannot

get the 8970-X and -Y data to agree, we can make no broad statements if the 8970-Z data does not match up either.

In general, even for the tightly spaced monitors of the St. Marys River, we should use the model both ways: on a baseline-by-baseline basis and with all baseline data combined. A comparison of the two approaches can indicate anomalous behavior in a particular propagation path and, perhaps, steer us towards resolution of a problem.

To complete this discussion, we should note that the goal of the model analysis is to obtain an estimate of dTD(n) and $\underline{C}(n)$. We choose the minimum mean square estimate (MMSE) approach which yields:

$$\begin{bmatrix} \widehat{dTD} \\ \underline{C} \end{bmatrix} = (\underline{A}^T\underline{A})^{-1}\underline{A}^T\,\underline{z}$$

This is a classical result which need not be derived here. We note, however, that a similar derivation is carried out in Appendix A.

Having obtained this estimate, we obtain a measure of the applicability of the model by checking the residual vectors, $\underline{r}$, where

$$\underline{r} = \underline{z}(n) - \underline{A}\begin{bmatrix} \widehat{dTD(n)} \\ \underline{C}(n) \end{bmatrix}$$

If the model has worked well, we should see that the residuals closely approximate the "white noise" sequence that Section 3 assumed describes the spatially independent component of the variations.

With this background, we should discuss some specifics about how we implement the model. We note that we do not want to apply the model directly to the data. Instead, we will subtract the appropriate SAM data records from the corresponding records of the other sites. We do this because we know that some of the variation in the SAM data does not fit the model. Specifically, notice that the SAM data record is not "zero" at all times. Thus, SAM does not follow a "blind" control law which says it must not allow any variation. Instead, the control law recognizes that the SAM is trying to detect minute signal variations in the presence of noise. Thus, SAM allows a small amount of variation in the signal to avoid "hunting."

It may be that the harbor monitor sites see much of the same variation that the SAM sees. In that case, those variations do not have the significance we want to assign to the estimated common error variations. Similarly, such variations, if they are present to the same degree in the data records of all the sites, will not fit the "dTD" portion of the model.

Thus, we remove the effects by subtracting the SAM observations from all the sites. We recognize we will also be subtracting variations that "SAM but nobody else sees," but the common error term in the model will pick this up. This approach keeps the model simple and simply requires that we remember to add the SAM data record back in to the picture if we try to predict what the observations would be at some site. A final note is that once we have subtracted the SAM data from all the sites (including the SAM data record itself), we must modify the A-matrix so that all elements corresponding to the SAM are 0.

The data records in figure 4-11 indicate the results of applying the model to the combined 8970-X and -Y data records for all 5 data collection sites.

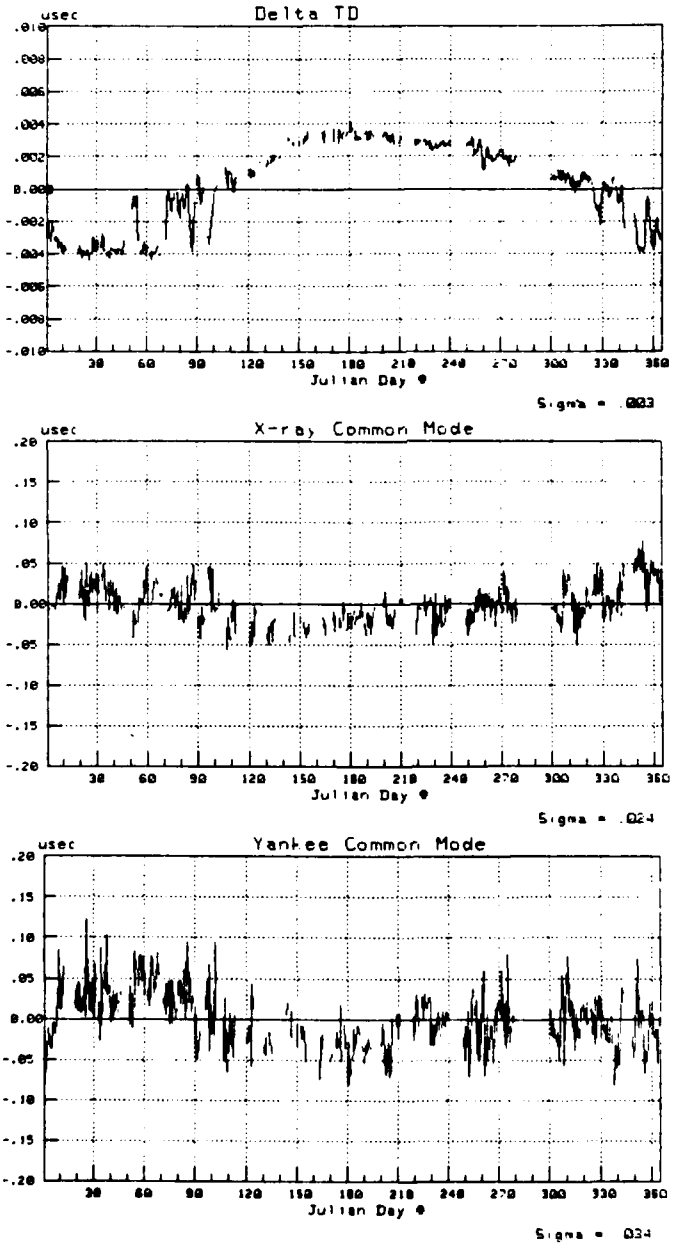

Figure 4-11 DRD Model MMSE Estimates

In Figures 4-12 and 4-13, we indicate the residuals of the estimation process.

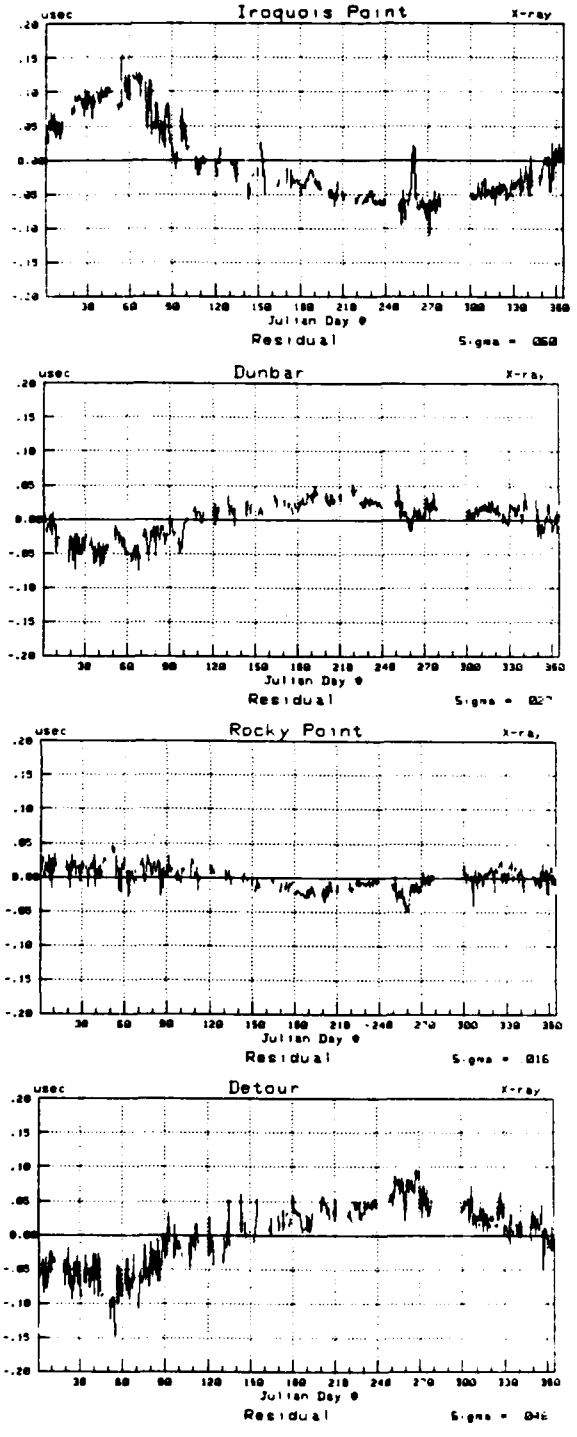

Figure 4-12 DRD Model MMSE Estimate Residuals - 8970-X

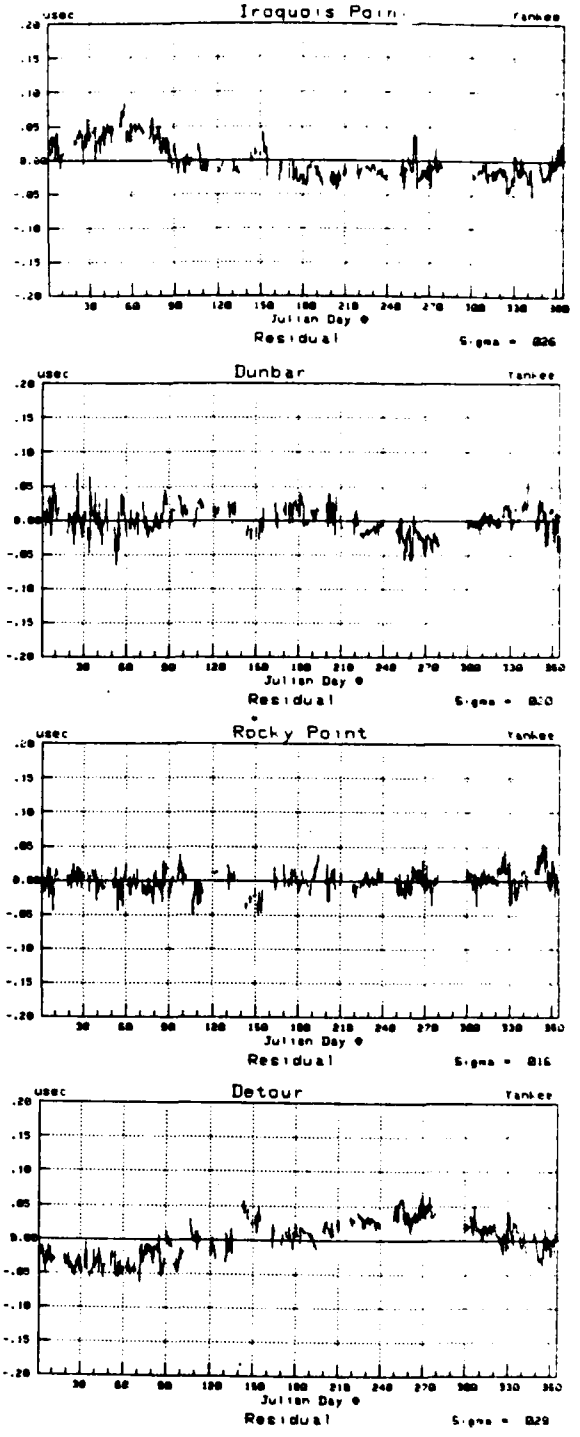

Figure 4-13 DRD Model MMSE Estimate Residuals - 8970-Y

Examining the results, we see that the dTD term is, essentially, as expected: "noise" superimposed on a year-long sinewave. We also see that the common error terms, with standard deviations of 24 and 34 nsec are much larger than the 11 nsec used in Section 3. This indicates a problem expected after the preceeding section.

Examining the residuals, we should first concentrate on the sites with large DRD's to see how this aspect of the model appears to be working. At these sites (Detour and Pt. Iroquois), we see some "structure" in the residuals which suggests a model problem. To scrutinize the plots we should bear in mind that a general characterization of the dTD plot of figure 4-11 is that it "bulges positive" in the summer. We should check to see if this general characteristic (or its inverse) is present in the residuals.

Beginning with the Pt. Iroquois Xray residuals, we see that the data generally "bulges negative" in the summer. This is the opposite of what the original Pt. Iroquois Xray data record, of figure 4-1 did. Thus, we can conclude that the Pt. Iroquois Xray data suggests the estimated dTD record bulges too much (it removed the positive bulge and then some). The Iroquois Yankee data suggests the model does a much better job. The residuals from the latter part of the year look pretty "flat" with only the slightest upturn in the last two weeks or so. The residuals from the first half of the year suggest a slight negative bulge - a trend consistent with the last few weeks of the year. In general, therefore, we can say the residuals have a slight negative bulge. This is the general characteristic of the original data record so we can say the Pt. Iroquois Yankee data suggests the estimated dTD record does not bulge enough.

Turning to a consideration of the Detour data, we see the Xray residual has a positive summer bulge to it. Again, this is what the original data record does so we again have the suggestion that the dTD record does not bulge enough to remove all the structure. The Detour Yankee data has a slight positive bulge, the opposite of what was in the original data record. Again, this suggests the dTD record bulges too much. This data record involves the largest DRD so we must downplay the importance of this finding. Nevertheless, we have two sites saying "too much" and two saying "not enough."

At this point, to resolve the conflict, we must turn to a baseline-by-baseline examination for insight. When we carry out the process, we obtain the estimates shown in figure 4-14 and the residuals shown in figures 4-15 and 4-16.

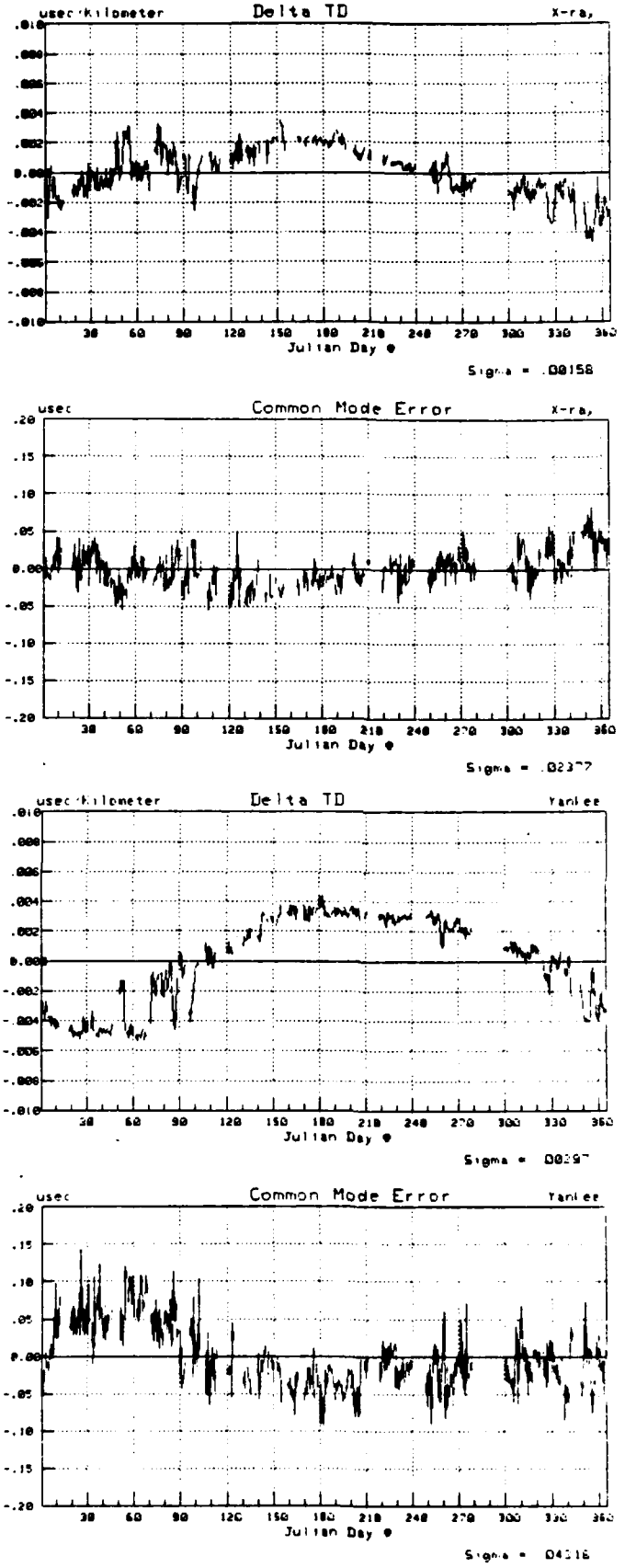

Figure 4-14 Baseline-by-Baseline DRD Model MMSE Estimates

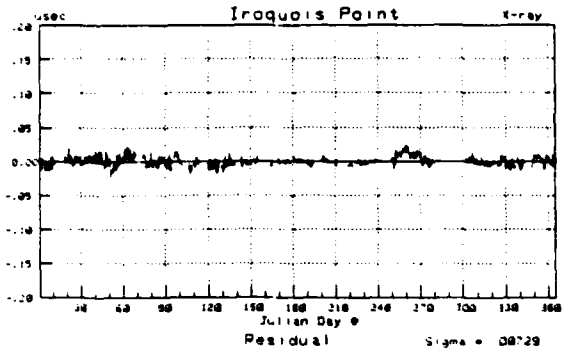

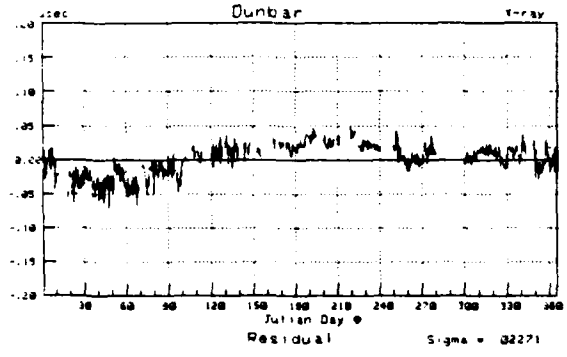

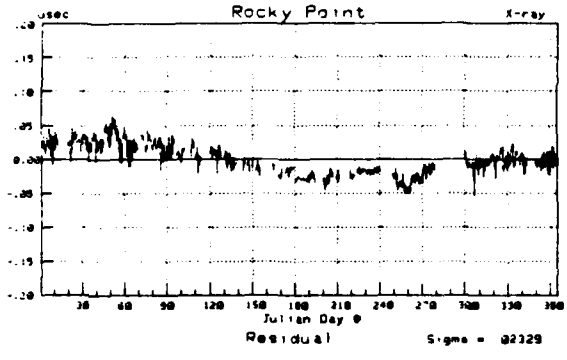

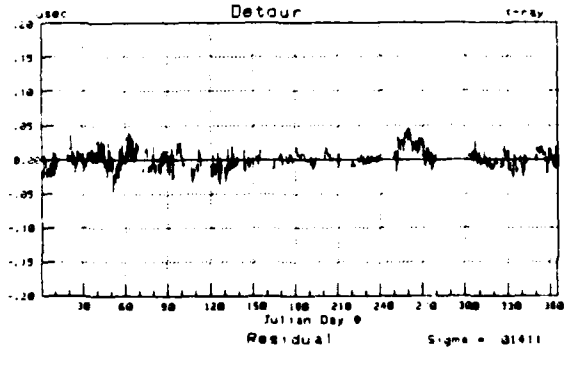

Figure 4-15 8970-X DRD Model
MMSE Estimate Residuals

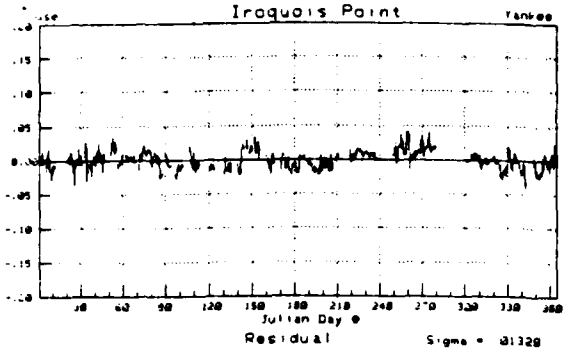

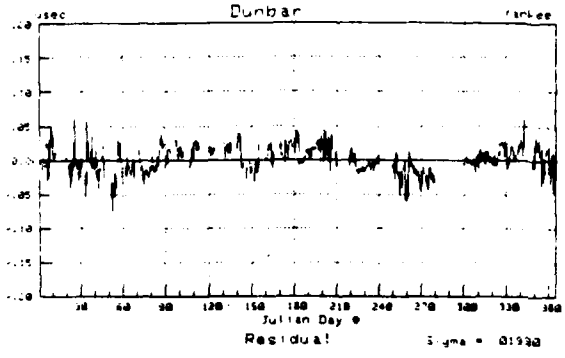

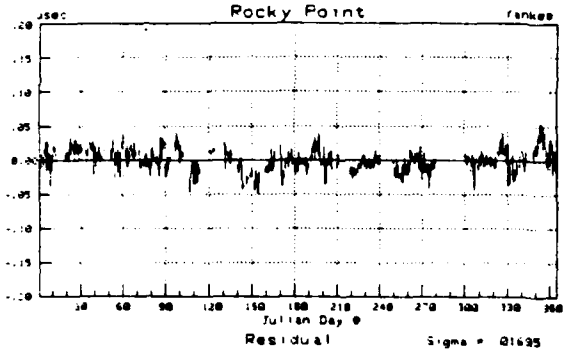

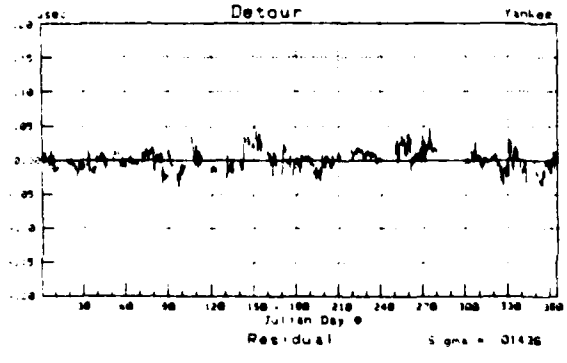

Figure 4-16 8970-Y DRD Model
MMSE Estimate Residuals

In examining these new results we first notice that the dTD_Y estimate of figure 4-14 is very similar to the "combined baseline" dTD estimate of figure 4-11. The dTD_X estimate of figure 4-14 looks very different from both other estimates. We feel the dTD_Y estimates (or the dTD) estimate is more correct than the dTD_X estimate and this stems from more than just a "majority vote."

Recall that we have already hinted there are some problems with the data. We can view these problems as "noise" and see, since we are trying to extract the basic "signal" from noise, we can run into some "signal-to-noise ratio" problems. Because of the way the LOP's are oriented (as belabored in Section 3), the 8970-Y DRD's are generally larger than the 8970-X DRD's for the sites of interest. As also belabored, the DRD's determine the expected size of the seasonal component, the signal we are trying to extract from the noise. Thus the 8970-Y data records contain the stronger signal so we will have an easier time in recovering that signal. This imbalance in the DRD's also explains why removal of the Xray data does little to change the 8970-Y estimate of dTD from the combined estimate of dTD.

A second, equally important reason for putting faith in the 8970-Y results comes from an examination of the residuals. The residuals of figure 4-16 may be noisy, but they are much "whiter" than other residuals, confirming the model has done a good job in expaining much of the variation structure. The residuals of figure 4-15, however, indicate considerable (relatively speaking) remaining structure. Having established this argument for believing the dTD_Y results, we should scrutinize the 8970-X analysis for hints of the problem.

We should first emphasize that the DRD is, essentially, zero for Dunbar and Rocky Point (and, of course, Riverside). Detour has a DRD_X of -16 km and Pt. Iroquois has a DRD_X of 30 km (so we think). Thus, Pt. Iroquois "counts" about twice as much as Detour in what the DRD_X decision should be. From the plots of figure 4-15, we see that the Pt. Iroquois data has a slight negative bulge. This is the opposite of what the original data shows so Pt. Iroquois Xray data suggests the dTD_X estimate is too <u>big</u>. This contradicts the conclusions obtained by comparing the dTD_X and dTD_Y estimates and may be the source of the problem (i.e., the factor that is "holding" dTD_X too low). If this is true, it is consistent with everything we have seen thus far. Pt. Iroquois may have the largest DRD_X and thus be able to dominate the estimation when we remove 8970-Y data from consideration but it cannot greatly affect the total estimate because of the large DRD_Y factors.

From figure 4-15 we also see that the Detour-X residual has a <u>slight</u> (almost imperceptible) negative bulge. Since the original data also had a negative bulge, data from Detour suggests dTD_X is too low. This confirms what the Yankee data tells us, and that Pt. Iroquois 8970-X data is the source of the problem.

Recall that an overall goal is to establish agreement between the 8970-X and 8970-Y data. The plots of figures 4-15 and 4-16 indicate this is not possible. We can, however, attempt to find a way to remove the Pt. Iroquois-X effects. One approach is to simply throw the data out. For

future reference, we will use a more general approach to accomplishing the same end. The approach features the use of a "weighting" matrix so that we obtain a "weighted MMSE estimate." As shown in Appendix A, the estimate now becomes

$$\begin{bmatrix} \widehat{dTD(n)} \\ \underline{C}(n) \end{bmatrix} = (\underline{A}^T \underline{W}\ \underline{A})^{-1}\ \underline{A}^T \underline{W}\ \underline{z}$$

where

$$\underline{W} = \begin{bmatrix} w_1 & 0 & . & . & 0 \\ 0 & w_2 & 0 & . & 0 \\ 0 & 0 & . & . & . \\ . & . & . & . & . \\ 0 & . & . & . & w_N \end{bmatrix}$$

where N/2 is the number of data sites. The w's indicate the relative amount of weight assigned to each data record. (The appearance of $\underline{W}$ inside the "inversion" parentheses as well as outside makes the results independent of the absolute size of the w-terms). Here, for two TD's, w_1 indicates the weight to be assigned to the X data from site 1, w_2 is the weight assigned to the Y data from site 1, w_3 is the weight to be assigned to the X data from site 2, etc. If all weights are equal (factoring out whatever actual value is assigned), the $\underline{W}$-matrix is replaced by the identity matrix and the estimate is as before.

Again, we could have accomplished the same purpose by simply throwing the Pt. Iroquois data out but prefer to introduce this more general approach for future reference. To proceed with the analysis, we "de-weight" the Pt. Iroquois 8970-X data by a factor of 1000 and obtain the results indicated in figures 4-17 through 4-19. (You have to live through the data collection process to appreciate our token inclusion of the data). A final note is that we could have presented similar results by modifying the Pt. Iroquois DRD_X value. We avoid this approach so that we can avoid having to provide an explantion for the use of this (type of) "force fit."

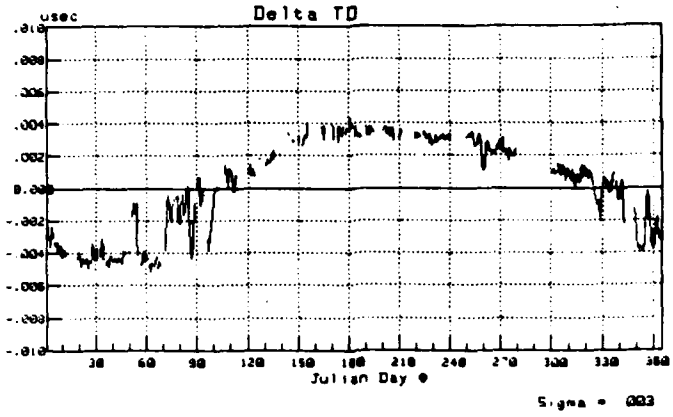

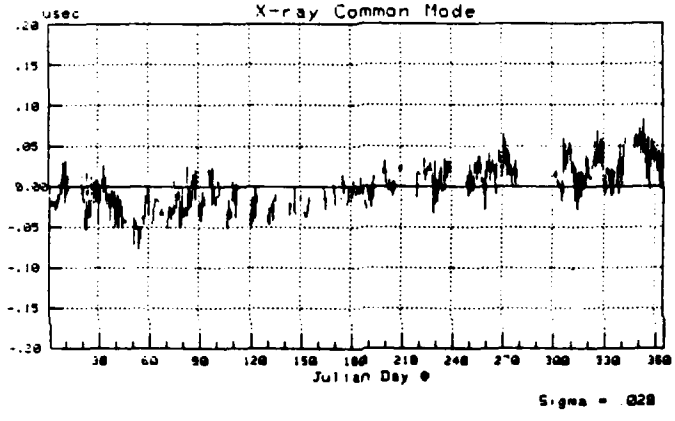

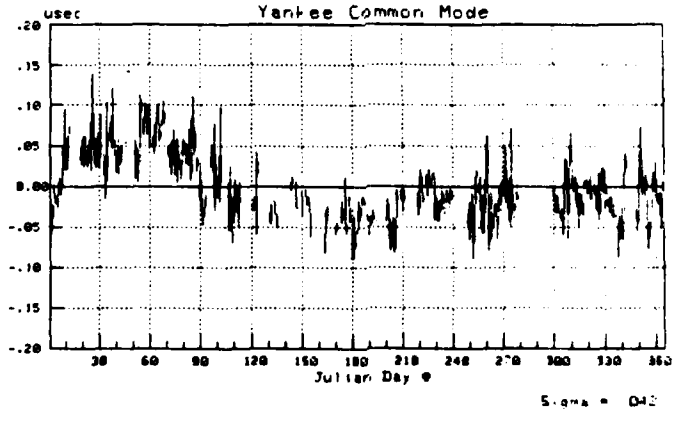

Figure 4-17 DRD Model Weighted MMSE Estimates

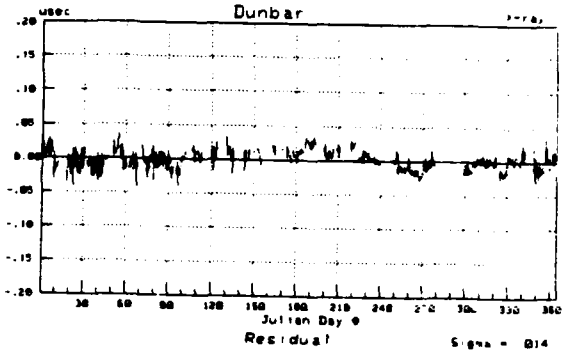

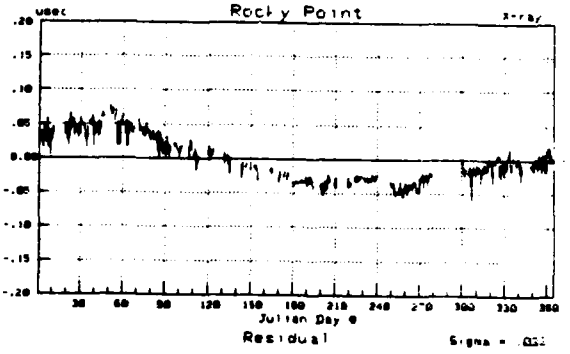

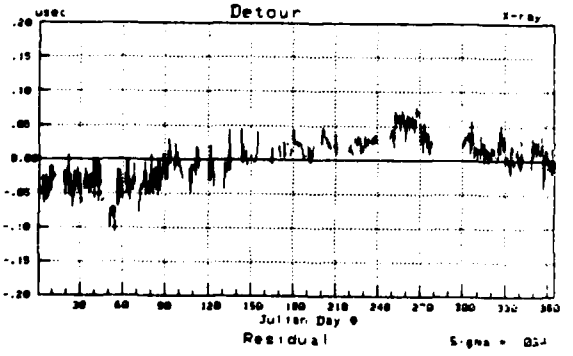

Figure 4-18 DRD Model Weighted MMSE Estimate Residuals - 8970X

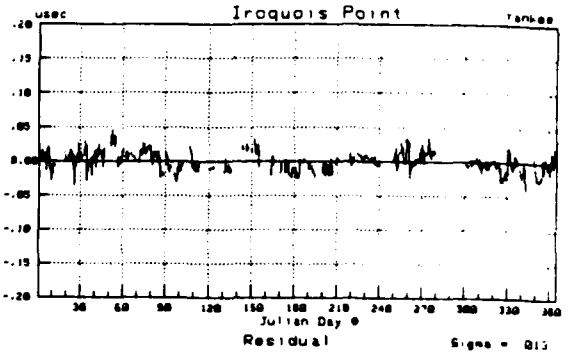

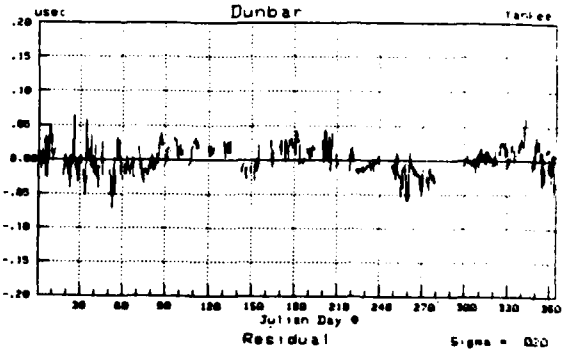

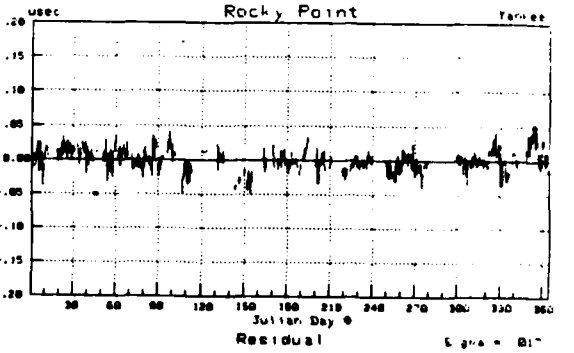

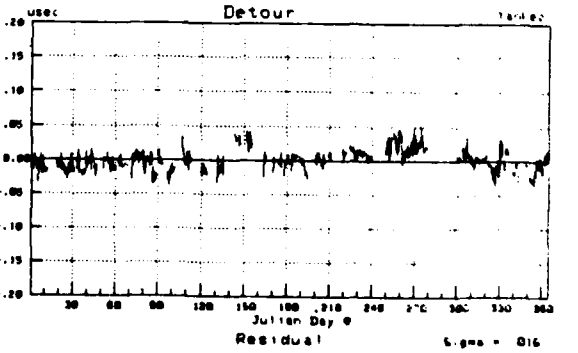

Figure 4-19 DRD Model Weighted MMSE Estimate Residuals - 8970-Y

The results indicate the dTD term is consistent with those shown in figure 4-11 and 4-14. By comparing the peak-to-peak swings as a convenient measure, we can make the stronger statement that the combined baseline results now agree, almost perfectly, with the "Yankee-only" results. The price we paid for this agreement was the requirement that we ignore the Pt. Iroquois-X data. If this were exclusively a "Loran-C propagation" study, we might be tempted to examine the signal paths more closely. There are, however, more far-reaching implications in the data and it is these that we want to explore. Additionally, we can note that preliminary examination indicates the data is simply not good enough to support the propagation study (as will be offered later, we feel this is a "system" problem as much as a data collection problem and that until the system questions are resolved, further propagation studies are not warranted - at least at this "extract the last ounce" level). For the purposes of this report we will have to be satisfied that the results are supported by 9 out of 10 sites. At this level, data from both baselines are in agreement.

Having stated this, we should examine what "level" we have arrived at. We notice that the common error term has a standard deviation of 28 nsec for the 8970-X baseline and 42 nsec for the 8970-Y baseline. This is approximately consistent with the results of the previous section in which, considering only the "close-in" harbor monitor sites, we suggested a value of 28.5 nsec for the standard deviation of the spatially independent component. Recognizing that we have now considered more sites, we see no reason to suggest we are not consistent.

We should notice that, ideally, we would want to argue the common error terms are exclusively representative of differences between the Austron 5000 and the Internav 404's. We must caution, however, that besides not knowing that our model is "complete," we have no grounds for asserting the two types of errors we allow for are "orthogonal." Thus, some of the model shortcoming are included in both the dTD and common terms. To illustrate this point, we can re-run the model - without considering the Austron 5000 data and by using one of the Harbor Monitor sites as the SAM (i.e., arguing it, by definition, has no common error). If we do this, the resulting common error terms have standard deviations of 23 nsec for 8970-X and 30 nsec for 8970-Y. Ideally, (i.e., if all Internavs were alike and if our model were complete), the residuals would not be nearly so large. We will explore the implications of this later. For now, we should get to the "bottom line" for the St. Marys River.

We begin by arguing that if we had to pick a single number to represent the standard deviation of the residuals, we would try some value in the range 25 to 35 nsec. The implication if we are "somewhat off" in this estimate will depend on how we use it. For reasons we will present later, our particular use dictates we choose the somewhat lower value of 20 nsec. Recall we want to attempt to predict performance in reaches other than those at which we have data collection sites. To do this we will follow the following procedure:

1. Multiply the dTD(n) sequence by the appropriate DRD.
2. Add the appropriate common error term to the result.
3. Add the appropriate Riverside data record back in.
4. Add white Gaussian noise with a standard deviation of 20 nsec.
5. Convert the resulting TD-records to a scatter plot.

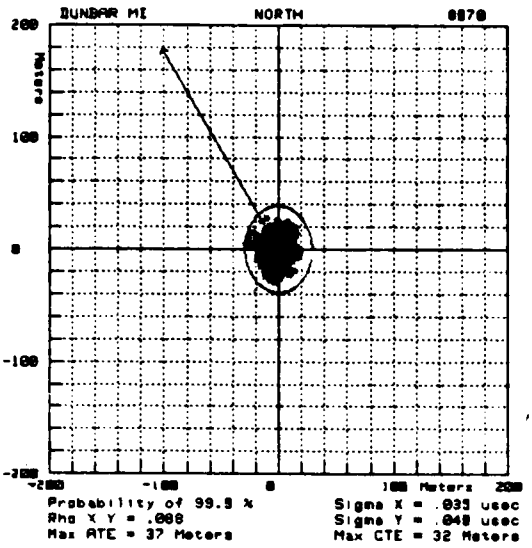

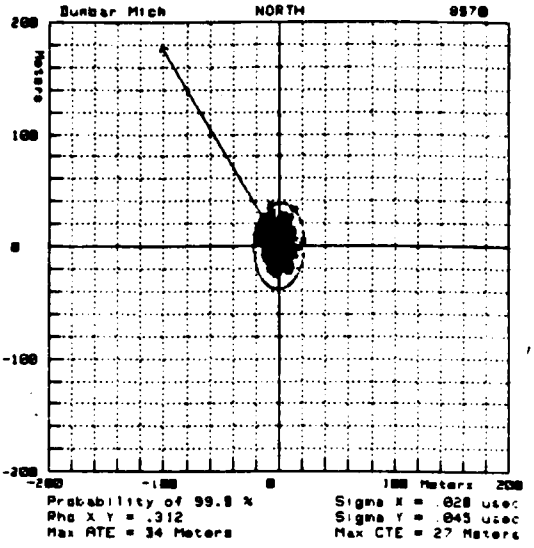

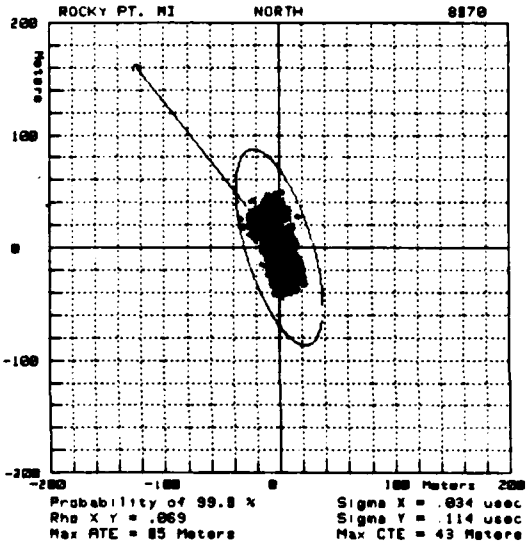

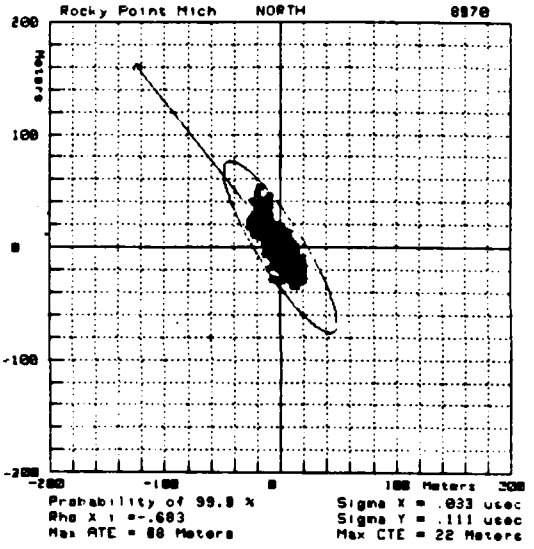

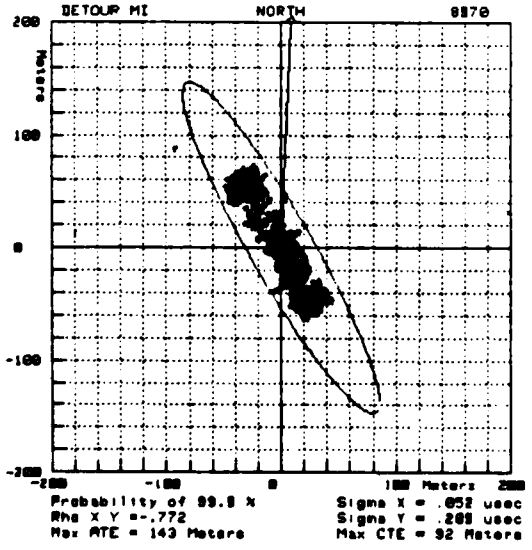

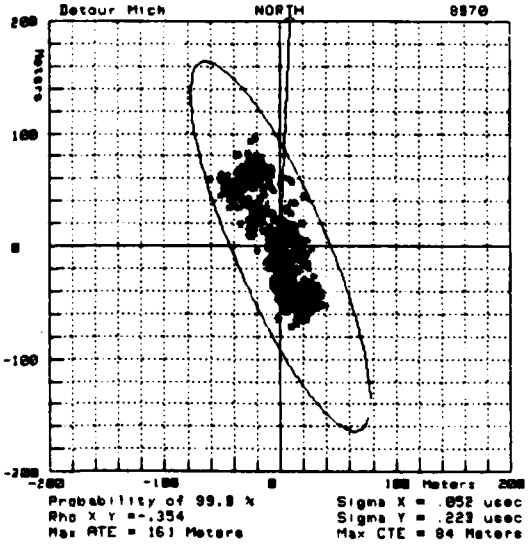

PREDICTED FROM MODEL

ACTUAL DATA

Figure 4-20 Comparison of Scatter Plots Based on Empirical Model Predictions to Measured Data Scatter Plots

Although the purpose of carrying out this procedure is to predict the performance at places other than where we have collected data, we carry out the prediction process for data sites to check ourselves. This procedure is carried out for Dunbar, Rocky Point and Detour and compared with the actual data scatter plots in figure 4-20.

We see the results of the prediction method are nearly identical to the observed data - actually being somewhat conservative. This can be explained from the use of our 20 nsec white noise estimate. First, we chose 20 nsec vice a number in the 25 to 35 nsec range because it was more representative of the residuals close to the SAM, i.e., at those locations which do not have a dominant DRD term and are thus more sensitive to the "spatially independent" terms. This would account for why we might have good agreement at the "close-in" sites. What makes the results conservative is that we have used white Gaussian noise to simulate the residuals. We can think of this type of noise as a "maximum disorder" one whereas the actual residuals have considerably more structure to them. Thus, although we can certainly compute a "standard deviation" for the actual residuals (actually, rms values), we don't expect a histogram to have "Gaussian tails." An analogous situation was discussed in reference 15 wherein we showed that, with large DRD's and a sinusoidal component, we expect the 95% probability ellipses to be actually more representative of "max error." A heuristic argument showed that for a sinusoid, the value not exceeded 95% of the time is about 99.7% of the value never exceeded. The Gaussian approximation allows more variation. Returning to the case at-hand, we argue similarly that although the residuals are not as structured as the pure sinewave, the same concepts apply: white Gaussian noise is a good simulator of "worst case." Thus, we use 20 nsec "sigma" white Gaussian noise to approximate 25-35 nsec "sigma" structured noise.

At this point we have said all we need to about the empirical DRD model. Before extending the prediction technique to other reaches, we should examine the 8970-Z data.

4.4 Supplemental LOP Data and Final Performance Prediction

Section 2 presented background discussions which indicate there were substantial problems with the data from early 1981. This is an explanation for why we have concentrated on later data. Since 8970-Z data is only available for this "problematic" period, we are forced to use the results of that period to dig out whatever information we can. As can be expected, data collection efforts matured throughout the 5-1/2 month period of the 8970-Z operation so that "things were starting to look reasonable" by May. Unfortunately, this is at about the beginning of the "uninteresting" time of the year. Examination of data records shows we have no usable 8970-Z data from Pt. Iroquois, Rocky Point or Dunbar until May. Thus, we will have to base our comparisons on data from Detour alone.

Although this site is not located in the narrow portion of the river, it does feature the largest DRD. Thus, we have a way of checking this "more interesting" feature of the model. To accomplish the check, however, we will use the dTD estimates from 1982 to compare to the "usable" 1981 8970-Z observations. This rules out a direct residual computation but does let us

examine the "gross" behavior of the data as recorded as compared to the predictions. To obtain an estimate of the common term, since we do not have enough sites to use the model to obtain one, we will simply average the previously determined C_X and C_Y terms. Thus, we will add together the appropriately scaled dTD term, the average C-term, the Riverside data and the 20 nsec standard deviation white noise term. This results in the data record shown in the plot of figure 4-21. The figure also contains a plot of the actual data record for visual comparison purposes.

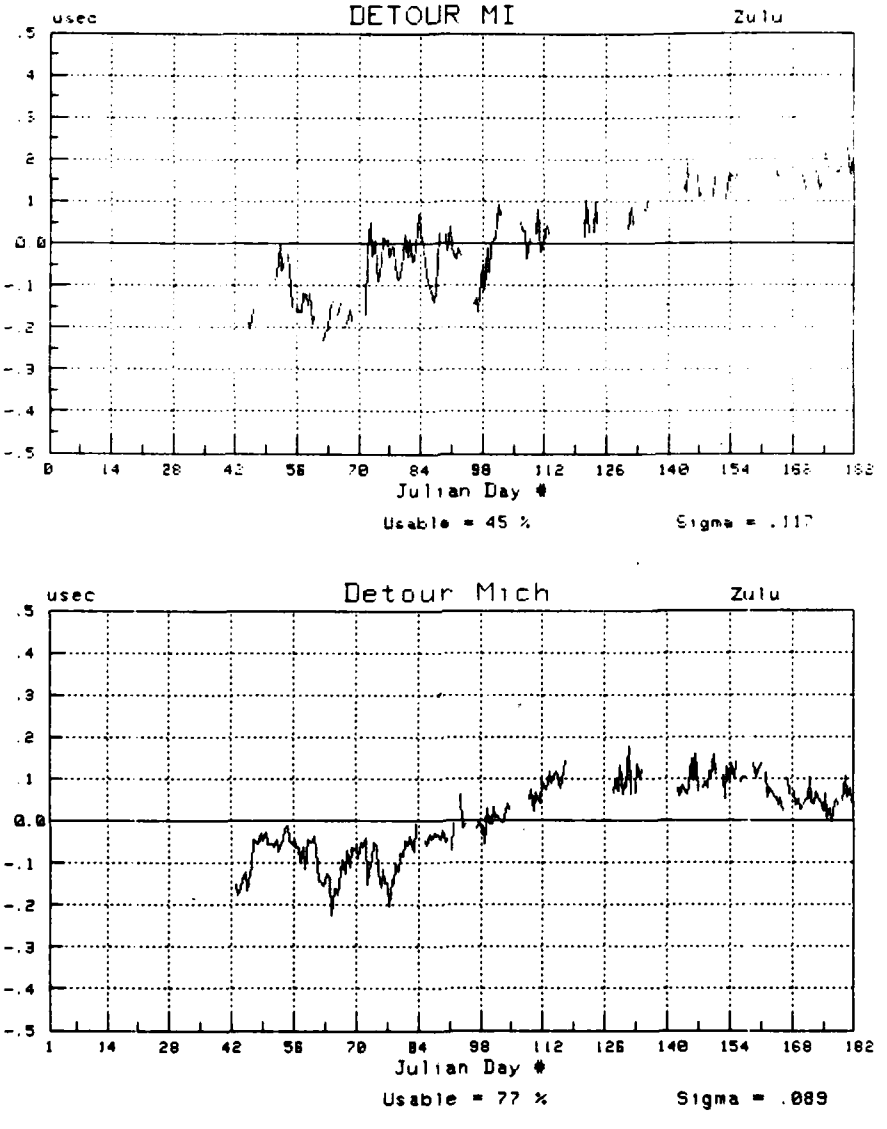

Figure 4-21 Comparison of Predicted and Observed 8970-Z Data Records

This visual comparison, admittedly, is a poor substitute for a full analysis but we must remember the times and the circumstances. The harbor monitor program was in its infancy and lessons were being learned the hard way. Postponement of the experiment for a year would have been desired but,

given the limited resources (few Coast Guard personnel were familiar with the mini-station equipment), the opportunity had to be taken or lost forever. Given these circumstances, we must settle for the good agreement indicated by the comparison of figure 4-21 and conclude the "XY" derived MMSE estimates adequately describe the 8970-Z variations. We call this a "proof by lack of contradiction - type II." (Type I refers to the case in which there is no supporting data).

With this (expected) agreement established as well as possible, we are ready to make our final performance predictions. To accomplish this, we generated data sequences from the estimates, as previously described, for all baselines and for all reaches. From these sequences we generate CTE plots for all the reaches - both for the MXY case and the MXYZ case. The results are as indicated in figures 4-22 and 4-23. We use Dunbar as the SAM.

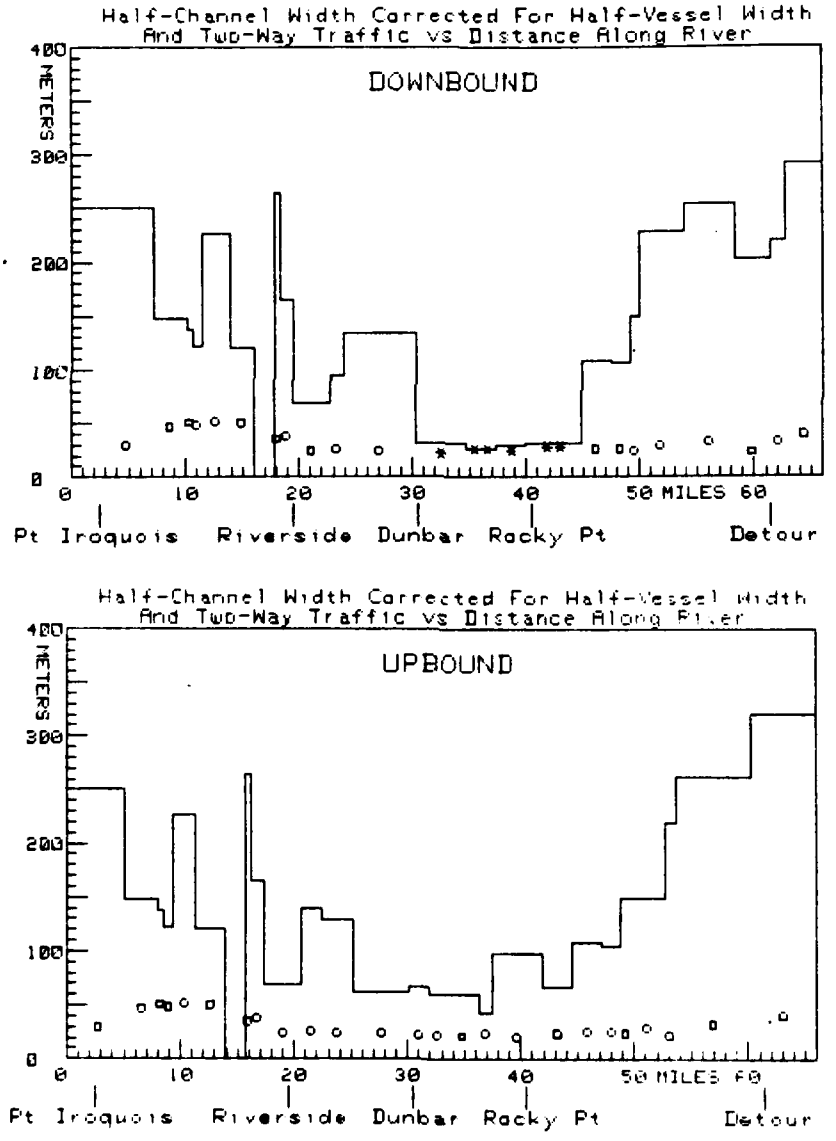

Figure 4-22 8970-X and -Y Empirical Model Fix Performance Predictions

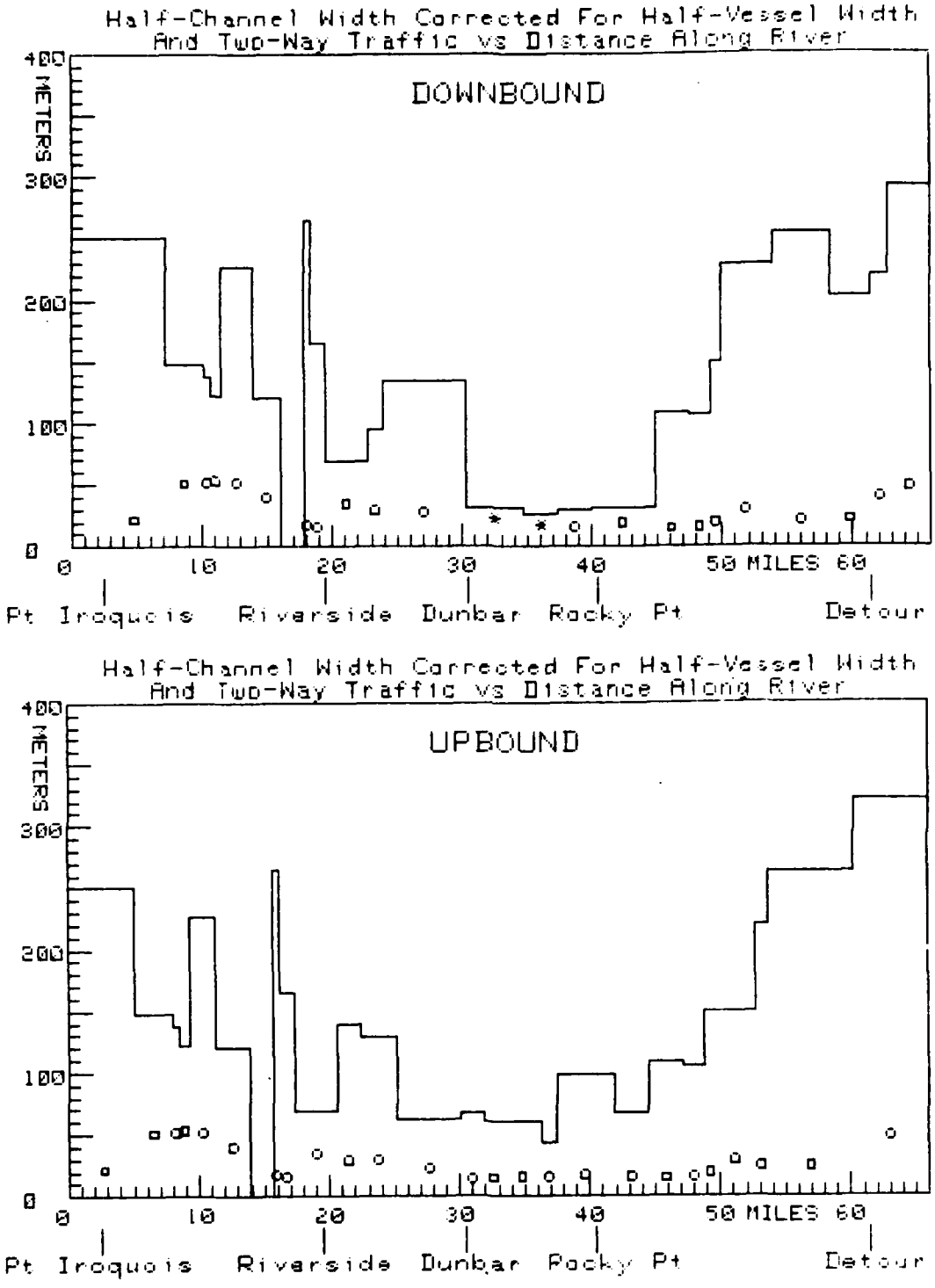

Figure 4-23 8970-X, -Y, and -Z Empirical Model Fix Performance Predictions

As stated earlier, we did not expect to overturn the "Gordon Lake utility" decision based on these results. We simply comment, however, that we again see no pressing advantage of the extra baseline. We can note that the SAM has now actually been established at Dunbar Forest and we can characterize existing performance as "25 meters, 99.9%, in the narrow reaches. As with the mini-chain conclusions, this cannot be considered

adequate for "blind transit" of the tight reaches. When combined with conventional radar, however, use of the existing Loran-C provides a complete navigation package.

One final comment is in order before we finish our consideration of the St. Marys River region. Note that as in reference 3, we computed DRD as a direct function of range. In reference 15, when considering the Notheast U.S. Chain (9960), we saw the need to make a refinement on this direct calculation. Specifically, we found that when significant amounts of seawater were involved, the seasonal variations did not directly follow the DRD model. Good agreement with the model was restored, however, when the seawater portions of the paths were omitted from the DRD calculations.

For the paths involved in the St. Marys River, we have "freshwater" lakes which freeze during the winter. We have experimented with various "weighting factors" to assign to the water portions of the path. Depending upon which sites we use in the model, we find the best results when we "count" water somewhere between 90 and 115% of land. Here "best results" means the sum of the squares of the residuals is minimized. The analysis shows the "freshwater factor" definitely belongs somewhere in this region but we cannot pinpoint its value. Thus we used a factor of 100%, i.e., we made no distinction between freshwater and land in the DRD calculations. We mention this so that there is no implied disagreement with reference 15. We fully expect stability studies in other areas with "non-freezing" water paths will confirm the approach of reference 15.

The matter of the St. Marys River having been put to rest, we want to resume examination of the data as it applies to "larger" performance areas.

4.5 Data Record Problems - An Introduction To Loran-C Phase Modulation

We have concluded the analysis of the data, as it applies to the St. Marys River, with a certain amount of disagreement with the predictions of Section 3. We found we could not demonstrate the validity of the claim that, as one moves closer to the SAM (or a Differential Loran-C control station), one approaches the performance "floor" determined by a TD standard deviation of 11 nsec. In view of the background discussions in Section 1, we see a determination of the actual "floor" must be a prime objective of the stability studies. Thus we will focus on this single issue in the remaining sections of the report.

A major hint provided by the analysis of Section 4.1 is that the Riverside (Austron 5000) data actually supported the "ballpark" 11 nsec claim. We used this fact, along with the precedent set in reference 3, to include a "common error" term in the MMSE DRD model estimates. The argument was that Austron 5000 receivers are different than Internav 404 receivers. This suggests we are seeing "receiver problems." Further scrutiny, we feel, will show there is considerably more involved.

To pursue the issue somewhat further, we ignored the Riverside data and used Dunbar (Internav 404 data) as the simulated SAM. We saw a slight

reduction in the common error/residual terms but the 11 nsec figure remained elusive. Thus, we cannot support the argument that the problem is simply due to different generic types of receivers. Within a generic type, what we might call "ensemble differences" appear to be significant. Given a small number of sites, known anamolies at some of the sites, and only one Austron 5000 data record, we really cannot do a full scale analysis of the variations. Nevertheless, and recognizing the point is not fully supportable, we want to suggest there is a significant difference between Austron 5000's and Internav 404's, between one Internav 404 and another, and between one Austron 5000 and another. Moreover, we suggest these are all manifestations of a far-reaching Loran-C system characteristic. This characteristic has several other practical manifestations and we can demonstrate two of them.

Recall the discussions of Section 2 indicated there was an effective shift of antenna location when the Internav 204 equipment was removed from three of the harbor monitor sites in July 1981. This caused a substantial TD change which was detected and removed from the data records. This was an equipment grounding problem and independent of the problem we want to concentrate on in this section. While the "antenna move" offsets were being examined, however, a very interesting side issue was noticed. We begin the discussion of this side issue by presenting the 8970-X data record from Dunbar as it was before the "antenna effects" were removed. The data is plotted in figure 4-24.

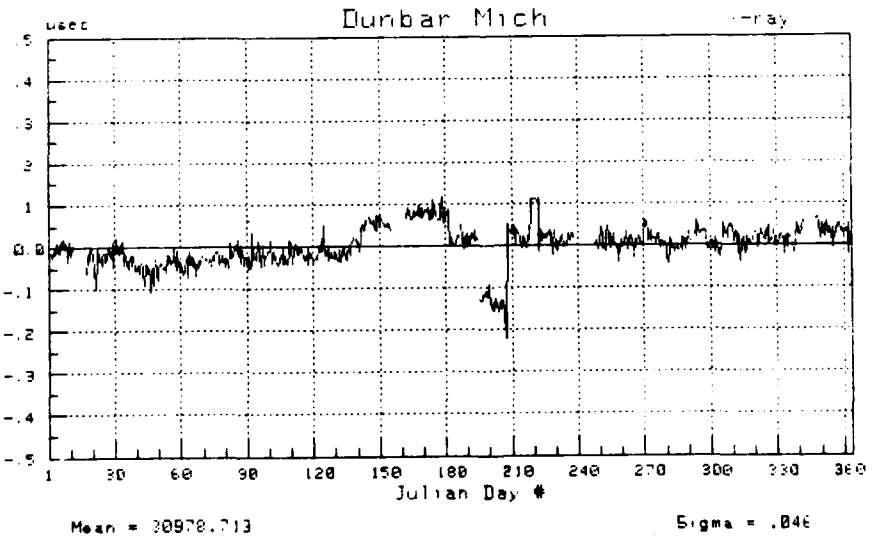

Figure 4-24 Dunbar 8970-X Harbor Monitor Data Before "204 Equipment Removal Effects" Were Removed

The plot shows the abrupt offset caused when the 204 set was removed - it happened on J.D. 182. Several other abrupt shifts can also be discerned, however, and these comprise the "side issue" we wish to point out. As discussed in Section 2, mini-chain and R&D Center personnel were able to re-construct the ground system tie-in and thus determine the offset caused by the removal of the 204 equipment. (The positive jump in the TD plot of Figure 4-24 at about J.D. 220 is a result of the ground being re-connected for a 3-day test.) With that offset removed, the plot of figure 4-25 shows the "side-issue" alone.

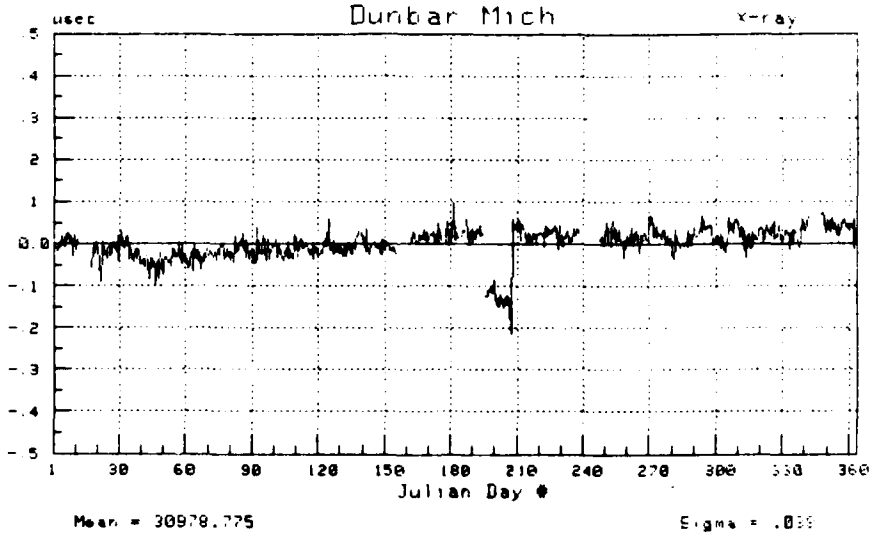

Figure 4-25 Dunbar 8970-X Harbor Monitor Data After "204 Equipment Removal Effects" Were Removed

The events surrounding the whole incident are worth relating since they help illustrate another point of Section 2 regarding how to conduct these experiments. While the incident was taking place, knowledgable R&D Center personnel (the installation team) were travelling around the country looking for suitable sites for future harbor monitor installations. While they were away, people less familiar with the intricacies of the system were checking the operation of the sites (via phone line access) and collecting the data. One day they discovered all the receivers in the St. Marys River area were tracking all the secondaries "10 usec low" (or so they thought). They recorded the discrepancy and dutifully "forced all the secondaries back where they belong."

When the installation team personnel returned to the Center they noticed the first problem immediately. It was not until the "204 removal" problem was resolved that they detected the "side issue." The side issue, of course, is that it was not "all the secondaries" that had "slipped a cycle," the master station had slipped a cycle. Thus, because of the improper "corrective action," all the signals were being tracked on a

different cycle than normal and although the TD's were approximately correct, there was a noticable (if you know what to look for) offset. We say "off course" the problem was with the master station but caution one can never be really sure right away. The proper corrective action was to have the receiver re-acquire all the stations. This is what the installation team personnel did and is what removed the offset and closed the incident.

Some final discussion regarding the "mechanics" of the incident is in order before we get to the point we wish to illustrate. The Internav 404 receiver can be operated in a mode in which it would have detected (and corrected) the problem with the master station on its own in a reasonable time. There were reasons, however, that we did not want to operate in this mode. Thus, we were operating in a mode (called "cycle jumps disabled") in which, if a cycle slip took place, the receiver would stay with the wrong track point. The question of how the cycle slip happened should be mentioned so that we do not leave the impression this is a receiver problem.

The problem, we suspect, (it is enormously difficult to reconstruct) happened because of a short master station off-air. Loran-C station signals go off the air in several ways. One way we can call "dying quickly and quietly." This way generally causes no problems. Other ways can be called "dying in agony" and "taking receivers with them." Typically this is caused by injecting considerable error into the receiver servo loop "velocity word." This causes the receiver loop to drive and, if a phase error in excess of 5 usec accumulates by the time a signal returns on-air, a receiver with its "cycle checking circuity" disabled will "slip a cycle." We should mention that we have studied the Internav 404 receiver by use of a simulator and noted that unless we "get the loop moving" before we take a signal away, signal losses for as much as 15 minutes will not cause cycle slips.

Upgraded versions of the harbor monitor sets routinely check for cycle slips and we think we no longer have this type of problem. We note that we have corrected the data records to remove this known source of TD offset. Whereas the incident is unfortunate (when you have to correct data records for problems like this, you are never sure how much of the problem - as opposed to the experiment - you are removing), it gives us an opportunity to illustrate several points. One is in regard to the difficulty typically encountered in executing massive data collection efforts, over a long period, with the goal of straining the last bit of information out of the signals. Another point ties in with our consideration of why the data record does not approach the ideal model we think it should: why do receiver TD readings change so significantly when the track point is changed one cycle? We claim the answer is the same system characteristic which caused the inter-receiver differences noted above. We also claim it causes the next problem we which to illustrate. To illustrate this problem, we turn to the substantial data base we have now accumulated under the harbor monitor program. The 9960-X data record accumulated by the Avery Point (R&D Center) harbor monitor set provides a good example. A segment of the data record is illustrated in figure 4-26.

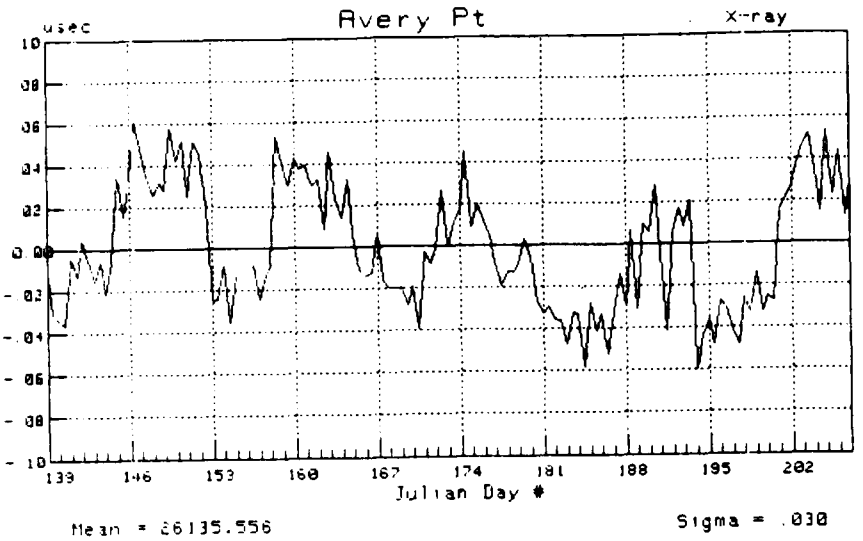

Figure 4-26 Avery Point Harbor Monitor Set 9960-X Data Record

The characteristic of the data record which should appear striking is the periodic offset that appears to occur, almost like clockwork, every week. We should note right away that what we are about to discuss is a phenomenon noticable in almost all Loran-C baselines. There are very definite reasons why this baseline happens to illustrate our point so "cleanly."

Those familiar with Loran-C chain operations realize that, at dual transmitter stations, the goal is to routinely switch transmitters every two weeks. Chain operators confirm, however, that the Nantucket station was changing transmitters every week during the period illustrated above. To complete the picture, we note that the 9960-Master station, Seneca, is equipped with a single, solid state transmitter and thus performs no transmitter switches. (For those whose subconscious mind generates answers while the conscious mind is concentrating on reading, the Dana and Baudette stations have dual transmitters. Thus, the 8970-X baseline - i.e., the one with the 26 nsec common error term standard deviation - features only one dual transmitter station whereas the 8970-Y baseline - the one with the 40 nsec common error term standard deviation - features two dual transmitter stations.)

We have obtained a record of Nantucket transmitter switches and constructed the "squarewave" sequence shown in figure 4-27. We recognize the pattern as reflected in the data. If we attempt a MMSE curve fit of the data of figure 4-27.a to the waveform of figure 4-27.b, we obtain a square wave peak-to-peak amplitude of 40 nsec. This represents the difference between the way the Avery Point Internav 404 receiver sees the transmitter switches and the way the Sandy Hook (9960-X SAM) Austron 5000 sees the switches. We remove this pattern from the data to obtain the data record plotted in figure 4-28.

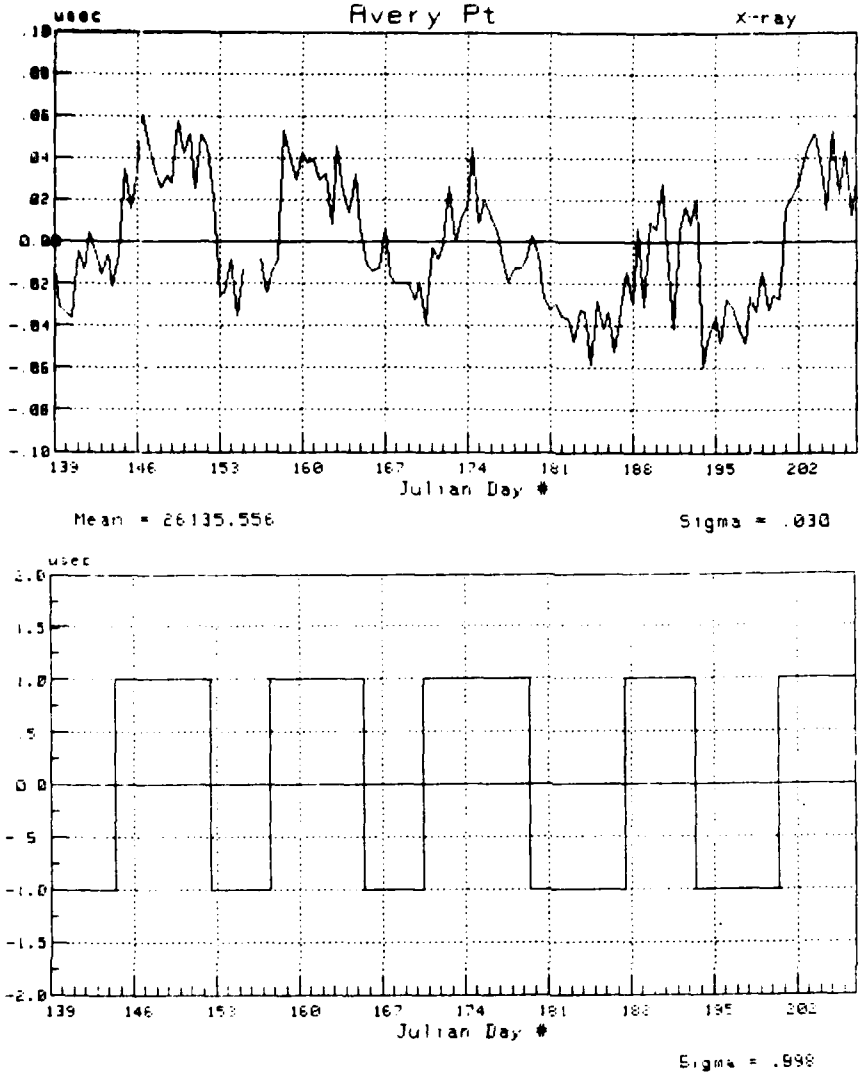

Figure 4-27 Avery Point 9960-X Data vs Nantucket Transmitter Record

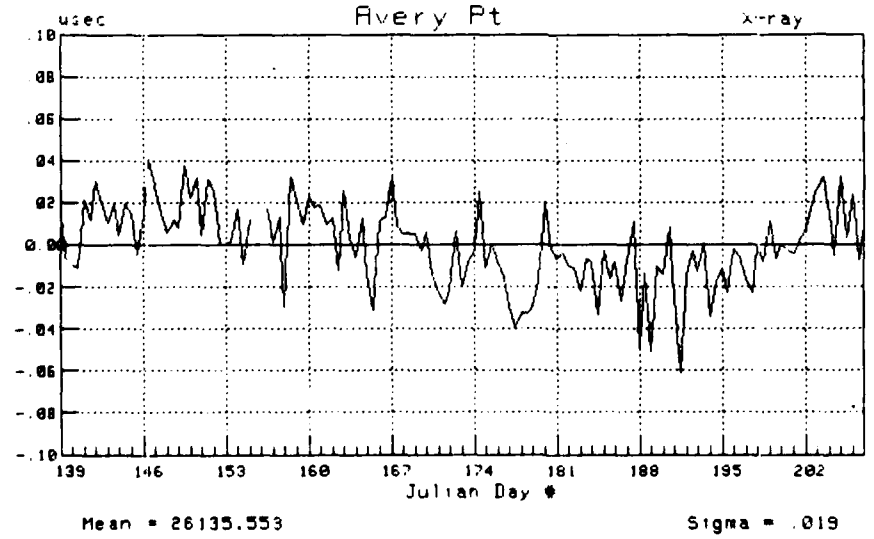

Figure 4-28 Avery Point Data With Estimated Transmitter Effects Removed

Again, we point out the only things special about our choice of the Nantucket signal are that the master station of the baseline has a single transmitter and that the particular data segment illustrated was otherwise "clean." Other segments of the same data record show independent effects and, like records for other baselines, obscure the phenomenon we wish to illustrate clearly.

At this point we have exhausted our collection of simple examples which illustrate there are areas to explore if we are not satisfied with the residuals/common term errors of the St. Marys River data analysis. Again, we mention there are other manifestations of the underlying problem but note we do not have simple ways of illustrating them. The problems are all caused by what, in Loran-C circles, is called "phase modulation." Newcomers to Loran-C may be somewhat surprised that so many effects are attributed to one system "parameter." To put the matter in perspective we suggest the following line of thinking.

When one first begins to explore the Loran-C system, one encounters the idea that the first goal of a receiver is to process the signal "envelope" to obtain a "coarse" estimate of the signal timing. If that goal is achieved, the correct cycle has been selected and the rest of the problem is to simply track the phase of the signal at the indicated track point and thus estimate the "fine" timing of the signal. Proceeding a little further, one discovers there is this almost mythical quantity called "ECD." It can be easy or difficult to describe and difficult or easy to understand (probably in that order) but the net result is that it is the system parameter which determines the ultimate utility of the system - i.e., whether or not the desired tracking cycle can be located by a receiver. Pursuing the matter further, one finds that there are many sources of ECD problems and many manifestations of the problems. All of these are lumped into one simple term because they have the simple consequence: the desired cycle is either found (pass) or not found (fail).

When viewed this way, it is perhaps not so surprising that there should be a simple term to represent the many things which can cause errors in the "fine" timing measurement. We will describe phase modulation in the next section. For now, we want to discuss the role it plays in the stability studies of the past and of the future.

Reference 3 (in its final form) mentioned phase modulation as a suspected source of remaining uncertainty about the mini-chain. In the summary of reference 3, one can detect a certain air of frustration illustrated by the conclusion: "the data and analysis presented here represents about as far as one can go given the resource investment..." If we recall the discussion of Section 1, we see a reason for the concern that we are no longer faced with. The mini-chain was a test bed. It was a "target of opportunity" to explore the ultimate precision of Loran-C. At the same time, however, it was extremely difficult to operate. The climate was difficult, the area was not convenient to sources of significant Loran-C engineering expertise, and the equipment was "non-Coast Guard standard." Thus the persistent fear that "we're missing something at the transmitting stations and the conclusions will not be representative of Loran-C in other areas."

In the present and future studies, we no longer need have this fear about the sources of the signals. Equally important, we no longer are tied to a distant, difficult to support area of experimentation. Finally, we have the advantage of confirming our suspicions that the observations are representative of "general" Loran-C.

Thus, we will differ somewhat with the summary of the mini-chain experiment regarding the St. Marys River area. Like reference 3, we suspect "phase modulation" (with two years of additional experience, our suspicions are much stronger). Like reference 3, we feel the phase modulation matter should be pursued. Unlike reference 3, however, we will not say: this is about as far as we can go in the St. Marys River. Instead, we say: we have gone as far as we should go in the St. Marys River. The examples of this section were obtained in a fortuitous manner. Whereas they are useful in illustrating the problem, they are insufficient to indicate whether or not anything can be done about it. If we are to find out what, if anything, can be done, we will have to proceed with a more carefully designed experiment. We must recognize the enormous difficulty in attempting to pinpoint this ultimate limitation of a high performance system and that our efforts may be unsuccessful. To maximize our chances of success, we must chose our own arena. Whereas we want to leave our options open, we can already say the arena will not be in the St. Marys River.

4.6 Phase Modulation of the Loran-C Signal

To begin the discussion, we turn to the description of the Loran-C pulse provided by reference 13. For our purposes we can re-write the formula as:

$$i(t) = x(t) \sin w_c t$$

This expression represents the transmitting antenna current waveform and we should note all the variables are supposed to be real valued (i.e., no imaginary numbers are involved). The carrier frequency is 100 Khz, i.e., $w_c = 2\pi \times 100{,}000$ with time (t) expressed in seconds.

The Loran-C system user generally does not have the opportunity to examine the antenna current waveform directly. If we were to examine it, however, we would want to do so with a spectrum analyzer. Typically, the spectrum analyzer would show that the current waveform spectrum is not perfectly symmetrical about 100 Khz.

Any number of textbooks which describe Fourier Transform theory are available. Early in the discussion, they establish how one can compute the spectrum of a waveform such as what we have shown for i(t) in terms of the spectrum of x(t), i.e., by use of what is generally called the "shifting" property. Application of this principle shows that if i(t) is not symmetrical about 100 Khz, then the spectrum of x(t) is not symmetrical about zero frequency. Further discussions of Fourier Transform properties show that this means x(t) cannot be real-valued. Indeed, this demands that x(t) have non-zero real and imaginary parts.

Complex numbers allow extremely powerful mathematical concepts but cannot directly represent so concrete a quantity as a current measurement. The implication is that, since we can only conceptually have a complex envelope, and since we want to take the discussion to more practical areas, we should seek a different representation of i(t). Such a representation exists, of course, and is:

$$i(t) = y(t) \sin w_c t + z(t) \cos w_c t$$

Here we see we have a so-called "in-phase" term and a so-called "quadrature" term. All quantities are real-valued and w_c still equals 2π x 100,000.

The ultimate goal of a Loran-C receiver is to measure the time difference of the received signals. Reference 13 calls this the "phase time difference" and we prefer this term. We want to talk about both phase and time. Starting with time, we note reference 13 states that time is defined by the sine-component. We see, therefore, that we can talk about phase in conventional electronics engineering terms using the sine wave as the reference. Given an in-phase and quadrature component, the phase is traditionally defined as:

$$|\phi(t)| = \tan^{-1}(y(t)/z(t))$$

(We have used the absolute value sign to avoid presently unimportant arguments about sign-conventions).

Examination of actual antenna current spectra shows that, whatever the actual values of y(t) and z(t), they are not DC-signals. Indeed, they change as functions of time across the "leading edge" of the pulse (the important portion of the signal for our purposes) so that $\phi(t)$ changes throughout the leading edge of the pulse. This changing nature of the pulse phase is what has led to use of the term "phase modulation."

From the discussion thus far, we have seen that phase modulation and "spectral asymmetry" are equivalent. Thus, anything that prevents the signal, at any stage in the system, from being perfectly symmetrical about 100 Khz, introduces what is called phase modulation.

Returning to the time domain description of reference 13, we see that the ideal envelope, x(t), is positive-valued. In practice, this is true throughout the leading edge. Thus, for the ideal situation, i(t) can be zero only when sin $w_c t$ is zero (since $x(t) > 0$). Consequently, "zero-crossings" would be found in the ideal antenna current at precisely spaced intervals of 10 usec. For the more general expression with both an in-phase an quadrature term, zero crossing are determined by the solutions of the more complex equation:

$$y(t) \sin w_c t + z(t) \cos w_c t = 0$$

At this point, then, we can see how reference 13 handles "phase-modulation-type" imperfections in the signal. A table is provided which describes "tolerances" on the zero-crossing locations. In short, the $x(t) \sin w_c t$ signal is offered as the ideal and deviations from this ideal are specified with the required "frame of reference" provided by defining the "30 usec point" as the standard reference point. Thus, reference 13 is consistent with our development. We have taken a different approach because, rather than providing a specification, we are trying to explore the implications.

The implications are determined by the effect phase modulation has on receivers. We can begin the discussion by noting that at the transmitting station, direct meaurements of the standard reference point, the 30 usec point, are possible. A receiver in the service area must contend with the fact that noise is received along with the signal. Thus, filters must be used and this makes it impossible to directly measure one point on the received signal. To examine how this effects the "final answer" determined by the receiver, we need to present a mathematical model for the process involved in the receiver.

We will start the development of the model by imagining an undistorted version of the antenna current waveform is delivered to the receiver. To keep the discussion simple, we will leave the details to Appendix B and present only the important results here. We will call the received signal $r(t)$ and note there is a time-varying phase waveform, $\phi(t)$ associated with the signal. If there is no phase modulation in the received signal, $\phi(t)$ is zero and we are dealing with a pure (amplitude modulated) sinewave.

In thinking about how receiver signal processing is implemented after the filter, we generally think of a zero-crossing detector. We will stick with this line of thinking but first note it does not have to be done that way - any convenient way of measuring the phase can be used. A zero crossing detector turns out to be the easiest method to implement. If we avoid the "ease of implementation" issue momentarily, we see an initial step in the design is to choose a "track point." (Arguing that it does not <u>have to be</u> a zero-crossing allows us to explore general concepts. More important, it begins to break us away from thinking that a single zero-crossing, defined in the signal specification and measured at the transmitting station, somehow "makes it" to the receiver phase locked loop "unscathed.")

Selection of the track point is the result of a complicated series of design tradeoffs - primarily determined by the desired skywave interference vs man-made noise interference tradeoff. We can denote the selected track point as T and note that the "voltage" delivered to the phase locked loop circuitry is

$$V = \int_{-\infty}^{T} r(t)\, h(T-t)\, dt$$

i.e., the phase locked loop input is determined by the convolution of the received signal with the receiver "front end" impulse response. Here we should introduce the fact that the actual quantities processed have "in-phase" and "quadrature" components which we will represent by the

notation $r_I(t)$ and $r_Q(t)$ (these represent the baseband signals). As with our description of the received signal, we must also represent the receiver "front end" response with an in-phase and quadrature component. The implied phase will be deignated by $\theta(t)$.

Let us first imagine that both the received signal and the "front end" response have spectra which are symmetrical about 100 Khz. Thus, there is no phase modulation and $\phi(t)$ and $\theta(t)$ are zero. In this case, as shown in Appendix B, we get:

$$V = A \sin w_c T + B \cos w_c T,$$

where A and B are constants determined by the filter characteristics. If we choose to implement a "zero-crossing" detector circuit, this means we have T determined by the equation

$$\tan w_c T = -B/A, \text{ or}$$

$$T = \delta + N \cdot \pi / w_c = \delta + N \cdot 5 \text{ usec}$$

The δ indicates the filter output need not be exactly in phase with the input. The particular "sense" of the zero-crossing to be tracked is a designer's choice. With this choice made, we have determined whether N is odd or even. The specific odd or even number is determined by the envelope circuit design.

Appendix B goes on to consider the case wherein the receiver response is still ideal (i.e., with a spectrum of the impulse response symmetrical about 100 Khz), but the received signal contains some phase modulation. Thus, r(t) has an in-phase part and a quadrature part. Using the argument that phase modulation is typically small (i.e., although $\phi(t)$ may not be zero, it is small), the Appendix shows that phase modulation in the received signal causes the receiver to move to a slightly different track point, $T' = T + \Delta T$ where,

$$\Delta T \simeq k \int_{-\infty}^{T} r_I(t)\, \phi(t)\, h(T-t)\, dt$$

where k is a constant.

This is an extremely important result for visualizing phase modulation effects. It shows that the time offset is a weighted integral of the signal phase, $\phi(t)$. The "weighting" function is determined by the envelope of the received signal and a "folded" version of the receiver impulse response envelope (folded about the desired track point).

To use this to explain the difference between the response of an Austron 5000 and a nearby Internav 404, we note first that $r_I(t)$ and $\phi(t)$ will be essentially the same in both cases. We can imagine that the desired track point is the same for both receivers (this is approximately true, as it turns out). The h(t) waveforms are significantly different, however.

The Austron 5000 is fairly wideband while the Internav 404 is fairly narrow band. Thus, the Austron time domain response "rises and decays rapidly," while the Internav response does so slowly. When "folded" about the track point, this means the Austron "emphasizes" the $\phi(t)$ values just before the track point and "forgets" earlier values. The Internav, conversely, remembers the phase errors from a much earlier portion of the received signal. Thus, the two receivers obtain different values of ΔT.

We can use the above discussion to visualize what occurs when Nantucket switches transmitters. After the switch, receivers in the field are provided significantly different $\phi(t)$ waveforms than before. The Austron 5000 at Sandy Hook probably sees a difference between the two transmitters (i.e., ΔT_1) and corrects for the offset (a SAM prerogative). The Internav at Avery Point, however, sees a slightly different ΔT (i.e., ΔT_2) so SAM's corrective actions do not restore the Avery Point TD to the value measured before the switch. Thus we record a TD offset of $\Delta T_2 - \Delta T_1$.

Appendix B continues by examining the situation obtained when the received signal is ideal (no phase modulation) but the spectral symmetry of the receiver response is disturbed. The result is that

$$\Delta T = k \int_{-\infty}^{T} r(t)\ \theta(T-t)\ h_I(T-t)\ dt$$

which, by analogy with the preceeding example, is as expected. Here, the $\theta(t)$ is associated with the spectral asymmetry of the receiver response.

We can use the above results to show what happens when we "slip a cycle" on <u>one</u> of the received signals. With an ideal received signal and receiver response, the TD changes 10 usec, i.e., we change N by 2 where, in the ideal case, $T = N \cdot 5 \text{ usec} + \delta$. If there is phase modulation in the receiver response (or in the received signal), however, we will get an additional ΔT change where

$$\Delta T = k \int_{-\infty}^{T} r(t)\ \phi(t)\ h(T+10-t)\ dt$$

This can be thought of as an effective filter change since we are significantly changing the weight being applied to $\phi(t)$ by the $h(\cdot)$ term.

The results can also show how a much less expected result can occur. This phenomenon was observed (but not fully understood) in the early stages of the mini-chain experiment and startled most project people. Suppose a receiver, with a "non-symmetrical front end," i.e., with a non-zero $\theta(t)$ term, is provided a signal which has no phase modulation. Now suppose we change the received signal - not by introducing any phase modulation, but by changing the ECD. We see now we have changed (shifted) the r(t) term and, thus, changed the weight assigned to $\theta(t)$. Thus, even with ideal signals (for a "real world" receiver), changing the ECD will cause a <u>phase shift</u> - just like changing the track point will. On further thought, this should not be too surprising since, in the extreme, we recognize a "10 usec ECD shift" as the same as a cycle slip.

We can extend the above results to show what happens when, for example, a receiver notch filter is adjusted. This distorts the receiver response symmetry and causes a TOA offset. Notice that the notch filter can be adjusted by the user or by the SAM with the same ultimate effect. We can note also that if the filter is adjusted in one receiver but not another of the same generic type, we must expect a difference between the two receivers.

This last example is very uninteresting for most Loran-C applications because, under the assumed "ideal signal" conditions, the same TOA shift occurs for the master and secondary signals so there is no TD offset. A similar result occurs if the received signals (master and secondary) are "identically distorted."

In general, of course, we expect spectral asymmetry due to both sources - the imperfections in the receivers and the imperfections in the received signals. As Appendix B shows, the offset, ΔT, in this case is approximately represented as

$$\Delta T = k \int_{-\infty}^{T} R_I(t) \, [\phi(t) + \theta(T-t)] \, H_I(T-t) \, dt$$

Since the "$\phi(t)$'s" will be different for the master and secondary stations, the above expression shows how even a seemingly harmless notch filter adjustment will produce different TOA changes and, thus, a TD shift.

To expand the concept, we should view the entire system in view of the model we now have. Specifically, we can define the start of the system as some timing reference signal at the transmitting station. We can imagine that an "impulse" is generated at some time determined by that reference and that there are a series of filters between the impulse and the end of the system - the receiver phase locked loop. We can say the filters are: the transmitter, the antenna/antenna coupler, the "filter" which describes the antenna current-to-far field transformation, the propagation path, and the receiver front end. We can see that each of these filters are sources of phase modulation and, ultimately, can limit the performance of the Loran-C system.

To get to the bottom line, we should emphasize that none of this causes insurmountable problems for HHE applications unless the factors change. The fact, for example, that an Austron 5000 and an Internav 404 will give different TD readings at a given site can be handled as long as the difference does not significantly change from time to time and over a small area. If the effects do not significantly change, for example, a trackline survey can be conducted with one type of receiver and, given a single site, one-time calibration, any receiver can use the same results.

If phase modulation effects change over a short period of time or over a small area, however, there is no simple solution. This is why we must be concerned with the effects of transmitter switches. We must note, however, that the only difference between transmitter switch effects and any other

manifestation of phase modulation, as far as we can presently demonstrate, is that the transmitter switch effects, which happen abruptly, can be easily illustrated. It is not so easy, for example, to determine how much propagation path changes effect phase modulation since these occur very slowly. Similarly, since there is only one antenna/antenna coupler per transmitting station, we do not have an easy way of seeing quick changes in these filters.

Ultimately, we have to find some way of determining how much each of the possible sources of phase modulation contribute to the total error budget. We note, for example, that there is something we can do to improve the tuning of transmitters. The improvement, of course, will involve some expense. Thus, to advocate the improvements, we must be able to show that imperfect transmitter performance causes a major portion of the problem. If, alternatively, it turns out that propagation path changes, i.e., something we cannot control, contribute most heavily to the problem, there is little to be gained from improving transmitter performance. In such a case, we must conclude we have reached (i.e., determined) the practical limit of system performance.

We note in closing, that reference 14 addressed all of these questions. We feel the matter must be further pursued for two important reasons, however. First, reference 14 was written without consideration of stringent HHE requirements. Thus, for example, effects on the order of 50 nsec were considered insignificant. Second, reference 14 had very little empirical data to work with. Indeed, observations obtained with the harbor monitor sets to date indicate the problems can be considerably different from those hypothesized in reference 14. Given that we now have the opportunity, if we are clever, to do a more empirical analysis, we should re-examine the entire issue.

The results of our efforts will be featured in future stability study reports.

5. Summary and Conclusions

To begin this report, we outlined the entire USCG HHE Loran-C R&D program, concentrating on the St. Marys River which, for years, was the only available test bed. With this background established, we summarized the deliberations relating to use of the Gordon Lake station as a supplemental LOP for the Great Lakes Loran-C Chain.

Continuation of one of the Mini-Chain stations, for at least a short experimental period, presented the opportunity to examine the final method of chain enhancement techniques featured in the HHE Loran-C strategy. It was recognized, however, that the studies might show there was some advantage to operating the station on a permanent basis. Thus, plans were made to include this possibility. The implementation decision had to be made at some point and, for reasons indicated, events forced the decision to be made just as the experiment was starting in January 1981. Besides documenting the considerations of the decision-making process, this report provides an opportunity to compare the results of one approach to estimating precision Loran-C performance to the more empirical approach featured in Section 4. Although the empirical approach will be the prime one used, both approaches will be featured in the HHE Loran-C Stability Studies, the remaining element in the USCG HHE Loran-C R&D Program.

The analysis indicated the following:

- Data from the 8970-X and -Y signals was available for the last 7 Months of 1980. This data was sufficient to show that "raw" Loran-C yielded inadequate performance in the St. Marys River. We note that the reaches of the river can be broadly classified as "wide" or "narrow" and that, as indicated in the Mini-Chain Final Report, Loran-C is not really needed for the narrow channels.

- Loran-C can serve a useful purpose in the wide reaches - indeed it is extremely useful in any reaches where alternate radio aids to navigation such as radar are not effective (e.g., due to lack of good radar targets). Such is the case in the wide reaches of the St. Marys River so an argument for providing "decent" Loran-C can be made. Since it is necessary to "enhance" existing Loran-C to provide this service in the St. Marys River, an argument can be made for the supplemental LOP approach - assuming it provides adequate performance.

- Before examining the supplemental LOP performance, we consider the expected performance when the existing system is operated with a mild (e.g., daily) form of differential corrections. We find this provides adequate performance in the wide reaches but not in the narrow reaches. We note, however, that Differential Loran-C - of any form, is a "new start" for the Coast Guard whereas operating another transmitting station (and a monitor) would not be. Thus we claim the "daily correction technique" should not be automatically assumed to be the desired approach, no matter how inexpensive it may appear on the surface.

- We simulate "ideal" performance of the new station and combine this

third TD record with the available observations from the other two stations. The results indicate the supplemental LOP approach does not measure up to the daily correction approach. Indeed, it does not satisfy performance requirements in all of the wide reaches. Again, this is for "ideal" 8970-Z performance which we know we cannot achieve.

- We caution that this is not a general conclusion regarding the Supplemental LOP concept. "Geometry improvement" is a prime advantage of a Supplemental LOP as an examination of the Houston/Galveston area will show. In the St. Marys River, however, the Loran-C geometry for the existing chain is near optimum so the full power of the technique cannot be effectively demonstrated.

- When we examine expected performance of the two enhancement techniques combined (i.e., daily corrections and the supplemental LOP), we find we have adequate performance, assuming ideal 8970-Z behavior, in all reaches - but only with one combination of 2-TD's. Suboptimal performance for the remaining combinations is offered as one reason for avoiding this "solution" even if the ideal could be achieved. We note, however, that once we add a small amount of expected seasonal variation to the 8970-Z simulated data, we are back to the situation wherein adequate performance is available only in the wide reaches. To add the consideration of seasonal variations, we had to employ the so-called "double-range-difference" (DRD) model, the classical approach to explaining this type of Loran-C variations.

- At this point in the deliberations regarding the fate of 8970-Z, it was recognized that there was no reason to expect any substantive improvement in performance by the addition of the supplemental LOP in the St. Marys River. Thus, the decision was made to cancel permanent implementation plans and to complete the Gordon Lake R&D experiment in mid-1981.

- Concern about possible problems at the Muskegon monitor site prompted a temporary move of the prime 8970 chain control station to Riverside in May 1981. This afforded several advantages to the R&D studies. First, it made the stability studies much easier to conduct. Additionally, it came close to simulating real-time differential Loran-C performance in the St. Marys so that guidance equipment demonstration could continue. Finally, and perhaps most importantly, it allowed a "graceful" exit from the area.

- Recognizing the improved performance implications of this move, we re-examined the expected performance - with or without the supplemental LOP - to be sure there was still no reason for continuing Gordon Lake. With control at Riverside, performance was expected to be adequate in all but one reach - without the supplemental LOP. With the supplemental LOP, one of the possible 2-TD combinations was expected to yield adequate performance in all reaches. The other two 2-TD combinations provided "borderline" performance in the narrow reaches and the expected 3-TD performance was expected to be inadequate in some reaches. Thus, there was no substantive change from previous findings.

- A final refinement involved a more optimum selection of a local

monitor site - specifically, Dunbar Forest. Under this condition, performance was predicted to be adequate in all reaches - without the supplemental LOP. Similar results were expected for all other 2-TD possibilities and the 3-TD performance appeared "borderline" in only one reach. As a general note, there is no theoretical reason that the 3-TD performance could not be made better than any of the 2-TD combinations. This would require a different "weighting function" than that used in PILOT. As described in Appendix A, the PILOT approach is to optimize "tracker jitter" performance. Thus, the importance of a TD in the 3-TD position solution is driven by expected received signal strength rather than hyperbolic distance to the SAM (i.e., rather than DRD considerations).

- Thus, even with a local monitor at a nearly optimal location there is no performance advantage to the supplemental LOP in the St. Marys River. We conclude the performance prediction section by claiming care must be taken in offering any "redundancy" argument in support of the supplemental LOP. The system is still "Loran-C - one system" - and one achieves true redundancy better by the use of a completely different system such as radar. Since locals feel this is an adequate approach to the narrow channels, the final argument in favor of the St. Marys River Supplemental LOP evaporates.

- Turning to an examination of data obtained later in the study, we use an empirical application of the DRD model. In this approach, the goal is to obtain MMSE estimates of the expected prime components of the variation.

- Initial application of the model yields disappointing results. Further examination of the data shows that the 8970-X data record from the Pt. Iroquois site is the main source of problems. When this data record is "de-emphasized," essentially all of the "gross" structure in the variation can be removed. The "residuals" and the "common error" terms show larger variations than used in the predictions of Section 3. This is identified as an area for later study

- Proceeding with the analysis, we show the signal components estimated from the 8970-X and -Y data are consistent with the limited 8970-Z data. This forms the basis for concluding there is no substantive difference between long and short baselines. This allows us to use available data records to generate performance predictions for both 2-TD and 3-TD cases.

- The results show that the existing chain provides 25 meters, 99.9% probability, cross-track error performance in the narrow reaches, with no significant improvement offered by the third LOP. This is the final statement about the St. Marys River Loran-C situation.

- Turning to a consideration of the implications on further studies outside the St. Marys River, we examine some of the problems indicated in the data record. Sufficient examples are given to indicate the prime contributor to Loran-C performance limitations is phase modulation.

- Use of data from outside the St. Marys River shows this is an

endemic system problem. We conclude this will determine the best possible performance level of HHE Loran-C.

- The Loran-C transmitters are known to contribute to the phase modulation total and we suspect this contribution is the largest part of the whole. Of the several sources of phase modulation, the tranmitter is the one amenable to improvement. Thus the report concludes future studies should be conducted under controlled conditions not possible in the St. Marys River, to determine if transmitter improvements are warranted.

APPENDIX A

ERROR ELLIPSES FOR 3-TD FIXES

Reference 2 contains an extensive series of Appendices describing the derivation of the so-called G-matrix, the linear transformation between a 3-TD space and the 2-dimensional position space (Lat/Long). Since an understanding of the method is important in following the presentations in this report, the derivation should be discussed in some detail herein. A prime motivation for including a separate presentation (i.e., as opposed to simply saying "see ref 2") is that the Appendices of reference 2 are simply a progression of technical notes. That method of presentaion makes it extremely difficult to follow the flow of the derivations. Additionally, the reference 2 Appendices devote considerable time to examining the area over which a single G-matrix calculation is valid. This is extremely important when the goal is to "translocate" several kilometers from a given waypoint as PILOT must do. Since we are concerned with much smaller areas, however, we can ignore this refinement. Thus, we can shorten the presentation and concentrate on only those considerations which are an important introduction to the discussion of error ellipses.

Appendix A of reference 15 presented an in-depth discussion of 2-TD error ellipses. Much of what is presented herein will draw upon that reference source and, wherever possible, comments will be made to indicate how the results here can be reduced to those of reference 15.

The 3-TD System of Equations

As in the 2-TD case discussed in reference 15, we recognize that for a small area, a "flat earth/linear grid" model adequately describes TD variations. Thus,

$$\Delta TD_1 = \frac{\partial TD_1}{\partial x}\Delta x + \frac{\partial TD_1}{\partial y}\Delta y$$

$$\Delta TD_2 = \frac{\partial TD_2}{\partial x}\Delta x + \frac{\partial TD_2}{\partial y}\Delta y \qquad \text{(A-1)}$$

$$\Delta TD_3 = \frac{\partial TD_3}{\partial x}\Delta x + \frac{\partial TD_3}{\partial y}\Delta y$$

or, in matrix form,

$$\begin{bmatrix} \Delta TD_1 \\ \Delta TD_2 \\ \Delta TD_3 \end{bmatrix} = \begin{bmatrix} \frac{\partial TD_1}{\partial x} & \frac{\partial TD_1}{\partial y} \\ \frac{\partial TD_2}{\partial x} & \frac{\partial TD_2}{\partial y} \\ \frac{\partial TD_3}{\partial x} & \frac{\partial TD_3}{\partial y} \end{bmatrix} \begin{bmatrix} \Delta x \\ \Delta y \end{bmatrix} = \underline{A} \begin{bmatrix} \Delta x \\ \Delta y \end{bmatrix}$$

Also as in reference 15, $TD_i = \gamma_i + \frac{r_i - r_m}{v}$

so that

$$\frac{\partial TD_i}{\partial x} = \frac{1}{v} \left(\frac{\partial r_i}{\partial x} - \frac{\partial r_m}{\partial x} \right)$$

$$\frac{\partial TD_i}{\partial y} = \frac{1}{v} \left(\frac{\partial r_i}{\partial y} - \frac{\partial r_m}{\partial y} \right)$$

and

$$\frac{\partial r_i}{\partial x} = - \sin \beta_i \qquad \frac{\partial r_i}{\partial y} = - \cos \beta_i$$

where: the r_i's are ranges to the secondary stations, the r_m's are ranges to the master station

γ_i is the baseline emission delay which varies as a function of time but not as a function of x or y (i.e., position)

the β's represent the bearing from the observer to the appropriate transmitting station and are measured counter-clockwise from North.

Thus, in the 3-TD case,

$$\underline{A} = \frac{-1}{v} \begin{bmatrix} (\sin \beta_1 - \sin \beta_m) & (\cos \beta_1 - \cos \beta_m) \\ (\sin \beta_2 - \sin \beta_m) & (\cos \beta_2 - \cos \beta_m) \\ (\sin \beta_3 - \sin \beta_m) & (\cos \beta_3 - \cos \beta_m) \end{bmatrix}$$

The difference between this and the 2-TD case is that here, A^{-1} does not exist so we cannot simply say

$$\begin{bmatrix} \Delta x \\ \\ \Delta y \end{bmatrix} = \underline{A}^{-1} \begin{bmatrix} \Delta TD_1 \\ \Delta TD_2 \\ \Delta TD_3 \end{bmatrix}$$

The solution is to recognize that in (A-1) we have 3 equations with 2 unknowns (Δx and Δy). The partial derivatives can be calculated, as shown above, and the TD's are measured. In general, because of measurement errors, there will be no solution - i.e., the 3 equations are "inconsistent."

We avoid this dilemma by explicitly acknowledging the errors and introducing three more "degrees of freedom."

$$\begin{bmatrix} \Delta TD_1 \\ \Delta TD_2 \\ \Delta TD_3 \end{bmatrix} = \underline{A} \begin{bmatrix} \Delta x \\ \\ \Delta y \end{bmatrix} + \begin{bmatrix} e_1 \\ e_2 \\ e_3 \end{bmatrix}$$

The e's represent the measurement errors. We now have 3 equations and 5 unknowns. This system of equations has an <u>infinite</u> number of solutions - a better situation to be in than the one wherein there is <u>no</u> solution. The rest of the problem simply involves choosing <u>one</u> of the infinite alternatives available to us.

There are at least three classical approaches to the choice worth mentioning. In the first, we choose that solution which results in the minimum mean squared error (MMSE), i.e., our solution features a minimum value of the quantity:

$$(e_1^2 + e_2^2 + e_3^2)/3$$

Minimization of the above quantity, of course, is guaranteed by minimization of the quantity representing simply the sum of the squares:

$$e_1^2 + e_2^2 + e_3^2$$

The above quantity can be written:

$$\underline{e}^T\underline{e} \qquad \text{where} \qquad \underline{e} = \begin{bmatrix} e_1 \\ e_2 \\ e_3 \end{bmatrix}.$$

The second choice is to minimize a "weighted" average of the squares of the errors:

$$w_1 e_1^2 + w_2 e_2^2 + w_3 e_3^2$$

or $$\underline{e}^T \underline{W}\, \underline{e}$$

where $$\underline{W} = \begin{bmatrix} w_1 & & \underline{0} \\ & w_2 & \\ \underline{0} & & w_3 \end{bmatrix}$$

The third choice minimizes $\underline{e}^T \underline{W}\, \underline{e}$ where $\underline{W}$ need not be diagonal. It is, however, symmetrical:

$$\underline{W} = \begin{bmatrix} w_{11} & w_{12} & w_{13} \\ w_{12} & w_{22} & w_{23} \\ w_{13} & w_{23} & w_{33} \end{bmatrix}$$

Matrix/Vector Differentiation

The Appendices of reference 2 utilize an involved method to show that an "arrived at" (somehow) solution is indeed an MMSE solution or weighted MMSE solution. The authors prefer an approach which is similar to the minimization problem addressed in basic calculus. This approach has the nice feature of deriving the solution and requires only that we be familiar with matrix/vector differentiation techniques.

The following results can be found in any number of references (e.g., reference 16). All vectors are column vectors and all vector/matrix multiplications satisfy conformal requirements. Matrices are shown in upper case and vectors are in lower case. Both matrices and vectors are underscored. A lower case element with no underscoring is a scalar. All matrices shown here are constant and $\underline{z}$ is not a function of $\underline{x}$.

Rule 1: $\dfrac{\partial k}{\partial \underline{x}} = \underline{0}$ (the null vector)

Rule 2: $\dfrac{\partial \underline{a}^T \underline{x}}{\partial \underline{x}} = \underline{a}$

Rule 3: $\dfrac{\partial \underline{x}^T \underline{A}\, \underline{x}}{\partial \underline{x}} = \underline{A}\, \underline{x} + \underline{A}^T \underline{x}$

MMSE, Weighted MMSE and G-Matrix Solutions

For ease of notation, let

$$\underline{z} = \begin{bmatrix} \Delta TD_1 \\ \Delta TD_2 \\ \Delta TD_3 \end{bmatrix} \qquad \underline{x} = \begin{bmatrix} \Delta x \\ \Delta y \end{bmatrix} \qquad \underline{e} = \begin{bmatrix} e_1 \\ e_2 \\ e_3 \end{bmatrix}$$

$\underline{A}$ is as before.

We have $\underline{z} = \underline{A}\, \underline{x} + \underline{e}$

$$\underline{e} = \underline{z} - \underline{A}\, \underline{x}$$

$$\underline{e}^T \underline{e} = (\underline{z} - \underline{A}\, \underline{x})^T (\underline{z} - \underline{A}\, \underline{x})$$

$$= \underline{z}^T \underline{z} - \underline{z}^T \underline{A}\, \underline{x} - (\underline{A}\, \underline{x})^T \underline{z} + (\underline{A}\, \underline{x})^T \underline{A}\, \underline{x}$$

$$= \underline{z}^T \underline{z} - \underline{z}^T \underline{A}\, \underline{x} - \underline{x}^T \underline{A}^T \underline{z} + \underline{x}^T \underline{A}^T \underline{A}\, \underline{x}$$

Note that $\underline{z}^T\underline{A}\,\underline{x}$ is a scalar and, since a scalar is equal to its transpose,

$$\underline{z}^T\underline{A}\,\underline{x} = \underline{x}^T\underline{A}^T\underline{z}$$

so that

$$\underline{e}^T\underline{e} = \underline{z}^T\underline{z} - 2\,\underline{z}^T\underline{A}^T\underline{x} + \underline{x}^T\underline{A}^T\underline{A}\,\underline{x}$$

We want to choose $\underline{x}$ to minimize $\underline{e}^T\underline{e}$. To do this we set

$$\frac{\partial \underline{e}^T\underline{e}}{\partial \underline{x}} = \underline{0}$$

and solve for $\underline{x}$. We should also check that $\frac{\partial}{\partial \underline{x}}\left(\frac{\partial \underline{e}^T\underline{e}}{\partial \underline{x}}\right)$, which will be a matrix, is positive definite.

$$\frac{\partial \underline{e}^T\underline{e}}{\partial \underline{x}} = \frac{\partial}{\partial \underline{x}}(\underline{z}^T\underline{z} - 2\,\underline{z}^T\underline{A}\,\underline{x} + \underline{x}^T\underline{A}^T\underline{A}\,\underline{x})$$

(rule 1) (rule 2) (rule 3)

$$= \underline{0} - 2\,\underline{A}^T\underline{z} + \underline{A}^T\underline{A}\,\underline{x} + \underline{A}^T\underline{A}\,\underline{x}$$

so

$$\frac{\partial \underline{e}^T\underline{e}}{\partial \underline{x}} = 2\,\underline{A}^T\underline{A}\,\underline{x} - 2\,\underline{A}^T\underline{z}$$

For $\frac{\partial \underline{e}^T\underline{e}}{\partial \underline{x}} = \underline{0}$,

$$\underline{A}^T\underline{A}\,\underline{x} = \underline{A}^T\underline{z}$$

The $\underline{A}$-matrix has rank 2 unless the observer is simultaneously on two baseline extensions (when on the baseline extension for LOP_i, $\beta_i = \beta_m$). Thus, $\underline{A}^T\underline{A}$, a 2 x 2 matrix, is generally invertible and

$$\text{MMSE estimate} = \hat{\underline{x}} = (\underline{A}^T\underline{A})^{-1}\underline{A}^T\underline{z}, \quad \text{a classical result.}$$

Checking the second derivative, we find:

$$\frac{\partial}{\partial \underline{x}} \left(\frac{\partial \underline{e}^T \underline{e}}{\partial \underline{x}} \right) = \frac{\partial}{\partial \underline{x}} (2\,\underline{A}^T\underline{A}\,\underline{x} - 2\,\underline{A}^T\underline{z})$$

(rule 2) (rule 1)

$$= 2\,A^TA - \underline{0}$$

Since $\underline{A}^T\underline{A}$ is positive definite, we have found a minimum.

Similarly, for $\underline{W} = \begin{bmatrix} w_1 & & \underline{0} \\ & w_2 & \\ \underline{0} & & w_3 \end{bmatrix}$

$$\underline{e}^T\underline{W}\,\underline{e} = (\underline{z} - \underline{A}\,\underline{x})^T\,\underline{W}\,(\underline{z} - \underline{A}\,\underline{x})$$

$$= \underline{z}^T\underline{W}\,\underline{z} - \underline{z}^T\underline{W}\,\underline{A}\,\underline{x} - \underline{x}^T\underline{A}^T\underline{W}\,\underline{z} + \underline{x}^T\underline{A}^T\underline{W}\,\underline{A}\,\underline{x}$$

$$= \underline{z}^T\underline{W}\,\underline{z} - 2\,\underline{z}^T\underline{W}\,\underline{A}\,\underline{x} + \underline{x}^T\underline{A}^T\underline{W}\,\underline{A}\,\underline{x}$$

and

$$\frac{\partial \underline{e}^T \underline{e}}{\partial \underline{x}} = \frac{\partial}{\partial \underline{x}} (\underline{z}^T \underline{W}\, \underline{z} - 2\, \underline{z}^T \underline{W}\, \underline{A}\, \underline{x} + \underline{x}^T \underline{A}^T \underline{W}\, \underline{A}\, \underline{x})$$

(rule 1) (rule 2) (rule 3)

$$= \underline{0} - 2\, \underline{A}^T \underline{W}^T \underline{z} + \underline{A}^T \underline{W}\, \underline{A}\, \underline{x} + \underline{A}^T \underline{W}^T \underline{A}\, \underline{x}$$

Note that $\underline{W}$ is diagonal so that $\underline{W}^T = \underline{W}$ and

$$\frac{\partial \underline{e}^T \underline{W}\, \underline{e}}{\partial \underline{x}} = 2\, \underline{A}^T \underline{W}\, \underline{A}\, \underline{x} - 2\, \underline{A}^T \underline{W}\, \underline{z}$$

For $\frac{\partial \underline{e}^T \underline{W}\, \underline{e}}{\partial \underline{x}} = \underline{0}$,

$$\underline{A}^T \underline{W}\, \underline{A}\, \underline{x} = \underline{A}^T \underline{W}\, \underline{z}$$

or $$\hat{\underline{x}} = (\underline{A}^T \underline{W}\, \underline{A})^{-1}\, \underline{A}^T \underline{W}\, \underline{z} \qquad \text{(Weighted MMSE estimate)}$$

Also, $$\frac{\partial}{\partial \underline{x}} \left(\frac{\partial \underline{e}^T \underline{W}\, \underline{e}}{\partial \underline{x}} \right) = \underline{A}^T \underline{W}\, \underline{A} \qquad \text{(positive definite)}$$

Note that for $\underline{W} = \underline{I}$, we have

$\hat{\underline{x}} = (\underline{A}^T \underline{A})^{-1}\, \underline{A}^T \underline{z}$; i.e., the MMSE solution previously identified

Also note that in the 2-TD case, unless a baseline extension is involved, A^{-1} exists and

$$\underline{x} = (\underline{A}^T\underline{A})^{-1}\,\underline{A}^T\underline{z} = \underline{A}^{-1}(\underline{A}^T)^{-1}\,\underline{A}^T\underline{z} = \underline{A}^{-1}\,\underline{z},$$

as expected and as used in reference 15.

In the third case, the derivation follows just as above since the only quality of the $\underline{W}$-matrix we really needed to invoke was that $\underline{W}^T = \underline{W}$. This is also true in the third case since $\underline{W}$ is symmetrical. This third alternative is what is chosen in PILOT where, per reference 2, the so-called G-matrix is used:

$$\underline{G} = (\underline{A}^T\underline{W}\,\underline{A})^{-1}\,\underline{A}^T\underline{W}$$

The $\underline{W}$-matrix used in PILOT is the inverse of $\underline{R}$ where $\underline{R}$ is the covariance matrix for the short term jitter in the TD measurements. Specifically,

$$\underline{R} = \begin{bmatrix} r_{11} & r_{12} & r_{13} \\ r_{21} & r_{22} & r_{23} \\ r_{31} & r_{32} & r_{33} \end{bmatrix}$$

where

$$r_{ij} = \rho_{ij}\,\sigma_i\,\sigma_j = \begin{cases} \sigma_i^2, & i = j \\ \rho_{ij}\,\sigma_i\,\sigma_j, & i \neq j \end{cases}$$

At this point we must make an important distinction. The statistics used in the PILOT formulation are appropriate for considering tracker performance. They differ entirely, however, from those used in the body of this report - as discussed several times. The PILOT formulation assumes that variations other than those associated with short-term signal jitter have been removed - either by "full differential Loran-C," or the periodic insertion of manual corrections. The PILOT terminal features a mechanism for inserting these corrections. In the report, however, we want to discuss the implications if these corrections (which we have no easy way of obtaining) are not inserted. To keep the distinction clear, we will refer to the PILOT statistics as "jitter" statistics. To see how reference 2 arrives at estimates of them we note that:

$$TD_i = TOA_i - TOA_m$$

The "jitter" derivation assumes the variations in the times of arrival (TOA) are independent. (In considering longer-term variations, we recognize this is not true - temperature effects are strongly correlated from path to path). Using this independence assumption yields:

$$E((TD_i - \overline{TD_i})^2) \triangleq \sigma_i^2 = \sigma^2_{TOA_i} + \sigma^2_{TOA_m}$$

and

$$\rho_{ij}\,\sigma_i\,\sigma_j \triangleq E((TD_i - \overline{TD_i})(TD_j - \overline{TD_j})) = \sigma^2_{TOA_m}, \quad i \neq j$$

In the Appendices of reference 2 it is argued (defendably) that

$$\sigma_i^2 = k_1 \left(\frac{r_i^2}{P_i} + \frac{r_m^2}{P_m} \right)$$

$$\rho_{ij}\,\sigma_i\,\sigma_j = k_1 \frac{r_m^2}{P_m}, \quad i \neq j$$

where, k_1 is a scale factor and the P's represent transmitted power levels.

Having stated that this is defendable (i.e., that variations increase with the square of the distance to the transmitting station), we note this violates all known theories and every known Loran-C measurement. It is just not quite all this simple. This is, however, the only easy thing to say about the variations and can be modified in a manner that is approximately valid for a given HHE area by adjustments to the P's after a local survey.

Thus, to compute the G-matrix, one must obtain information regarding transmitted power (see reference 13) and compute the appropriate ranges (simple routines for great circle distances prove entirely adequate).

Summary of G-Matrix Construction

1. Compute the A-matrix as described in reference 15.
2. Obtain transmitted power values from reference 13.

3. Compute great circle ranges from the point of interest to appropriate transmitting stations.

4. Compute the elements and construct the R-matrix:

$$r_{ij} = \begin{cases} k_1 \left(\frac{r_i^2}{P_i} + \frac{r_m^2}{P_m} \right), & i = j \\ k_1 \frac{r_m^2}{P_m}, & i \neq j \end{cases}$$

Alternatively, let $k_1 \frac{r_m^2}{P_m} = k_2$ and note that

$$k_1 \frac{r_i^2}{P_i} + k_1 \frac{r_m^2}{P_m} = k_1 \frac{r_m^2}{P_m} \frac{r_i^2}{P_i} \frac{P_m}{r_m^2} + k_1 \frac{r_m^2}{P_m}$$

$$= k_2 \left(1 + \left(\frac{r_i}{r_m} \right)^2 \frac{P_m}{P_i} \right)$$

so that

$$r_{ij} = \begin{cases} k_2 \left(1 + \left(\frac{r_i}{r_m} \right)^2 \frac{P_m}{P_i} \right) & i = j \\ k_2, & i \neq j \end{cases}$$

For this computation we can let $k_2 = 1$. See the note at the end of step 6.

5. Let $\underline{W} = \underline{R}^{-1}$

6. Compute $\underline{G} = (\underline{A}^T \underline{W} \underline{A})^{-1} \underline{A}^T \underline{W}$

Note: Since $(\underline{A}^T \underline{W} \underline{A})^{-1}$ is directly proportional to k_2 and $\underline{W}$ is inversely proportional to k_2, the G-matrix is independent of k_2. Thus any value of k_2 (e.g., 1, as used above) can be used in calculating $\underline{R}$.

3-TD Error Ellipse

We now have

$$\begin{bmatrix} \Delta x \\ \Delta y \end{bmatrix} = \underline{G} \begin{bmatrix} \Delta TD_1 \\ \Delta TD_2 \\ \Delta TD_3 \end{bmatrix}$$

As in reference 15, we will simplify the notation. Let

$$\begin{bmatrix} \Delta x \\ \Delta y \end{bmatrix} = \underline{v} \qquad \text{and} \qquad \begin{bmatrix} \Delta TD_1 \\ \Delta TD_2 \\ \Delta TD_3 \end{bmatrix} = \underline{u}$$

The probability density function associated with the random vector $\underline{u}$ is:

$$p_{\underline{u}}(\underline{U}) = \frac{1}{(2\pi)^{N/2} |\underline{K}|^{1/2}} \exp\left(-1/2\ \underline{U}^T \underline{K}^{-1} \underline{U} \right)$$

The N = 2 situation was described in reference 15 where

$$\underline{K} = \begin{bmatrix} \sigma_1^2 & \rho_{12}\,\sigma_1\,\sigma_2 \\ \rho_{12}\,\sigma_1\,\sigma_2 & \sigma_2^2 \end{bmatrix}$$

We must emphasize that here the parameters represent the "total" statistics described in the main body of the report, not just what we have called the "jitter" statistics. In the N = 3 case that we want to consider now,

$$\underline{K} = \begin{bmatrix} \sigma_1^2 & \rho_{12}\,\sigma_1\,\sigma_2 & \rho_{13}\,\sigma_1\,\sigma_3 \\ \rho_{12}\,\sigma_1\,\sigma_2 & \sigma_2^2 & \rho_{23}\,\sigma_2\,\sigma_3 \\ \rho_{13}\,\sigma_1\,\sigma_3 & \rho_{23}\,\sigma_2\,\sigma_3 & \sigma_3^2 \end{bmatrix}$$

In reference 15, the transformation from $\underline{u}$ to $\underline{v}$ was invertible (i.e., $\underline{v} = \underline{A}^{-1}\underline{u}$). Thus, we proceeded directly to "v-space" to determine the ellipses of interest. Here, we will stay in $\underline{u}$-space to determine the ellipse (ellipsoid). As in reference 15, we are interested in finding some contour, $p_{\underline{u}}(\underline{U}) = k_3$, and in knowing the probability of an observation falling within that contour. We have

$$p_{\underline{u}}(\underline{U}) = k_3 = \frac{1}{(2\pi)^{3/2}|\underline{K}|^{1/2}} \exp\left(-1/2\ \underline{U}^T\underline{K}^{-1}\underline{U}\right)$$

so that

$$k_3(2\pi)^{3/2}|\underline{K}|^{1/2} = \exp(-\underline{U}^T\underline{K}^{-1}\underline{U}/2)$$

or

$$\underline{U}^T\underline{K}^{-1}\underline{U} = -2\ \ln(k_3(2\pi)^{3/2}|\underline{K}|^{1/2}) = c^2$$

$\underline{U}^T\underline{K}^{-1}\underline{U} = c^2$ defines an ellipsoid and, as shown in reference 17, the probability of falling within that ellipsoid, for a Gaussian random vector, is P, where

$$1-P = \frac{N}{(2)^{N/2}\Gamma(N/2+1)} \int_c^\infty x^{N-1} e^{-x^2/2}\, dx$$

For N = 3, we have

$$1 - P = \frac{3}{2^{3/2}\,\Gamma(5/2)} \int_c^\infty x^2 e^{-x^2/2}\, dx$$

Recall that $\Gamma(1/2) = \sqrt{\pi}$ and $\Gamma(x+1) = x\,\Gamma(x)$

so that

$$\Gamma(5/2) = (3/2)\,\Gamma(3/2) = (3/2)(1/2)\,\Gamma(1/2) = 3\sqrt{\pi}/4$$

and

$$1 - P = \sqrt{2/\pi} \int_c^\infty x^2 e^{-x^2/2}\, dx$$

This integral cannot be expressed in closed form. Integrating by parts, however, shows that

$$\int_c^\infty x^2 e^{-x^2/2}\, dx = c\, e^{-c^2/2} + \int_c^\infty e^{-x^2/2}\, dx$$

Note that $\int_c^\infty e^{-x^2/2}\, dx = \sqrt{2\pi}\,(1 - F(c))$

where $F(c) = \int_{-\infty}^{c} (1/\sqrt{2\pi})\, e^{-x^2/2}\, dx$ and is well-tabulated.

Thus, we have

$$P = 1 - \sqrt{2/\pi} \int_c^\infty x^2 e^{-x^2/2}\, dx$$

$$= 1 - \sqrt{2/\pi}\,\{\, c\, e^{-c^2/2} + \sqrt{2\pi}\,(1 - F(c))\,\}$$

$$= 1 - \sqrt{2/\pi}\, c\, e^{-c^2/2} - 2\,(1 - F(c))$$

Representative values of c^2 are:

$P = 0.50$	$c^2 = 2.37$
$P = 0.90$	$c^2 = 6.25$
$P = 0.95$	$c^2 = 7.81$
$P = 0.99$	$c^2 = 11.35$
$P = 0.999$	$c^2 = 16.2$

Having selected an appropriate value of c^2, we return to the discussion of the contour:

$$\underline{U}^T\underline{K}^{-1}\underline{U} = c^2$$

This defines, at the desired probability level, a contour in the 3-TD space. We now want to consider a projection of the enclosed ellipsoid onto the two-dimensional x-y space. We follow the procedure outlined in the Appendices of reference 18 which considers the set:

$$\Omega_{\underline{x}} = \{ \underline{X}: \ \underline{X}^T\underline{\Gamma}^{-1}\underline{X} \leq 1 \}$$

With $\underline{y} = \underline{G}\,\underline{x}$ where $\underline{G}^{-1}$ does not exist, we obtain the projection of the $\underline{x}$-vectors contained in $\Omega_{\underline{x}}$ to the $\underline{y}$-plane to find they are contained in $\Omega_{\underline{y}}$ where

$$\Omega_{\underline{y}} = \{ \underline{Y}: \ \underline{Y}(\underline{G}\,\underline{\Gamma}\,\underline{G}^T)^{-1}\underline{Y} \leq 1 \}$$

Here, we have

$$\Omega_{\underline{u}} = \{ \underline{U}: \ \underline{U}^T\underline{K}^{-1}\underline{U} \leq c^2 \}$$

which, for $\underline{v} = \underline{G}\,\underline{u}$, yields

$$\Omega_{\underline{v}} = \{ \underline{V}: \ \underline{V}^T(\underline{G}\,\underline{K}\,\underline{G}^T)^{-1}\underline{V} \leq c^2 \}$$

(using $\underline{\Gamma} = \underline{K}$, $\underline{x} = \underline{u}/c$, $\underline{y} = \underline{v}/c$)

Note that in the N = 2 case, where $\underline{G} = \underline{B}$ and $\underline{B}^{-1}$ exists, we have

$$\Omega_{\underline{v}} = \{ \underline{V}: \ \underline{V}^T(\underline{B}\,\underline{K}\,\underline{B}^T)^{-1}\underline{V} \leq c^2 \}$$

but $$(\underline{B}\,\underline{K}\,\underline{B}^T)^{-1} = (\underline{B}^{-1})^T\underline{K}^{-1}\underline{B}^{-1}$$

This latter quantity was defined in reference 15 as $\underline{H}^{-1}$

Using the same notation, we have

$$\underline{\Omega}_{\underline{V}} = \{ \underline{V}: \underline{V}^T \underline{H}^{-1} \underline{V} \leq c^2 \}$$

which is the same result as that obtained, in a much different fashion, by reference 15.

Summary of Procedure for Generating Error Ellipses

1. Determine the elements of the covariance matrix $\underline{K}$. The method, which uses the double range difference model, is presented in reference 15 and carried out in the body of this report.

2. Compute the G-matrix as described earlier in this Appendix.

3. Select a desired probability contour and compute c^2.

4. Compute the $\underline{H}$ matrix:

$$\underline{H} = (\underline{G}\ \underline{K}\ \underline{G}^T)$$

5. Plot the ellipse: $\underline{V}^T \underline{H}^{-1} \underline{V} = c^2$.

APPENDIX B

PHASE MODULATION DERIVATIONS

The derivations in this Appendix support the discussions of Section 4.6 of the report. In that section, we establish that although the ideal antenna current waveform is expressed

$$i(t) = x(t) \sin w_c t,$$

the actual signal contains phase modulation and is more properly expressed

$$i(t) = y(t) \sin w_c t + z(t) \cos w_c t.$$

In discussions of the effects, we want to determine what happens when a waveform with phase modulation is processed by a Loran-C receiver. This causes us to focus our attention on what we denote as V(T), the voltage sampled by the phase locked loop circuitry at the receiver track point, T. V(T) is the result of the convolution of the received signal with the impulse response of the receiver "front end," i.e.,

$$V(T) = \int_{-\infty}^{T} r(t)\, h(T-t)\, dt \qquad \text{(B-1)}$$

In general,

$$r(t) = R_I(t) \sin w_c t + R_Q(t) \cos w_c t$$

and,

$$h(t) = H_I(t) \sin w_c t + H_Q(t) \cos w_c t$$

so that,

$$V(T) = \int_{-\infty}^{T} [\, R_I(t) \sin w_c t + R_Q(t) \cos w_c t \,] \times [\, H_I(T-t) \sin w_c(T-t) + H_Q(T-t) \cos w_c(T-t) \,]\, dt$$

where $R_I(t)$, $R_Q(t)$, $H_I(t)$, and $H_Q(t)$ are "baseband" representations of the in-phase and quadrature "envelopes" of r(t) and h(t).

We should mention that reference 14 contains a related discussion of these matters. Reference 14, however, begins with the assumption that essentially everything developed herein is well known to the reader and proceeds to examine the size of TD variations for representative changes in r(t) and h(t). Thus, the purpose of this Appendix will be to develop the concepts used in the report. We will concentrate on establishing what factors will cause phase variations (and why), leaving consideration of "how much?" to reference 14.

Returning to the discussion of the voltage sampled by the phase locked loop, we have

$$V(T) = \int_{-\infty}^{T} [\, R_I(t) \sin w_c t + R_Q(t) \cos w_c t \,] \; x$$

$$[\, H_I(T-t) (\sin w_c T \cos w_c t - \sin w_c t \cos w_c T)$$

$$+ H_Q(T-t) (\cos w_c T \cos w_c t + \sin w_c t \sin w_c T) \,] \; dt$$

$$= \sin w_c T \int_{-\infty}^{T} R_I(t) H_I(T-t) \sin w_c t \cos w_c t \, dt$$

$$- \cos w_c T \int_{-\infty}^{T} R_I(t) H_I(T-t) \sin^2 w_c t \, dt$$

$$+ \cos w_c T \int_{-\infty}^{T} R_I(t) H_Q(T-t) \sin w_c t \cos w_c t \, dt$$

$$+ \sin w_c T \int_{-\infty}^{T} R_I(t) H_Q(T-t) \sin^2 w_c t \, dt$$

$$+ \sin w_c T \int_{-\infty}^{T} R_Q(t) H_I(T-t) \cos^2 w_c t \, dt \qquad \text{(B-2)}$$

$$- \cos w_c T \int_{-\infty}^{T} R_Q(t) H_I(T-t) \sin w_c t \cos w_c t \, dt$$

$$+ \cos w_c T \int_{-\infty}^{T} R_Q(t) H_Q(T-t) \cos^2 w_c t \, dt$$

$$+ \sin w_c T \int_{-\infty}^{T} R_Q(t) H_Q(T-t) \sin w_c t \cos w_c t \, dt$$

Implications With No Phase Modulation

To begin to consider some special cases, suppose that

$$H_Q(t) = R_Q(t) = 0.$$

Then, B-2 becomes

$$V(T) = \sin w_c T \int_{-\infty}^{T} R_I(t)\, H_I(T-t) \sin w_c t \cos w_c t$$

$$- \cos w_c T \int_{-\infty}^{T} R_I(t)\, H_I(T-t) \sin^2 w_c t \, dt$$

Without loss of generality, we can consider the "zero-crossing detector" implementation of the phase locked loop so that loop action makes $V(T_1) = 0$, where T_1 = the estimate of the signal time of arrival.

With $V(T_1) = 0$, we have

$$\tan w_c T_1 = \frac{\int_{-\infty}^{T} R_I(t)\, H_I(T-t) \sin^2 w_c t \, dt}{\int_{-\infty}^{T} R_I(t)\, H_I(T-t) \sin w_c t \cos w_c t \, dt} = \frac{B}{A}$$

and,

$$T_1 = (1/w_c) \tan^{-1}(B/A) = (1/w_c)\,(N \cdot \pi + \text{P.V. } [\tan^{-1}(B/A)]) \qquad \text{(B-3)}$$

(P.V. denotes "principle value").

Since $w_c = 2\pi \times 10^5$,

$$T_1 = N \cdot \pi/(2\pi \times 10^5) + (1/w_c)\ \text{P.V.}\ [\tan^{-1}(B/A)]$$

$$= N \cdot 5\ \text{usec} + (1/w_c)\ \text{P.V.}\ [\tan^{-1}(B/A)]$$

Implementation (i.e., whether a positive-going or negative-going zero crossing detector is used) determines whether N is to be odd or even. Cycle detection circuitry (i.e., the envelope processor) determines the actual value of N. Notice that, in general,

$$\text{P.V.}\ [\tan^{-1}(B/A)] \neq 0$$

so that zero-crossings of the processed signal are not generally aligned with zero-crossings of the incoming signal - even for these "ideal" waveforms. Thus, the "30-usec point" has become simply a "concept" long before the phase locked loop of any actual Loran-C receiver.

There are several other things we should say about these "ideal" waveforms before we complicate the matter by returning the non-zero quadrature components. First, suppose we change the track point - for one of the signals only - by "10 usec." Specifically, suppose we want the receiver to "seek" the zero crossing at $T_2 = T_1 - 10\ \text{us} + \Delta T$. We have,

$$\sin w_c T_1 \int_{-\infty}^{T_1} R_I(t)\, H_I(T_1 - t) \sin w_c t \cos w_c t\, dt$$

$$- \cos w_c T_1 \int_{-\infty}^{T_1} R_I(t)\, H_I(T_1 - t) \sin^2 w_c t\, dt = 0$$

and

$$\sin w_c(T_1 - 10 + \Delta T) \int_{-\infty}^{T_1 - 10 + \Delta T} R_I(t)\, H_I(T_1 - 10 + \Delta T - t) \sin w_c t \cos w_c t\, dt$$

$$- \cos w_c(T_1 - 10 + \Delta T) \int_{-\infty}^{T_1 - 10 + \Delta T} R_I(t)\, H_I(T_1 - 10 + \Delta T - t) \sin^2 w_c t\, dt = 0$$

This means

$$\sin w_c T_1 \int_{-\infty}^{T_1} R_I(t)\, H_I(T_1-t) \sin w_c t \cos w_c t$$

$$-\cos w_c T_1 \int_{-\infty}^{T_1} R_I(t)\, H_I(T_1-t) \sin^2 w_c t\, dt \qquad \text{(B-4)}$$

$$= [\sin w_c T_1 \cos w_c \Delta T + \cos w_c T_1 \sin w_c \Delta T] \quad x$$

$$\int_{-\infty}^{T_1-10+\Delta T} R_I(t)\, H_I(T_1-10+\Delta T-t) \sin w_c t \cos w_c t\, dt$$

$$- [\cos w_c T_1 \cos w_c \Delta T - \sin w_c T_1 \sin w_c \Delta T] \quad x$$

$$\int_{-\infty}^{T_1-10+\Delta T} R_I(t)\, H_I(T_1-10+\Delta T-t) \sin^2 w_c t\, dt$$

Very little is gained by trying to solve the above "mess" for ΔT. The point to notice is that, in general, $\Delta T \neq 0$. Thus, even with this "ideal" signal and receiver response, a "change in cycle" on one signal of a baseline will cause a slight TD change (equal to ΔT in this case) - in addition to the "expected" 10 μsec change.

Another "ideal" situation we should examine arises from consideration of ECD changes. We note that, again in general, the signal delivered to the receiver does not fit the ideal envelope description. Let us ignore this technicality however and note that, according to the Loran-C signal specification, we have

$$R_I(t,\tau) = R_I(t-\tau)$$

so B-2 becomes

$$V(T,\tau) = \sin w_c T \int_{-\infty}^{T} R_I(t-\tau)\, H_I(T-t) \sin w_c t \cos w_c t\, dt$$

$$- \cos w_c T \int_{-\infty}^{T} R_I(t-\tau)\, H_I(T-t) \sin^2 w_c t\, dt$$

Note that $R_I(t-\tau) = 0$ for $t < \tau$, so

$$V(T,\tau) = \sin w_c T \int_{\tau}^{T} R_I(t-\tau)\, H_I(T-t) \sin w_c t \cos w_c t\, dt$$

$$- \cos w_c T \int_{\tau}^{T} R_I(t-\tau)\, H_I(T-t) \sin w_c t \cos w_c t\, dt$$

For $V(T_2,\tau) = 0$, we require

$$T_2 = N \cdot 5 \text{ usec} + (1/w_c) \tan^{-1}\left[\frac{\int_{\tau}^{T_2} R_I(t-\tau)\, H_I(T_2-t) \sin^2 w_c t\, dt}{\int_{\tau}^{T_2} R_I(t-\tau)\, H_I(T_2-t) \sin w_c t \cos w_c t\, dt}\right] \qquad \text{(B-5)}$$

Letting $T_2 = T_1 + \Delta T$, we compare equations B-3 and B-5 to find $\Delta T = 0$ if (and, essentially, only if)

$$\frac{\int_{\tau}^{T} R_I(t-\tau)\, H_I(T-t) \sin^2 w_c t\, dt}{\int_{\tau}^{T} R_I(t-\tau)\, H_I(T-t) \sin w_c t \cos w_c t\, dt} = \frac{\int^{T} R_I(t)\, H_I(T-t) \sin^2 w_c t\, dt}{\int^{T} R_I(t)\, H_I(T-t) \sin w_c t \cos w_c t\, dt}$$

Again, without "cranking through" the above mess to see what gory requirements have to be satisfied by $H_I(t)$ for ΔT to be zero (for any given value of τ), we can see that even an "ideal ECD" change will cause a ΔT, i.e., a TOA change.

To summarize the "ideal" cases,

- a cycle change for one of the signals will result in a TD change (modulo 10 usec),
- an ECD change (for one of the signals) will cause a change in the time difference reading.

Phase Modulation in the Received Signal

Here we have $R_Q(t) \neq 0$ (but $H_Q(t) = 0$ still). We have already encountered "messes" and can expect the equations to become even messier as we add non-zero terms to equation B-2. Thus, we will have to make some simplifying approximations in the course of subsequent discussions. To begin, let

$$\phi(t) = \tan^{-1}\left[\frac{R'_Q(t)}{R'_I(t)}\right]$$

for small $\phi(t)$,

$$\phi(t) \simeq \frac{R'_Q(t)}{R'_I(t)}$$

so that,

$$R'_Q(t) \approx R'_I(t)\ \phi(t)$$

We have used the notation R'_Q and R'_I to allow a comparison with the previously discussed "no phase modulation case."

From B-2, we have

$$V(T) = \sin w_c T \left[\int_{\infty}^{T} R'_I(t) H_I(T-t) \sin w_c t \cos w_c t\, dt + \int_{\infty}^{T} R'_Q(t)\, H_I(T-t) \cos^2 w_c t\, dt \right]$$

$$- \cos w_c T \left[\int_{\infty}^{T} R'_I(t) H_I(T-t) \sin^2 w_c t\, dt + \int_{\infty}^{T} R'_Q(t) H_I(T-t) \sin w_c t \cos w_c t\, dt \right]$$

Let's say $V(T) = 0$ for $T = T_2$, so

$$0 = V(T_2) = \sin w_c T_2 \left\{ \int_{\infty}^{T_2} H_I(T_2-t) \left[R'_I(t) \sin w_c t + R'_Q(t) \cos w_c t\right] \cos w_c t\, dt \right\}$$

(B-6)

$$- \cos w_c T_2 \left\{ \int_{\infty}^{T_2} H_I(T_2-t) \left[R'_I(t) \sin w_c t + R'_Q(t) \cos w_c t\right] \cos w_c t\, dt \right\}$$

Recall that when we considered the "no phase modulation case," we had $V(T) = 0$ for $T = T_1$. In that case, we had $R_Q(t) = 0$ and the received signal was composed exclusively of its in-phase component which we called, and will continue to call, $R_I(t)$ (i.e., no prime).

In the no phase modulation case we had

$$0 = V(T_1) = \sin w_c T_1 \int_{\infty}^{T_1} H_I(T_1-t) \left[R_I(t) \sin w_c t\right] \cos w_c t\, dt$$

(B-7)

$$- \cos w_c T_1 \int_{\infty}^{T_1} H_I(T_1-t) \left[R_I(t) \sin w_c t\right] \sin w_c t\, dt$$

With $T_1 = T_2 + \Delta T$, we have

$$\sin w_c T_1 = \sin w_c T_2 \cos w_c \Delta T - \sin w_c \Delta T \cos w_c T_2$$

and (B-8)

$$\cos w_c T_1 = \cos w_c T_2 \cos w_c \Delta T + \sin w_c \Delta T \sin w_c T_2$$

Since we use the same voltage level detector in each case, we have $V(T_1) = V(T_2)$ (= 0, generally). Thus, we can combine equations B-6, B-7 and B-8 to obtain

$$\sin w_c T_2 \left\{ \int_{\infty}^{T_2} H_I(T_2-t) \left[R'_I(t) \sin w_c t + R'_Q(t) \cos w_c t\right] \cos w_c t \, dt \right\}$$

$$- \cos w_c T_2 \left\{ \int_{\infty}^{T_2} H_I(T_2-t) \left[R'(t) \sin w_c t + R'_Q(t) \cos w_c t\right] \sin w_c t \, dt \right\} \quad \text{(B-9)}$$

$$= (\sin w_c T_2 \cos w_c \Delta T - \sin w_c \Delta T \cos w_c T_2) \int_{\infty}^{T_1} H_I(T_1-t)[R_I(t) \sin w_c t] \cos w_c t \, dt$$

$$- (\cos w_c T_2 \cos w_c \Delta T + \sin w_c \Delta T \sin w_c T_2) \int_{\infty}^{T_1} H_I(T_1-t)[R_I(t) \sin w_c t] \sin w_c t \, dt$$

For small amounts of phase modulation (or, more generally, small changes in phase modulation), we have

$$\Delta T \simeq 0; \qquad \cos w_c \Delta T \simeq 1; \qquad \sin w_c \Delta T \simeq 0$$

$$R'_I(t) \simeq R_I(t); \quad \text{and} \quad R'_Q(t) \simeq R'_I(t) \, \phi(t)$$

Using these approximations in B-9, we get

$$\sin w_c T_2 \int_{-\infty}^{T_2} H_I(T_2-t)\,[R'_I(t)\sin w_c t + R'_I(t)\,\phi(t)\cos w_c t]\cos w_c t\,dt$$

$$- \cos w_c T_2 \int_{-\infty}^{T_2} H_I(T_2-t)\,[R'_I(t)\sin w_c t + R'_I(t)\,\phi(t)\cos w_c t]\sin w_c t\,dt$$

$$\simeq \sin w_c T_2 \int_{-\infty}^{T_1} H_I(T_1-t)\,[R'_I(t)\sin w_c t]\cos w_c t\,dt$$

$$- \cos w_c T_2 \int_{-\infty}^{T_1} H_I(T_1-t)\,[R'_I(t)\sin w_c t]\sin w_c t\,dt$$

or, with $H_I(T_1-t) \simeq H_I(T_2-t)$,

$$\sin w_c T_2 \int_{T_1}^{T_2} H_I(T_2-t)\,R'_I(t)\sin w_c t\cos w_c t\,dt$$

$$- \cos w_c T_2 \int_{T_1}^{T_2} H_I(T_2-t)\,R'_I(t)\sin^2 w_c t\,dt$$

$$\simeq \cos w_c T_2 \int_{-\infty}^{T_2} R'_I(t)\,\phi(t)\,H_I(T_2-t)\sin w_c t\cos w_c t\,dt$$

$$- \sin w_c T_2 \int_{-\infty}^{T_2} R'_I(t)\,\phi(t)\,H_I(T_2-t)\cos^2 w_c t\,dt$$

Note that with $\phi(t) = 0$, the "right side" of this equation equals zero, forcing the "left side" to zero and, thus, T_2 to equal T_1 - the expected result for no phase modulation. Conceptually, therefore, the above equation tells us the following:

- With no phase modulation, the receiver tracks at T_1, i.e., the phase locked loop sees zero voltage from the filtered signal at T_1.

- With phase modulation, a weighted integral of $\phi(t)$ up to time T_1 will, generally, cause a small but non-zero value of $V(T_1)$. The loop must "average some RF" (from T_1 to T_2) to cancel this slight voltage. Thus, $T_1 \neq T_2$.

To be a bit more specific, we can re-write the preceeding equation as:

$$\sin w_c T_2 \int_{T_1}^{T_2} H_I(T_2-t)\, R'_I(t)\, (\sin 2w_c t)/2\, dt$$

$$- \cos w_c T_2 \int_{T_1}^{T_2} H_I(T_2-t)\, R'_I(t)\, (1-\cos 2w_c t)/2\, dt$$

$$\simeq \cos w_c T_2 \int_{-\infty}^{T_2} H_I(T_2-t)\, R'_I(t)\, \phi(t)\, (\sin 2w_c t)/2\, dt$$

$$- \sin w_c T_2 \int_{-\infty}^{T_2} H_I(T_2-t)\, R'_I(t)\, \phi(t)\, (1+\cos 2w_c t)/2\, dt$$

A further approximation recognizes that $R'_I(t)$ and $\phi(t)$ are slowly varying. Thus, the 200 Khz components ($\sin 2w_c t$ and $\cos 2w_c t$) contribute negligibly to the right side of the above equation. Thus, we have

$$\sin w_c T_2 \int_{T_1}^{T_2} H_I(T_2-t)\, R'_I(t) \sin 2w_c t\, dt$$

$$- \cos w_c T_2 \int_{T_1}^{T_2} H_I(T_2-t)\, R'_I(t)\, (1-\cos 2w_c t)\, dt$$

$$\simeq - \sin w_c T_2 \int_{-\infty}^{T_2} H_I(T_2-t)\, R'_I(t)\, \phi(t)\, dt$$

or,

$$\int_{T_1}^{T_2} H_I(T_2-t)\, R'_I(t) \sin 2w_c t\, dt - \cot w_c T_2 \int_{T_1}^{T_2} H_I(T_2-t)\, R'_I(t)\, (1-\cos 2w_c t)\, dt \qquad \text{(B-10)}$$

$$\simeq - \int_{-\infty}^{T_2} H_I(T_2-t)\, R'_I(t)\, \phi(t)\, dt$$

For $T_2 - T_1 = \Delta T$ = small, we have

$$\int_{T_1}^{T_2} H_I(T_2-t)\, R'_I(t) \sin 2w_c t\, dt \simeq -k_1 \Delta T$$

and

$$\cot w_c T_2 \int_{T_1}^{T_2} H_I(T_2-t)\, R'_I(t)\, (1-\cos 2w_c t)\, dt \simeq k_2 \Delta T$$

Thus, B-10 becomes

$$\Delta T \simeq k \int_{-\infty}^{T_2} H_I(T_2-t)\, R'_I(t)\, \phi(t)\, dt$$

where $k = (k_1 + k_2)^{-1}$.

This is the principle result used in the report and, for purposes of providing insight into the effects of phase modulation, seems to be the best representation of the important waveforms. The concept is:

> the change in TOA is determined by a weighted integral of the phase error term. The weighting function is primarily determined by the envelope of the receiver impulse response.

Phase Modulation in the Receiver Response

In this case we have $R_Q(t) = 0$ but $H_Q(t) \neq 0$. The derivation proceeds just as in the "phase modulated received signal" case using:

$$\theta(t) = \tan^{-1}\left[\frac{H'_Q(t)}{H'_I(t)}\right]$$

where, for small $\theta(t)$,

$$H_I(t) \simeq H'_I(t); \qquad H'_Q(t) \simeq H'_I(t)\, \theta(t)$$

Using a procedure similar to the one which led to equation B-11, we obtain

$$\Delta T \simeq k' \int_{-\infty}^{T_2} R_I(t)\, H'_I(T_2-t)\, \theta(T_2-t)\, dt$$

Phase Modulation in the Received Signal AND the Receiver Response

For non-zero $R_Q(t)$ and $H_Q(t)$, we use the approximations

$$R'_Q(t) \simeq R'_I(t)\, \phi(t) \quad \text{and} \quad H'_Q(t) \simeq H'_I(t)\, \theta(t)$$

in equation B-2 to get

$$\begin{aligned}
V(T) \simeq\ & \sin w_c T \int_{-\infty}^{T} H'_I(T-t)\, R'_I(t) \sin w_c t \cos w_c t\, dt \\
& - \cos w_c T \int_{-\infty}^{T} H'_I(T-t)\, R'_I(t) \sin^2 w_c t\, dt \\
& + \cos w_c T \int_{-\infty}^{T} R'_I(t)\, H'_I(T-t)\, \theta(T-t) \sin w_c t \cos w_c t\, dt \\
& + \sin w_c T \int_{-\infty}^{T} R'_I(t)\, H'_I(T-t)\, \theta(T-t) \sin^2 w_c t\, dt \\
& + \sin w_c T \int_{-\infty}^{T} R'_I(t)\, H'_I(T-t)\, \phi(t) \cos^2 w_c t\, dt \\
& - \cos w_c T \int_{-\infty}^{T} R'_I(t)\, H'_I(T-t)\, \phi(t) \sin w_c t \cos w_c t\, dt \\
& + \cos w_c T \quad R'_I(t)\, H'_I(T-t) \quad (t) \quad (T-t) \cos^2 w_c t\, dt \\
& + \sin w_c T \int_{-\infty}^{T} R'_I(t)\, H'_I(T-t)\, \phi(t)\, \theta(T-t) \sin w_c t \cos w_c t\, dt
\end{aligned}$$

With both $\phi(t)$ and $\theta(t)$ small, terms featuring the product $\phi(t)\ \theta(t)$ are negligible. We also note that $V(T_1) = V(T_2)\ (\ = 0)$, where T_1 is the track point when $\phi(t) = \theta(t) = 0$ and T_2 is the track point otherwise. These two facts lead to:

$$\sin w_c T_2 \int_{-\infty}^{T_2} R'_I(t)\ H'_I(T_2-t) \sin w_c t \cos w_c t\ dt$$

$$- \cos w_c T_2 \int_{-\infty}^{T_2} R'_I(t)\ H'_I(T_2-t) \sin^2 w_c t\ dt$$

$$+ \cos w_c T_2 \int_{-\infty}^{T_2} R'_I(t)\ H'_I(T_2-t)\ \theta(T_2-t) \sin w_c t \cos w_c t\ dt$$

$$+ \sin w_c T_2 \int_{-\infty}^{T_2} R'_I(t)\ H'_I(T_2-t)\ \theta(T_2-t) \sin^2 w_c t\ dt$$

$$+ \sin w_c T_2 \int_{-\infty}^{T_2} R'_I(t)\ H'_I(T_2-t)\ \phi(t) \cos^2 w_c t\ dt$$

$$- \cos w_c T_2 \int_{-\infty}^{T_2} R'_I(t)\ H'_I(T_2-t)\ \phi(t) \sin w_c t \cos w_c t\ dt$$

$$+ \text{negligible terms}$$

$$\simeq \sin w_c T_1 \int_{-\infty}^{T_1} R'_I(t)\ H'_I(T_1-t) \sin w_c t \cos w_c t\ dt$$

$$- \cos w_c T_1 \int_{-\infty}^{T_1} R'_I(t)\ H'_I(T_1-t) \sin^2 w_c t\ dt$$

(The right-hand side of the above equation comes from the "no phase modulation" discussion on page B-3 and represents $V(T_1)$.) Using $T_1 \simeq T_2$ and $H'_I(T_2-t) \simeq H'_I(T_1-t)$, this becomes

$$\simeq \sin w_c T_2 \int_{-\infty}^{T_1} R'_I(t)\ H'_I(T_2-t) \sin w_c t \cos w_c t\ dt$$

$$- \cos w_c T_2 \int_{-\infty}^{T_1} R'_I(t)\ H'_I(T_2-t) \sin^2 w_c t\ dt$$

Further manipulation of the equation yields

$$\sin w_c T_2 \int_{T_1}^{T_2} R'_I(t)\, H'_I(T_2-t) \sin w_c t \cos w_c t\, dt$$

$$- \cos w_c T_2 \int_{T_1}^{T_2} R'_I(t)\, H'_I(T_2-t) \sin^2 w_c t\, dt$$

$$\simeq - \cos w_c T_2 \int_{-\infty}^{T_2} R'_I(t)\, H'_I(T_2-t)\, \theta(T_2-t) \sin w_c t \cos w_c t\, dt$$

$$- \sin w_c T_2 \int_{-\infty}^{T_2} R'_I(T_2-t)\, H'_I(T_2-t)\, \theta(T_2-t) \sin^2 w_c t\, dt$$

$$- \sin w_c T_2 \int_{-\infty}^{T_2} R'_I(t)\, H'_I(T_2-t)\, \phi(t) \cos^2 w_c t\, dt$$

$$+ \cos w_c T_2 \int_{-\infty}^{T_2} R'_I(t)\, H'_I(T_2-t)\, \phi(t) \sin w_c t \cos w_c t\, dt$$

$$\simeq \cos w_c T_2 \int_{-\infty}^{T_2} R'_I(t)\, [\phi(t) - \theta(T_2-t)]\, H'_I(T_2-t)\, (\cos 2w_c t)/2\, dt$$

$$- \sin w_c T_2 \int_{-\infty}^{T_2} R'_I(t)\, [\phi(t)\,(1+\cos 2w_c t) + \theta(T_2-t)\,(1-\cos 2w_c t)]/2\, H'(T_2-t)\, dt$$

The interval defined by the integration limits on the left-hand side of the above equation is small with respect to the period of the sinusoids inside the integral. Thus, as before, we can represent the left-hand side as $k_1 \Delta T$. The first integral on the right-hand side of the equation, as well as the "RF" part of the second integral, approximates the integral of a sinusoid over several periods and can be considered negligible when compared to the contribution of the "DC" portion of the second integral on the right side. Thus, we have

$$k_1 \Delta T \simeq \sin w_c T_2 \int_{-\infty}^{T_2} R'_I(t)\, [\phi(t) + \theta(T_2-t)]\, H'_I(T_2-t)\, dt$$

This reduces to

$$\Delta T \simeq k \int_{-\infty}^{T_2} R'_I(t)\,[\phi(t) + \theta(T_2-t)]\,H'_I(T_2-t)\,dt$$

which, again, shows the TOA change to be a weighted integral, up to the track point, of the phase modulation - as indicated in the body of the report.

REFERENCES

1. "Department of Transportation National Plan for Navigation," U.S. Department of Transportation, April 1972.

2. Olsen, D.L., Ligon, J.L., Sedlock, A.J., and Isgett, C.E., "Precision Loran-C Navigation for the Harbor and Harbor Entrance Area," May 1980. U.S. Coast Guard Report No. CG-D-34-80. Avaialble from the National Technical Information Service, Springfield, Virginia 22161 as AD-A086001.

3. Olsen, D.L., "St. Marys River Loran-C Mini Chain Final Report," July 1981. U.S. Coast Guard Report No. CG-D-11-82. Available from the National Technical Information Service, Springfield, Virginia 22161 as PB82-255183.

4. Gupta, R.R., Healy, R.D., and Warren, R.S., "Design and Calibration of a Grid Prediction Algorithm for the St. Marys River Loran-C Chain," The Analytical Sciences Corporation, March, 1978, Published as U.S. Coast Guard Report No. CG-D-32-80. Available from the National Technical Information Service, Springfield, Virginia 22161 as AD-A096004.

5. Gupta, R.R., "Application of Semi-Empirical TD Grid Calibration to the West Coast Loran-C Chain," The Analytical Sciences Corporation, July 1979. Published as U.S. Coast Guard Report No. CG-D-29-81. Available from the National Technical Information Service, Springfield, Virginia 22161 as AD-A103804.

6. Lewicki, J.P., Milne, T.J., and Sedlock, A.J., "Time Difference Survey System," April 1981. Published as U.S. Coast Guard Report No. CG-D-72-81. Available from the National Technical Information Service, Springfield, Virginia 22161 as AD-A115588.

7. Sedlock, A.J., "HHE Loran-C Time Difference Surveying, Final Report," November 1982. Published as U.S. Coast Guard Report No. CG-D-54-82. Available from the National Technical Information Service, Springfield, Virginia 22161 as AD-A124343.

8. Baer, G.E. and Harrison, J.F., Jr., "PILOT, A Precision Intercoastal Loran Translocator, Volume 3 - Software," The Johns Hopkins University Applied Physics Laboratory, March 1982. Published as U.S. Coast Guard Report No. CG-D-21-81,III. Available from the National Technical Information Service as AD-A121759.

9. DePalma, L.M. and Gupta, R.R., "Seasonal Sensitivity Analysis of the St. Marys River Loran-C Time Difference Grid," The Analytic Sciences Corporation, June 1978. Published as U.S. Coast Guard Report No. CG-D-33-80. Available from the National Technical Information Service as AD-A085825.

10. Creamer, P.M. and DePalma, L.M., "Quantification of St. Marys River Loran-C Time Difference Grid Stability," The Analytic Sciences Corporation, August 1980. Published as U.S. Coast Guard Report No. CG-D-52-81. Available from the National Technical Information Service, Springfield, Virginia 22161 as AD-A108074.

11. Campbell, L.W., Doherty, R.H., and Johler, J.R., "Loran-C System Dynamic Model: Temporal Propagation Variation Study," Analytical Systems Engineering Corporation and Colorado Research and Prediction Laboratory, Inc., July 1979. Published as U.S. Coast GUard Report No. CG-D-57-79. Available from the National Technical Information Service, Springfield, Virginia 22161 as AD-A076214.

12. Samaddar, S.N., "Weather Effects on Loran-C Propagation," Navigation: Journal of the Institute of Navigation, Vol. 27, No.1, Spring 1980, pp. 39-53.

13. "Specification of the Transmitted Loran-C Signal", U.S. Coast Guard, July 1981

14. Feldman, D.A., "The Effects of Phase Modulation on Accuracy of the Loran-C System," IEEE 1978 Position Location and Navigation Symposium (PLANS) Procedings.

15. Slagle, D.C., and Wenzel, R.J. "Loran-C Signal Stability Study: St. Lawrence Seaway," July, 1982. Published as U.S. Coast Guard Report No. CG-D-39-82. Available from the National Technical Information Service, Springfield, Virginia 22161 as AD-A122476.

16. Standard Mathematical Tables, The Chemical Rubber Co., Cleveland, Ohio, 18th Edition, Selby, S.M., Ed., 1970.

17. Van Trees, H.L., Detection, Estimation and Modulation Theory, Part I, John Wiley and Sons, Inc., New York, 1968.

18. Schweppe, F.C., Uncertain Dynamic Systems, Prentice-Hall, Inc., Englewood Cliffs, N.J., 1973.